ANALYTICA CHIMICA ACTA

International monthly devoted to all branches of analytical chemistry
Revue mensuelle internationale consacrée à tous les domaines de la chimie analytique
Internationale Monatsschrift für alle Gebiete der analytischen Chemie

ELSEVIER PUBLISHING COMPANY
AMSTERDAM

Anal. Chim. Acta, Vol. 45, No. 3, 365–556, May 1969
Published monthly
Completing Volume 45

Provisional Publication Schedule for 1969

In the interests of rapid publication it has been found necessary to schedule 5 volumes for appearance in 1969. Since monthly publication will be maintained, this implies that 2 of the volumes will each consist of three issues, while 3 of the volumes will each consist of only 2 issues. The following provisional schedule applies:

Vol. **44**, No. **1**	January 1969	
Vol. **44**, No. **2**	February 1969	**(completing Vol. 44)**
Vol. **45**, No. **1**	March 1969	
Vol. **45**, No. **2**	April 1969	
Vol. **45**, No. **3**	May 1969	**(completing Vol. 45)**
Vol. **46**, No. **1**	June 1969	
Vol. **46**, No. **2**	July 1969	**(completing Vol. 46)**
Vol. **47**, No. **1**	August 1969	
Vol. **47**, No. **2**	September 1969	
Vol. **47**, No. **3**	October 1969	**(completing Vol. 47)**
Vol. **48**, No. **1**	November 1969	
Vol. **48**, No. **2**	December 1969	**(completing Vol. 48)**

Subscription price: $ 17.50 or Dfl. 63.— per volume plus postage. Total subscription price for 1969: $ 87.50 or Dfl. 315.— plus postage. Additional cost for copies by airmail available on request. For subscribers in the U.S.A. and Canada, 2nd class postage paid at Jamaica, N.Y. For advertising rates apply to the publishers.

Subscriptions should be sent to:

ELSEVIER PUBLISHING COMPANY P.O. Box 211, Amsterdam, The Netherlands

GENERAL INFORMATION

Languages

Papers will be published in English, French or German.

Submission of papers

Papers should be sent to:

PROF. PHILIP W. WEST,
Coates Chemical Laboratories,
College of Chemistry and Physics,
Louisiana State University,
Baton Rouge 3,
La. 70803 (U.S.A.)

or to:

DR. A. M. G. MACDONALD,
Department of Chemistry,
The University,
P.O. Box 363
Birmingham 15 (Great Britain)

Reprints

Fifty reprints will be supplied free of charge. Additional reprints (minimum 100) can be ordered at quoted prices. They must be ordered on order forms which are sent together with the proofs.

They're all in the BDH Catalogue...

a range of more than 5,000 chemicals

BDH can supply almost every reagent in regular demand in laboratory practice today, as well as many developed for special applications in research and industry — reagents of the highest standards of purity and reliability.

Items of particular interest include:

'Aristar' ultra-pure chemicals: for analytical, research and industrial applications in which extreme purity is essential.

'AnalaR' analytical reagents: More than 300 guaranteed analytical reagents conforming to the recently revised 'AnalaR' specifications.

BDH Biochemicals: A comprehensive selection of high quality biochemicals and reagents including Amino acids and derivatives, enzymes and enzyme substrates, nucleotides, nucleosides and nucleic acids, carbohydrates and sugar phosphates, highly pure fatty acids and methyl esters.

Materials for chromatography and electrophoresis
Micro-analytical reagents
Organic Analytical Standards
General laboratory chemicals
Clinical reagents
Solvents for spectroscopy
Microscopical stains and sundries
Ion exchange resins
Volumetric solutions
Indicators
Test papers

If you do not already receive our monthly publication 'New Entries in the BDH Catalogue', ask your distributor to add you to the mailing list.

BDH Chemicals Ltd
Poole · England BH12 4NN

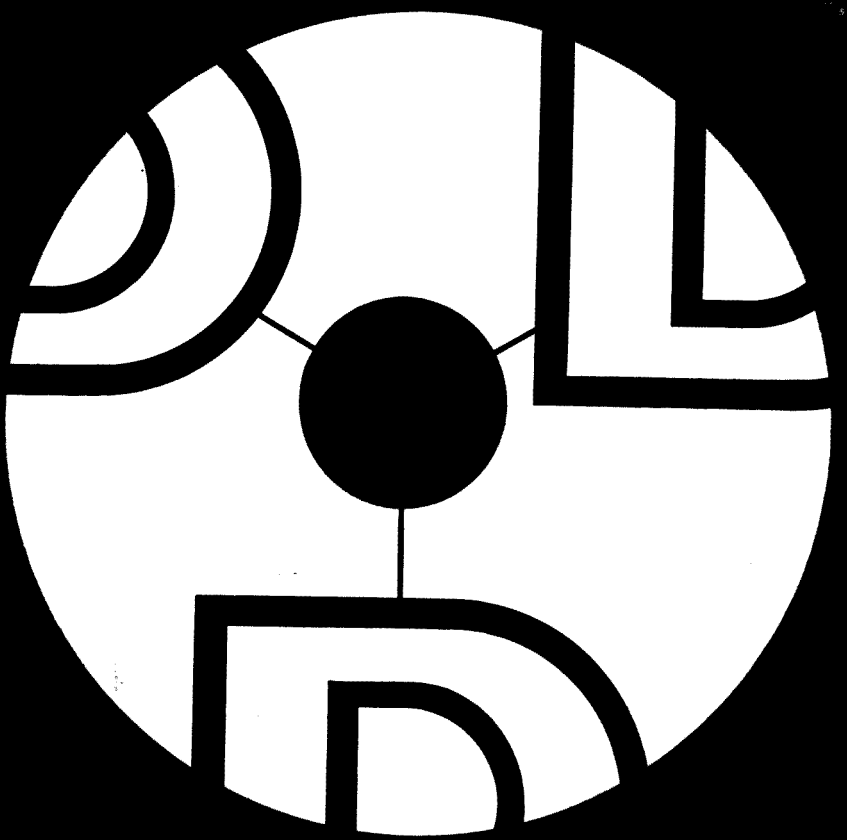

SUMMARIES OF PAPERS PUBLISHED IN ANALYTICA CHIMICA ACTA

Vol. 45, No. 3, May 1969

DETERMINATION OF TRACES OF LITHIUM, BERYLLIUM OR PHOSPHORUS BY X-RAY ANALYSIS

New indirect X-ray methods have been developed for the determination of traces of lithium, beryllium and phosphorus. In the lithium method which is suitable for 1–100 μg Li, 50 μg of ammonium ion, 100 μg of sodium and 1 mg of K, Rb or Cs can be tolerated; larger amounts require an extraction process. Other interfering ions may require a cation-exchange separation. For the determination of beryllium (0–40 μg), there are very few interferences when beryllium is precipitated as phosphate in the presence of EDTA. For the determination of phosphorus (1–40 μg), beryllium is used as precipitant.

C. L. LUKE,
Anal. Chim. Acta, 45 (1969) 365–376

DETERMINATION OF TRACES OF BORON OR SODIUM BY X-RAY ANALYSIS

New indirect X-ray methods have been developed for the determination of 0–40 μg of boron or sodium. Methods are suggested for the removal of interfering elements.

C. L. LUKE,
Anal. Chim. Acta, 45 (1969) 377–381

LIQUID ION-EXCHANGE ELECTRODES AS END-POINT DETECTORS IN COMPLEXIMETRIC TITRATIONS. DETERMINATION OF CALCIUM AND MAGNESIUM IN THE PRESENCE OF SODIUM

PART I. THEORETICAL CONSIDERATIONS

Chemical and potentiometric titration curves are derived based on theoretical assumptions, for EGTA and DCTA as titrants. The problem of locating the equivalence point on practical titration curves is discussed. Linear extrapolation methods are outlined that should enable this point to be determined more accurately. It is concluded that complexiметric titrations monitored with liquid ion-exchange electrodes such as the Orion calcium activity electrode and divalent electrode should be useful for the analysis of calcium and magnesium in natural waters.

M. WHITFIELD AND J. V. LEYENDEKKERS,
Anal. Chim. Acta, 45 (1969) 383–398

LIQUID ION-EXCHANGE ELECTRODES AS END-POINT DETECTORS IN COMPLEXIMETRIC TITRATIONS

PART II. DETERMINATION OF CALCIUM AND MAGNESIUM IN THE PRESENCE OF SODIUM

A calcium-selective electrode was used to monitor EGTA and DCTA titrations of aqueous mixtures of calcium, magnesium and sodium salts. The solution concentrations were selected to span the range of natural waters, and the results were analysed statistically. The pattern of titration curves observed with changing solution composition agreed qualitatively with that predicted theoretically, but the overall potential drop was usually lower than that predicted; end-points were determined by graphical and numerical methods. The technique is suitable for the determination of calcium and magnesium in sea water with an estimated accuracy of 0.5%.

M. WHITFIELD, J. V. LEYENDEKKERS AND J. D. KERR,
Anal. Chim. Acta, 45 (1969) 399–410

SYSTEMATIC TITRATION ERRORS IN REDOX TITRATIONS

Exact and approximate expressions have been derived for the calculation of systematic titration errors in redox titrations. Some numerical examples are calculated, and it is shown that the proposed expressions yield higher values for the titration errors than are given by some recently suggested expressions.

U. A. TH. BRINKMAN,
Anal. Chim. Acta, 45 (1969) 411–416

CONTROLLED-POTENTIAL COULOMETRIC DETERMINATION OF AMERICIUM

Controlled-potential coulometry has been studied as a means for the precise and accurate determination of americium. Americium is chemically oxidized to the hexavalent state, and then coulometrically reduced from Am(VI) to Am(V) at a platinum electrode controlled at 1.05 V *vs.* S.C.E. The results of repetitive analysis of standard solutions prepared from high-purity americium-243 dioxide agree within a few tenths percent with standard values for 0.4–1.3 mg of americium.

J. R. STOKELY, JR. AND W. D. SHULTS,
Anal. Chim. Acta, 45 (1969) 417–424

THE SPECTROFLUORIMETRIC DETERMINATION OF GALLIUM, INDIUM AND ZINC WITH 2,2′-PYRIDYLBENZIMIDAZOLE

The spectrofluorimetric determination of nanogram amounts of gallium, indium and zinc with 2,2′-pyridylbenzimidazole is described. Zinc can be determined in the range 15–800 ng/ml, gallium 70–700 ng/ml and indium 110–1,000 ng/ml, with standard deviations of 1.1%, 4.8% and 2.3%, respectively. Interferences can be avoided by extraction, reduction or precipitation procedures. Methods are proposed for the determination of zinc in the presence of gallium and indium, and for gallium or indium in the presence of zinc.

L. S. BARK AND A. RIXON,
Anal. Chim. Acta, 45 (1969) 425–432

Elsevier Titles in Chemistry

INORGANIC CHEMISTRY

A Guide to Advanced Study
Third, completely revised edition

by **R. B. Heslop** and **P. L. Robinson**

6×9″, viii+774 pages, 155 tables, 400 illus., 227 lit. ref., 1967, Dfl. 32.50, 65s.

Contents: Modern inorganic chemistry. The atomic nucleus: genesis of the elements. Radiochemistry. Electronic structures of atoms. The periodic table. Valency; nature and classification of chemical bonding. Structure and shape of molecules. Bonding and structure in compounds of non-transition elements. Bonding in transition-metal complexes. The solid state. Oxidation-reduction: redox reactions. Acids and bases. Hydrogen. The hydrides. The noble gases. The alkali metals. Beryllium, magnesium and the alkaline earth metals. Boron and aluminium. Gallium, indium and thallium. Carbon and silicon. Organometallic compounds. Germanium, tin and lead. Nitrogen and phosphorus. Arsenic, antimony and bismuth. Oxygen, sulphur, selenium, tellurium and polonium. The oxides. Peroxides and peroxo-compounds. The halogens. The halides and pseudohalides. The transition metals. Complex or co-ordination compounds and ions. Substitution reactions of metal complexes. The lanthanides, scandium and yttrium The actinides. Titanium, zirconium and hafnium. Vanadium, niobium and tantalum. Chromium, molybdenum and tungsten. Manganese, technetium and rhenium. Iron, cobalt and nickel. The platinum metals. Copper, silver and gold. Zinc, cadmium and mercury. Index.

INTRODUCTION TO THE ATOMIC NUCLEUS

Volume 3 in a collection of monographs on "*Topics in Inorganic and General Chemistry*" edited by P. L. Robinson

by **J. G. Cuninghame**

5½×8½, xi+220 pages, 3 tables, 58 illus., 170 lit. refs., 1964, Dfl. 15.00, 35s.

Contents: Historical introduction. General definitions and properties. Nuclear forces. Stable nuclides. Radioactivity. Nuclear models. Nuclear reactions. Fission. Alpha-decay. Beta-decay. Gamma-emission. Interaction of particles and rays with matter. Index.

INTRODUCTION TO NUCLEAR CHEMISTRY

by **D. J. Carswell**

5½×8½″, ix+279 pages, 23 tables, 69 illus., 1967, Dfl. 32.50, 70s.

Contents: The development of nuclear chemistry. Fundamental particles and nuclear structure. Nuclear reactions and radioactivity. Properties of nuclear radiations. The detection and measurement of nuclear radiation. Nuclear instrumentation. Radiation chemistry. Isotope measurement and separation methods. Charged particle accelerators, neutron sources, production and properties of the actinide elements. Uses of isotopes. Experimental nuclear chemistry. Index.

RADIOCHEMICAL SURVEY OF THE ELEMENTS

Principal Characteristics and Applications of the Elements and their Isotopes

by **M. Haïssinsky** and **J.-P. Adloff**

6×9″, ix+177 pages, 1965, Dfl. 32.50, 75s.

Contents: Introduction. The elements in alphabetical order. Element 102. Element 104.

THE STRUCTURE OF INORGANIC RADICALS

An Application of Electron Spin Resonance to the Study of Molecular Structure

by **P. W. Atkins** and **M. C. R. Symons**

6×9″, x+280 pages, 57 tables, 74 illus., 357 lit. refs., 1967, Dfl. 60.00, £7.0.0.

Contents: Introduction. An introduction to electron spin resonance. Formation and trapping of radicals. Trapped and solvated electrons. Atoms and monatomic ions. Diatomic radicals. Triatomic radicals. Tetra-atomic radicals. Penta-atomic radicals. Summary and conclusions.
Appendices: The language of group theory. The spin hamiltonian. Calculation of *g*-values. Determination of spin-density distribution and bond angles. Analysis of electron spin resonance spectra. Index.


Elsevier Publishing Company

Amsterdam London New York

THE SOLVENT EXTRACTION OF ALKALI METAL TETRAPHENYLBORATES

The extraction of sodium and small amounts of potassium, rubidium and cesium from aqueous solutions containing sodium tetraphenylborate (TPB), sodium perchlorate and perchloric acid has been studied for nitromethane, nitroethane, nitrobenzene, methyl isobutyl ketone and tributyl phosphate. Nitromethane gives the highest distribution ratio (org/aq) for the perchlorates, and nitrobenzene gives the highest distribution ratio and separation factor for the tetraphenylborates. Most distribution data could be explained by assuming that the tetraphenylborates were fully dissociated in both phases. The equilibrium constants and distribution ratios increase in the order sodium<potassium<rubidium<cesium. The distribution ratio of small amounts of the heavy alkali metal ions will thus not be appreciably influenced by the concentration of sodium tetraphenylborate, but will decrease on the addition of sodium chloride or perchlorate. The effect of perchloric acid can be explained by irreversible acid hydrolysis of the tetraphenylborate ion.

T. Sekine and D. Dyrssen,
Anal. Chim. Acta, 45 (1969) 433–446

STUDIES WITH DITHIZONE. PART XVII. THE EXTRACTION CONSTANTS OF ORGANOMERCURY(II) DITHIZONATES

Extraction constants are reported for the distribution of fourteen different organomercury(II) dithizonates, RHg(HDz), between carbon tetrachloride and aqueous phases of constant ionic strength containing complexing halide ions.

H. M. N. H. Irving and A. M. Kiwan,
Anal. Chim. Acta, 45 (1969) 447–455

AN INDIRECT GRAVIMETRIC–AMPEROMETRIC DETERMINATION OF HIGH CALCIUM CONTENTS WITH EDTA

(in French)

A gravimetric–amperometric determination of high percentages of calcium is proposed. An exactly weighed amount of EDTA, slightly less than the theoretical amount, is added and the determination is then completed amperometrically. The proposed method is more precise than direct amperometric titration for large amounts of calcium; relative errors in determining 50 mg Ca are: $\pm$ 1–2‰ for the proposed method, $\pm$7‰ for the direct method. A theoretical study of the errors involved confirms the greater precision of the proposed method at the 50-mg Ca level.

W. Haerdi, D. Monnier and A. Daïna,
Anal. Chim. Acta, 45 (1969) 457–466

ADVANCES IN COLLOID AND INTERFACE SCIENCE

An international journal devoted to experimental and theoretical developments in interfacial and colloidal phenomena and their implications in chemistry, physics, technology and biology

Contents of Volume 1

Contents of the first two issues of Volume 2

Subscription price:
Dfl. 75.00, £ 8.14.6 or $ 21.00 per volume of four quarterly issues plus postage Dfl. 3.50, 8s. 3d., or $1.00.

Orders for single issues or full subscriptions may be sent to your regular bookseller or to Elsevier Publishing Company, P.O. Box 211, Amsterdam, The Netherlands.

Elsevier Publishing Company Amsterdam London New York

210 E

THE USE OF THERMOGRAVIMETRIC ANALYSIS IN KINETIC STUDIES OF THE THERMAL DEGRADATION OF POLYMERS

Various thermogravimetric methods can be used to determine the activation energy and the rate constant of the pyrolysis of compounds, when only one mechanism is involved or when several mechanisms occur simultaneously with a relative extent which does not depend much on the temperature. Although the experimental results can be explained by simple kinetic theory, the mechanism of the pyrolysis is in most, if not all, cases much more complicated than is indicated by the thermogravimetric results. This is certainly true in the pyrolysis of polyethyleneglycol adipate. This does not reduce the interest of thermogravimetric analysis but illustrates the great difficulties which can be encountered in accounting for thermogravimetric measurements.

F. FARRÉ-RIUS, J. HURET, M. PUYO AND G. GUIOCHON,
Anal. Chim. Acta, 45 (1969) 467–483

THE SYNTHESIS OF SOME NITRATED POLYAMINE RESINS AND THEIR USE AS ION-EXCHANGERS FOR THE ALKALI AND ALKALINE EARTH METALS

Five polyamines were synthesized by the condensation of an amine with its corresponding amine hydrochloride salt and the polyamines were nitrated, averaging 1 nitro group per monomer unit. The nitro-polyamines were found to be weak cation-exchangers. The resins did not have the same selectivity towards potassium as the exchanger synthesized by SKOGSEID, who incorporated dipicrylamine onto a polystyrene resin.

C. A. JANICKI AND C. E. MOORE,
Anal. Chim. Acta, 45 (1969) 485–491

POTENTIOMETRIC TITRATIONS WITH ION-EXCHANGING MEMBRANE ELECTRODES

PART V. TITRATION CURVES FOR PRECIPITATION TITRATIONS INVOLVING IONS OF HIGHER VALENCIES

Theoretical titration curves were calculated for the cases when univalent and bivalent or univalent and trivalent ions are present in the titration system. As was found previously, the factor that primarily determines the shape of the titration curves for a given combination of ionic valencies is the ratio of the diffusion coefficients of the counter-ions present in the solution to be titrated and in the titrant. The experimental results obtained with solutions containing univalent and bivalent ions are in accordance with the theoretical expectations. The use of a simplified method for the calculation of the intramembrane diffusion potential is justified.

F. P. IJSSELING AND E. VAN DALEN,
Anal. Chim. Acta, 45 (1969) 493–503

THE ELECTROMETRIC DETERMINATION OF HYPOBROMITE AND BROMITE

(in German)

Factors influencing the determination of hypobromite and bromite are discussed. A simultaneous determination of hypobromite and bromite is possible by chronopotentiometry with a gold electrode or by conventional polarography.

H. FUCHS AND R. LANDSBERG,
Anal. Chim. Acta, 45 (1969) 505–510

SUBMICRO METHODS OF ORGANIC ANALYSIS

by R. BELCHER
Professor of Analytical Chemistry,
The University of Birmingham, Great Britain

6 × 9″, ix + 173 pages, 12 tables, 35 illus., 186 lit. refs., 1966, Dfl.27.50, 65s.

Contents: 1. Introduction. 2. The balance. 3. General apparatus. 4. The determination of nitrogen. 5. Carbon and hydrogen. 6. Chlorine. 7. Bromine and iodine. 8. Fluorine. 9. Sulphur. 10. Phosphorus and arsenic. 11. Carboxyl groups. 12. Organic bases in non-aqueous media. 13. Alkoxyl and N-methyl groups. 14. Acetyl groups. 15. The carbonyl group. 16. Olefinic unsaturation. 17. Oxidation with periodate. 18. The determination of nitro and nitroso groups. 19. Thiol groups. 20. The cryoscopic determination of molecular weight. Index.

TECHNIQUES OF OSCILLOGRAPHIC POLAROGRAPHY

Second Edition, completely revised and enlarged

by R. KALVODA
Institute of Polarography, Czechoslovak Academy of Sciences, Prague, Czechoslovakia
with a preface by Professor J. Heyrovský

6 × 9″, 214 pages, 3 tables, 90 illus., 263 lit. refs., 1965, Dfl. 30.00, 70s.

Contents: Preface (J. Heyrovský); Author's Preface; 1. Introduction. 2. Examples of application of the oscillopolarographic method. 3. Practical oscillopolarographic exercises. 4. Maintenance of apparatus and construction of auxiliary electrical circuits. Index.

TABLE OF META-STABLE TRANSITIONS FOR USE IN MASS SPECTROMETRY

by J. H. BEYNON, R. A. SAUNDERS AND A. E. WILLIAMS
Research Department, Imperial Chemical Industries Ltd.,
Manchester, Great Britain

9½ × 6½″, xix + 392 pages, 1965, Dfl. 50.00, £6.10.0.

These tables are intended to make it easy to determine the ionic reaction which gives rise to any meta-stable peak in a mass spectrometer, and will prove indispensable to any laboratory possessing this equipment. The introduction is given in English, German, French and Russian, to make the tables more generally useful.

STATIONARY PHASE IN PAPER AND THIN-LAYER CHROMATOGRAPHY

Second International Symposium organized by the Chromatography Group of the Czechoslovak Chemical Society, at Liblice
by K. MACEK AND I.M.HAIS

7 × 10″, 358 pages, 69 tables, 135 illus., 494 lit. refs., 3 coloured plates, 1965, Dfl. 47.50, £5.15.0.

Contents: List of participants in the discussion. Introduction. Opening speech. I. Chromatography papers. II. Thin-layer materials. III. Stationary liquids and adsorbents in paper chromatography. IV. Stationary liquids and impregnations for thin layers. V. General problems of the stationary phase. Discussion. Closing remarks. Author index. Subject index.


Elsevier Publishing Company

P.O. Box 211, Amsterdam

Ripple Rd., Barking, Essex, London

52 Vanderbilt Ave. N.Y. 10017, New York

A SCHEME FOR THE SEPARATION OF CATIONS BY SOLVENT EXTRACTION

(in German)

A simple and rapid cation separation scheme has been developed, covering about 60 cations, many of them being quantitatively separable in the micro- and milligram ranges. By analogy with the classical hydrogen sulphide–ammonia separation process, the cations are divided with decreasing acidity by BPHA and DDDC extraction into five main groups. In group I the transition elements of groups 4 to 7 of the periodic system are extracted from 2 *N* mineral acidic solution, as BPHA complexes; in group II, from the same acid concentration, cations of the hydrogen-sulphide group are extracted by DDDC; in group III, from neutral solution, cations of the ammonia and ammonium sulphide group are extracted by BPHA and DDDC; and in group IV, from 1 *N* ammoniacal solution are extracted the alkaline earths as BPHA complexes. For further separation, the differing reextractability of these chelate complexes dissolved in chloroform with solutions of reagents is utilised.

H. FÖRSTER AND K. SCHWABE,
Anal. Chim. Acta, 45 (1969) 511–523

COLORIMETRIC DETERMINATION OF ORGANIC PEROXIDES

(Short Communication)

J. BELISLE,
Anal. Chim. Acta, 45 (1969) 525–526

A RAPID METHOD FOR CALIBRATION OF MICROPIPETS

(Short Communication)

J. F. GOGGINS AND J. M. TANZER,
Anal. Chim. Acta, 45 (1969) 526–527

DETERMINATION OF PLUTONIUM BY CONTROLLED-CURRENT COULOMETRY

(Short Communication)

J. R. STOKELY, JR. AND W. D. SHULTS,
Anal. Chim. Acta, 45 (1969) 528–532

SEPARATION OF THE ACIDIC SULFIDES OF ARSENIC, ANTIMONY AND TIN FROM MIXTURES WITH BASIC SULFIDES BY MEANS OF ALKALINE MONOCHLOROACETATE

(Short Communication)

A. CALDAS,
Anal. Chim. Acta, 45 (1969) 532–534

DIFFRACTION OF X-RAYS BY CHAIN MOLECULES

by B. K. VAINSHTEIN

Foreword by M. F. PERUTZ

6 x 9″, xiii + 414 pages, 3 tables, 258 illus., 256 lit.refs., 1966, Dfl. 65.00, £7.10.0.

Contents: 1. Principles of the theory of X-ray diffraction. 2. Structures of chain molecules and assemblies. 3. Diffraction by an isolated chain molecule. 4. Scattering intensity and structure of object. 5. Properties of the distribution and interference functions. 6. Diffraction by assemblies of parallel chain molecules. 7. Diffraction by assemblies with nonparallel packing of chain molecules and by amorphous polymers. Subject index.

INFRA RED INSTRUMENTATION AND TECHNIQUES

by A. E. MARTIN

5½ x 8½″, x + 180 pages, 13 tables, 94 illus., 86 lit.refs., 1966, Dfl. 32.50, 75s.

Contents: 1. Historical. 2. Modern infra-red spectrometers. 3. Miscellaneous instruments. 4. Interferometric spectrometers. 5. Accessories. 6. Experimental methods and techniques. Index.

ENERGY TRANSFER IN RADIATION PROCESSES

Chemical, Physical and Biological Aspects

Proceedings of the International Symposium held in Cardiff, 1965

edited by G. O. PHILLIPS

5½ x 8½″, xvi + 182 pages, 10 tables, 81 illus., 273 lit.reft., 1966, Dfl. 32.50, 75s.

Contents: Introductions to the sections by F. S. Dainton, G. F. J. Garlick and Tikvah Alper. Invited papers by E. J. Bowen, Jett C. Arthur, N. Riehl, R. Mason. Contributed papers.

MASS SPECTROMETRIC ANALYSIS OF SOLIDS

edited by A. J. AHEARN

5½ x 8½″, viii + 175 pages, 13 tables, 46 illus., 242 lit.refs., 1966, Dfl. 30.00, 70s.

Contents: 1. Introductory survey. 2. The production of ions from solids. 3. Photographic emulsions as ion detectors in quantitative mass spectrography. 4. Analysis of special samples. 5. Mass spectrographic microprobe analysis. Subject index.

RADIOCHEMICAL SURVEY OF THE ELEMENTS

Principal characteristics and applications of the elements and their isotopes

by M. HAISSINSKY
and
J.-P. ADLOFF

6 x 9″, ix + 177 pages, 1965, Dfl. 32.50, 75s.

Contents: Introduction. The elements in alphabetical order. Element 102. Element 104.

Elsevier Publishing Company

P.O. Box 211, Amsterdam

Ripple Rd., Barking, Essex, London

52 Vanderbilt Ave. N.Y. 10017, New York

EFFECT OF SUBSTITUENTS ON DISSOCIATION CONSTANTS OF PICRAMINE REAGENTS CONTAINING THE *o,o'*-DIHYDROXYAZO GROUP

(Short Communication)

A. A. MUK AND M. B. PRAVICA,
Anal. Chim. Acta, 45 (1969) 534–538

BEAM CENTERING IN A NEUTRON GENERATOR

(Short Communication)

L. KOSTA, F. CVELBAR AND V. RAMŠAK,
Anal. Chim. Acta, 45 (1969) 539–541

SOME OBSERVATIONS ON THE DETERMINATION OF IODIDE BY ITS CATALYTIC EFFECT ON THE DECOMPOSITION OF THE MONOTHIOCYANATE COMPLEX OF IRON(III)

(Short Communication)

J. M. OTTAWAY, C. W. FULLER AND W. B. ROWSTON,
Anal. Chim. Acta, 45 (1969) 541–544

AN IMPROVED TITRIMETRIC METHOD FOR THE DETERMINATION OF URANIUM: OXYGEN RATIOS

(Short Communication)

S. R. DHARWADKAR AND M. S. CHANDRASEKHARAIAH,
Anal. Chim. Acta, 45 (1969) 545–546

THE DETERMINATION OF SULPHIDE IN WATERS BY AN AUTOMATIC METHOD

(Short Communication)

P. CASAPIERI, R. SCOTT AND E. A. SIMPSON,
Anal. Chim. Acta, 45 (1969) 547–550

THE MASS SPECTRA OF ORGANIC MOLECULES

by J. H. Beynon, R. A. Saunders and A. E. Williams, Research Department, Imperial Chemical Industries Ltd., Manchester, Great Britain

7 x 10″, ix + 510 pages, 20 tables, 181 illus., 547 lit. refs., 1968, Dfl. 97.50

Contents: 1. The principles and methods of mass spectrometry. 2. Types of ions in the mass spectra of organic compounds. 3. The mass spectra of hydrocarbons. 4. The mass spectra of oxygenated compounds. 5. The mass spectra of nitrogen compounds. 6. The mass spectra of sulphur compounds. 7. The mass spectra of halogenated compounds. 8. The mass spectra of boron compounds. 9. The mass spectra of phosphorus compounds. 10. The mass spectra of silicon compounds. 11. Examples of structure determination from mass spectra. Appendix 1. Peaks commonly encountered in the mass spectra of organic compounds. Appendix 2. The masses and abundances of nuclides commonly encountered in the mass spectra of organic compounds. References. Indexes.

MASS SPECTROMETRIC ANALYSIS OF SOLIDS

edited by A. J. Ahearn, Member of Technical Staff, Bell Telephone Laboratories, Inc., Murray Hill, New Jersey, U.S.A.

5½ x 8½″, viii + 175 pages, 13 tables, 46 illus., 242 lit. refs., 1966, Dfl. 30.00

Contents: 1. Introductory survey. 2. The production of ions from solids. 3. Photographic emulsions as ion detectors in quantitative mass spectrography. 4. Analysis of special samples. 5. Mass spectrographic microprobe analysis. Indexes.

ATOMIC-ABSORPTION SPECTROSCOPY

and Analysis by Atomic-Absorption Flame Photometry

by J. Ramírez-Muñoz, Principal Applications Chemist at Beckman Instruments Inc. and Scientific Research Collaborator of the C.S.I.C., Spain

6 x 9″, xii + 493 pages, 23 tables, 156 illus., 950 lit. refs., 1968, Dfl. 80.00

Contents: *Part I: Fundamentals.* 1. Origins of the method and nomenclature. 2. General principles and characteristics. 3. Absorption and emission. 4. The literature of atomic-absorption spectroscopy. 5. Theory. *Part II: Instrumental Systems.* 6. Instrumental systems. 7. Emission systems. 8. Absorption system. 9. Selection system. 10. Photometric system. 11. Instruments. *Part III: Range and Limitations of Atomic Absorption Methods.* 12. Determinable elements. Choice of lines. 13. Sensitivity. 14. Limitations in atomic absorption. *Part IV: Experimental Methods.* 15. Experimental process. 16. Standard solutions. 17. Preparation of the sample. 18. Experimental measurements and calibration. *Part V: Applications.* 19. Applications. Appendix. Bibliography.

Still available:

MASS SPECTROMETRY AND ITS APPLICATIONS TO ORGANIC CHEMISTRY

by J. H. Beynon

7 x 10″, xii + 640 pages, 11 tables, 185 illus., 2213 lit. refs., 1960, reprinted 1964 and 1967, Dfl. 85.00

TABLE OF META-STABLE TRANSITIONS FOR USE IN MASS SPECTROMETRY

by J. H. Beynon, R. A. Saunders and A. E. Williams

10 x 7″, xix + 392 pages, 1965, Dfl. 50.00

MASS AND ABUNDANCE TABLES FOR USE IN MASS SPECTROMETRY

by J. H. Beynon and A. E. Williams

10 x 7″, xxi + 570 pages, 1963, Dfl. 60.00


Elsevier Publishing Company Amsterdam London New York

408 E

Analytica Chimica Acta
Elsevier Publishing Company, Amsterdam
Printed in The Netherlands

DETERMINATION OF TRACES OF LITHIUM, BERYLLIUM OR PHOSPHORUS BY X-RAY ANALYSIS

C. L. LUKE
Bell Telephone Laboratories, Incorporated, Murray Hill, N. J. 07904 (U.S.A.)
(Received December 10th, 1968)

It has seemed desirable to develop suitable X-ray methods for the determination of traces of lithium, beryllium or phosphorus to supplement the methods commonly used for these elements. Investigations have shown that new indirect X-ray methods[1] for the determination of 1–100 μg of lithium or 1–40 μg of beryllium and a coprecipitation–X-ray method[2] for the determination of 1–40 μg of phosphorus are possible.

DETERMINATION OF LITHIUM

In the first part of this series on indirect X-ray analysis, methods were described for the determination of traces of fluorine and sulfur[1]. The same approach has been used in the present work, namely to precipitate lithium as a stoichiometric inorganic compound which contains a heavy element that can be determined by X-ray analysis. Thus, it has been shown that traces of lithium can be quantitatively precipitated as arsenate or phosphate and then determined by measuring the amount of arsenic or phosphorus present in the precipitate with an X-ray spectrograph[2].

Reagents

Standard lithium solutions. Dissolve 0.611 g of lithium chloride in water and dilute to 100 ml (1 mg Li/ml). Prepare solutions containing 100 μg Li/ml and 10 μg Li/ml by volumetric dilution.

Arsenate–ethanol solution. Add 2 drops of a 1% (w/v) solution of phenolphthalein in ethanol to 40 ml of a 0.2% (w/v) solution of potassium dihydrogen arsenate. Add 160 ml of ethanol, neutralize to the red color with a 10% (w/v) solution of potassium hydroxide and add 0.1 ml in excess.

Phosphate–ethanol solution. Mix 60 ml of a 0.2% (w/v) solution of trisodium phosphate dodecahydrate with 140 ml of ethanol.

Preparation of calibration graphs

Transfer aliquots of standard lithium solutions covering the range of 0–10 μg or 0–100 μg of lithium to 50-ml beakers. Add an aliquot containing 20 μg of lithium to each of the beakers. Evaporate the solutions just to dryness on a low temperature (150°) hot plate. Cool, add 10 ml of arsenate–ethanol or phosphate–ethanol solution and allow to stand for 5 min with occasional swirling. Police the beaker thoroughly and filter on a 2 μ, carbon-stained, PVC disk[1]. Allow the solution to drain completely

but do not wash the beaker or filter funnel. Dry the disk thoroughly and then take a 10-sec count on an X-ray spectrograph at the wavelength of the Kα line of arsenic in a helium atmosphere using a lithium fluoride crystal and a tungsten target; or take a 100-sec count at the wavelength of the Kα line of phosphorus in a helium atmosphere using a PET crystal and a chromium target[2]. Prepare suitable calibration graphs.

Analysis of sample

If the sample to be analyzed consists only of alkali chlorides, dissolve in water and evaporate the solution just to dryness in a 150-ml beaker on a low hot plate and finally, if more than about 2 mg of salt is present, in a 100° oven to prevent decrepitation or creeping up the walls of the beaker. Cool and proceed to the acetone extractions described subsequently.

Otherwise, isolate the lithium from organic matter and from the bulk of the matrix cations or anions of the sample by suitable separations. Then evaporate the acid solution containing the lithium to a volume of 0.25 ml in a 50-ml beaker. Avoid evaporation to dryness otherwise hydrolysis of certain salts may occur. Add 5 ml of water, swirl and warm to dissolve all the salts present and then pour into a water-equilibrated cation-exchange column and allow to drain. Wash the beaker into the column with an additional 5 ml of water and allow to drain. Discard the effluent.

The column used in the present work was made from a cut-down 50-ml buret and the liquid was introduced through a funnel that extended down to near the top of the resin bed. The latter was supported and covered with a layer of glass wool and measured 1 × 10 cm. The resin used was Dowex 50-X8 (100–200 mesh, hydrogen form). The elution rate was about 1.5 ml/min when 1+9 hydrochloric acid was used as the eluent.

If the sample solution added to the column contains no cations whose affinity for the resin is low, nor anions other than chloride, elute the lithium with four successive 10-ml portions of 1+9 hydrochloric acid, catching the effluent in a 250-ml beaker. Otherwise elute with 10 ml of water, discard the effluent and then elute the lithium. Evaporate the collected effluent on a low hot plate just to dryness and cool.

Add 10 ml of acetone down the walls of the beaker so as not to loosen the precipitate. Swirl gently 2 or 3 times and then repeat the swirling once a minute for 5 min. After the 6th swirling, carefully decant the acetone completely into a 50-ml beaker while retaining all of the salt in the first beaker. Add 1 ml of 1+9 hydrochloric acid to the first beaker, swirl to dissolve salts and evaporate to dryness. Cool and repeat the acetone extraction, collecting the extract in the second beaker. If the sample being extracted contains over 2 and less than 100 mg of alkali salt, dissolve and extract a third time. If still larger amounts of alkali salts are present, one or more additional extractions will probably be required. If it is suspected that more than about 50 μg of ammonium ion is present at this point, evaporate the combined acetone extracts just to dryness under an air jet on a low hot plate and repeat the acetone extraction. Finally, in any event, add an aliquot containing 20 μg of lithium to the last acetone extract or extracts and again evaporate to dryness. Then add 10 ml of arsenate–ethanol or phosphate–ethanol solution and proceed as directed in *Preparation of calibration graphs.*

Discussion

Attempts to precipitate the lithium as a complex periodate[3] or as $LiKFeIO_6$[4] were not successful. However, tests showed that traces of lithium could be precipitated with tribasic potassium arsenate or sodium phosphate from 80% or 70% ethanol solution, respectively. Sodium phosphate is not entirely soluble in 80% ethanol solution. The lithium precipitate could then be filtered on a PVC disk and lithium determined by measuring the arsenic or phosphorus present with an X-ray spectrograph. Alternatively, of course, if an X-ray spectrograph is not available, it should be possible to filter on Millipore paper, destroy the paper by wet oxidation and then determine the arsenic or phosphorus present by the spectrophotometric molybdenum blue method. Analysis of the lithium arsenate precipitate has shown that it consists of $Li_2KAsO_4 \cdot H_2O$. No attempt was made to characterize the lithium phosphate precipitate.

The X-ray count for arsenic or phosphorus obtained with a given amount of lithium decreases somewhat as the arsenate–ethanol solution ages and a precipitate is sometimes seen to form in the phosphate–ethanol solution on standing, which suggests that the reagent solutions should not be kept too long. Because of this and because the counts obtained for arsenic and, to a lesser extent, for phosphorus vary somewhat from batch to batch of reagent, it will be best, where high accuracy is desired, to prepare new calibration disks each time an analysis is to be made. The pH of the arsenate or phosphate–ethanol solution is about 12.5.

There does not appear to be much to choose between the arsenate and phosphate methods for lithium. However, it is true that the arsenate method is more sensitive and that the count obtained for arsenic is influenced less by variations in the flow of the helium or by the presence of water in the disks. Incidentally, it follows from this that when the phosphate method is used, it is imperative that the disks be thoroughly dry at the time of the X-ray analysis. Also it would appear desirable to use the arsenate method if arsenate is present at the time of precipitation or the phosphate method if phosphate is present.

The precipitation of the lithium as arsenate or phosphate is increasingly incomplete as the amount of lithium present decreases. However, if 20 μg of lithium is added to all of the samples in the calibrations and analyses the calibration graphs obtained are reasonably linear and as little as 1 μg of lithium can be precipitated and determined (Table I).

Interference of the alkali and the alkaline earth elements. As much as 1 mg of potassium, rubidium and cesium, 100 μg of sodium, or 50 μg of ammonium ion, all

TABLE I

TYPICAL CALIBRATION GRAPH DATA FOR LITHIUM

Lithium added (μg)	*Counts/sec*		*Lithium added (μg)*	*Counts/sec*	
	Arsenate	*Phosphate*		*Arsenate*	*Phosphate*
0	2380	264	10	4357	474
1	2528	284	25	7400	728
2.5	2833	313	50	12261	1059
5	3358	364	75	16526	1304
7.5	3900	420	100	21223	1505

as chlorides, causes no interference in the precipitation and determination of lithium as arsenate or phosphate. Larger amounts of sodium or potassium cause high results and larger amounts of ammonium ion cause low results. The four common alkaline earths tend to precipitate as arsenate or phosphate. The interference of calcium and magnesium is severe but if no more than about 20 μg of barium or strontium is present, good results for lithium can be obtained. However, in general, it will be necessary to completely remove these four alkaline earths before analysis for lithium. Beryllium chloride becomes very insoluble on evaporation to dryness and occludes appreciable amounts of lithium. For this reason beryllium must be removed before attempting the lithium analysis.

BROWN AND REEDY[5] have shown that lithium can be isolated from the other alkalis and ammonium ion by one or more extractions of the mixed chlorides with acetone. Experience with this method has shown that the separation is good provided that the salts are completely dry at the time of the extraction, but that the filtration recommended by these workers is not necessary. Because of the severe interference of ammonium ion it is desirable, when two or more extractions have been made to separate the lithium from ammonium chloride, to make an additional acetone extraction on the residue from the evaporation of the acetone extracts.

Attempts to remove ammonium chloride by volatilization were not successful since, no matter how carefully the temperatures were controlled, loss of lithium chloride by volatilization was noted[6]. However, if the temperature during volatilization does not exceed 175°, appreciable amounts of ammonium acetate can be safely removed. Volatilization losses of lithium have also been noted when organic matter has been destroyed with nitric and perchloric acids and the acids are subsequently removed by evaporation to dryness. Hence in such evaporations the temperature should be as low as possible.

The acetone extraction separation used for the removal of the alkalis serves equally well for the removal of barium or strontium but small amounts of magnesium and appreciable amounts of calcium accompany the lithium. Nevertheless, if precautions are taken to cool the dried salts rapidly before the extraction so as to prevent takeup of water and also to swirl the solutions very gently during the acetone extraction, it is possible to separate the lithium from all but traces of barium, strontium and magnesium and from much of the calcium. In fact, good recoveries of traces of lithium in the presence of up to 1 mg of barium, strontium and magnesium can be had. The acetone extraction fails in the presence of calcium and beryllium and hence these elements must be removed by cation-exchange separation. Typical data on the determination of traces of lithium in mixtures with alkalis or alkaline earths, by means of the acetone extraction separations are shown in Table II.

Lithium perchlorate can be extracted with 1,4-dioxane but some of the other alkalis and the alkaline earths tend to accompany it. Lithium sulfate can be extracted with 80% ethanol and readily separated from calcium but magnesium and some of the other alkalis accompany it. Moreover, sulfate cannot be tolerated in the precipitation of the lithium as arsenate or phosphate.

Interference of other elements. As much as 100 μg of such elements as Au, Pt, Ru, Rh, Os, Ir, Re, Tl(I), Pb, Ga, Al, Zn, Hg(II), Sb(V), and Sn(IV) do not interfere in the determination of 50 μg of lithium by the arsenate or phosphate methods. Palladium and the 35 or more elements that precipitate as hydroxide[7] all cause

TABLE II

DETERMINATION OF TRACES OF LITHIUM IN ALKALI AND ALKALINE EARTH CHLORIDES BY THE ARSENATE METHOD

Element added (mg)	*Li added (μg)*	*Li found (μg)*	*Element added (mg)*	*Li added (μg)*	*Li found (μg)*
1 K	50.0	50	1 NH_4	10.0	11
100 K	10.0	10	1 NH_4	50.0	49
100 K	50.0	50	100 NH_4	10.0	10
1 Na	50.0	49	100 NH_4	50.0	50
100 Na	10.0	10	1 Ba	10.0	11
100 Na	50.0	49	1 Ba	50.0	49
1 Rb	10.0	10	1 Sr	10.0	11
1 Rb	50.0	49	1 Sr	50.0	49
1 Cs	10.0	9	1 Mg	10.0	9
1 Cs	50.0	49	1 Mg	50.0	49

varying degrees of high results, presumably as a result of occlusion of some of the reagent or by partial precipitation as arsenate or phosphate. Tests on 100-μg quantities of elements that normally appear as anions show that no interference is caused by Te(IV), Se(IV), Se(VI), V(V), Mo(VI), W(VI), Cr(VI), Br^-, I^-, BrO_3^-, IO_3^-, NO_2^-, NO_3^- and, in the absence of appreciable amounts of potassium, perchlorate. On the other hand, IO_4^-, AsO_3^{3-}, AsO_4^{3-}, SO_3^{2-}, SO_4^{2-}, PO_4^{3-} and F^- precipitate lithium and can cause low results. In addition, silicate, germanate and borate become insoluble on evaporation to dryness. In so doing they occlude lithium and cause low results for this element.

As much as 500 μg of sodium tartrate, citrate, acetate, thiocyanate or EDTA causes little or no interference but the same amount of cyanide or oxalate causes very low recoveries of lithium. The fact that small amounts of EDTA do not prevent precipitation of the lithium suggested that it might be used to complex some of the hydroxide elements so as to prevent their interference, but subsequent work has shown that this is not a safe practice since lithium itself tends to be complexed if the ratio of the weight of EDTA to lithium present exceeds a certain value.

In considering ways of overcoming the interferences described above it seemed that this could best be done by means of a cation-exchange separation. Thus if the lithium from a sample to be analyzed is put on a suitable cation-exchange column, it can then be eluted with 1+9 hydrochloric acid ahead of much of each of the other alkali elements and ammonium ion present in microgram quantities and from microgram amounts of almost all of the other common cations that have been retained on the column[8]. The amount of each of the alkali elements which will accompany the lithium will be greater, the greater the alkali content of the sample, the lower the atomic weight of the alkali and, of course, the coarser the resin mesh size and the shorter the column length. Fortunately, the alkalis and ammonium ion which accompany the lithium can be subsequently removed by acetone extraction. This double separation makes possible an elegant isolation of the lithium in preparation for an analysis.

One of the distinct advantages of the cation-exchange separation is that it also provides a simultaneous separation of lithium from traces of most of the interfering anions including cyanide and oxalate[9] and from an appreciable number of

simple and complex cations whose affinity for the resin is low, since most of each of such anions and cations can be flushed through the column with water before the elution of the lithium is started. When the sample to be put on the cation exchanger contains elements which are capable of hydrolyzing, it is necessary to maintain an adequate acidity in the solution. However, the acidity should be kept to the minimum if interfering anions or cations are to be washed out of the column with water, otherwise a small amount of the lithium may also be eluted. On the other hand, if there is no need to remove such interfering anions or cations the acidity is not as critical since the elution with water can be omitted.

The cation-exchange separation is by no means perfect. Thus, sulfate appears to be particularly difficult to wash through the column without incurring some loss of lithium. Moreover, incomplete separation of certain elements, especially those that are eluted immediately after the lithium, may occur. However, if the amount of interfering cations that accompanies the lithium in the elution with 1+9 hydrochloric acid is small and if these cations hydrolyze or otherwise remain insoluble in acetone, no harm is done provided that a double acetone extraction is made in order to recover the lithium that is trapped by the insoluble salts. On the other hand, certain interfering elements such as cadmium and indium tend to accompany the lithium through both the ion-exchange and acetone separations. In such instances, additional separations will be required.

The cation-exchange separation is not required when the sample to be analyzed consists only of alkali or ammonium chlorides. However, if the anion present is not chloride or cannot be readily converted to chloride, the ion-exchange separation must be made.

Since many elements are difficult to remove from a cation-exchange column by elution with 3 *M* hydrochloric acid, it is usually easier and quicker to prepare a fresh column for each analysis rather than to attempt to cleanse the column of cations after an analysis.

TABLE III

DETERMINATION OF TRACES OF LITHIUM IN MIXTURES WITH VARIOUS ELEMENTS AND COMPOUNDS

Ions added (100 μg)	*Li found (μg)*	*Acid or anion added*	*Li found (μg)*
Ba, Sr, Ca, Mg, Be	49	Acetic acid[a]	49
Cu, Th, Pb, As^{5+}, Cr	49	Nitric acid[a]	48
Co, Bi, La, Pd, U^{6+}	51	Perchloric acid[a]	48
Mn, Zn, Ga, Al, V^{5+}	48	Phosphoric acid[a]	50
Ni, Ce, Hg^{2+}, Te^{4+}, Sb^{5+}	47	Sulfuric acid[a]	41
Fe^{3+}, Tl^{+}, Ti^{4+}, Se^{4+}	51	Cyanide[b]	50
Au, Pt, Ru, Ir, Rh	49	Oxalate[b]	50
Os, Sn^{4+}, Y, Mo^{6+}, W^{6+}	48	Citrate[b]	48
Ge, Sm, Re, Dy, Tl^{3+}	48	Tartrate[b]	48
Zr, Hf, Nb, Ta	50	Thiocyanate[b]	49
P, Nd, S	48	Fluoride[b]	49
Cd	60	Borate[b]	49
In	58	Arsenate[b]	48
		Iodate[b]	49

[a] 1 drop of the concentrated acid added.
[b] 0.5 mg of the sodium salt added.

It is evident that the cation-exchange separation will only suffice to isolate the lithium from traces of other elements. In general it will be necessary to remove organic matter and the bulk of the matrix elements, in a sample to be analyzed, by such separations as wet oxidation, distillation, solvent extraction, precipitation, electrolysis or ion exchange[10,11] before proceeding to the cation-exchange and acetone separations. In a typical analysis it will be best, before proceeding to other required separations and the two basic separations, to remove organic acids or cyanide by wet oxidation with nitric plus perchloric acids, remove silica and fluoride by evaporation with hydrofluoric plus perchloric acids in a platinum dish, remove silver by precipitation as a halide and remove germanium, selenium, tellurium, arsenic, antimony and tin by distillation as bromide from hydrobromic plus perchloric acids.

In order to demonstrate the usefulness of the cation-exchange separation, mixtures of 50 μg of lithium plus measured amounts of various elements or compounds were evaporated to 0.25 ml, and carried through the proposed analysis, with the arsenate method. The results obtained are shown in Table III.

DETERMINATION OF BERYLLIUM

Beryllium can be precipitated from pH 5 solution with the arsenate or phosphate reagent solutions used in the lithium determination. If 20 μg of beryllium is added to the samples in the preparation of the calibration graphs and the analyses, the calibration graphs obtained for arsenic or phosphorus are reasonably linear and as little as 1 μg of beryllium can be precipitated and determined (Table IV). Interference from a host of other trace elements can be eliminated by complexing them with EDTA and precipitating the beryllium as phosphate. EDTA severely suppresses the precipitation of beryllium arsenate.

TABLE IV

TYPICAL CALIBRATION GRAPH DATA FOR BERYLLIUM

Be added (μg)	*Counts/sec*		
	No EDTA added		*EDTA added*
	Arsenate	*Phosphate*	*Phosphate*
0	7000	939	821
1	7700	964	870
5	9100	1159	1030
10	11180	1318	1223
20	14285	1650	1615
30	17532	1896	1879
40	20177	2118	2102

Reagents

Standard beryllium solution. Dissolve 0.197 g of air-dried, tested-purity, beryllium sulfate tetrahydrate in a mixture of 10 ml of water plus 50 mg of sodium tartrate dihydrate plus 1 ml of nitric acid. Dilute to 100 ml in a volumetric flask (100 μg Be/ml). Dilute 10.0 ml of this solution plus 50 mg of sodium tartrate plus 1 ml of nitric acid to 100 ml (10 μg Be/ml).

Buffer solution (pH 5). Dissolve 72 g of anhydrous sodium acetate plus 20 ml of glacial acetic acid in water and dilute to 1 l.

Preparation of calibration graphs

Transfer aliquots of standard beryllium solutions covering the range of 0–10 μg or 0–40 μg of beryllium to 50-ml beakers. Add an aliquot containing 20 μg of beryllium plus 3 drops of hydrochloric acid plus 0.1 ml of 0.5% (w/v) tartaric acid solution plus 0.1 ml of 10% (w/v) EDTA solution. Evaporate the solutions on a low hot plate and finally at about 75° just to dryness to remove all acid odor and add 2 ml of pH 5 buffer solution. Warm to dissolve all salts, cool, add 10 ml of phosphate–ethanol solution and allow to stand for 15 min. Then proceed as directed in *Preparation of phosphate calibration graphs* for lithium.

Analysis of sample

Remove organic matter and all but traces of other elements by suitable chemical separations. Then add 20 μg of beryllium plus 3 drops of hydrochloric acid and proceed as directed in *Preparation of calibrations graphs* for beryllium.

Discussion

In the preparation of the beryllium calibration graphs it was noted that a very low count for arsenic or phosphorus was obtained when a standard beryllium solution (10 μg/ml) containing no tartrate was used. Apparently the beryllium in such a dilute solution hydrolyzes in spite of the nitric acid present. The presence of tartrate is beneficial even at higher concentrations of beryllium. Thus, the calibration graph covering the range of 0–40 μg of beryllium is more linear in the presence of tartrate than in its absence. Apparently tartrate complexes beryllium strongly enough to prevent hydrolysis but does not prevent the precipitation of the beryllium as arsenate or phosphate. In contrast to this, the citrate complex is so strong that it prevents complete precipitation of the beryllium as arsenate or phosphate.

Interference of other elements. As expected, several elements, among the 50 or more tested, tend to accompany the beryllium when this element is precipitated as arsenate or phosphate at pH 5. In so doing the results obtained for beryllium are

TABLE V

DETERMINATION OF TRACES OF BERYLLIUM IN MIXTURES WITH ELEMENTS AND COMPOUNDS

Ions added (100 μg)	*Be found (μg)*	*Ions added (100 μg)*	*Be found (μg)*
Al, Mg, Ca, Fe^{3+}, Cu	49	Br, I, Si, Mn, P	48
La, U^{6+}, Nd, Y, Ce	48	Zr, Hf	46
V^{5+}, Ti^{4+}, Dy, Sr, Ba	47	Nb, Ta	40
Rb, Cs, Sb^{5+}, Sn^{4+}, Au	49	Te^{4+}	60
Mo, W, Re, Th, Se^{4+}	45	F^-	38
NH_4, S, Li, Tl^+, Sc	50	Citrate[a]	37
Co, Zn, Ni, In, Cr^{3+}	49	Tartrate[a]	48
Sm, Tl^{3+}, Hg, Gd, Ge	51	Oxalate[a]	49
Bi, Ga, Ag, Cd, Pb	51	Borate[a]	49
Rh, Pt, Pd, Os, Ir, Ru	49	AsO_4^{3-}[a]	48
		CN^-[a]	49

[a] 0.5 mg of the sodium salt added.

often 10 to 15% high. The fact that the results are not excessively high suggests that the offending elements are undergoing only partial precipitation as phosphate or arsenate. A notable exception to this pattern is to be found in the case of aluminum which is strongly precipitated as arsenate.

In order to prevent high results for beryllium it seemed desirable to try to prevent the precipitation of the interfering elements by complexing them with EDTA. When this was done, however, it was found that precipitation of beryllium as arsenate was severely suppressed. Fortunately, this does not occur when the beryllium is precipitated as phosphate. Under the conditions of the proposed method, the addition of the EDTA has little or no effect on the precipitation of the beryllium as phosphate (Table IV). Data obtained on the effect of 100-μg portions of 50 or more of the common elements on the determination of 50-μg portions of beryllium, by the proposed method, show that in the presence of 10 mg of EDTA very few of the elements precipitate and the results for beryllium are usually good (Table V).

X-Ray analysis of the disks has shown that some tellurium, barium, tungsten, silicon, tantalum and, to a lesser extent, niobium, thorium and titanium accompanies the beryllium but the counts obtained for phosphorus in these samples usually tend, if anything, to be low rather than high. This suggests that the offending elements precipitate by hydrolysis and may cause slightly low results by absorbing phosphorus radiation. Tests showed that high counts for phosphorus are obtained when tellurium accompanies the beryllium phosphate because of line interference due to the Lβ radiation of tellurium. Silver precipitates on adding EDTA and is then reduced to the metal by the ethanol but, in spite of this, recoveries of beryllium are good. Fluoride causes low results for beryllium because it complexes this element and prevents complete precipitation of the beryllium phosphate. Sulfate, if present in more than trace amounts, causes low results by precipitating part of the beryllium as sulfate. Excess of acid must be removed from the sample to be analyzed before the addition of the pH 5 buffer, otherwise low recoveries of the beryllium may occur.

From what has been said it is evident that while the use of EDTA will suppress the interference of traces of a host of elements it will be necessary, in most instances, to remove all organic matter and the bulk of the cations and anions in the sample by chemical separations, as described in the lithium method, before the determination of beryllium. Nevertheless, it has been shown that 10 mg of EDTA will suppress the precipitation of at least 1 mg of copper. This makes it possible to determine 0.5–2% of beryllium in beryllium–copper alloys. Thus, when two NBS standard beryllium–copper alloys were dissolved in nitric acid and analyzed (in both cases 1 mg of the sample was used in the analysis), the results obtained were as follows: for sample A, present 1.91% Be, found 1.95% Be; and for Sample B, present 0.44% Be, found 0.44% Be.

DETERMINATION OF PHOSPHORUS

Just as traces of beryllium can be precipitated as phosphate in 70% ethanol solution, so traces of phosphate can be precipitated under the same conditions by the addition of an excess of beryllium. If arsenate is added to act as a coprecipitant the precipitation of 1–40 μg of phosphorus is quantitative and the calibration graph obtained is perfectly linear (Table VI).

TABLE VI

TYPICAL CALIBRATION GRAPH DATA FOR PHOSPHORUS

P added (μg)	*Counts/sec*	*P added (μg)*	*Counts/sec*
0	143	20	1775
1	194	30	2550
5	541	40	3402
10	991		

Reagents

Standard phosphorus solutions. Dissolve 0.6138 g of trisodium phosphate dodecahydrate in water and dilute to 500 ml (100 μg P/ml). Dilute 10.0 ml of this solution to 100 ml (10 μg P/ml).

Arsenic solution (ca. 2 mg As/ml). Dissolve 0.8 g of disodium hydrogen arsenate heptahydrate in water and dilute to 100 ml.

Beryllium solution (ca. 5 mg Be/ml). Dissolve 10 g of beryllium nitrate trihydrate in 5 ml of nitric acid, add 95 ml of water and filter.

Preparation of calibration graphs

Transfer aliquots of standard phosphorus solutions covering the range of 0–10 μg or 0–40 μg of phosphorus to 50-ml beakers. Add 0.1 ml of 0.5% (w/v) tartaric acid solution plus 0.1 ml of 10% (w/v) EDTA solution. Evaporate the solution to 0.2 ml, cool, add 2 ml of pH 5 buffer solution followed by 0.1 ml of arsenic solution, 0.1 ml of beryllium solution and then 10 ml of 70% (v/v) ethanol solution, swirling the solutions after each addition. Allow to stand for 15 min and then proceed as directed in *Preparation of phosphate calibration graphs* for lithium except use a graphite crystal in place of a PET crystal in the X-ray measurement.

Analysis of sample

Convert the phosphorus to orthophosphate and remove organic matter and all but traces of other elements by suitable chemical separations. Add 3 drops of hydrochloric acid plus 0.1 ml of tartaric acid solution plus 0.1 ml of EDTA solution and then evaporate on a low hot plate and finally at about 75° just to dryness to remove all odor of hydrochloric acid. Add 2 ml of pH 5 buffer solution, warm to dissolve all salts, cool and then proceed as directed in *Preparation of calibration graphs* for phosphorus.

Discussion

In the indirect X-ray method for the determination of beryllium it was not possible to precipitate very small amounts of this element quantitatively as phosphate because one could not make use of a coprecipitant. Hence it was necessary to add 20 μg of beryllium to the samples in the calibration and the analyses. In the present method, however, this restriction does not apply and hence as little as 1 μg of phosphorus can be precipitated and determined as beryllium phosphate provided that arsenate is used as a coprecipitant. Since the affinity of beryllium for arsenate in the presence of EDTA is not great it is necessary to use a rather large amount of arsenate in order to obtain enough precipitated beryllium arsenate to coprecipitate the phosphate.

In spite of the appreciable solubility of beryllium arsenate it seemed possible that a suitable method for the determination of traces of arsenate could be had by using phosphate as a coprecipitant. However, tests showed that recoveries of arsenate are increasingly incomplete below 20 μg of arsenic. For this reason further attempts to determine arsenic by this method were abandoned.

In the proposed method for phosphorus, beryllium was chosen to precipitate the phosphate because the beryllium is not appreciably complexed by EDTA and because it causes only minimal absorption of phosphorus radiation in the X-ray measurement. In the phosphate methods for the determination of lithium or beryllium described above, a PET crystal could be used in the X-ray analysis since the ratio of the weight of phosphorus to lithium or beryllium in the lithium or beryllium phosphate molecules was rather high and hence adequate sensitivity in the X-ray analysis was available. In the proposed method for the determination of phosphorus, however, it is desirable to use a graphite crystal to assure adequate sensitivity in the phosphorus determination. The graphite crystal provides a 10-fold increase in sensitivity over the PET crystal in the phosphorus determination.

Work on the possible interference of 100-μg portions of 50 or more of the common elements in the precipitation of 20 μg of phosphorus as beryllium phosphate has shown that the data obtained are quite similar to those shown in Table V. For this reason, and in order to save space, the data obtained for phosphorus have not been included in this report. Nevertheless, a few observations regarding this work are appropriate. It was noted that traces of sodium arsenate, molybdate, tungstate, silicate, germanate, chromate or vanadate do not interfere in the method for phosphorus if the solution is not acidified before evaporation to 0.2 ml and addition of the pH 5 buffer. However, if the mixtures of aliquots of solutions of the various anions are acidified with hydrochloric acid and then evaporated to 0.2 ml before the addition of the buffer, very low results for phosphorus are obtained in the presence of silicate, arsenate and molybdate. This suggests that soluble heteropoly compounds are being formed. These difficulties can be eliminated or at least minimized by removal of all the hydrochloric acid by evaporation before addition of the buffer solution.

Fluoride and probably also citrate do not interfere in the phosphorus method. This is understandable since fluoride or citrate complexes beryllium and not phosphate and since a large excess of beryllium is present in this method. As expected, most of the same elements that accompany beryllium also accompany phosphorus in the precipitation. In addition, lead accompanies the phosphorus as lead arsenate. In considering methods to be used to isolate the phosphate before its determination by the proposed method, it would appear advantageous to remove interfering cations on a cation-exchange resin.

SUMMARY

New indirect X-ray methods have been developed for the determination of traces of lithium, beryllium and phosphorus. In the lithium method which is suitable for 1–100 μg Li, 50 μg of ammonium ion, 100 μg of sodium and 1 mg of K, Rb or Cs can be tolerated; larger amounts require an extraction process. Other interfering ions may require a cation-exchange separation. For the determination of beryllium

(0–40 μg), there are very few interferences when beryllium is precipitated as phosphate in the presence of EDTA. For the determination of phosphorus (1–40 μg), beryllium is used as precipitant.

RÉSUMÉ

De nouvelles méthodes d'analyse aux rayons-X ont été mises au point pour le dosage indirect de traces de lithium, béryllium et phosphore. Lors du dosage du lithium pour des quantités allant de 1 à 100 μg Li, on peut tolérer 50 μg d'ammonium, 100 μg de sodium et 1 mg de potassium, rubidium ou césium. Des quantités plus grandes nécessitent une extraction. D'autres ions gênants exigent une séparation avec échangeur de cations. Pour le dosage du béryllium (0–40 μg), il n'y a que très peu d'interférences, s'il est précipité comme phosphate, en présence d'EDTA. Quant au dosage des phosphates (1–40 μg), le béryllium est utilisé comme précipitant.

ZUSAMMENFASSUNG

Es wurden neue indirekte röntgenspektralanalytische Methoden zur Bestimmung von Spuren Lithium, Beryllium und Phosphor entwickelt. Das Lithium lässt sich im Bereich von 1–100 μg Li bestimmen, dabei sind 50 μg Ammoniumionen, 100 μg Natrium und 1 mg K, Rb oder Cs zulässig; grössere Mengen erfordern einen Extraktionsprozess. Andere störende Ionen werden mit Hilfe eines Kationenaustauschers abgetrennt. Bei der Bestimmung von Beryllium (0–40 μg) treten es nur sehr wenige Störungen auf, wenn das Beryllium in Gegenwart von ÄDTA als Phosphat gefällt wird. Bei der Bestimmung von Phosphor (1–40 μg) wird Beryllium als Fällungsmittel verwendet.

REFERENCES

1 C. L. LUKE, *Anal. Chim. Acta*, 43 (1968) 245.
2 C. L. LUKE, *Anal. Chim. Acta*, 41 (1968) 237.
3 L. B. ROGERS AND E. R. CALEY, *Ind. Eng. Chem., Anal. Ed.*, 15 (1943) 209.
4 E. B. SANDELL, *Colorimetric Determination of Traces of Metals*, 2nd Edn., Interscience, New York, 1950, p. 414.
5 M. H. BROWN AND J. H. REEDY, *Ind. Eng. Chem., Anal. Ed.*, 2 (1930) 304.
6 T. Y. KOMETANI, *Anal. Chem.*, 38 (1966) 1596.
7 G. E. F. LUNDELL AND J. I. HOFFMAN, *Outlines of Methods of Chemical Analysis*, John Wiley, New York, 1951, p. 82.
8 H. HERING, *Anal. Chim. Acta*, 6 (1952) 340.
9 R. L. GRISWOLD AND N. PACE, *Anal. Chem.*, 28 (1956) 1035.
10 C. L. LUKE, *Anal. Chem.*, 36 (1964) 2036.
11 O. SAMUELSON, *Ion Exchange Separations in Analytical Chemistry*, John Wiley, New York, 1963, p. 310.

Analytica Chimica Acta
Elsevier Publishing Company, Amsterdam
Printed in The Netherlands

DETERMINATION OF TRACES OF BORON OR SODIUM BY X-RAY ANALYSIS

C. L. LUKE
Bell Telephone Laboratories, Incorporated, Murray Hill, N. J. 07904 (U.S.A.)
(Received December 13th, 1968)

As a result of continuing investigations on the determination of light elements by indirect X-ray analysis[1,2], new X-ray methods have been developed for the determination of 1–40 μg of boron or sodium.

DETERMINATION OF BORON

It has been shown that traces of boron can be precipitated in 15% ethanol solution as barium borotartrate[3,4] and then determined by measuring the amount of barium present in the precipitate by X-ray analysis.

Reagents

Standard boron solution. Dissolve 0.572 g of pure boric acid in water and dilute to 100 ml (1 mg B/ml). Prepare solutions containing 100 μg B/ml and 10 μg B/ml by volumetric dilution.

Sodium hydroxide solution (1 M). Dissolve 4 g of sodium hydroxide in 100 ml of water in a plastic bottle. Dispense with a plastic pipet.

Barium tartrate solution. Dissolve 1 g of barium chloride dihydrate, 1 g of tartaric acid and 5 g of ammonium chloride in 250 ml of water in a 500-ml volumetric flask. Add 75 ml of ethanol, cool, dilute to the mark with water and mix.

Preparation of calibration graphs

Transfer aliquots of standard boron solutions, of total volume no greater than 0.5 ml and covering the range of 0–10 μg or 0–40 μg of boron, to 50-ml boron-free beakers. Add 0.2 ml of standard boron solution (100 μg/ml) to each of the beakers. Add 0.5 ml of 1 *M* sodium hydroxide solution followed by 10.0 ml of barium tartrate solution and then 2 drops of ammonium hydroxide. The pH of the solution at this point should be about 9.5. Swirl and allow to stand for 30 min. Filter on a carbon-stained 0.6-μ PVC disk[1] and allow the solution to drain completely. The carbon black used for staining the disk should be suspended in 15% (v/v) ethanol. Do not wash the beaker or funnel. Dry the disk and then take a 100-sec count on an X-ray spectrograph at the wavelength of the Kα line of barium using a lithium fluoride crystal, a tungsten target, a 10-mil Soller slit and a dual counter, at a setting of 60 kVP and 60 mA. Prepare suitable calibration graphs.

Analysis of sample

Isolate the boron by methanol distillation from phosphoric acid, using boron-free glassware throughout[5]. The receiving flask should contain no alkali. Transfer the distillate to a boron-free beaker or dish, add 0.5 ml of 1 *M* sodium hydroxide solution and evaporate to 0.5 ml. Cool, add 0.2 ml of standard boron solution (100 μg B/ml) plus 10.0 ml of barium tartrate solution and proceed as directed in *Preparation of calibration graphs.*

Discussion

No attempt was made to determine which elements interfere in the precipitation of boron as barium borotartrate. However, since precipitation is made at pH 9.5 it is evident that, in most instances, the boron will have to be isolated by methanol distillation before attempting the analysis. Tests have shown that, in order to precipitate traces of boron, ethanol must be added to reduce the solubility of the borotartrate. On the other hand, the concentration of ethanol used must not be greater than about 15%, otherwise barium tartrate will precipitate on standing. The precipitation of the boron appears to be more rapid when ammonium hydroxide alone is used to adjust the solution to pH 9.5 and the precipitation is slow and incomplete in the presence of milligram quantities of alkali chlorides. Hence, in the isolation of the boron by methanol distillation it will be desirable to neutralize the sample with the minimum amount of hydrochloric acid before distillation or, preferably, to distil from a nonvolatile acid such as phosphoric acid. Perhaps this difficulty with alkali chloride might be overcome by saponifying the methyl ester with tetramethylammonium hydroxide. If the methanol distillate contains more than about 50 μg of boron, it will be necessary to take an aliquot of the distillate for the saponification and analysis.

The precipitation of less than 10 μg of boron is slow and incomplete. However, if 20 μg of boron is added to all samples, the calibration graph obtained is reasonably linear provided that the Kα line of barium is used in the X-ray analysis (Table I).

TABLE I

TYPICAL CALIBRATION GRAPH DATA FOR BORON

B added (μg)	*Counts/sec*	*B added (μg)*	*Counts/sec*
0	1389	20	2410
1	1430	30	2797
5	1670	40	3236
10	1896		

DETERMINATION OF SODIUM

Tests have shown that traces of sodium can be precipitated in 50% ethanol solution as sodium zinc uranyl acetate and determined by measuring the uranium content of the precipitate on an X-ray spectrograph.

Reagents

Standard sodium solutions. Dissolve 0.0635 g of pure sodium chloride in water

and dilute to 250 ml (100 μg Na/ml). Dilute 10.0 ml of this solution to 100 ml (10 μg Na/ml).

Zinc uranyl acetate–ethanol solution. Transfer 10 mg of sodium chloride, 3 ml of glacial acetic acid, 3 g of hydrated zinc acetate and 10 g of hydrated uranyl acetate to a beaker containing 100 ml of water. Heat until almost all of the salt has been dissolved. Cool, add 100 ml of ethanol, cool and allow to stand for 1 h. Filter on a 5-μ MF-Millipore paper disk and store the filtrate in the dark in a glass bottle that is kept stoppered when not in use. Discard the solution if it turns dark.

Sodium zinc uranyl acetate. Dissolve 10 mg of sodium chloride in 0.1 ml of water. Add 10 ml of zinc uranyl acetate–ethanol solution, allow to stand for 5 min, filter on a 5-μ Millipore paper disk and wash with two 5-ml portions of 95% ethanol.

Ethanol wash solution. Transfer the sodium zinc uranyl acetate precipitate and 1.5 ml of glacial acetic acid to 500 ml of 95% ethanol. Allow to stand overnight and then filter on a 5-μ Millipore paper disk. Store the filtrate in the dark in a glass bottle that is kept stoppered when not in use.

Preparation of calibration graphs

Transfer aliquots of standard sodium solutions covering the range of 0–10 μg or 0–40 μg of sodium to 10- or 30-ml beakers, respectively. Evaporate the solutions to dryness, using only gentle heat (175°), in order to avoid loss of sodium by volatilization or decrepitation. Cool, and add 2.0 ml of zinc uranyl acetate–ethanol solution to the 10-ml beakers or 5.0 ml to the 30-ml beakers. Allow the solutions to stand with occasional swirling for 15 min.

Police the beaker thoroughly and filter on a 2-μ carbon-stained PVC disk[1], pouring the solution directly onto the paper disk rather than down the walls of the reservoir. Allow the solution to drain completely. Wash down the policeman and walls of the beaker with 5 ml of ethanol wash solution, swirl and pour to the reservoir, washing down the walls of the latter in the process. Allow to drain completely. Repeat the wash once more. Dry the disks and then take a 100-sec count on an X-ray spectrograph at the Lα line of uranium, using a lithium fluoride crystal, a tungsten target, a 10-mil Soller slit and a dual counter. Prepare suitable calibration graphs.

Analysis of sample

Obtain the sample, free from interfering elements, in dilute hydrochloric acid solution. Evaporate to dryness on a 175° hot plate in a 10- or 30-ml beaker. Add 2 or 5 ml of the zinc uranyl acetate–ethanol reagent solution and proceed as directed above in *Preparation of calibration graphs.*

Discussion

The precipitation of sodium with zinc uranyl acetate is more rapid and complete in 50% ethanol solution than it is in aqueous solution[6]. Moreover, the precipitated salt is more finely divided, which is advantageous from the standpoint of the X-ray analysis. If precipitation is made in 5 ml of zinc uranyl acetate–ethanol solution, recovery of sodium is complete when more than 10 μg is being determined. In order to obtain complete recovery of 1–10 μg of sodium it is necessary to precipitate in 2 ml of the reagent solution.

If desired, the zinc uranyl acetate–ethanol solution can be prepared in the manner directed except that 10 g of commercially available, hydrated zinc uranyl acetate is used in place of the separate acetates. When magnesium uranyl acetate is used in place of the zinc salt, the recoveries of traces of sodium are nil or very incomplete.

TABLE II

TYPICAL CALIBRATION GRAPH DATA FOR SODIUM

Sodium added (μg)	*Counts/sec 2 ml reagent used*		
	1	*2*	
0	382	477	
1	758	923	
5	2481	2537	
10	4721	4461	
	5 ml reagent used		
	1	*2*	*3*[a]
0	501	524	446
10	4694	4228	4251
20	8164	7890	7527
30	12009	11437	11900
40	16145	15318	15188

[a] Reagent solution prepared from zinc uranyl acetate.

Typical calibration graph data for the determination of sodium are shown in Table II. When these data are plotted it is seen that all of the graphs are linear, although the counts obtained decrease and the slope of the graphs changes somewhat as the reagent solution ages. This emphasizes the need for calibration each time an analysis is made.

Phosphate, arsenate and molybdate are precipitated by the reagent and must be completely removed before a sodium determination is attempted. Potassium and lithium also precipitate if present in amounts of more than 25 μg or 100 μg, respectively. Thus, if appreciable amounts of these elements are present, they will have to be removed before sodium can be determined. Lithium can be removed by acetone extraction[2] and potassium can probably be removed as perchlorate. As much as 1 mg of such elements as Ba, Sr, Ca, Mg, Cs, Rb, Ni and Fe^{3+} causes no interference when precipitation is made from 5-ml volume, but it will probably be necessary, in most instances, to isolate the sodium by ion-exchange separation before its determination[2].

SUMMARY

New indirect X-ray methods have been developed for the determination of 0–40 μg of boron or sodium. Methods are suggested for the removal of interfering elements.

RÉSUMÉ

De nouvelles méthodes aux rayons-X sont proposées pour le dosage indirect du bore ou du sodium (0 à 40 μg). Des procédés sont décrits pour l'élimination des éléments gênants.

ZUSAMMENFASSUNG

Neue, indirekte röntgenspektralanalytische Methoden wurden für die Bestimmung von 0–40 μg Bor oder Natrium entwickelt. Für die Beseitigung störender Elemente werden Methoden vorgeschlagen.

REFERENCES

1 C. L. LUKE, *Anal. Chim. Acta*, 43 (1968) 245.
2 C. L. LUKE, *Anal. Chim. Acta*, in press.
3 J. A. GAUTIER AND P. PIGNARD, *Mikrochem. Ver. Mikrochim. Acta*, 36/37 (1951) 793.
4 A. A. NEMODRUK AND Z. K. KARALOVA, *Analytical Chemistry of Boron*, English Translation, Israel Program for Scientific Translation, Jerusalem, 1965, p. 33.
5 A. A. NEMODRUK AND Z. K. KARALOVA, *Analytical Chemistry of Boron*, English Translation, Israel Program for Scientific Translation, Jerusalem, 1965, p. 100.
6 E. R. CALEY, C. T. BROWN AND H. P. PRICE, *Ind. Eng. Chem., Anal. Ed.*, 6 (1934) 202.

Analytica Chimica Acta
Elsevier Publishing Company, Amsterdam
Printed in The Netherlands

LIQUID ION-EXCHANGE ELECTRODES AS END-POINT DETECTORS IN COMPLEXIMETRIC TITRATIONS. DETERMINATION OF CALCIUM AND MAGNESIUM IN THE PRESENCE OF SODIUM

PART I. THEORETICAL CONSIDERATIONS

M. WHITFIELD AND J. V. LEYENDEKKERS
Division of Fisheries and Oceanography, CSIRO, P.O. Box 21, Cronulla, Sydney, N.S.W. 2230 (Australia)

(Received November 26th, 1968)

Over the last few years, ion-exchange electrodes have been developed that exhibit an appreciable selectivity for calcium and magnesium in the presence of monovalent cations[1,2]. Liquid ion-exchange electrodes in which the ion-exchange oil is held in an inert matrix are now available commercially*. These electrodes are analogous in many respects to the more familiar glass electrodes[3,4] which are solid ion-exchangers. In both solid and liquid exchangers equilibrium boundary (ion-exchange) processes and non-equilibrium (diffusion, migration) processes contribute to the electrode potential and to the selectivity of the electrode for a given ion. The ion mobilities in the membrane largely determine the selectivity of a solid exchanger whereas the selectivity of a liquid ion-exchanger is dominated by its equilibrium ion-exchange properties[3]. The mobilities of divalent cations in glasses at room temperatures are much lower than those of alkali metal cations and this limits the use of glass electrodes as divalent cation sensors in solutions containing appreciable amounts of alkali metal ions[4]. However, even though more selectivity towards divalent cations is attained by liquid ion-exchangers, complete specificity has not been achieved. In addition, the theoretical treatment is complicated because the ion-exchange sites are effectively mobile[5]. The solid exchanger investigated by SHATKAY[1] might present a useful alternative to glass electrodes in this respect.

In this paper, liquid ion-exchange electrodes represented by the Orion calcium activity electrode and the Orion divalent electrode are discussed. These electrodes respond to calcium and magnesium ion activities but can also be used to measure concentrations of these ions. This can be done directly if the electrodes are suitably calibrated, but the accuracy is limited[6,7]. The relationship between electrode potential and ion concentration is complicated by ion association and by pH and ionic strength effects. The maximum response attainable is 29.6 mV for a ten-fold change in concentration at 25°. The limit of discrimination of most pH meters is ± 0.001 pH units (± 0.06 mV) and the accuracy of measurement is seldom better than ± 0.15 mV. Direct potentiometric techniques are therefore unlikely to give an accuracy better than $\pm 5\%$ even in simple solutions. In complex solutions the electrode response to a ten-fold change in concentration is less than the ideal value and the accuracy is

* Orion Res. Inc., Cambridge, Mass.; Corning Glass Works, Corning, N.Y.

correspondingly decreased. The spiking method developed by GARRELS[8] overcomes many of these problems but even so an accuracy better than $\pm 3\%$ would be difficult to achieve with the present electrodes.

If the electrode is used to indicate the end-point of a titration it is only necessary that the point of stoichiometry be effectively indicated. The method no longer depends on the exact interpretation of small changes in voltage and is not restricted by the accuracy of the electrode response to changes in solution concentration. If the form of the titration curve is reproducible and the equivalence point can be located theoretically, the titration technique should yield more accurate results than those obtained by the direct method. The literature on the application of complexometric titrations for alkaline earth metals is extensive[9-12]. The problems associated with such titrations when a liquid ion-exchange electrode is used to indicate the end-point are considered in this series of papers.

CHEMICAL CONSIDERATIONS

Apart from the method of end-point detection in complexometric titrations, it is necessary to consider the most suitable complexing reagent, the relative rates of complexation reactions, and the effects of pH and various side reactions.

Complexones

Available complexones and their stability constants are listed in several books[13-16]. RINGBOM[11] presents useful tables of equilibrium constants collected from the literature and converted (with some exceptions) to values observed under well-defined conditions, approximating those common in analytical work (Table I).

TABLE I

CONCENTRATION STABILITY CONSTANTS[a] OF ALKALINE EARTH COMPLEXES[11] AT 20°

(Ionic strength $\mu = 0.1$)

Cation	*log* $K_{M'L'}$		
	EGTA	*DCTA*	*EDTA*
H^+ $n = 1$	9.54	11.78	10.34
$n = 2$	8.93	6.2	6.24
$n = 3$	2.73	3.6	2.75
$n = 4$	2.08	2.51	2.07
Mg^{2+}	5.2	10.3	8.7
Ca^{2+}	11.0	12.5	10.7
Ba^{2+}	8.4	8.0	7.8
Sr^{2+}	8.5	10.0	8.6

[a] Conditional constants at pH 11.

Ethylenediaminetetraacetic acid (EDTA) is the most generally useful complexone for metals[9-11,16], and EDTA titrations monitored with a calcium activity electrode have been reported[17-19]. Mixtures of calcium, barium, magnesium and zinc ions give a single inflection point and alkali metals are said to improve the accuracy[17,19].

Various other complexones form more stable alkaline earth metal complexes than those formed with EDTA, but some of the acid dissociation constants of these

complexones are larger than the corresponding values for EDTA (Table I). Thus, as the pH falls, the conditional stability constants for the metal complexes decrease more rapidly than do the equivalent constants of EDTA complexes. Nevertheless, these complexones have advantages for the titration of calcium–magnesium mixtures. It has been reported that EGTA (ethyleneglycol bis(2-aminoethylether) tetraacetic acid) is more suitable than EDTA for the selective titration of calcium in the presence of magnesium[20–23], and that DCTA (1,2-diaminocyclohexanetetraacetic acid) is the most suitable for magnesium or magnesium + calcium titrations[10,12,24] (*cf.* Table I). RINGBOM[11] shows that a much higher accuracy can be obtained with DCTA than with EDTA in titrations of calcium ions at low concentration (provided that the precision in detecting the equivalence point is high enough).

Rates of complexing

RINGBOM[11] has outlined the general principles concerning rates of complexation reactions. Although SCHWARZENBACH[9] points out that DCTA complexes with metals are formed more slowly than the corresponding EDTA complexes, no special mention of slow complexing of DCTA with alkaline earth metals is made by RINGBOM[11] or PŘIBIL[10]. On the other hand, the slow reaction of magnesium with EDTA has been reported[25]. EGTA and DCTA appeared to be the most suitable reagents for the titrations discussed here.

Side reactions

For an aqueous mixture of calcium, magnesium and sodium salts, only the influence of pH on complex formation, and buffer ion effects need be considered.

The *apparent* formation constant[9], or the *conditional* constant[11] simplifies the analysis of complex formation, since these constants cover a whole series of side reactions: hydrolysis of the complexing agent and of the metal ion, formation of acidic or basic chelate complexes, and competing side reactions involving the complex and other metal ions and buffering or masking substances. The *conditional* constant $K_{M'L'}$ is defined by:

$$K_{M'L'} = [ML]'/[M]'[L]' \qquad (1)$$

where $[M]'$ = the total concentration of metal incorporated in species other than the metal chelate;

$[L]'$ = the concentration of the free ligand plus the concentrations of all species of the complexing agent not bound to the metal;

$[ML]'$ = the sum of the concentrations of all species containing the chelating agent and metal ion in 1:1 ratio.

A dashed symbol indicates that the concentration of a particular component has been corrected to allow for the effects of side reactions.

In considering the titration of calcium the formation of the magnesium chelate can be considered as a side reaction. The change in the conditional constant of the calcium complex is[11] a linear function of the magnesium ion concentration [Mg], *viz.*

$$K_{CaL'} = K_{CaL}/K_{MgL}[Mg] \quad \text{if} \quad [Mg]K_{MgL} > 1 \qquad (2)$$

The decrease in $K_{CaL'}$ can be minimised by reducing the value of [Mg], *e.g.* by adding a suitable masking agent for magnesium[11,12].

RINGBOM[11] gives plots of the conditional constants of DCTA, EGTA and EDTA calcium complexes as functions of pH. For all the complexes, log $K_{CaL'}$ is 2 or less at pH 4 and increases to a value of 10–11 at pH 10. Changes for the corresponding magnesium complexes are similar although the values of the constants are smaller. Calcium and magnesium form only weak hydroxo complexes. The highest stability constant is $K_{MgOH}=10^{2.6}$ and in any case magnesium hydroxide precipitates from highly alkaline solutions. To avoid precipitation with the possibility of co-precipitation of calcium, the pH should not be higher than 10. Even at this pH in a buffered solution the maximum concentration of magnesium which can exist without precipitating the hydroxide is around 10^{-2} mole/l[26]. Since the conditional constants of the DCTA and EGTA complexes decrease as the pH is lowered, a pH value of 9–10 is optimal for the titrations considered here. However, for the selective titration of calcium with EGTA, lower pH values are acceptable in potentiometric titrations[15,20]. An ammonia buffer is suitable for pH 9–10 since its buffer capacity is greatest around pH 9.3. This buffer would have little effect on the conditional constants of the metal chelates since complexes of calcium or magnesium with ammonia are weak[11,26]. The corresponding sulphate complexes that occur in natural waters are also weak and should have little effect on the form of the titration curve.

Because the side reactions have only a small effect on the conditional constants of the calcium and magnesium complexes, the values shown in Table I were used for calculating the titration curves.

Chemical titration curves

The following equation[27] was used to calculate the concentrations of magnesium and calcium as functions of the reagent volume, V.

$$p[\mathrm{M}]^3+[\mathrm{M}]^2\{p(C_y-C)+C_Mk+C_N\}+[\mathrm{M}]\{C_Mk(C_y-C)-pC_M/K_{ML}\}$$
$$-C_M{}^2k/K_{ML}=0 \qquad (3)$$

where [M] represents the concentration of metal ion

$C_M=C_{M_0}V_0/(V_0+V)$ $\quad$ C_{N_0}, C_{M_0} = original concentrations of metal ions

$C_N=C_{N_0}V_0/(V_0+V)$ $\quad$ V_0 = starting volume

$C_y=C_{y_0}V/(V_0+V)$ $\quad$ C_{y_0} = concentration of ligand

$k = K_{NL}/K_{ML}$

$p = 1-k$ $\quad$ $C = C_M+C_N$

Log [M] values were calculated for various solution compositions and plotted against f, the ratio of volume of titrant added to equivalent volume (Figs. 1 and 2). For EGTA titrations (Fig. 1), provided that the Mg/Ca ratio is $\leqslant 1$, the curve remains vertical over a wide range of concentrations when $f=1.0$ (curves a, e), but the gradient progressively decreases as the ratio increases (curves b, c, d). For the solution represented by curve a, the changes in the concentration of magnesium (curve a'') and in the concentration of the sum of calcium and magnesium (curve a') are also given. These curves indicate that, with appropriate indicators, it would be possible to estimate both calcium and magnesium from a single titration with EGTA. In Fig. 2 (DCTA titrations) curves a' and c' show changes in calcium ion concentration, and

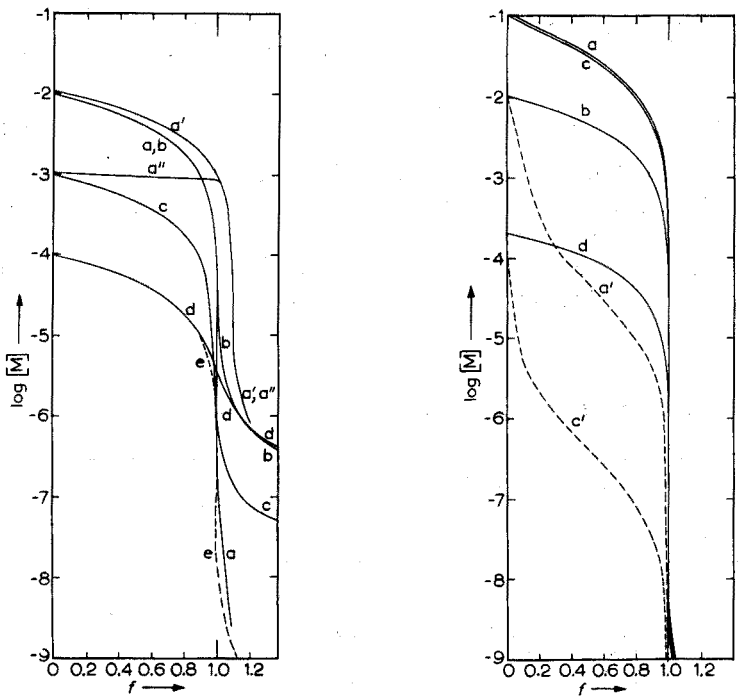

Fig. 1. EGTA titration curves calculated from eqn. (3).
f = volume titrant added/equivalence volume.

pCa_0 \ pMg_0	3	3	3	1	4
2	a	a′	a″	b	
3				c	
4				d	e
[M] plotted	[Ca]	sum	[Mg]	[Ca]	[Ca]

Curve e is dashed for clarity.

Fig. 2. DCTA titration curves calculated from eqn. (3).
f = volume titrant added/equivalence volume.

pCa_0 \ pMg_0	1	1	4
2	a	a′	b
4	c	c′	d
[M] plotted	sum	[Ca]	sum

Two curves are drawn dashed for clarity.

curves a, b, c and d changes in the total concentration of the metal ions. No distinctive end-point occurs for calcium because of the small difference between the DCTA–metal stability constants of magnesium and calcium (Table I).

Concentration of metal ion at equivalence point

Since the electrodes (see POTENTIOMETRIC CONSIDERATIONS) only respond to changes in metal ion concentration above a certain threshold concentration, it is of

interest to estimate the concentration of metal ion to be expected at the equivalence point. For the EGTA titration of calcium, the equivalence point can be approximated by[11]:

$$[Ca]_{eq} = (C_{Ca_0}/K_{CaEGTA'})^{\frac{1}{2}} \text{ for } K_{ML'} \geqslant ca.\ 10^7 \quad (4)$$

When magnesium is present the formation of its EGTA complex can be considered as a side reaction so that the conditional constant of the calcium complex can be calculated from eqn. (2). The concentration of calcium at the equivalence point can also be calculated from eqn. (3) by substituting in $V_{eq} = V_0 C_{Ca_0}/C_{Y_0}$. Examples are given in Table II, where concentrations are given in moles/l.

TABLE II

ESTIMATES OF THE CONCENTRATION OF CALCIUM IONS AT THE EQUIVALENCE POINT IN EGTA TITRATIONS

Titration	C_{Ca_0}	C_{Mg_0}	K_{CaEGTA}	K_{MgEGTA}	$K_{CaEGTA'}$	$[Ca]_{eq}$	
						eqns. (2) and (4)	*eqn. (3)*
1	10^{-2}	10^{-1}	$1.0 \cdot 10^{11}$	$1.6 \cdot 10^5$	$6.2 \cdot 10^6$	$4.0 \cdot 10^{-5}$	$4.0 \cdot 10^{-5}$
2	10^{-2}	10^{-4}	$1.0 \cdot 10^{11}$	$1.6 \cdot 10^5$	$6.2 \cdot 10^9$	$1.3 \cdot 10^{-6}$	$1.2 \cdot 10^{-6}$
3	10^{-4}	10^{-1}	$1.0 \cdot 10^{11}$	$1.6 \cdot 10^5$	$6.2 \cdot 10^6$	$4.0 \cdot 10^{-6}$	
4	10^{-4}	10^{-4}	$1.0 \cdot 10^{11}$	$1.6 \cdot 10^5$	$6.2 \cdot 10^9$	$1.3 \cdot 10^{-7}$	$1.3 \cdot 10^{-7}$
5	10^{-2}	Zero	$1.0 \cdot 10^{11}$	$1.6 \cdot 10^5$	$1.0 \cdot 10^{11}$	$3.2 \cdot 10^{-7}$	

The concentrations of the metal ions at the equivalence points for calcium (*i.e.* when the amount of ligand added is equivalent to the original concentration of calcium), and for the sum of calcium and magnesium, for DCTA titrations can also be calculated from eqn. (3), *e.g.* for titration 1 (Table II) the values would be:

At calcium equivalence point, [Ca] $2.0 \cdot 10^{-3}$ *M*
[Mg] $8.9 \cdot 10^{-2}$ *M*

At calcium + magnesium equivalence point, [Ca] zero
[Mg] $3.1 \cdot 10^{-7}$ *M*

In consequence, there is little to be gained, as far as these chelating agents are concerned, by extending the threshold limit of the electrodes below 10^{-7} *M*. In fact, the present threshold of 10^{-5} *M* should be adequate for most titrations and will avoid interference from traces of heavy metals.

In practice, some easily distinguishable point on the titration curve (*e.g.* a point of inflection or the midpoint of the section of maximum slope) is chosen as the "end-point", and it is assumed that the consumption of the ligand in going from this point to the equivalence point, or *vice versa*, is small. The exact position of the equivalence point on the titration curves is considered below.

Location of equivalence point on titration curve

MEITES AND MEITES[28] have given exact general descriptions of the slopes, the relative precisions, and the locations of the inflection points obtained in potentiometric titrations of a metal ion M with a complexone L to give the soluble 1:1

chelate ML, for an ideally cation-responsive indicator electrode. The precision of one titration relative to another depends on K_{ML}, C_{M_0} and C_{M_0}/C_{Y_0} $(=r)$.

When there is a point of maximum slope on the titration curve (Figs. 1 and 2) it always precedes the equivalence point. If r exceeds a certain value dependent on $K_{ML}C_M$, a point of minimum slope also appears. In titrations for which $K_{ML}C_M$ is large (*i.e.* $>ca.$ 200) the locations of the inflection point can be obtained from:

$$f_{max.\,slope} = 1 - A/K_{ML}C_{M_0} \quad (5)$$

$$f_{min.\,slope} = B + C/K_{ML}C_{M_0} \quad (6)$$

where $A = (6r^3 + 11r^2 + 6r + 1)/(r+1)^2$

$B = (2r+1)(r-1)/r(3r+1)$

$C = b(1+Br)/(1-B)$, $b = (13r^3 + 9r^2 - r - 1)/r(3r+1)^2$

Examples for EGTA titrations, with magnesium complexing considered as a side reaction, are given in Table III. If the end-point is taken as the point of maximum slope in these titrations, an error of as much as 1% can result (*e.g.* titration 4). In general, however, provided that a satisfactory value of r is chosen the error can be made small.

TABLE III

INFLECTION POINTS OF EGTA TITRATION CURVES

Titration	C_{Ca_0}	C_{Mg_0}	C_{Y_0}	$K_{CaEGTA'}$	r	$f_{max.\,slope}$	$f_{min.\,slope}$
1	10^{-2}	10^{-1}	10^{-1}	$6.2 \cdot 10^6$	0.1	1.0000	—
2	10^{-2}	10^{-1}	10^{-2}	$6.2 \cdot 10^6$	1.0	0.9999	0.0000
3	10^{-4}	10^{-1}	10^{-3}	$6.2 \cdot 10^6$	0.1	0.9977	—
4	10^{-4}	10^{-1}	10^{-4}	$6.2 \cdot 10^6$	1.0	0.9900	0.0020
5	10^{-4}	10^{-4}	10^{-4}	$6.2 \cdot 10^9$	1.0	1.0000	0.0000

If DCTA is used instead of EGTA for titration 4, it can be assumed that

$C_{M_0} = C_{Ca_0} + C_{Mg_0} = 0.1001$ and $K_{ML} = K_{MgDCTA'} = 2 \cdot 10^{10}$

so that $f_{max.\,slope} = 1.0000$

Thus for most practical compleximetric titrations, provided that an ideal end-point detector is used, the end-point may be taken as the point of maximum slope. If any doubt exists, eqns. (5) and (6) can be used to check this assumption for a particular titration. However, the electrodes considered here are not ideal, hence it is necessary to consider the type of titration curves likely to be obtained in practice.

POTENTIOMETRIC CONSIDERATIONS

Recently, SANDBLOM *et al.*[5] have discussed the factors governing the electrode properties of liquid ion-exchange membranes for both steady state and transient situations. The parameters controlling electrode selectivity are also discussed and a general equation for the electrode potential of an ion-exchange membrane, whether solid or liquid, has been derived. This equation consists of three terms, the first (dealing with equilibrium boundary properties) being common to solid and liquid

exchangers; the remaining two (concerned with diffusion within the membrane) are zero for a solid exchanger but may have a finite value in the case of the liquid exchanger. EISENMAN[3] has used this equation to describe and compare the principal features of the electrode potentials experimentally observed with solid and liquid ion-exchange membranes.

For the liquid ion-exchange electrodes discussed here the well-established theory applicable to solid exchangers[5] may be used to illustrate some of the problems introduced by the lack of specificity of the electrodes. Marked deviations from the equation for a solid exchanger are only expected when the mole fraction of interfering ions in the solution is very much greater than that of the selected ion. This situation arises in the critical region near the end-point in the titrations discussed here. In this case diffusion effects become significant and the electrode potential becomes time-dependent[2,3].

When a reference electrode and either the calcium or the divalent electrode are immersed in an aqueous solution containing calcium, magnesium and sodium ions, the potential of the resulting cell, E, may be expressed as:

$$E = E'' + S n \log \left[[\mathrm{Ca}]^{1/n} + \left(K_{\mathrm{CaMg}} \frac{\gamma_{\mathrm{Mg}}}{\gamma_{\mathrm{Ca}}} [\mathrm{Mg}] \right)^{1/n} + \left(K_{\mathrm{CaNa}} \frac{\gamma_{\mathrm{Na}}^2}{\gamma_{\mathrm{Ca}}} [\mathrm{Na}]^2 \right)^{1/n} + L^{1/n} \right] \quad (7)$$

where $E'' = E' + S n \log \gamma_{\mathrm{Ca}}$ (8)

E' is a parameter that depends on the type of reference electrode, the internal construction of the membrane electrode and the liquid junction potential between the reference electrode and the solution. It is effectively constant for a series of solutions of fixed ionic strength and pH, at a given temperature and pressure. The square brackets denote concentrations; γ denotes the activity coefficient of the subscripted ion. L represents the lower limit of detection of the electrode; this is related to the finite solubility of the ion-exchange oil. S is the slope factor of the electrode. If the electrode is behaving ideally, S is related to the gas constant (R), the Faraday (F) and the absolute temperature (T) by the equation

$$S = 2.303 RT/2F \quad (9)$$

S therefore has the same dimensions as an e.m.f. and can be expressed in millivolts. This implies that eqn. (7) is dimensionally incorrect. However, the log term is actually an activity *ratio* with the denominator taken as unity when the activities are expressed in moles/litre. The values n, K_{CaMg} and K_{CaNa} are empirical coefficients. The K values are generally used to characterise the selectivity of the electrode to the given pair of ions, and are often considered as constants. For simplicity it can be assumed that $n = 1$; variations in its value can then be incorporated into K_{CaMg} and K_{CaNa} which thus become selectivity functions rather than constants. MOORE AND ROSS[29] used this approach in their investigation of potassium-selective glasses and found a better fit for their data than that obtained when n was considered as the variable. For the present purpose, however, it can be assumed that K_{CaMg} and K_{CaNa} do not change significantly with solution composition. The values of the activity coefficient ratios $\gamma_{\mathrm{Mg}}/\gamma_{\mathrm{Ca}}$ and $\gamma_{\mathrm{Na}}^2/\gamma_{\mathrm{Ca}}$ must also be considered, although no completely satisfactory method exists for estimating the activity coefficients of individual ions in complex mixtures[8,30].

TABLE IV

VALUES USED IN Figs. 3–6 FOR ORION CALCIUM ACTIVITY ELECTRODE (MODEL 92-20)

Parameter	*Value*	*Reference*
K_{CaMg}	0.014	Orion Handbook[a]
K_{CaNa}	0.0005	Estimated experimentally
γ_{Mg}/γ_{Ca}	1.3[b]	31
$\gamma_{Na}^2/\gamma_{Ca}$	2.0	31
L	$5 \cdot 10^{-6}$ M	Orion Handbook[a]

[a] Orion Ionalyser, Instruction Manual, Calcium ion electrode model 92-20, Orion Res. Inc., Cambridge, Mass., 1966.
[b] A value of 1.0 was assumed for solutions containing no sodium ions.

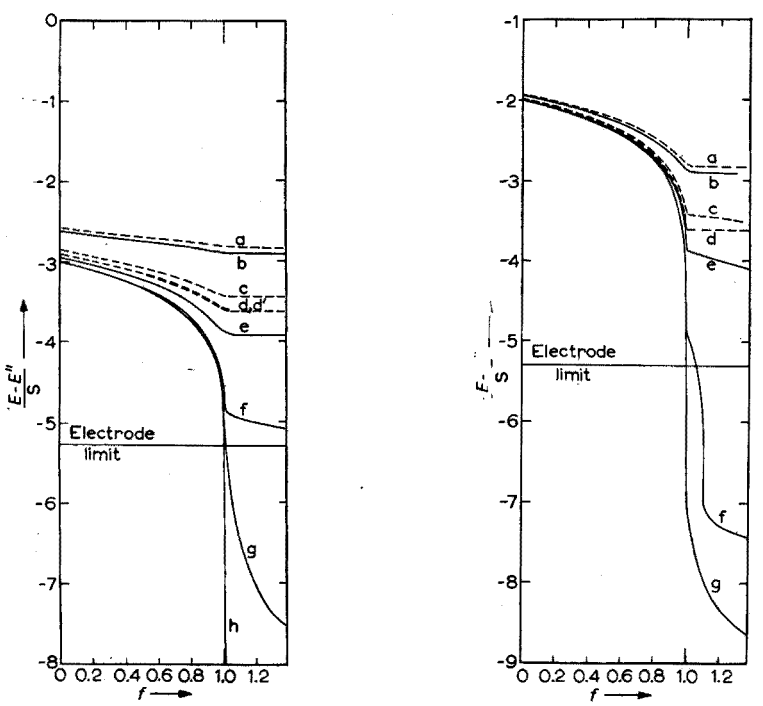

Fig. 3. Potentiometric EGTA titration curves for the Orion calcium activity electrode calculated from eqn. (7).

f = volume titrant added/equivalence volume.

pCa$_0$ \ pMg$_0$	1	2	3	4
3	a,b	c,e	d,f	d',g

Curve h represents the titration of a pure 10^{-3} M calcium chloride solution
——— [Na] = 0; --- [Na] = 0.5 M.

Fig. 4. Potentiometric EGTA titration curves for the Orion calcium activity electrode, calculated from eqn. (7).

f = volume titrant added/equivalence volume.

pCa$_0$ \ pMg$_0$	1	2	3	4
2	a,b	c,e	d,f	g

——— [Na] = 0; --- [Na] = 0.5 M.

The mixtures considered here consist of calcium chloride and magnesium sulphate; some of the mixtures also contain 0.5 M sodium chloride. For the mixtures containing sodium, the activity coefficient values given by GARRELS AND THOMPSON[31] for the ions in sea water were used. For the mixtures without sodium, the method of SHATKAY[32] for estimating the ratio γ_{Mg}/γ_{Ca} was considered, but because of the presence of sulphate ions in the mixtures and the problem of complexing, it was finally decided to take the value of 1 for simplicity; in the relatively dilute solutions

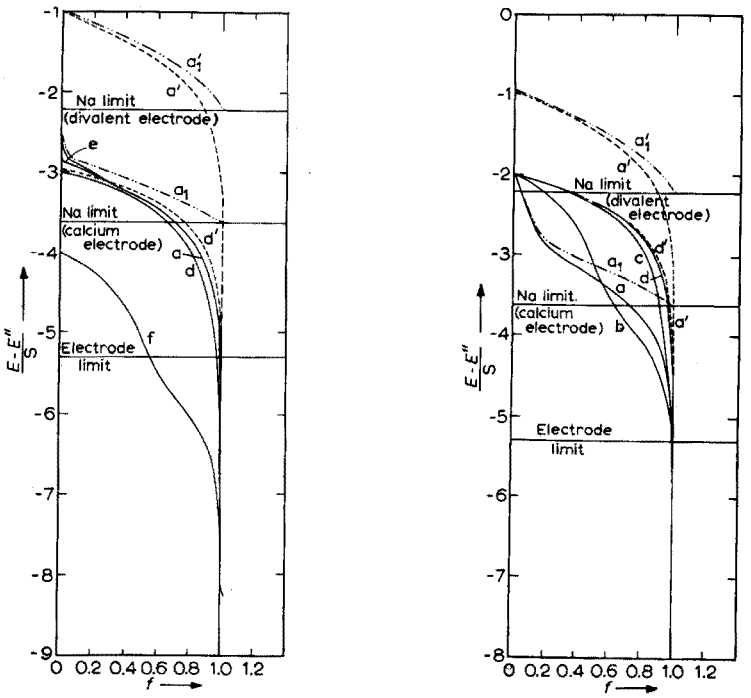

Fig. 5. Potentiometric DCTA titration curves based on eqn. (7).
f = volume titrant added/equivalence volume.

pCa$_0$ \ pMg$_0$	1	1	4
3	a	a_1	d
4	e		f
[Na]	0	0.5	0

——— calcium activity electrode, $K_{CaMg} = 0.014$, $K_{CaNa} = 0.0005$;
------ and dashed symbols: divalent electrode, $K_{CaMg} = 1.0$, $K_{CaNa} = 0.012$;
–·–·–·– sodium interference included.

Fig. 6. Potentiometric DCTA titration curves based on eqn. (7).
f = volume titrant added/equivalence volume.

pCa$_0$ \ pMg$_0$	1	1	2	3	4
2	a	a_1	b	c	d
[Na]	0	0.5	0	0	0

——— calcium activity electrode;
------ and dashed symbols: divalent electrode;
–·–·–·– sodium interference included.
Parameter values are the same as for Fig. 5.

used, deviations from this value will be small and will not appreciably affect the form of the titration curve.

Theoretical potentiometric titration curves

The log function of eqn. (7) (equivalent to $(E-E'')/S$) was calculated (with the values in Table IV) for various solution compositions and plotted as a function of f, eqn. (3) being used to calculate changes in ion concentration (Figs. 3–6). The concentration of sodium is considered to change only by dilution; this was taken into account.

The divalent electrode would generally be unsuitable for EGTA titrations since it would follow the pattern of curve a′ in Fig. 1, hence the theoretical titration curves for this electrode are restricted to DCTA titrations (Figs. 5, 6). It was assumed that this electrode responds equally to calcium and magnesium, *i.e.* $K_{CaMg}=1.00$, and γ_{Mg}/γ_{Ca} was taken as unity.

The curves in Figs. 3–6 only approximate the practical titration curves since, apart from uncertainties in the values listed in Table IV, variations in E'' and S can be expected during the titration. However, these curves should show how the shape of the titration curve is affected by changes in solution composition. This information can be used to predict the feasibility of a particular titration and to locate regions where difficulty may be expected in interpreting the titration curves. Essentially, these curves may be considered as a combination of the chemical titration curves (Figs. 1 and 2) and a horizontal line representing either the electrode limit or the level of interference from other ions in solution. This horizontal line sets a lower limit or a "levelling-off potential" for the titration curve. The ammonium ion introduced with the buffer sustains monovalent cation interference when sodium is absent and hence the actual electrode limit is masked. Only sodium ion interference is considered here. However, ammonium ion effects could be included in eqn. (7) if the appropriate value for K_{CaNH_4} was known. In the absence of interference the titration curves would level off just above the electrode limit. When interfering ions are present, little advantage would be gained by extending this limit unless the increased sensitivity was coupled with increased selectivity for divalent cations.

In the EGTA titrations (Figs. 3 and 4) changes in the concentration of magnesium are small until the calcium end-point is reached. In the absence of sodium the titration curves become progressively shallower as the magnesium concentration rises from 10^{-4} to 10^{-1} M, corresponding to an increase in the level of magnesium interference. After the end-point the magnesium concentration decreases at a rate that is proportional to $r(C_{Mg_0}/C_{Y_0})$. For example, in curve f (Fig. 4, $r=0.01$) the magnesium end-point can be located, whereas in curve b (Fig. 4, $r=1.0$) the rate of magnesium removal is low. Addition of sodium raises the interference level, giving even shallower titration curves. Since the sodium concentration is approximately constant a second "effective electrode limit" is established (curve d, Figs. 3 and 4). These effects are most noticeable in Fig. 3 where the initial calcium concentration is lowest. The theoretical curves indicate clearly the level at which interference effects limit the usefulness of the titration procedure (*e.g.* curves a, b, Fig. 3).

If the titrant is added as a sodium complex then the level of interference will rise progressively throughout the titration and may effectively swamp the end-point. Where the level of interference is not severe the equivalence point may be identified

with the point of maximum slope of the titration curve. Where there is appreciable interference the point of maximum slope also coincides with the heel of the curve (point of maximum inflection) just before the levelling-off potential is reached. In practical titrations, the electrode potential may drift considerably in the region close to the end-point, especially when the equivalence point has been passed. Under these circumstances it will probably be simpler to locate the point of maximum slope on the titration curve rather than the heel of the curve.

When DCTA is used as a titrant (Figs. 5 and 6) both the calcium and magnesium ions are reduced to low levels at the equivalence point and the response of the electrode reflects the monovalent cation activity level (*viz.* Na^+, NH_4^+, H^+). The divalent electrode (curves a' and d', Figs. 5 and 6) shows a greater potential drop than the calcium electrode because of its higher selectivity towards magnesium ions. However, this electrode also has a higher selectivity towards sodium ions than does the calcium electrode. This restricts its use for solutions such as sea water that contain a relatively high concentration of sodium (compare curves a_1 and a_1' with curves a and a', Figs. 5 and 6).

In Figs. 5 and 6 the full curves are shown for all titrations with the level of sodium interference or the electrode limit indicated by horizontal lines. The same curves can then be used to assess similar electrodes with different selectivity properties. For example, Orion have recently replaced the divalent ion-exchange resin considered in these studies with one of higher sensitivity (electrode limit 10^{-8} *M*, *cf.* 10^{-5} *M*). The selectivity towards sodium ions is also increased (K_{MgNa} 0.12, *cf. ca.* 0.012 for the original resin). This resin might be useful in fresh water analysis if the increased selectivity for sodium is not accompanied by a corresponding increase in its selectivity for ammonium ions, and provided that the enhanced interference from iron(II) and zinc(II) is not prohibitive.

The curves for the calcium electrode show varying degrees of complexity according to the relative and absolute concentrations of calcium and magnesium (compare curves a, Figs. 5 and 6) and this might hamper the identification of the end-point, especially in the presence of sodium. In practice, discrepancies between the "assumed" equivalence point (end-point) and the "true" equivalence point will not affect the accuracy greatly, provided that the slope between the two points is very steep ($\Delta V < ca.$ 0.01 ml).

Extrapolation methods to determine the end-point

When the unsymmetrical shape of a curve makes the end-point hard to identify, the titration data could be presented in a linear form, so that an extrapolation to the equivalence point can be made. GRAN[33] advocated this method for asymmetrical titration curves as early as 1952.

If all the factors except $[Ca]^{1/n}$ in the log term of eqn. (7) are assumed to remain approximately constant before the equivalence point is reached in an EGTA titration and n is 1, then

$$10^{(E-E'')/S} = [Ca] + (K'[Mg] + Na_f + L) \qquad (10)$$
$$= [Ca] + P$$

where P is constant, $K' = K_{CaMg}(\gamma_{Mg}/\gamma_{Ca})$ and $Na_f = K_{CaNa}(\gamma_{Na}^2/\gamma_{Ca})[Na]^2$

Thus $10^{E/S}=10^{E''/S}([Ca]+P)$

$$=a[Ca]+b \qquad (10a)$$

where a and b are assumed constant.

By neglecting terms of small value, *ca.* 10^{-9}, eqn. (3) can be reduced to:

$$(V_0+V)[Ca]=C_{y_0}(V_{eq}-V) \qquad (3a)$$

For EGTA titrations, eqn. (10a) then becomes:

$$(V_0+V)10^{E/S}=aC_{y_0}(V_{eq}-V)+b(V_0+V) \qquad (10b)$$

After the equivalence point for calcium (*i.e.* $V>V_{eq}$), the EGTA will complex the magnesium and it can be shown that:

$$(V_0+V)[Mg]=C_{Mg_0}V_0+C_{y_0}(V_{eq}-V)$$

Since $E=E''+S\log(K'[Mg]+Na_f+L)$

$$10^{E/S}=10^{E''/S}(K'[Mg]+Na_f+L)$$

thus $(V_0+V)10^{E/S}=a'C_{y_0}(V_{eq}-V)+b'(V_0+V)$ (10c)

where $a'=aK'$ and $b'=a\{Na_f+L+(K'C_{Mg_0}V_0)/(V_0+V)\}$

At the point of intersection of (10b) and (10c):

$$(V_{eq}-V)=(V_0+V)(b-b')/C_{y_0}(a'-a)$$

where $b-b'=aK'\{[Mg]-C_{Mg_0}V_0/(V_0+V)\}$

Thus $V=V_{eq}$ provided that only a small amount of magnesium has been complexed by the EGTA at the equivalence point of calcium, and provided that the above assumptions hold.

In practice, $(V_0+V)10^{E/S}$ is plotted against V. The curve should show two linear sections of different slope before and after the end-point. These are extrapolated and the point of intersection taken as the end-point. It will be necessary to know S: this is discussed below.

Equation (10b) will apply in DCTA titrations after $[Ca]_{eq}$ has been reached or when [Ca] is small. This equation may be expressed:

$$(V_0+V)10^{E/S}=a'C_{y_0}(V'_{eq}-V)+b''(V_0+V) \qquad (10d)$$

where $C_{y_0}V'_{eq}=(C_{Mg_0}+C_{Ca_0})V_0$, $b''=a(Na_f+L)$

If the line is extrapolated to $(V_0+V)10^{E/S}=0$

$$V'_{eq}-V=-b''(V_0+V)/a'C_{y_0}$$

$$=-(Na_f+L)(V_0+V)/C_{y_0}K'$$

If the quantity on the right-hand side is significant, it could probably be estimated fairly accurately and added to V to give the equivalent volume.

If the line is extrapolated to $(V_0+V)10^{E_L/S}$ where E_L is the levelling-off potential,

$$V=V'_{eq}$$

provided $(V_0+V)10^{E_L/S}=b''(V_0+V)$

i.e. $E_L=E''+S\log(Na_f+L)$

These methods are the most convenient to use when a computer is available. However, in practice their application might be limited because of changes in the values of E'' and S during the titration.

Evaluation of S. S can either be determined by normal standardisation procedures or it can be evaluated from the titration data in the following way. At the start of an EGTA titration, S will be constant and the cell potential should vary linearly with changes in [Ca] unless C_{Ca_0} is small relative to C_{Mg_0}, or $(C_{Ca_0}+C_{Mg_0})$ is small relative to [Na]

$$i.e.\ E=E''+S\log[\mathrm{Ca}].$$

From eqn. (3a):

$$[\mathrm{Ca}]=(V_{eq}-V)C_{y_0}/(V_0+V).$$

If V_{eq} is estimated, then [Ca] can be calculated for a number of values of V near the start of the titration (up to $f=0.5$). A plot of E *versus* log [Ca] or a computerised solution will give an estimate of S in this region. The value of S near the end-point will probably be lower than this estimate but the difference should not affect the results greatly.

In the case of the DCTA titration

$$E=E''+S\log([\mathrm{Ca}]+K'\log[\mathrm{Mg}])$$

unless $(C_{Ca_0}+C_{Mg_0})$ is small relative to [Na]. S can be obtained by the same procedure as before by substituting in the known value for K' and by assuming that [Mg] $\simeq C_{Mg_0}$ at the start of the titration.

CONCLUSIONS

Ion-exchange electrodes such as the Orion calcium activity electrode and the Orion divalent electrode should be useful as end-point detectors in chelometric titrations of calcium–magnesium mixtures. The calcium electrode functions as a selective indicator for calcium in EGTA titrations. Satisfactory results should be obtained when $[\mathrm{Ca}]>10^{-4}$ M and $[\mathrm{Mg}]/[\mathrm{Ca}]<ca.$ 100. The divalent electrode monitors the sum of calcium and magnesium in DCTA titrations and useful results should be obtained provided that $[\mathrm{Ca}]+[\mathrm{Mg}]>ca.\ 10^{-4}$ M. Interfering ions such as sodium should not be added with the chelating agent, or should be replaced by ions with smaller interference (*i.e.* the acid, just neutralised with ammonium hydroxide, should be used rather than the tetrasodium or disodium salt of the complexone).

The point of maximum slope should closely approximate the equivalence point in terms of equivalent volume of titrant. If ambiguities exist regarding the location of this point on the experimental curve, a linear extrapolation method could be used or a suitable computerised analysis of the data made (*e.g.* curve fitting and calculation of the point of maximum slope).

When a relatively high concentration of sodium is present the calcium electrode is preferred to the divalent electrode which has greater sensitivity to sodium.

Since many methods have been developed for "masking" or limiting the effects of interfering ions during complexiметric titrations of complex mixtures[10–12], the limits suggested above could probably be extended. PŘIBIL AND VESELY[12] have described a method whereby the calcium is masked with EGTA whilst magnesium is titrated with DCTA, and the calcium is then determined by back-titration of the excess EGTA with calcium chloride solution.

The titration method considered in this paper should be useful for analysis of calcium and magnesium in natural waters, particularly sea water. EGTA and DCTA titrations monitored with a calcium activity electrode have been made on a series of calcium–magnesium–sodium mixtures (covering the range of concentrations of these metals in natural waters). The results are discussed in another paper[34].

SUMMARY

Chemical and potentiometric titration curves are derived based on theoretical assumptions, for EGTA and DCTA as titrants. The problem of locating the equivalence point on practical titration curves is discussed. Linear extrapolation methods are outlined that should enable this point to be determined more accurately. It is concluded that complexiметric titrations monitored with liquid ion-exchange electrodes such as the Orion calcium activity electrode and divalent electrode should be useful for the analysis of calcium and magnesium in natural waters.

RÉSUMÉ

Courbes de titrage chimiques et potentiométriques sont deduites en se basant sur suppositions théoriques et en utilisant EGTA et DCTA comme titrants. Le problème de localisation du point équivalent sur courbes de titrage pratiques est discuté. Un aperçu est donné des méthodes d'extrapolation linéaires qui devraient donner le moyen de déterminer ce point avec une plus grande précision. La conclusion en est tirée que titrages complexométriques surveillées avec électrodes d'échange d'ions liquides telles que Orion électrode calcium activité et l'électrode divalente pourraient être utiles pour l'analyse de calcium et magnésium dans les eaux naturelles.

ZUSAMMENFASSUNG

Chemische und potenziometrische Titration Kurven werden hergeleitet auf Grund von theoretischen Annahmen unter Benutzung von EGTA und DCTA als Titrierflüssigkeiten. Das Problem den Equivalenz Punkt auf den praktischen Titration Kurven zu lokalisieren wird besprochen. Lineare Extrapolation Verfahren die ermöglichen sollen diesen Punkt genau zu bestimmen werden umgerissen. Es wird gefolgert dass komplexometrische Titrationen, kontrollieıt mit einer flüssigen Ionenaustausch Elektrode, wie Z.B., die Orion Kalzium Aktivität Elektrode und die zweiwertige Elektrode, würden nützlich sein können für die Analyse von Kalzium und Magnesium in natürlichen Gewässer.

REFERENCES

1 A. SHATKAY, *Anal. Chem.*, 39 (1967) 1056.
2 J. W. ROSS, JR., *Science*, 158 (1967) 1378.
3 G. EISENMAN, *Anal. Chem.*, 40 (1968) 310.
4 G. EISENMAN (Editor), *Glass Electrodes for Hydrogen and Other Cations: Principles and Practice*, M. Dekker, New York, 1967, pp. 293–321.
5 J. SANDBLOM, G. EISENMAN AND J. L. WALKER, JR., *J. Phys. Chem.*, 71 (1967) 3862, 3871.
6 G. A. RECHNITZ, *Chem. Eng. News*, 45 (1967) 146.

7 G. A. RECHNITZ, Ref. 4, p. 323.
8 R. M. GARRELS, Ref. 4, Ch. 13.
9 G. SCHWARZENBACH, *The General, Selective, and Specific Formation of Complexes by Metallic Cations, Advances in Inorganic Chemistry and Radiochemistry*, Vol. III, Academic Press, New York, 1961; *Complexometric Titrations*, Interscience, New York, 1957.
10 R. PŘIBIL, *Komplexometrie, I and II*, VEB Deutscher Verlag für Grundstoffindustrie, Leipzig, 1959, 1962; *Talanta*, 13 (1966) 1223.
11 A. RINGBOM, *Complexation in Analytical Chemistry: A Guide for the Critical Selection of Analytical Methods Based on Complexation Reactions*, Interscience, New York, 1963.
12 R. PŘIBIL AND V. VESELÝ, *Talanta*, 13 (1966) 233.
13 J. BJERRUM, G. SCHWARZENBACH AND L. G. SILLÉN, *Stability Constants, Chem. Soc. (London), Spec. Publ.*, 7 (1958).
14 K. B. YATSIMIRSKII AND V. P. VASILEV, *Instability Constants of Complex Compounds*, Pergamon Press, New York, 1960.
15 L. MEITES (Editor), *Handbook of Anal. Chem.*, McGraw Hill, New York, 1963.
16 G. SCHWARZENBACH AND H. A. FLASCHKA, *Die komplexometrische Titration*, Springer-Verlag, Berlin, 1963.
17 J. A. KING AND A. K. MUKHERJI, *Naturwissenschaften*, 53 (1966) 702.
18 S. C. GLAUSER, E. IFKOVITS, E. M. GLAUSER AND R. W. SEVY, *Proc. Soc. Exptl. Biol. Med.*, 124 (1967) 131.
19 A. K. MUKHERJI, *Anal. Chim. Acta*, 40 (1968) 354.
20 A. RINGBOM, G. PENSAR AND E. WANNINEN, *Anal. Chim. Acta*, 19 (1958) 525.
21 R. W. SCHMID AND C. N. REILLEY, *Anal. Chem.*, 29 (1957) 264; F. S. SADEK, R. W. SCHMID AND C. N. REILLEY, *Talanta*, 2 (1959) 38.
22 YOSHIKO DATE AND KYOJI TOEI, *Bull. Chem. Soc. Japan*, 36 (1963) 518.
23 F. CULKIN AND R. A. COX, *Deep-Sea Res.*, 13 (1966) 789.
24 R. PŘIBIL, Z. ROUBAL AND E. SVATEK, *Collection Czech. Chem. Commun.*, 18 (1953) 43.
25 C. L. WILSON AND D. W. WILSON (Editors), *Comprehensive Analytical Chemistry*, IB, Elsevier, Amsterdam, 1959.
26 J. N. BUTLER, *Ionic Equilibrium*, Addison-Wesley, Reading, Mass., 1964, Ch. 10.
27 U. HANNEMA AND G. DENBOEF, *Anal. Chim. Acta*, 39 (1967) 167, 479.
28 L. MEITES AND T. MEITES, *Anal. Chim. Acta*, 37 (1967) 1.
29 E. W. MOORE AND J. W. ROSS, *Science*, 148 (1965) 71.
30 R. G. BATES, *Electrometric pH Determinations*, Wiley, New York, 1954, p. 35.
31 R. M. GARRELS AND M. E. THOMPSON, *Amer. J. Sci.*, 260 (1962) 57.
32 A. SHATKAY, *J. Phys. Chem.*, 71 (1967) 3858.
33 G. GRAN, *Analyst*, 77 (1952) 661.
34 M. WHITFIELD, J. V. LEYENDEKKERS AND J. KERR, *Anal. Chim. Acta*, 45 (1969) 399.

Analytica Chimica Acta
Elsevier Publishing Company, Amsterdam
Printed in The Netherlands

LIQUID ION-EXCHANGE ELECTRODES AS END-POINT DETECTORS IN COMPLEXIMETRIC TITRATIONS

PART II. DETERMINATION OF CALCIUM AND MAGNESIUM IN THE PRESENCE OF SODIUM

M. WHITFIELD, J. V. LEYENDEKKERS AND J. D. KERR*
Division of Fisheries and Oceanography, CSIRO, P.O. Box 21, Cronulla, Sydney, N.S.W. 2230 (Australia)
(Received January 27th, 1969)

Liquid ion-exchange electrodes have previously been used to determine calcium and magnesium concentrations directly in the presence of a considerable excess of sodium[1,2]. A theoretical analysis[3] has shown that such electrodes should be useful as end-point indicators in the determination of calcium and magnesium by complexiметric titration. This procedure should produce more accurate and more precise results than the direct method. The general applicability of such titrations to the determination of calcium and magnesium in natural waters is discussed in this paper. The sodium, calcium and magnesium concentrations were chosen to cover the range normally found in sea, estuarine and river water. Since many titration curves were obtained over a wide composition range, a reasonable test of the theoretical approach was also possible. Ethyleneglycolbis-(β-aminoethylether)-N,N'-tetraacetic acid (EGTA) was used to titrate calcium selectively, and 1,2-diaminocyclohexane-N,N,N',N'-tetraacetic acid (DCTA) to titrate the total calcium and magnesium.

EXPERIMENTAL

Reagents

EGTA and DCTA (95% minimum; Hopkin and Williams, Ltd) were used without further purification; *ca.* 0.1 *M*, 0.01 *M* and 0.001 *M* solutions, just neutralised with dilute ammonia solution, were standardised by potentiometric titration with a calcium chloride solution prepared from primary standard carbonate[4] (Mallinckrodt, assay 99.95–100.05%, dried at 130° for 2 h). The titration was monitored with the Orion calcium activity electrode and the end-point was taken as the point of maximum slope on the titration curve[3].

Magnesium solutions were prepared from magnesium sulphate heptahydrate (A.R., 99.5–100.5%) and standardised against DCTA. The presence of sulphate ions in the solutions provides an ionic atmosphere that is fairly representative of natural waters.

* Present address: Division of Mathematical Statistics, CSIRO, Mill Rd, St Lucia, Qld. 4067, Australia.

Buffer pH 10. Ammonium chloride (67.5 g) and concentrated ammonia (570 ml) were dissolved in water, diluted to 1 l with distilled water and stored in a plastic bottle.

Apparatus

Calcium activity electrode. An Orion model 92-20 calcium activity electrode was used. This electrode is selective to various divalent cations, *viz.* Zn^{2+} (3.2), Ca^{2+} (1.0), Fe^{2+} (0.80), Pb^{2+} (0.63), Cu^{2+} (0.27), Ni^{2+} (0.080), Sr^{2+} (0.017), Mg^{2+} (0.014), Ba^{2+} (0.010); the numbers indicate the approximate value of the selectivity ratios. The ratio for Na^+ is around 0.0005, those for K^+ and NH_4^+ are somewhat less. The electrode is suitable for use in the pH range 5.5–11, and temperature range 0°–50°. RECHNITZ AND LIN[5] have studied the performance of this electrode in solutions buffered by tetraethylammonium borate. The values they obtained for the selectivity ratios differed considerably from those quoted above ($K_{CaNa}=0.001$, $K_{CaMg}=0.04$).

The divalent ion electrode (Orion model 92-32) has equal selectivity for calcium and magnesium and might seem better suited than the calcium activity electrode for determining the end-point of the DCTA titrations. However, it is more sensitive to sodium than the calcium activity electrode, so that its use is restricted to fresh-water analysis. The use of the calcium activity electrode throughout the series simplified the statistical analysis.

Reference electrode. A Jenaer thalamide electrode was employed, with a saturated potassium chloride filling-solution. The electrode had a restricted flow liquid-junction of the porous pot type.

Voltmeter. The electrodes were connected directly to a Dynamco potentiometric digital voltmeter (DM2022), which has an input impedance greater than 10^4 MΩ. The long-term accuracy of the voltmeter is rated as 0.0025% f.s.d. ±0.01% of the reading, which gives an accuracy of ±100 μV for the measurements quoted. The digital display gives high resolution, so that titration curves can be plotted accurately despite the relatively small changes in potential observed.

Procedure

The titrations (Table I) were performed in random order to minimise the effects of systematic error. The experiment was designed to test the feasibility of the technique over a wide range of solution composition rather than to assess the absolute accuracy at any point. In some instances, duplicate titrations were run to check unusual features in the titration curves; in such cases, reproducibility was good (see Fig. 8). The calcium ion in the mixture was titrated with the appropriate EGTA solution, and then the sum of calcium and magnesium was titrated in an identical sample with the appropriate DCTA solution. A Metrohm Herisau motor-driven piston burette (E412 Dosimat) with digital counter indication (accuracy ±0.005 ml after calibration) was used for the titrations, which were performed at room temperature (20°–24°).

The appropriate volumes of standard calcium and magnesium solutions were added to the titration vessel from a Vernier piston burette (precision ±0.001 ml); the solution was diluted to 100 ml (or 50 ml for samples 0.1 *M* in magnesium) with distilled water and, where appropriate, with 2.5 *M* sodium chloride solution from a piston burette. The electrodes were inserted through O-ring sealed holes in the perspex

TABLE I

DEVIATIONS OF CONCENTRATION ESTIMATES FROM TRUE VALUES

(units 10^{-5} M)

Consecutive no.	True concentration			Deviations									
				Graphical						Least squares		Extrapolation	
				[Ca] + [Mg]			[Ca]			[Ca] + [Mg]	[Ca]	[Ca] + [Mg]	[Ca]
				Observers									
	[Na]	[Mg]	[Ca]	A	B	C	A	B	C				
22	0	10000	10	−102	—[a]	—	—	—	—	−175	—	—	—
17		10060	100	10	—	—	—	—	—	−18	—	—	—
19		10060	1000	−16	−24	−22	−20	—	—	−7	—	10	−5
16	0	1006	10	−9	—	—	—	—	—	−7	—	—	—
23			100	−3	2	−3	−4	−4	−3	16	0	17	−1
2			1000	−1	−6	−3	−5	−12	−10	8	−3	32	3
3	0	101	10	4	7	8	—	—	—	6	5	11	1
8			100	0	−1	1	1	0	−1	−3	−1	2	0
15			1000	2	4	4	0	−5	−8	24	−26	15	6
24	0	10	10	0	—	—	0	0	0	0	4	−1	1
18			100	−1	−1	−1	0	−1	0	−9	−1	−1	0
9			1000	−6	−6	−6	0	−4	0	−3	−5	3	−5
12	50000	10060	10	58	—	—	—	—	—	100	—	—	—
5			100	−109	—	—	−6	—	—	−76	−11	—	—
6			1000	−35	−46	−53	−20	14	10	−35	—	11	−3
13	50000	1006	10	−41	—	—	—	—	—	−34	—	—	—
20			100	−9	−10	−35	−1	0	0	−33	−17	1	1
7			1000	−1	3	0	5	0	0	−6	−26	24	−5
21	50000	101	10	—	—	—	—	—	—	—	—	14	3
4			100	2	6	5	0	−1	−1	—	—	8	−1
10			1000	−34	−42	−39	−5	−10	−10	−49	−25	−2	−3
11	50000	10	10	—	—	—	1	0	0	—	0	—	3
1			100	3	4	5	−1	−1	−1	2	−2	4	1
14			1000	−8	−4	15	0	−10	−12	−8	−15	5	−3

[a] A dash indicates that no estimate was made because the titration curve was too flat.

cap of the titration vessel. The titration was commenced when the e.m.f. reading became stable, usually 10 min after immersion; the average titration time was 20 min. Voltage readings were taken 30 sec after each addition of titrant near the end-point. The electrodes were immersed in 0.1 M calcium chloride between titrations. For samples which were 0.1 M in magnesium the buffer was added after about half the titrant had been added, to avoid precipitation of magnesium hydroxide. The performance of the electrode system was checked regularly by calibration in a series of solutions of known calcium ion activity.

RESULTS AND DISCUSSION

Titration curves

Figures 1–4 show e.m.f. *versus* f, the titrated fraction of the metal ions (V/V_{eq}).

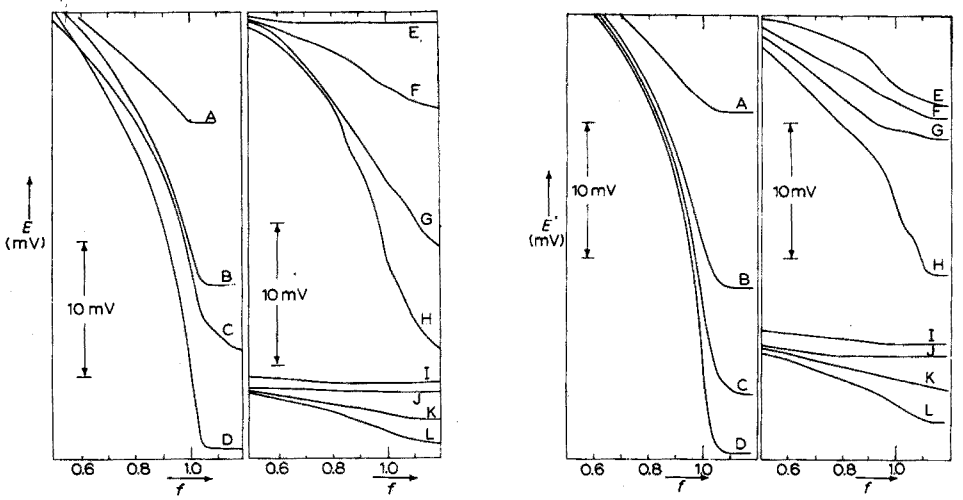

Fig. 1. Sections of EGTA titration curves. Solution composition:

pCa \ pMg	1	2	3	4
2	A	B	C	D
3	E	F	G	H
4	I	J	K	L

($p\mathrm{M} = -\log_{10}[\mathrm{M}]$). f is the titrated fraction of the metal ions.

Fig. 2. Sections of EGTA titration curves. Solution compositions were the same as for Fig. 1 except that 0.5 M sodium chloride was added.

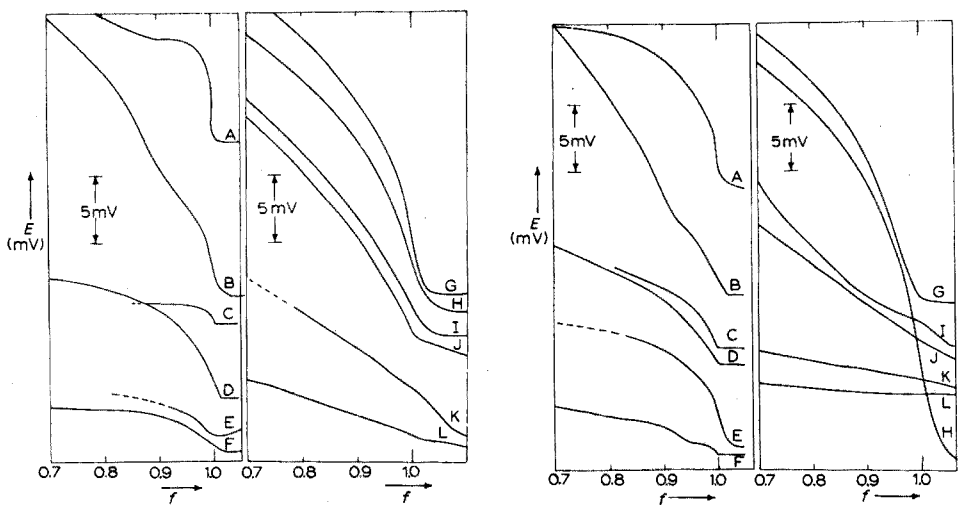

Fig. 3. Sections of DCTA titration curves. Solution composition:

pCa \ pMg	1	2	3	4
2	A	B	G	H
3	C	D	I	J
4	E	F	K	L

Fig. 4. Sections of DCTA titration curves. Solution compositions are the same as for Fig. 3 with the exception that 0.5 M sodium has been added to level.

Only the section near the end-point ($f=0.5$–1.2) has been plotted and the vertical scale has been exaggerated in comparison with the theoretical curves described previously (30 mV on the present scale is approximately equivalent to a decade span of the vertical scales used in Part I[3]).

The variation in form of the EGTA titration curves (Figs. 1 and 2) correlates with changes in the calcium and magnesium concentration as predicted theoretically. An interesting feature of curve C (Figs. 1 and 2) is the appearance of the magnesium end-point which is quite clearly defined despite the small potential drop. For the DCTA titrations (Figs. 3 and 4) the curve pattern is more complex, as was apparent in the theoretical analysis.

The potential drop near the end-point is rather small even for the best titrations. However, the drop is often quite sharply defined, the point of maximum slope being at $f=1.0$. In some cases the end-point occurs at the heel of the curve, *e.g.* curves A (Fig. 1), E (Fig. 3) and C, F and G (Fig. 4). This feature is associated with high concentrations of magnesium and/or sodium ion, as discussed previously[3].

When the experimental response of the electrode is compared directly with the theoretical response by means of the equation

$$E=E''+S \log ([\mathrm{Ca}]+K_1[\mathrm{Mg}]+K_2[\mathrm{Na}]^2)$$

the agreement is not good. It is difficult to estimate the activity and selectivity coefficients incorporated in K_1 and K_2 since little is known about their variation in such complex solutions. Accordingly, the changes in the concentrations of the titrated ions were plotted against the cell potential to illustrate the effect of changing solution composition on the electrode response. These concentrations can be estimated quite accurately from equations given earlier[3] and the resulting curves (Figs. 5 and 6) provide a concise summary of the practical electrode performance. For DCTA titrations (Fig. 6), the curves are affected by uncertainties in the values of K_{CaMg}.

The curves all follow the same general pattern with the electrode response gradually levelling off as the end-point is approached. For EGTA titrations (Fig. 5)

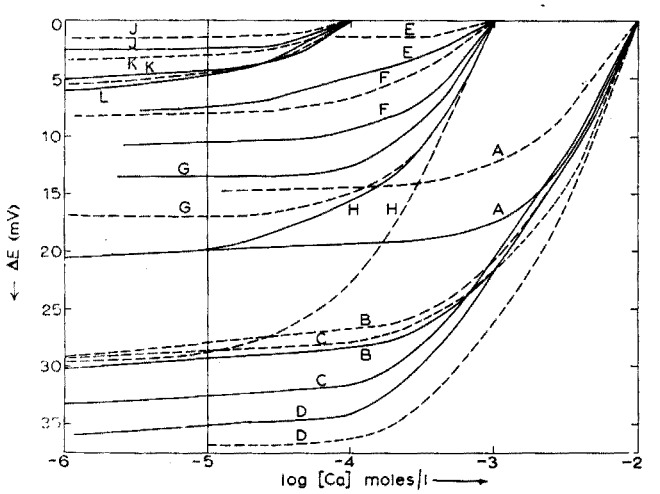

Fig. 5. Log [Ca] *vs.* change in e.m.f. Solution compositions are the same as for Fig. 1. A solid curve indicates that sodium has been added to the 0.5 *M* level; vertical line indicates electrode limit.

the curves with and without sodium are similar which suggests that the influence of sodium is limited. However, the situation is complicated by the presence of varying concentrations of ammonium ion which also interferes with the electrode response; this effect would be most significant in solutions that do not contain sodium. In general, the response of the electrode is satisfactory except when the magnesium–calcium ratio exceeds ten. The pattern of curves is more complex for the DCTA titrations because of the shift in electrode response observed in some curves when the influence of magnesium ions becomes significant (*e.g.*, curves B and D, Fig. 6).

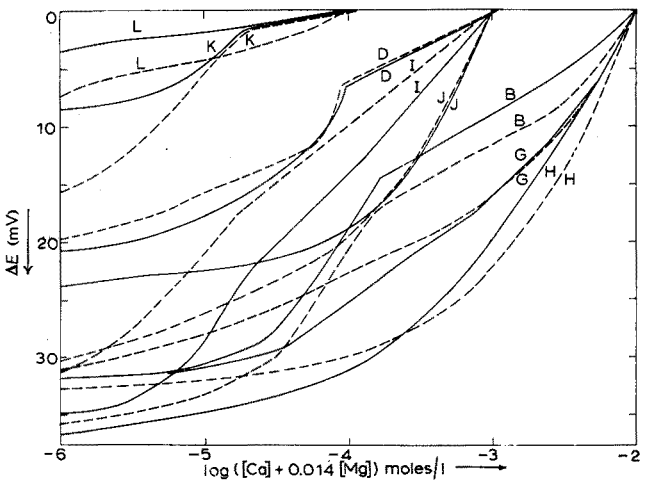

Fig. 6. Log ([Ca] + 0.014[Mg]) *vs.* change in e.m.f. Solution compositions are the same as for Fig. 3. A solid curve indicates that sodium has been added to the 0.5 *M* level.

Estimation of the equivalence point

The problems associated with the selection of an end-point have been discussed previously[3]. Three methods were used.

1. Titration curves were plotted (Figs. 1–4) and the mid-point of the section of maximum slope taken as the end-point. Three observers, A, B and C, made independent estimates of this point for each curve.

2. A computer program (based on least squares) was used to test the titration data (e.m.f. *vs.* titrant volume) for polynomial fit up to degree 6, and the corresponding points of inflection were computed. The point of maximum slope on the degree 6 curve was taken as the end-point since this degree gave the best fit for most, though not all, titrations. Only a section of the titration curve was used; the flat portion after the end-point was omitted.

3. The "Gran" extrapolation method described in the previous paper[3] was also used. An approximate value for the end-point was obtained from method 1. The expression:

$$(V_0 + V)10^{E/S} \tag{3}$$

where V_0 is the starting volume, V the volume of titrant added, E the recorded e.m.f., and S a parameter, was assumed to be a linear function of V in the titration region bounded by f values of 0.9–1.0. For the EGTA titrations the expression was also

assumed to be a linear function of V after the end-point (to $f=1.05$), the value of V common to both functions being the end-point (Fig. 7). It can be shown that

$$\frac{\partial V_{eq}}{\partial S} = \frac{(V_0+V_{eq})\cdot E''}{S^2}\left[1-\frac{C_{y_0}(1-K')}{K'\Delta Mg}\right]^{-1}$$

by differentiating with respect to S the equation describing the point of intersections of the two lines[3]. ΔMg is the amount of magnesium complexed before the calcium equivalence point. V_0, E'', C_{y_0} and K' are constants defined previously[3]. For the titrations described here, the error in V_{eq} will be small, even when $\partial S/S$ is as large as 30%, if [Ca] is greater than 10^{-4} M, and if the small f range specified above is used. For the DCTA titrations, the levelling-off potential E_L (reached after the end-point, Figs. 3 and 4) was substituted in the first function and the corresponding V taken as the end-point (Fig. 8). This relationship applies when the calcium concentration is low[3]. The change in V_{eq} per millivolt change in S is given by

$$\partial V_{eq} = \frac{(E_L-E'')C_4\,10^{(E_L-E'')/S}}{S^2}$$

where

$$C_4=(V_0+V_L)/[K'C_{y_0}-(Na_f+L)].$$

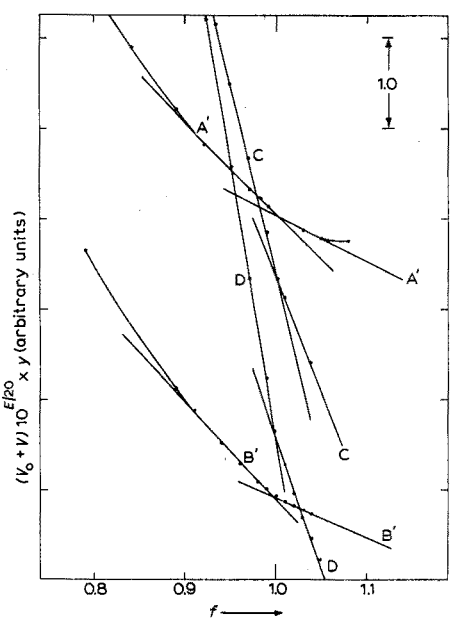

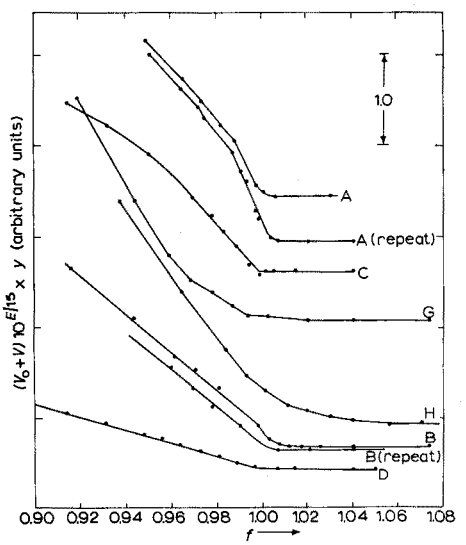

Fig. 7. $(V_0+V)10^{E/20}$ *vs.* f for EGTA titrations. Solution compositions correspond to those of Fig. 1. A dashed symbol indicates that 0.5 M Na is also present. The ordinate scales vary for the individual curves.

Curve	A′	B′	C	D
$\log_{10} y$	−44	−44	−42	−40

Fig. 8. $(V_0+V)10^{E/15}$ *vs.* f for DCTA titrations. Solution compositions correspond to those of Fig. 4. The ordinate scales vary for the individual curves. For curves A,C,G $y = 10^{-58}$; for curves H,B,D $y = 10^{-57}$.

and V_L is the volume of titrant added when the electrode limit is reached. Since C_4 is as large as 10^5, the error in V_{eq} could be quite large. The approximate range for these titrations, in percent error of V_{eq} per millivolt change in S, is 0.04% (titration I, Fig. 3) to 20% (titration L, Fig. 4). An average value of S near the end-point was estimated from Fig. 5 for the EGTA titrations (20 mV) and from Fig. 6 for the DCTA titrations (15 mV). Some representative plots of the exponential function (eqn. (3)) *vs.* f are shown in Figs. 7 and 8. The DCTA titration curves (Fig. 8) are concave when the Mg/Ca ratio is less than 1, becoming convex as the ratio increases. The calculation of the exponential, derivation of the linear equations (by least squares) and determination of the end-points were made by means of a C.D.C. 3600 computer.

COHEN[6] has described a simple graphical method for locating the end-point of a potentiometric titration, in which the $\Delta E/\Delta V$ *vs.* V relationships before and after the end-point are used. This method is unsuitable for the present titrations because the response of the electrode after the end-point is limited by the effect of interfering ions.

Since the curves of Fig. 5 are approximately linear up to $f=0.6$, an estimate of the initial concentration of calcium C_{Ca_0} can be made as follows. The starting potential E_0 is given by

$$E_0 = E' + S \log C_{Ca_0}$$

After V_1 ml of titrant of concentration C_{y_0} have been added, the potential will be

$$E_1 = E' + S \log (C_{Ca_0} - V_1 C_{y_0}/V_0)$$

and

$$\Delta E = E_0 - E_1 = S \log [C_{Ca_0}/(C_{Ca_0} - (V_1/V_0)C_{y_0})]$$

thus

$$C_{Ca_0} = (V_1/V_0)C_{y_0}\ x_1/(x_1 - 1) \qquad (4)$$

where

$$\log x_1 = \Delta E_1/S \text{ and } V_1/V_{eq} \leqslant 0.6$$

A value of 24 mV for S was assumed at the beginning of the titration, and eqn. (4) was used to calculate the calcium concentration of the samples used in the EGTA titrations. With the exception of the samples low in calcium (10^{-4} M), the results were within 1–5% of the actual values. The use of eqn. (4) therefore provides a rapid estimate of C_{Ca_0} from only two measurements of the potential. There were insufficient data points at the start of all the titrations to justify a more detailed analysis on the basis of eqn. (4).

Statistical analysis

The experiments covered a wide range of solution compositions, which resulted in considerable variation in the form of the titration curves (Figs. 1–4). It is therefore difficult to make a rigorous statistical comparison of the various end-point procedures. Estimates of calcium and magnesium were obtained by the three methods described above for determining the equivalence point. Table I lists the actual concentrations and the deviations from the true values of the estimates obtained by each method. An analysis of variance of the deviations was made for each of the methods. In the analysis of the results for calcium plus magnesium, while no factors or interactions were significant, substantial residuals occurred where no estimates

could be obtained for calcium. Therefore, the only values analysed were those for which calcium estimates were also available.

The estimates of bias for the various methods are shown in Table II. For method 1, the calcium effect is significant for observer B and approaches significance for observer C, $p < 0.10$. The only significant effect for the determination of the sum of calcium and magnesium with this method is an average bias of $-10 \cdot 10^{-5}$ M for observer C. For method 2, the only significant bias was one that increased with the concentration of calcium. Method 3 showed significant biases in the analysis of DCTA titrations; these were related to the magnesium concentration. The calcium–magnesium interaction approached significance. Estimates at high magnesium levels were possible only when the calcium level was also high. The estimates at other levels are consistent with a linear bias.

TABLE II

ESTIMATE OF BIAS

(units 10^{-5} M)

Estimation of	*Level*		*Method*				
			1A[a]	*1B*	*1C*	*2*	*3*
[Ca] (EGTA)	[Ca]	10	—	−2	−3	−1	—
		100	—	−3	−3	−2	—
		1000	—	−10	−10	−13	—
[Ca] + [Mg] (DCTA)	All levels		—	—	−10	—	—
[Ca] + [Mg] (DCTA)	[Mg]	10	—	—	—	—	2
		100	—	—	—	—	8
		1000	—	—	—	—	20
		10000	—	—	—	—	11

[a] Method 1 with observers A, B, C.

TABLE III

ESTIMATED STANDARD ERRORS

(units 10^{-5} M)

Method	*[Ca] + [Mg]*	*[Ca]*	*[Mg]*
1A	10	3	10
1B	14	4	15
1C	14	4	15
2	19	7	20
3	7	3	8

For each method, Table III shows estimates of the standard error from the analysis of variance after accounting for bias. Estimation of the magnesium errors was made on the assumption of independence of errors.

The values given in Tables II and III are based on a collective analysis of all the available data. However, it is clear from Table I that many of the solutions can be analysed with a much smaller standard error than that represented in Table III. In

general, the graphical method gives the best results for the DCTA titrations (Ca + Mg) although the end-point is easier to locate if the exponential form of graph is used (Fig. 8). The extrapolation method gives the best results for the EGTA titrations (Ca). The least squares method is not satisfactory because of the problems inherent in fitting a polynomial expansion to a rather complex exponential function.

ANALYSIS OF NATURAL WATERS

The results indicate that the method would be useful for the determination of calcium and magnesium in sea water, supplementing other methods now in use. These and earlier methods, including various EDTA titrations, have been reviewed by CULKIN[1]. EDTA titrations with visual end-points give overall accuracy within $\pm 0.5\%$ for calcium and within $\pm 0.3\%$ for magnesium[8], if done by experienced workers. EGTA titrations have also been used[9]. JAGNER[10] used a potentiometric titration method to determine magnesium in sea water: magnesium was precipitated as the hydroxide (in a nitrogen atmosphere), the hydroxyl ion concentration being monitored by a glass calomel electrode system and an accuracy of *ca.* 0.2% being obtained. A visual indicator method can be used to determine calcium in sea water with an accuracy of 0.1%, if empirical corrections are made for magnesium interference[11].

The method described here is particularly simple and can be readily automated and adapted to microtitration. With a voltmeter similar to the one used here, accuracy should be better than 0.5% for calcium (this could probably be improved by masking the magnesium[3]), and better than 0.5% for magnesium.

The calcium activity electrode has a selectivity ratio of *ca.* 0.017 for strontium. This gives an "effective" concentration in sea water of about 10^{-6} *M* which is beyond the electrode's detection limit. Thus, although the stability constant of the strontium–EGTA complex is higher than that for the magnesium–EGTA complex ($\log K_{SrY} = 8.5$ *vs.* $\log K_{MgY} = 5.4$), errors due to strontium should be small. The stability constant for the strontium–DCTA complex is approximately the same as that for the corresponding magnesium complex ($\log K = 10.0$ *vs.* $\log K = 10.3$). The results for magnesium (titration D) can therefore be used to estimate the strontium error. This should not be greater than 0.1%.

The electrode also responds to zinc, iron, lead, copper, nickel and barium. In sea water free of coastal influences the concentrations of these elements are too low to cause interference. However, in inshore samples these elements might have to be masked[3,8]. Figure 9 shows the titration curves (e.m.f. *vs.* titrant volume) for a sample of inshore sea water ($S^0/_{00}$ 35.2) titrated with EGTA (curve a) and DCTA (curve b). The values for magnesium and calcium obtained by the various end-point methods are given in Table IV. The data are consistent with molality/chlorinity ratios reported by other workers in the western Pacific[1].

The EGTA method examined here for the determination of calcium in sea water has recently been investigated by DYRSSEN *et al.*[12], who reported deviations from the true concentration as high as 1–2%. They determined the end-points by extrapolating the Gran function before the equivalence point to intercept a function related to the limiting potential after the equivalence point (see Fig. 9). With this technique the errors introduced by variations in S will be greater than in the method

outlined in the present study[3]. This is apparent from the analysis of the DCTA titrations considered earlier where the limiting potential was also used as one of the intercepts in the Gran plot. The lack of precision reported by DYRSSEN *et al.* may, in part, be caused by the addition of monovalent interfering ions (*e.g.* NH_4^+, Na^+) at a higher level than is necessary in the titrant and in the buffer, and by the method of storing the electrode. These effects will cause S to vary unless a consistent pattern of titrant addition and potential read-out is adhered to from one titration to the next. This, in turn, will affect the reproducibility of the Gran plot.

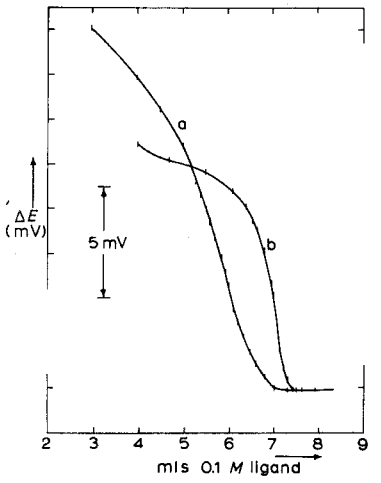

Fig. 9. Sea water titration curves ($S^0/_{00} = 35.2^0/_{00}$). (a) 60 ml sea water titrated with 0.1 *M* EGTA; (b) 50 ml sea water (diluted 1/5) titrated with 0.1 *M* DCTA.

TABLE IV

RESULTS OF SEA WATER ANALYSIS (Fig. 9)

(units 10^{-5} *M*)

Titrant	*Parameter*	*Method*		
		1	*2*	*3*
EGTA	V_{eq}	5.95	5.83	5.97
	[Ca]	991.7	971.7	995.0
DCTA	V_{eq}	7.04	7.03	7.10
	[Ca] + [Mg]	6252	6243	6306
	[Mg]	5261	5272	5311

The titration of calcium in other natural waters by the method described here should give an accuracy of 1–2%, which could be improved by adding known amounts of calcium to bring the initial concentration of the sample to a suitable value (*e.g.* 10^{-2} *M*).

SUMMARY

A calcium-selective electrode was used to monitor EGTA and DCTA titrations of aqueous mixtures of calcium, magnesium and sodium salts. The solution concen-

trations were selected to span the range of natural waters, and the results were analysed statistically. The pattern of titration curves observed with changing solution composition agreed qualitatively with that predicted theoretically, but the overall potential drop was usually lower than that predicted; end-points were determined by graphical and numerical methods. The technique is suitable for the determination of calcium and magnesium in sea water with an estimated accuracy of 0.5%.

RÉSUMÉ

Une électrode sélective de calcium est proposée pour contrôler les titrages de calcium, magnésium et de sodium en milieu aqueux, à l'aide d'EGTA et de DCTA. Les concentrations ont été choisies de manière à embrasser tout le domaine des eaux naturelles. On analyse statistiquement les résultats afin d'étudier l'action réciproque des cations. Les courbes de titrage obtenues concordent qualitativement avec celles prévues théoriquement. Leur point final est déterminé graphiquement et numériquement. Cette technique convient au dosage du calcium et du magnésium dans l'eau de mer, avec une précision estimée à 0.5%.

ZUSAMMENFASSUNG

Für die Titration wässriger Mischungen von Calcium-, Magnesium- und Natriumsalzen mit EGTA und DCTA wurde eine calciumselektive Elektrode als Anzeige verwendet. Es wurden Konzentrationen untersucht, wie sie in natürlichen Wässern vorkommen. Die Ergebnisse wurden statistisch analysiert. Der beobachtete Verlauf der Titrationskurven mit wechselnden Lösungszusammensetzungen stimmt qualitativ mit dem theoretisch vorhergesagten überein. Jedoch ist der gesamte Spannungsabfall im Verlauf der Titration im allgemeinen kleiner als erwartet. Die Endpunkte wurden mit graphischen und numerischen Methoden bestimmt. Die Technik ist für die Bestimmung von Calcium und Magnesium im Seewasser geeignet und besitzt Genauigkeit von 0.5%.

REFERENCES

1 M. E. THOMPSON AND J. W. ROSS, *Science*, 154 (1966) 1643.
2 M. E. THOMPSON, *Science*, 153 (1966) 866.
3 M. WHITFIELD AND J. V. LEYENDEKKERS, *Anal. Chim. Acta*, 45 (1969) 383.
4 W. J. BLAEDEL AND H. T. KNIGHT, *Anal. Chem.*, 26 (1954) 743.
5 G. A. RECHNITZ AND Z. F. LIN, *Anal. Chem.*, 40 (1968) 696.
6 S. R. COHEN, *Anal. Chem.*, 38 (1966) 158.
7 F. CULKIN, in J. P. RILEY AND G. SKIRROW, *Chemical Oceanography*, Vol. 1, Academic Press, London, 1965, pp. 121–161.
8 B. J. SZABO, *Bull. Marine Sci.*, 17 (1967) 544.
9 F. CULKIN AND R. A. COX, *Deep-Sea Res.*, 13 (1966) 789.
10 D. JAGNER, *Report on the Chemistry of Seawater III*, Dept. Anal. Chem., University of Göteborg, Sweden, 1967.
11 S. TSUNOGAI, M. NISHIMURA AND S. NAYAKA, *Talanta*, 15 (1968) 385.
12 D. DYRSSEN, D. JAGNER AND H. JOHANSSON, *Report on the Chemistry of Seawater V*, Dept. Anal. Chem., University of Göteborg, Sweden, 1968.

Analytica Chimica Acta
Elsevier Publishing Company, Amsterdam
Printed in The Netherlands

SYSTEMATIC TITRATION ERRORS IN REDOX TITRATIONS

U. A. TH. BRINKMAN
Chemistry Laboratory, Free Reformed University, Amsterdam (The Netherlands)
(Received January 21st, 1969)

Less attention has been given to a rigorous mathematical treatment of redox reactions than to that of precipitation or neutralisation titrations. However, in the past decade, equations have been derived for the potential at the equivalence point for inhomogeneous reactions[1] and much work has been done on the calculation of the potential change during the progress of a redox titration[2,3]. On the other hand, only brief references have been made to the systematic titration error in redox titrimetry. A generally valid expression has been proposed by BRINKMAN[4,5]; the mode of calculation is indicated[5], but no detailed treatment is given. Recently, ERDEY AND SVEHLA[6] have published a fairly complete discussion of the problem in which four expressions are given for the value of the percentage error.

In the present paper, it will be shown that two equations, different from all four previous equations[6], suffice to cover the exact calculation of the percentage error at all stages of every homogeneous redox titration, whether oxidimetric or reductimetric.

DERIVATION OF THE PRECISE EXPRESSION

In titrimetric analysis a certain amount of titrant (x meq) is added to a solution containing p meq of material to be determined; p is therefore a constant and x is variable. The equivalence-point of the titration is reached when $x=\mathrm{p}$. In general, the indicator system used will give a signal to indicate that the titration is finished when $x\neq\mathrm{p}$. This point is called the end-point of the titration. By the term systematic titration error, also called titration[7] or chemical[8] error, is meant the error caused by the fact that the equivalence-point and end-point do not coincide because of errors inherent in the titration system. Therefore, when a titration is finished ($x\neq\mathrm{p}$), a systematic error is introduced

$$\Delta=(x-\mathrm{p})\ \text{meq} \tag{1}$$

giving the number of meq that has been added in excess. Let the two half-reactions involved in a redox equilibrium be

$$a\ \mathrm{ox}_1+ne\rightleftharpoons c\ \mathrm{red}_1 \tag{2a}$$

$$b\ \mathrm{red}_2\rightleftharpoons d\ \mathrm{ox}_2+ne \tag{2b}$$

$$a\ \mathrm{ox}_1+b\ \mathrm{red}_2\rightleftharpoons c\ \mathrm{red}_1+d\ \mathrm{ox}_2 \tag{2}$$

The following equations now apply, when red_2 is titrated with ox_1, and assuming that no titration products are present in the solution.

$$\mathrm{red_1}/c = \mathrm{ox_2}/d \tag{3}$$

$$\mathrm{ox_1}/a + \mathrm{red_1}/c = x/nv \tag{4}$$

$$\mathrm{ox_2}/d + \mathrm{red_2}/b = \mathrm{p}/nv \tag{5}$$

where v is the volume (ml) at the end-point of the titration and $\mathrm{ox_1}$, $\mathrm{red_1}$, etc., are expressed in moles/l.

Substitution of eqns. (3)–(5) into eqn. (1) yields

$$\Delta = nv\,(\mathrm{ox_1}/a - \mathrm{red_2}/b) \tag{6}$$

When the titration is carried out in the reverse order ($\mathrm{ox_1}$ with $\mathrm{red_2}$), the same result is obtained, but the equation now bears a minus sign; *i.e.*, for every redox titration, Δ can be represented by

$$\Delta = \pm nv\,(\mathrm{ox_1}/a - \mathrm{red_2}/b) \tag{7}*$$

For the percentage error one finds

$$\delta = \pm (100 \cdot nv/\mathrm{p})(\mathrm{ox_1}/a - \mathrm{red_2}/b) \tag{8}$$

HOMOGENEOUS REACTIONS

Consider the homogeneous redox equilibrium

$$a\ \mathrm{ox_1} + ne \rightleftharpoons a\ \mathrm{red_1} \tag{9a}$$

$$b\ \mathrm{red_2} \rightleftharpoons b\ \mathrm{ox_2} + ne \tag{9b}$$

$$a\ \mathrm{ox_1} + b\ \mathrm{red_2} \rightleftharpoons a\ \mathrm{red_1} + b\ \mathrm{ox_2} \tag{9}$$

with the corresponding Nernst equations, which for the sake of convenience may be written as

$$\mathrm{ox_1}/\mathrm{red_1} = 10^{n(\mathrm{E}-\mathrm{E_1}^0)/0.06a} \tag{10}$$

$$\mathrm{ox_2}/\mathrm{red_2} = 10^{n(\mathrm{E}-\mathrm{E_2}^0)/0.06b} \tag{11}$$

where the E^0 values are the formal redox potentials of the systems involved. As an additional equation we have

$$\mathrm{red_1}/\mathrm{ox_2} = a/b \tag{12}$$

δ is given by eqn. (8).

When considering an oxidimetric titration, *i.e.* when $\mathrm{ox_1}$ is the titrant,

$$\mathrm{ox_2} + \mathrm{red_2} = b\mathrm{p}/nv \tag{13}$$

From eqns. (11)–(13)

$$\mathrm{ox_2} = b\ \mathrm{red_1}/a = (b\mathrm{p}/nv)/(1 + 10^{-n(\mathrm{E}-\mathrm{E_2}^0)/0.06b}) \tag{14}$$

Combination of this equation with eqns. (10) and (11), and substitution into eqn. (8) yields

$$\delta = 100\ [10^{n(\mathrm{E}-\mathrm{E_1}^0)/0.06a} - 10^{-n(\mathrm{E}-\mathrm{E_2}^0)/0.06b}]/[1 + 10^{-n(\mathrm{E}-\mathrm{E_2}^0)/0.06b}] \tag{15}$$

* In deriving this equation, it has been assumed that the error due to interaction of the redox couples with the indicator present in the solution, is negligible. This assumption may in general be applied in neutralisation and redox, but not in precipitation[5], titrations.

For a reductimetric titration, *i.e.* when red_2 is the titrant, eqn. (13) must be replaced by

$$ox_1 + red_1 = ap/nv \tag{16}$$

Elaboration along the lines indicated above now yields

$$\delta = 100\ [10^{-n(E-E_2^0)/0.06b} - 10^{n(E-E_1^0)/0.06a}]/[1 + 10^{n(E-E_1^0)/0.06a}] \tag{17}$$

With the help of eqns. (15) and (17), the percentage systematic titration error for every homogeneous redox titration can be calculated exactly by substituting E_1^0, E_2^0, n and $E = E_{end}$.

Approximate expression

An approximate, but still reliable, value of the percentage error δ can be calculated by assuming that at the end-point of the titration, the titrand has been completely converted into the desired end-product. This implies that eqns. (13) and (16) may be replaced by

$$ox_2/b = red_1/a = p/nv \tag{18}$$

for both the oxidimetric and the reductimetric titration. Combination of eqns. (8), (10), (11) and (18) yields

$$\delta = \pm 100\ (10^{n(E-E_1^0)/0.06a} - 10^{-n(E-E_2^0)/0.06b}) \tag{19}$$

with the plus- and minus-sign referring to the oxidimetric and reductimetric titrations, respectively. As a further approximation, one may simply cancel the smallest term in eqn. (19); for example, in a reductimetric titration $10^{-n(E-E_2^0)/0.06b}$ and $10^{n(E-E_1^0)/0.06a}$ before and after the equivalence point, respectively, can be cancelled. This technique, which has also been adopted by ERDEY AND SVEHLA[6], may be employed when the percentage titration errors are not excessively small (*cf.* DISCUSSION).

INHOMOGENEOUS REACTIONS

Consider the inhomogeneous redox equilibrium represented by eqn. (2); the corresponding Nernst equations are

$$ox_1^a/red_1^c = 10^{n(E-E_1^0)/0.06} \tag{20}$$

and

$$ox_2^d/red_2^b = 10^{n(E-E_2^0)/0.06} \tag{21}$$

As an additional equation we have

$$red_1/ox_2 = c/d \tag{22}$$

An exact solution of the problem cannot easily be obtained here; this may be shown using as an example the titration of red_2 with ox_1. In this case

$$red_2/b + ox_2/d = p/nv \tag{23}$$

Hence

$$b\ ox_2 + d\ ox_2^{d/b} \cdot 10^{-n(E-E_2^0)/0.06b} = pbd/nv \tag{24}$$

For this equation there is no generally valid exact solution. However, often conditions such as $b = 1$ and $d = 2$ will apply; a quadratic equation now results, and calculation is simple.

Approximate expression

In order to obtain a generally valid expression for δ, we again assume that the conversion of the titrand into the desired end-product is complete at the end-point of the titration, *i.e.* (*cf.* eqn. (18))

$$\mathrm{red}_1/c = \mathrm{ox}_2/d = \mathrm{p}/nv \tag{25}$$

Substitution of eqn. (25) into eqns. (20) and (21) yields

$$\mathrm{ox}_1 = 10^{n(\mathrm{E}-\mathrm{E}_1{}^0)/0.06a}\,(\mathrm{p}c/nv)^{c/a} \tag{26}$$

and

$$\mathrm{red}_2 = 10^{-n(\mathrm{E}-\mathrm{E}_2{}^0)/0.06b}\,(\mathrm{p}d/nv)^{d/b} \tag{27}$$

By combining these results with eqn. (8) one finds for the percentage error

$$\delta = \pm 100\,[(nv/\mathrm{p})^{1-c/a}\cdot(c/a)^{c/a}\cdot 10^{n(\mathrm{E}-\mathrm{E}_1{}^0)/0.06a} - (nv/\mathrm{p})^{1-d/b}\cdot(d/b)^{d/b}\cdot 10^{-n(\mathrm{E}-\mathrm{E}_2{}^0)/0.06b}] \tag{28}$$

DISCUSSION

In the foregoing sections it has been shown that exact expressions for the (percentage) systematic titration error in redox titrations may easily be derived by substituting the various data into eqn. (7) or (8). However, the expressions so obtained differ from those given by ERDEY AND SVEHLA[6]. This may be explained as follows.

In the introduction to their paper, ERDEY AND SVEHLA state that the titration error arises because the values of the end-point and equivalence-point potential of the system are not identical. This definition—which *mutatis mutandis* is used in all textbooks and papers for every type of titration—amounts to the fact that the amount of titrant needed to shift the potential of the system from its end-point to its equivalence-point value yields the absolute error. As an example, the authors discuss a reductimetric titration, assuming that the end-point precedes the equivalence-point, *i.e.* some of the ox_1 remains untitrated. They then state that the absolute error is equal to the actual concentration of ox_1 at the end-point minus its equilibrium concentration at the equivalence point:

$$nv\,(\mathrm{ox}_{1,\mathrm{end}} - \mathrm{ox}_{1,\mathrm{equ}})/a \text{ meq} \tag{29}*$$

i.e., the error is defined here as the amount of ox_1 untitrated at the end-point. However, this amount of reactant untitrated at the end-point will always be smaller than the amount of titrant necessary to shift the end-point to the equivalence-point potential, as is shown below. In the example cited, $\mathrm{ox}_{1,\mathrm{end}} > \mathrm{ox}_{1,\mathrm{equ}}$, and $\mathrm{red}_{2,\mathrm{end}} < \mathrm{red}_{2,\mathrm{equ}}$. When, now, an amount of red_2 equivalent to $nv\,(\mathrm{ox}_{1,\mathrm{end}} - \mathrm{ox}_{1,\mathrm{equ}})/a$ is added to the solution to be titrated, the error as expressed by eqn. (29) indeed becomes equal to zero, but the same does not hold for the systematic titration error Δ: the amount of red_2 required to make $\mathrm{E}_{\mathrm{end}} = \mathrm{E}_{\mathrm{equ}}$, and therefore $\Delta = 0$, equals

$$nv\,[(\mathrm{ox}_{1,\mathrm{end}} - \mathrm{ox}_{1,\mathrm{equ}})/a + (\mathrm{red}_{2,\mathrm{equ}} - \mathrm{red}_{2,\mathrm{end}})/b] \text{ meq} \tag{30}$$

Since, however, at the equivalence-point

$$\mathrm{ox}_1/a = \mathrm{red}_2/b \tag{31}$$

* In this expression, meq is used instead of mole; moreover, instead of "concentrations", the correct total amounts, *i.e.* volume × "concentrations", are written.

(*cf.* eqns. (3)–(5); $x = p$), eqn. (30) reduces to

$$nv\,(ox_{1,end}/a - red_{2,end}/b) \qquad (32)$$

the expression already derived above (eqn. (7) with a minus sign). In summary, since $|ox_{1,end}/a - red_{2,end}/b| > |ox_{1,end}/a - ox_{1,equ}/a|$, the error calculated as described by ERDEY AND SVEHLA will always be too small. Analogous results are obtained when the end-point of the titration comes after the equivalence-point and when oxidimetric titrations are considered. Two examples are discussed below.

1. Consider the titration of red_2 with ox_1, according to

$$red_2 + ox_1 \rightleftharpoons ox_2 + red_1 \qquad (33)$$

$n = 1$, $E_1^0 = +0.76$ V and $E_2^0 = +0.40$ V. Table I summarizes the results of calculations of δ for various values of E_{end}, by means of eqn. (17), eqn. (19), eqn. (19) after cancelling of the smallest term and the precise expressions of ERDEY AND SVEHLA (*cf.* eqn. (29)).

TABLE I

CALCULATION OF $|\delta|$ FOR VARIOUS VALUES OF E_{end} FOR AN OXIDIMETRIC TITRATION ACCORDING TO EQN. (33)

$\lvert E_{end} - E_{equ} \rvert$ (mV)	*Eqn. (17)*	*Eqn. (19)*	*Simplified eqn. (19)*	*Erdey and Svehla*
5	0.04	0.04	0.12	0.02
10	0.08	0.08	0.15	0.05
20	0.17	0.17	0.21	0.11
40	0.45	0.45	0.47	0.37
60	0.98	0.99	1.00	0.90

2. ERDEY AND SVEHLA[6] discuss the titration of hexacyanoferrate(III) ($= ox_1$) with ascorbic acid ($= red_2$), in the presence of 2,6-dichlorophenolindophenol indicator; pH = 7, $E_1^0 = +0.44$ V, $E_2^0 = +0.07$ V and $E_{end} = +0.22$ V. For this titration

$$2\,ox_1 + red_2 \rightleftharpoons 2\,red_1 + ox_2 + 2\,H^+ \qquad (34)$$

with $n = 2$, a δ value of $-0.02_1\%$ is found by means of eqn. (17), eqn. (19) or the latter equation in its simplified form, here

$$\delta = 100 \cdot 10^{n(E - E_1^0)/0.06a} \qquad (35)$$

However, the error thus calculated differs fairly considerably from the value of $-0.01_4\%$ obtained by the precise expression given in ref. 6.

Both examples demonstrate that the precise expressions of ERDEY AND SVEHLA indeed yield too low values of δ.

SUMMARY

Exact and approximate expressions have been derived for the calculation of systematic titration errors in redox titrations. Some numerical examples are calculated, and it is shown that the proposed expressions yield higher values for the titration errors than are given by some recently suggested expressions.

RÉSUMÉ

Des expressions exactes et approximatives sont établies pour le calcul des erreurs systématiques dans les titrages redox. Quelques exemples numériques sont calculés. On constate que ces expressions fournissent des valeurs plus élevées pour les erreurs de titrage que certaines équations récemment proposées.

ZUSAMMENFASSUNG

Es wurden exakte und angenäherte Ausdrücke für die Berechnung systematischer Titrationsfehler bei Redoxtitrationen entwickelt. Einige numerische Beispiele werden berechnet und es wird gezeigt, dass die vorgeschlagenen Formeln höhere Werte für die Titrationsfehler ergeben als bei einigen jüngst vorgeschlagenen Formeln.

REFERENCES

1 U. A. TH. BRINKMAN, *Chem. Weekblad*, 59 (1963) 9.
2 J. A. GOLDMAN, *J. Electroanal. Chem.*, 11 (1966) 255; 16 (1968) 47.
3 E. BISHOP, *Anal. Chim. Acta*, 26 (1962) 397.
4 U. A. TH. BRINKMAN, *Talanta*, 10 (1963) 1103.
5 U. A. TH. BRINKMAN, *Chem. Techniek (Amsterdam)*, 19 (1964) 365.
6 L. ERDEY AND G. SVEHLA, *Anal. Chim. Acta*, 40 (1967) 473.
7 I. M. KOLTHOFF AND V. A. STENGER, *Volumetric Analysis*, Vol. I, 2nd Edn., Interscience, New York, 1942, p. 143.
8 E. BISHOP, *Anal. Chim. Acta*, 22 (1960) 205.

Analytica Chimica Acta
Elsevier Publishing Company, Amsterdam
Printed in The Netherlands

CONTROLLED-POTENTIAL COULOMETRIC DETERMINATION OF AMERICIUM*

J. R. STOKELY, JR. AND W. D. SHULTS
Analytical Chemistry Division, Oak Ridge National Laboratory, Oak Ridge, Tenn. 37830 (U.S.A.)
(Received December 16th, 1968)

In recent years large amounts of americium have become available for research purposes through heavy element production programs. Methods for the analysis of americium have been based on α-counting[1], calorimetry[2], spectrophotometry[3], and coulometry[4]. None of these methods is completely satisfactory for the precise and accurate determination of milligram amounts of americium. High precision is difficult to attain with α-counting and spectrophotometry, and calorimetry requires large samples and high radiochemical purity.

The only published coulometric method for americium—that of KOEHLY[4]—is rather lengthy and demanding, and gives somewhat biassed analytical results. KOEHLY's procedure does, however, emphasize the attractiveness of the coulometric technique for this application: good precision with milligram quantities of material and easy adaptability to remote operation. Accordingly, a detailed study of potentiostatic coulometry was made as applied to the determination of americium. These studies, and the significantly improved procedure, are reported in the present paper. PROPST[5] has recently studied the voltammetric behavior of americium at a conducting glass electrode by voltage-scanning coulometry.

Americium is normally present in aqueous solution as the trivalent ion. Conversion to the hexavalent state can be accomplished with powerful chemical oxidants or by electrolytic oxidation. KOEHLY[4] based his coulometric procedure on the electrolytic oxidation of Am(III) to Am(VI) and coulometric reduction of Am(VI) to Am(V) at a platinum electrode. A lengthy electrolysis at 1.9–2.0 V *vs.* N.H.E. was required to oxidize the americium quantitatively, and it was necessary to cool the solution in an ice bath during the electrolysis to prevent evaporation of the solution. Although the precision of this coulometric determination for 2–20 mg of americium is of the order of 0.5% (relative standard deviation), a negative bias of 1.7% was obtained which was attributed to the radiolytic reduction of americium(VI). This method has been improved by eliminating the lengthy electrolytic oxidation and by reducing the bias to a level that is insignificant for many applications. The electrolytic oxidation is replaced with a chemical oxidation which is rapid and quantitative. With carefully purified americium-243 dioxide as a standard, the analytical results obtained are both precise and accurate—a few tenths of a per cent—with 0.4–1.0 mg quantities of americium.

* Research sponsored by the U. S. Atomic Energy Commission under contract with the Union Carbide Corporation.

EXPERIMENTAL

Reagents

High-purity $^{243}AmO_2$ was required for the preparation of standard solutions of americium(III) to ascertain the accuracy of the method. ^{243}Americium was purified by three precipitations of potassium americium(V) carbonate, elution of americium-(III) from an anion-exchange column with 8 *M* hydrochloric acid, several precipitations of americium hydroxide with ammonia gas, and a final precipitation of americium oxalate from weakly acidic solution. Ignition in air at 900° for 5 h converted the oxalate to the dioxide. The purified dioxide was analyzed emission spectrographically for the following sixteen elements: Al (< 0.06%), Ca (< 0.2%), Ce (< 1.2%), Cr (< 0.06%), Cu (< 0.03%), Fe (< 0.1%), K (< 0.2%), La (< 0.3%), Mg (< 0.06%), Na (< 0.1%), Nd (< 2%), Ni (< 0.03%), Pr (< 6%), Si (< 0.3%), Y (< 0.1%), Zr (< 0.3%). Standard solutions of americium(III) in nitric acid were prepared from accurately weighed samples of the purified dioxide.

All other reagents were of reagent-grade quality. Solutions of ammonium persulfate were prepared daily.

Apparatus

An ORNL Model Q-2564 High-Sensitivity Coulometric Titrator[6], with provision for graphical readout of integrated current as a function of titration time, was used. Readout voltages from the integrator were measured with a Rubicon Potentiometer. The integrator was calibrated electrically.

A 25 × 50-mm weighing bottle was used as the vessel in a coulometric cell assemblage similar to that described previously[6]. The controlled electrode was a 1 × 6 cm, 45-mesh platinum gauze shaped to fit the inside of the weighing bottle. Rapid stirring was accomplished with a magnetic stirrer. During the electrolysis, argon was sparged through the solution to remove oxygen. All operations were carried out in glove boxes.

Procedure

Pipet an aliquot containing (preferably) greater than 400 μg of americium into the weighing bottle. Add nitric acid to give a final acid concentration in 10 ml of solution of 0.05–0.20 *M*. Add 2 drops of 0.02% silver nitrate and 0.5 ml of 1 *M* ammonium persulfate (prepared daily), and adjust the solution volume to *ca.* 10 ml with water. Heat on a hot plate so that the solution boils gently. After about 2 min the amber color of americium(VI) appears. Continue heating for 10–20 minutes, then remove the solution from the hot plate and allow to cool to near room temperature. Add water to make the total solution volume *ca.* 10 ml. Position the weighing bottle under the electrode assemblage and start the stirrer and sparge gas. Adjust the potential of the platinum electrode to 1.6 V *vs.* S.C.E. and allow pre-electrolysis to proceed for *ca.* 15 min. Stop the electrolysis, adjust the potential of the electrode to 1.05 V *vs.* S.C.E., and prepare the instrument for current integration. Then start the electrolysis, and integrate the current as americium(VI) is reduced to Am(V). After the current drops to a constant value, which should require less than 10 min, integrator readout voltages corresponding to at least two titration times are obtained.

DISCUSSION

Because of the high potential (1.7 V *vs.* N.H.E.) and irreversibility of the Am(III)–Am(VI) couple, strong oxidizing conditions are needed to oxidize Am(III) to Am(VI). Successful oxidation has been achieved with silver(II) oxide[7], ammonium persulfate[7], and ozone[8]. Both silver(II) oxide and ammonium persulfate were examined as possible oxidants for americium(III), and superior results were obtained with ammonium persulfate catalyzed with a trace of silver ion. Heating a solution of americium(III) with persulfate for a few minutes gave the characteristic rum color of americium(VI). Additional heating completes the oxidation and also serves to decompose the bulk of the persulfate. (Persulfate would interfere in the subsequent electrolytic reduction if present in large amounts.) Ozone was not investigated because of the hazard and the elaborate equipment involved in using it in a glove box.

As suspected from previous radiochemical studies[1,9], low acid concentrations are required if the chemical oxidation is to be quantitative. Table I shows analytical results obtained with various acid concentrations. Acid concentrations below 0.2 *M* are required for complete oxidation. Presumably the acid-catalyzed decomposition of persulfate to give hydrogen peroxide[10], which reduces Am(VI) and Am(V), prevents quantitative oxidation in stronger acid solution.

TABLE I

EFFECT OF ACID CONCENTRATION

Acid concn. (M)	*Continuous faradaic current (μA)*	*Am found (μg)*[a]
0.05	6.8	421.5
0.10	2.3	422.7
0.20	1.0	424.4
0.25	1.0	376.5
0.30	0.8	351.9

[a] Am added = 424.0 μg.

TABLE II

EFFECT OF HEATING TIME ON EXPERIMENTAL PARAMETERS

Heating time (min)	*Continuous faradaic current (μA)*	*Blank (μg Am)*	*Am found*[a] *(μg)*
5	40.5	17.2	418.9
10	10.0	16.7	420.9
15	3.8[b]	17.6	422.3
20	1.5	16.3	420.6
25	0.5	15.8	418.4

[a] Am added: 424.0 μg.
[b] Equivalent to 5.7 μg Am for 10 minute electrolysis.

Table II shows values of the continuous faradaic current corresponding to various heating times. The major portion of the continuous faradaic current is due to the slow electrolytic reduction of persulfate, hence the decrease in the current at longer heating periods reflects lower residual concentrations of persulfate. If the

continuous faradaic current remains constant during the course of the titration, elimination of its contribution to the total integrated current is possible by extrapolation of the integrator readout *vs.* time curve to the beginning of the titration[6,11]. Since the ultimate accuracy and precision of the titration depends on the ability to make valid and accurate corrections for the continuous current, it is desirable to reduce the current to the smallest possible value. The chemical oxidation was carried out by heating for 10–20 min to insure that the continuous faradaic current would be less than 10 μA, and then the readout voltage was numerically extrapolated to time zero in order to correct for the effect of the continuous faradaic current.

Corrections are also needed for the charging current and the faradaic current caused by reduction of impurities in the reagents. Corrections for these currents are conveniently obtained from a blank titration of all reagents except americium. Typical blank corrections are given in Table II. Even though these blank corrections are rather large (0.07 μeq) they are constant to within *ca.* 5% (Table II). When the same electrode and experimental conditions were used over a period of one month, the standard deviation of the value of the blank was found to be equivalent to 0.8 μg of americium. This uncertainty sets the ultimate sensitivity and precision that may be obtained by this method.

Figure 1 is a typical coulometric titration curve illustrating the manner in which corrections are applied. Q^{E} is the experimental integrator readout; Q^{F} is the integrated continuous faradaic current. The difference $Q^{E}-Q^{F}$ is obtained by numerical extrapolation of the integrator readout to time zero. Q^{NF} is the readout corresponding to a blank electrolysis, also corrected by extrapolation for the effect of any continuous faradaic current. In the determination of americium, Q^{F} and Q^{NF} are

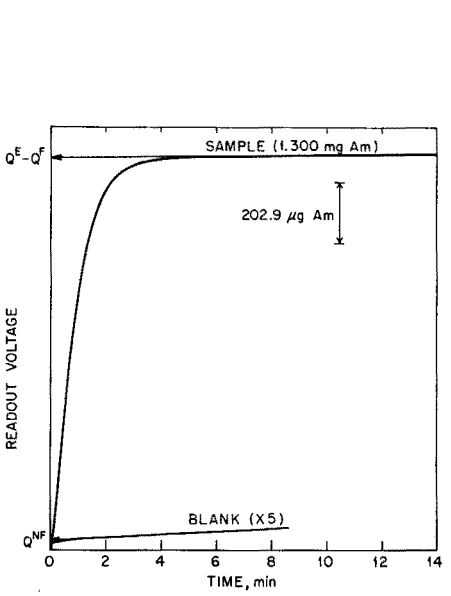

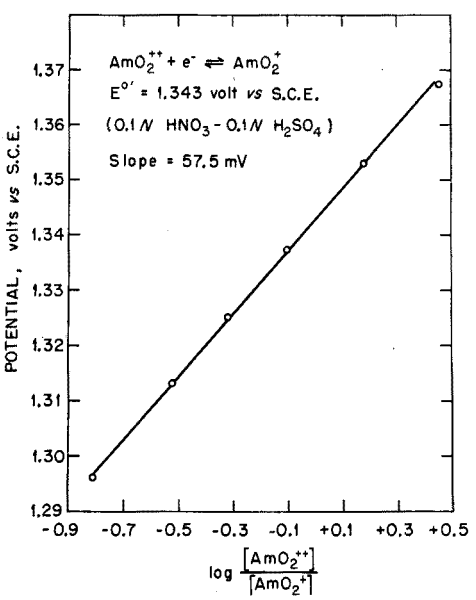

Fig. 1. Typical titration curve, illustrating corrections for continuous faradaic current and electrolysis blank.

Fig. 2. Curve showing potential of Am(VI)–Am(V) couple.

subtracted from Q^E to obtain Q^C, the corrected integrator readout corresponding to coulometric reduction of americium(VI). These factors, and two others which had to be considered in designing this procedure, are expressed in the following equation.

$$Q_t^C = Q_t^E - Q_t^F - Q_t^{NF} - \int_0^t \frac{d[Am(VI)]_{DISP.}}{dt}\,dt + \int_0^t \frac{d[Am(VI)]_{LOSS}}{dt}\,dt \qquad (1)$$

The subscripted variables are dependent on t, the titration time.

The fourth term on the right side of eqn. (1), $d[Am(VI)]_{DISP}$, represents the differential production of americium(VI) via disproportionation of americium(V). COLEMAN[12] observed that the disproportionation rate of americium(V) is a sensitive function of the acid concentration, the rate being slow at low acid concentrations. Estimation of the disproportionation rate of americium(V) from COLEMAN's data reveals that less than 0.01% of americium(V) disproportionates during the course of the coulometric reduction under the experimental conditions used here. The term representing the production of americium(VI) by disproportionation in eqn. (1) is thus small in comparison to the other terms and can be neglected.

The fifth term on the right side of eqn. (1) represents the differential loss of americium(VI) via non-electrolytic processes such as reaction with water or auto-reduction. It has been observed that the reduction rate depends on the total amount of americium present[13], *i.e.*,

$$\frac{d[Am(VI)]_{LOSS}}{dt} = kQ^C \qquad (2)$$

where k is the rate constant corresponding to loss of americium(VI). Substituting eqn. (2) into eqn. (1), integrating, and rearranging yields the final expression:

$$Q^C = \frac{Q^E - Q^{NF} - Q^F}{1 - kt} \qquad (3)$$

Values of k are 0.04 h^{-1} for ^{241}Am[13] and 0.004 h^{-1} for ^{243}Am[12]. Hence, if electrolysis conditions are such that 99.9% of americium(VI) is reduced in 10 min, errors of -0.7 and -0.07% are possible for ^{241}Am and ^{243}Am, respectively. Other α-emitters will increase k and cause larger errors. Equation (3) demonstrates the importance of short electrolysis times. For ^{241}Am particularly, it is imperative to use rapid stirring and a large-area working electrode to minimize the electrolysis time. With the cell assemblage described previously and the most rapid stirring rate possible, 99.9% of the americium(VI) can be electrolyzed in less than 6 min (Fig. 1).

During the preliminary studies, the analytical results obtained were in error (low) by several percent, depending on the treatment of the chemically oxidized sample. Since the americium(VI)–americium(V) couple is reversible and its potential is quite high, it was suspected that some americium(VI) was being reduced to americium(V) during the latter part of the chemical oxidation or during the few minutes between chemical oxidation and electrolytic reduction. A brief electrolytic oxidation at 1.6 V *vs.* S.C.E. just before the coulometric reduction was found to eliminate this error. This pre-oxidation insures that all americium is present in the hexavalent state when the coulometric reduction commences. The potentials for this pre-oxidation and for coulometric reduction are based on the curve in Fig. 2. This Fig. shows the experimentally measured potentials of solutions having known ratios

of americium(VI) to americium(V) [obtained by coulometric reduction of a pure solution of americium(VI)]. The linearity and slope (57.5 mV *vs.* theoretical 59 mV) of this curve attests the reversibility of the americium(VI)–americium(V) couple in this medium. The formal potential is 1.34 V *vs.* S.C.E., in excellent agreement with 1.35 V reported by PENNEMAN AND ASPREY[14]. Thus, americium can be rapidly and quantitatively converted between the hexa- and pentavalent oxidation states electrolytically at 1.60 V and 1.05 V *vs.* S.C.E., respectively; chemical oxidation surmounts the irreversible americium(III)–americium(VI) couple. This approach should be a convenient method for preparing pure solutions of americium(V) or americium(VI) for physical or chemical studies in which it is important to avoid extraneous oxidizing or reducing reagents.

RESULTS

The precision and accuracy of the titration were ascertained by repetitive analysis of pure ^{243}Am(III) solutions by the procedure given earlier. The results are summarized in Table III. The precision is excellent when a milligram or more of americium is determined. As the amount of americium determined decreases, the precision becomes poorer because of the proportionately larger blank and background

TABLE III

SUMMARY OF RESULTS OF ANALYSIS OF AMERICIUM-243 STANDARDS

^{243}Am *added* (μg)	^{243}Am *found* (μg)	*Relative standard deviation* (%)	*Error* (%)	*Number of determinations*
1300	1297	0.3	−0.2	8
441.2	440.4	0.6	−0.2	9
88.3	89.3	2.6	+1.1	8

current corrections which must be applied. For example, in the titration of 88 μg of americium, the corrections are comparable to about 25% of the americium determined. The method has not been tested with quantities of americium much above 1 mg, but the precision would probably remain good, and would perhaps improve slightly with larger amounts of americium because corrections would be relatively small. With regard to accuracy, the results agree within experimental error with the americium-243 added assuming that americium dioxide is a truly stoichiometric compound. Reports in the literature[15,16] indicate that the compound is very close to the predicted stoichiometric composition.

It was not possible to evaluate this method with $^{241}AmO_2$ of unequivocal purity. However, comparative analyses of americium-241 solutions by coulometric titration and by α-counting demonstrated that the accuracy of the coulometric method is at least as good as that of counting methods. (The precision of the coulometric results with americium-241 is comparable to that obtained with americium-243.) In one experiment, six replicate coulometric analyses of an americium-241 solution gave 787 ± 5 μg of ^{241}Am per ml, whereas α-activity measurements of the same solution gave 779 ± 10 μg ^{241}Am per ml. A 2π gas proportional counter was

used, and the half-life of americium-241 was taken as 433 years[17]. The accuracy of the coulometric procedure was checked further in a second experiment. A solution that contained both ^{241}Am and ^{243}Am was prepared carefully, from radiochemically pure ^{241}Am and ^{243}Am solutions that had been analyzed coulometrically. The ratio of the α-radioactivities of the two isotopes in this solution was determined with electrodeposited sources and a silicon surface barrier detector. Given this activity ratio, and the half-lives of the two isotopes[17,18], and the concentration of ^{243}Am in the original ^{243}Am solution, it is possible to compute the concentration of ^{241}Am in the original ^{241}Am solution. This result was 1.458 ± 0.06 mg ^{241}Am/ml for two replicate analyses. The result obtained by the coulometric procedure was 1.472 ± 0.004 mg ^{241}Am/ml for five replicate analyses.

Neptunium, plutonium, cerium and curium were considered as contaminants that might interfere in this method. Both neptunium and plutonium are oxidized to their hexavalent oxidation states by persulfate, but as the curve in Fig. 3 indicates, their hexavalent states are not reduced at 1.05 V *vs.* S.C.E. Neither neptunium or

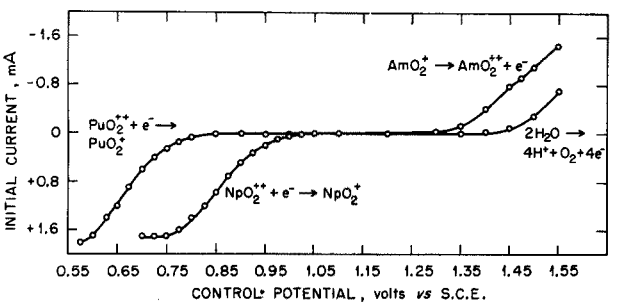

Fig. 3. Current–potential curves for pertinent couples.

plutonium interfered when present in amounts equal to americium. Cerium, another element which occasionally occurs with americium, interferes seriously, however, because it is partially oxidized by persulfate to cerium(IV) which is reducible at 1.05 V *vs.* S.C.E. There is no obvious method for eliminating cerium interference; separation is required. Although curium does not interfere directly, the high specific activity of ^{242}Cm or ^{244}Cm causes generation of radiolytic decomposition products from water which chemically reduce americium(VI) and cause low results in the titration. Determination of 1 mg of americium-243 in the presence of 0.2, 0.9, 1.8, and 3.6 mg of ^{244}Cm gave results which were in error by +0.4, −0.7, −2.1, and −6.4%, respectively. Determination of americium in the presence of ^{244}Cm is thus limited to ^{244}Cm levels of a few tenths of milligrams; otherwise a separation is required.

The controlled-potential coulometric determination described herein provides a relatively simple and straightforward means for determining milligram amounts of americium with excellent precision and accuracy. The method yields analytical results that are based upon electrical calibration, and compare well with chemical standards. The present method should be useful, not only for analysis of moderate-to-high-purity americium compounds, but also for studies aimed at evaluating and/or re-evaluating several fundamental chemical or physical properties of americium and its isotopes.

We gratefully acknowledge the assistance of W. R. MUSICK with the emission spectrographic analyses.

SUMMARY

Controlled-potential coulometry has been studied as a means for the precise and accurate determination of americium. Americium is chemically oxidized to the hexavalent state, and then coulometrically reduced from americium(VI) to americium-(V) at a platinum electrode controlled at 1.05 V *vs.* S.C.E. The results of repetitive analysis of standard solutions prepared from high-purity americium-243 dioxide agree within a few tenths percent with standard values for 0.4–1.3 mg of americium.

RÉSUMÉ

La coulométrie à potentiel contrôlé peut être appliquée au dosage précis et exact de l'américium. Ce dernier est oxydé chimiquement à l'état hexavalent et réduit ensuite coulométriquement de Am(VI) en Am(V) à une électrode de platine à potentiel contrôlé 1.05 V *vs.* ECS. Les résultats obtenus avec des dosages répétés de solutions standards, préparées à partir de dioxyde d'américium-243 extrèmement pur, correspondent, à quelques dizièmes de pour cent près, aux étalons d'américium de 0.4 à 1.3 mg.

ZUSAMMENFASSUNG

Die Coulometrie mit kontrolliertem Potential wurde untersucht, inwieweit sie sich zur genauen und richtigen Bestimmung von Americium eignet. Das Americium wird chemisch zur 6-wertigen Stufe oxidiert und dann coulometrisch an einer Platinelektrode mit einem kontrollierten Potential von 1.05 V vom Am(VI) zum Am(V) reduziert. Die Ergebnisse wiederholter Analysen mit Standardlösungen die aus hochreinem Americium-243-dioxid hergestellt wurden, stimmen bis auf wenige Zehntel Prozent mit Standardwerten von 0.4–1.3 mg Americium überein.

REFERENCES

1 F. L. MOORE, *Anal. Chem.*, 35 (1963) 715.
2 D. L. DAVIS AND F. L. OETTING, *Analysis of Americium by Calorimetry*, USAEC Rept. RFP-895, 1967.
3 G. R. HALL AND P. D. HERNIMAN, *J. Chem. Soc.*, (1954) 2214.
4 G. KOEHLY, *Anal. Chim. Acta*, 33 (1965) 418.
5 R. C. PROPST, private communication.
6 H. C. JONES, W. D. SHULTS AND J. M. DALE, *Anal. Chem.*, 37 (1965) 680.
7 T. B. ASPREY, S. E. STEPHANOU AND R. A. PENNEMAN, *J. Am. Chem. Soc.*, 73 (1951) 5715.
8 M. WARD AND G. A. WELCH, *J. Chem. Soc.*, (1954) 4038.
9 J. R. STOKELY, JR. AND F. L. MOORE, *Anal. Chem.*, 39 (1967) 994.
10 I. M. KOLTHOFF AND I. K. MILLER, *J. Am. Chem. Soc.*, 73 (1951) 3055.
11 L. MEITES AND S. A. MOROS, *Anal. Chem.*, 31 (1959) 23.
12 J. S. COLEMAN, *Inorg. Chem.*, 2 (1963) 53.
13 S. R. GUNN, *Thermodynamics of Aqueous Ions of Americium*, UCRL-2541, 1954.
14 R. A. PENNEMAN AND T. B. ASPREY, *The Formal Potential of Am(V)–Am(VI) Couple*, USAEC Rept. AECU-936, 1950.
15 T. B. ASPREY AND B. B. CUNNINGHAM, *Equilibria in the Oxide Systems of Praseodymium and Americium*, USAEC Rept. UCRL-329, 1955.
16 T. D. CHIKALLA AND T. EYRING, *J. Inorg. & Nucl. Chem.*, 29 (1967) 228.
17 F. OETTING AND S. R. GUNN, *J. Inorg. & Nucl. Chem.*, 29 (1967) 2659.
18 L. C. BROWN AND R. C. PROPST, A New Determination of the Half-Life of ^{243}Am, accepted for publication in the *J. Inorg. & Nucl. Chem.*

Analytica Chimica Acta
Elsevier Publishing Company, Amsterdam
Printed in The Netherlands

THE SPECTROFLUORIMETRIC DETERMINATION OF GALLIUM, INDIUM AND ZINC WITH 2,2'-PYRIDYLBENZIMIDAZOLE

L. S. BARK AND A. RIXON
Department of Chemistry, University of Salford, Salford, 5, Lancs. (England)
(Received January 4th, 1969)

The metals cadmium, gallium, indium and zinc are often produced from the same mineral source. Since there is now an industrial demand for high-purity samples of these metals, highly sensitive methods for the determination of each in the presence of the others are necessary. Most of the reagents reported for the fluorimetric determination of zinc and cadmium are based on the 8-substituted quinolines[1], but such methods suffer from interferences by small amounts of numerous metal ions so that their use is somewhat restricted.

From a consideration of molecules containing suitable functional groups for chelation with these metals and suitable groups for use as fluorimetric reagents, it was decided to investigate the use of 2,2'-pyridylbenzimidazole, which contains the =N=C=C=N= ferroin-grouping and which in chelation, will probably be sufficiently rigid to cause enhancement of the fluorescence. There is potentially a large pathlength for electronic delocalisation, which is highly favourable for fluorescence.

Although 2,2'-pyridylbenzimidazole has been previously reported as a colorimetric reagent for iron(II)[2], and studies of the stability and structures of some pyridylbenzazole metal complexes have been reported[3–6], no work has been previously reported on the fluorimetric aspects of any metal complexes of these reagents. In the present paper, methods are described for the determination of zinc and indium or gallium in presence of each other.

EXPERIMENTAL

Reagents and solutions

2,2'-Pyridylbenzimidazole. The compound was prepared by a published method[7]. The product was repeatedly recrystallised from ethanol until the melting point, elemental analysis and infrared spectra agreed with previously reported data, or did not change. $1.00 \cdot 10^{-3}$ *M* and $1.00 \cdot 10^{-4}$ *M* solutions of the reagent were prepared in fluorimetrically pure ethanol, and were stable for over 6 months.

Metal salt solutions. All metal salt solutions were prepared in deionised, distilled water which was fluorimetrically pure. The appropriate metal solutions were prepared from high-purity elements or from appropriate salts which had been purified and assayed by conventional methods.

Buffer solutions. A series of buffer solutions was prepared to cover the pH ranges of pH 3.0–5.0 (potassium hydrogen phthalate/hydrochloric acid/sodium hydroxide) and pH 4.0–7.0 (sodium acetate/acetic acid).

Treatment of glassware

To prevent adsorption of the metal ions onto the active surface of the glassware, all interior surfaces of all glass containers except the sample cells, were treated with a 0.1% (w/v) solution of tetrabutyl titanate in cyclohexane. The surfaces were allowed to drain in air, and dried at 40°–60° for 24 h. Slow hydrolysis of the titanate occurred, giving a polymeric layer of butoxy-titanium groups, which act as an effective barrier between the solution and the glass surface.

Instrumentation

The fluorescence measurements were made with an Aminco-Bowman spectrofluorimeter which had a modified cell carrier. This was fitted with aluminium mirrors to ensure total reflection of the emergent unabsorbed light and of the fluorescent light opposite the photomultiplier slit. Slit widths were adjusted to give a 10-nm band, both in the excitation and the emission monochromators. The solutions were contained in fused 10-mm quartz cells which were thermostatted at $25 \pm 0.1°$.

Calibration curves for zinc, indium, gallium

Calibration curves for the three metal species were prepared by adding a measured amount of standard solutions of the metal salts dissolved in fluorimetrically pure water. The appropriate buffer solution (5 ml) was then added, along with 10 ml of the reagent solution (10^{-4} *M* for Zn and In, or 10^{-3} *M* for Ga) in purified ethanol. The mixture was then diluted to 100 ml, stirred to achieve homogeneity and allowed to stand for a fixed time at $25 \pm 1°$. The fluorescence of each solution was measured at a previously determined wavelength.

The experimental conditions are summarised in Table I, and the ranges are also given. In each case, the plots were linear and passed through the origin.

TABLE I

CONDITIONS FOR CALIBRATION CURVES

Conditions	*Ga*	*In*	*Zn*
Excitation wavelength (nm)	347	335	330
Emission wavelength (nm)	413	411	398
Concn. of reagent	10^{-3} *M*	10^{-4} *M*	10^{-4} *M*
pH of buffer	4.09	5.2	5.8
Time of development (min)	30	30	30
Range for Beer's law 10^{-4} *M*		0–10 ml	0–10 ml
10^{-5} *M*	0–30 ml	0–20 ml	0–10 ml
Slope of Beer's law plot (Change of R.I./μM of Me).	2.68	1.35	3.4

Sensitivity

The minimum amount of ion which could be determined, was defined arbitrarily as that amount which, under the experimental conditions, would give a signal-to-noise ratio of 2:1. These amounts were determined for each metal. The minimum volume for convenient working is 5 ml of solution. This allows up to 2 ml for washing out of optical cells, and sufficient solution to fill two of the cells normally used for the measurements. This volume is comprised of 4 ml of the metal salt solution

(adjusted to about pH 7), 0.5 ml of 10^{-4} *M* or 10^{-3} *M* reagent (10^{-3} *M* for Ga) and 0.5 ml of the appropriate buffer.

The minimum determinable amounts of each metal ion, under these conditions, were:

Zinc 0.8 nmoles or 50 ng.
Gallium 4.0 nmoles or 280 ng.
Indium 4.0 nmoles or 450 ng.

RESULTS AND DISCUSSION

Spectral characteristics of the reagent and the metal complexes, and the effect of pH

The reagent spectra (both absorption and emission) consist of single narrow peaks, with pronounced maxima at 311 nm and 381 nm respectively. Similarly shaped spectra were recorded for each of the metal complexes (Table II). In all cases the complexes showed maximum fluorescence at a particular pH (Fig. 1). The reagent spectrum showed a decrease in fluorescence with increase in pH up to about pH 7.0, probably because of removal of protons from the protonated species formed in acidic solution; similar effects have been noted by many workers. The relative sharpness of the curves in Fig. 1 indicates the need to control the pH to $\pm$0.1 pH units, by means of suitable buffer systems.

TABLE II

SPECTRAL CHARACTERISTICS OF THE REAGENT AND METAL COMPLEXES

(All solutions are 10^{-5} *M*)

	λ_{ex}	λ_{em}	*pH*	*R.I.*[a]
Reagent	311	381	7.0	1.59
Zinc complex	330	398	5.8	2.23
Gallium complex	347	413	4.4	0.52
Indium complex	335	411	5.2	1.29

[a] Relative Intensity (R.I.) is the product of the reading of the meter multiplier galvanometer and the shunt stage of the instrument.

The effect of excess of reagent and time of development

At the very low concentrations of metal ion used, it was necessary to have a large excess of reagent in all cases. To establish the optimal amount of reagent for each case, the metal ion was treated with the same volume of reagent solution containing different concentrations, and the solution was allowed to attain maximum fluorescence, which was then measured against a blank solution containing the same amount of reagent, under the same experimental conditions. Both zinc and indium reached maximum fluorescence with a *ca.* 10-fold molar excess of reagent to metal (Fig. 2). For gallium it was necessary to use about 30 times the stoichiometric amount of reagent.

The necessity of a large excess of reagent (especially in the case of gallium) indicates not only the relative difficulty of forming the complex but also its relative instability. This latter point is confirmed by the shape of the Job's plots[8] (Fig. 3)

which were done to investigate the nature of the three metal complex systems; the shallowness of the gallium curve indicates a complex of low stability.

The development of maximum fluorescence is not instantaneous, but occurs slowly and reaches a maximum about 15 min after mixing. To allow for any variations caused by slight changes in ambient conditions, a development time of 30 min was

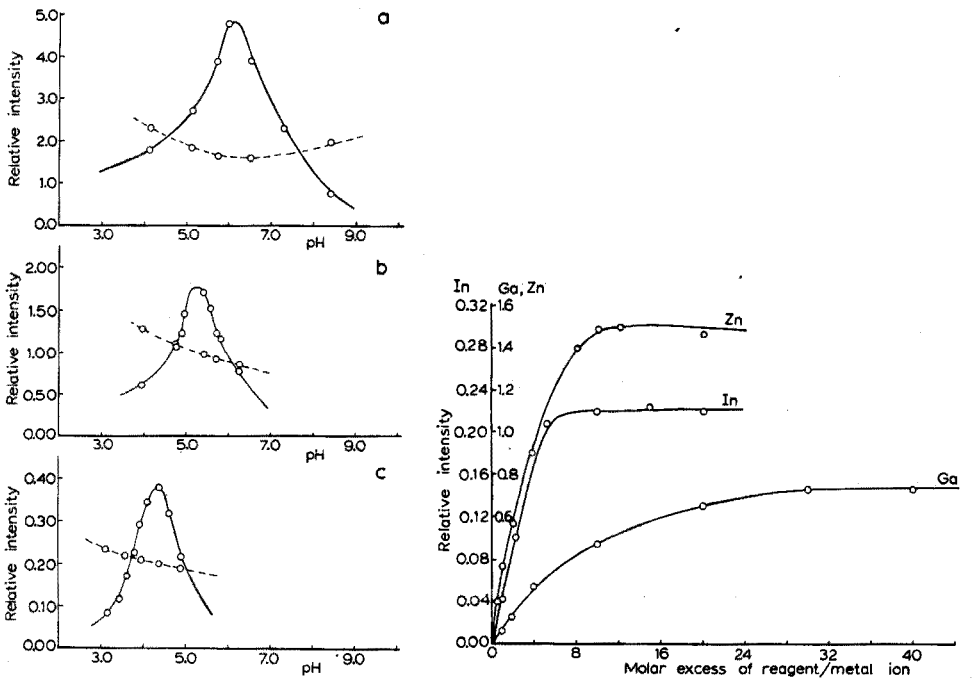

Fig. 1. Effect of pH. (———) Complex, (– – – –) reagent. 10^{-5} *M* solutions of zinc (a), indium (b) and gallium (c).

Fig. 2. Effect of excess of reagent. Initial metal concentrations: Zn^{2+} $2 \cdot 10^{-6}$ *M*, Ga^{3+} $1 \cdot 10^{-6}$ *M*, In^{3+} $1 \cdot 10^{-6}$ *M*.

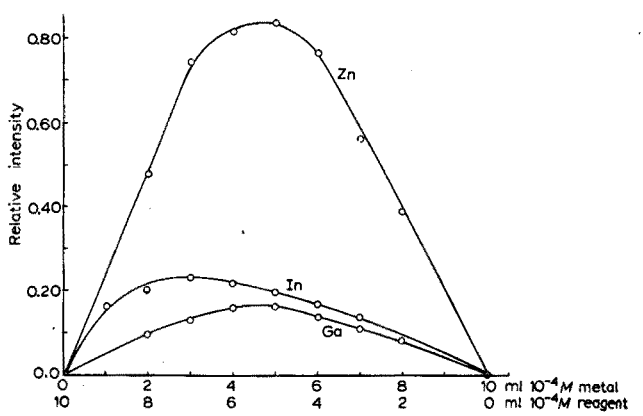

Fig. 3. Methods of continuous variations.

used. No significant variation in the amount of fluorescence occurred after this time; measurements made at intervals up to 10 days indicated that once the complexes are formed they are stable both photochemically and under the thermal variations encountered in a non-thermostatted laboratory.

The effect of foreign ions

The effects on each system of a 100-fold molar excess of each of the following ions were investigated: Al, Be, Sb(III), Ba, Bi(III), Cd, Cr(III), Co(II), Ca, Ce(III), Ce(IV), Cu(I), Cu(II), Fe(II), Fe(III), Ge, La(III), Pr(III), Nd(III), Sm(III), Eu(II), Gd(III), Tb(III), Dy(III), Ho(III), Er(III), Yb(III), Lu(III), Pb(II), Hg(I), Hg(II), Mg, Mn(II), Ni, Pt(II), Pt(IV), Pd(II), Os(VIII), Ag, Sr, Tl(I), Th, TiO^{2+}, UO_2^{2+}, VO^{2+}, Zr, F^-, Cl^-, Br^-, I^-, ClO_3^-, ClO_4^-, BrO_3^-, IO_3^-, oxalate, tartrate, benzoate, CN^-, SCN^-, SO_4^{2-}, SO_3^{2-}, $S_2O_3^{2-}$, S^{2-}, SeO_4^{2-}, MoO_4^{2-}, WO_4^{2-}.

The fluorescence was quenched by Co(II), Ce(IV), Cu(I), Cu(II), Fe(III), Hg(II), Ni(II), MoO_4^{2-}, Pt(IV), Pd(II), Ag(I), S^{2-}. Bismuth was precipitated at the pH values used and caused some interference, probably by adsorption of the reagent and also by coprecipitation of the zinc. Cadmium ions caused enhancement of the fluorescence. Of the interfering ions mentioned, cerium(IV) can be reduced to cerium(III), which does not interfere, and iron(III) can be reduced to iron(II).

For gallium and indium, it is possible to separate all the other interfering ions by addition of sodium benzoate at pH *ca.* 7.0, and extraction of the gallium and indium benzoates into ethyl acetate[9]. The gallium and indium may be re-extracted into an aqueous 0.1 *M* hydrochloric acid solution. In practice, it was found easier to allow the ethyl acetate layer to evaporate on a water bath; the benzoic acid subsequently formed did not interfere.

The removal of interfering ions in the zinc system presented greater difficulties. Whilst it is possible to separate zinc from the other ions by reduction with sodium dithionite, the excess of dithionite quenched the fluorescence. However, the removal of the interferences by reduction with hypophosphite was possible. The zinc complex was not apparently affected and even a 1,000-fold excess of hypophosphite had no effect on the reagent.

The most troublesome interference was that caused by cadmium ions. It was overcome by allowing maximum fluorescence to develop (30 min) and then by adding a 1–2 molar excess of sulphide ion (calculated on cadmium concentration). After the mixture had been allowed to stand for a further 10 min, the fluorescence was measured; this fluorescence was proved to be that of the zinc complex alone, the cadmium complex having been decomposed. When a large excess of sulphide ion was added, the fluorescence began to decrease after 20–30 minutes, the rate of decrease being related to the amount of sulphide ion. When the amount of sulphide ion added was exactly equivalent to the amount of cadmium ion present, then the fluorescence of the zinc/cadmium solution stayed constant over 6 days.

PROPOSED METHODS

Determination of zinc in the range 15–800 ng/ml

For solutions not containing interfering ions. To 4 ml of the sample solution add 0.5 ml of pH 5.8 buffer (sodium acetate/acetic acid) and 0.5 ml of 10^{-4} *M* 2,2′-

pyridylbenzimidazole in ethanol. Allow the solution to stand for 30 min and then irradiate at 330 nm; measure the fluorescent radiation at 398 nm. Compare the fluorescence with that of a blank solution containing the same amount of reagent at the same pH.

For solutions containing interfering ions other than gallium or indium. To 4 ml of the solution containing zinc, add 1 drop of 10% (w/v) aqueous sodium hypophosphite solution, warm to coagulate any precipitate formed, centrifuge, transfer the solution quantitatively to a 5-ml flask with a mixture of equal volumes of pH 5.8 buffer and 10^{-4} *M* 2,2'-pyridylbenzimidazole in ethanol and make up to the mark. Allow the fluorescence to develop for 30 min. Remove 1–2 ml for measurement as before. To 2 ml of the remainder, add 1 drop of 10^{-4} *M* sodium sulphide in water. Allow to stand for 5–10 min and measure the fluorescence. Any decrease in fluorescence is caused by removal of cadmium ions. The excess of sulphide and hypophosphite have no effect over the time range quoted.

For solutions containing gallium and indium and other interfering ions. Remove the gallium and/or indium by extraction as benzoates, using ethyl acetate as the extractant (see below). Then proceed as above.

Determination of gallium or indium

To *ca.* 10 ml of a solution containing 70–700 ng of gallium/ml or 110–1000 ng of indium/ml, add 1 ml of aqueous 50% (w/v) ammonium acetate solution and 1 ml of aqueous 25% (w/v) sodium benzoate solution. Mix well, add 2–3 ml of freshly distilled ethyl acetate, and shake vigorously for 1–2 min. Separate the two phases, re-extract the aqueous layer with more ethyl acetate, combine the organic phases, add 1–2 ml of water with 1–2 drops of 0.1 *M* hydrochloric acid, and warm gently until all the organic phase has evaporated. Transfer the aqueous phase to a standard flask with the appropriate buffer (pH 5.2 for indium; pH 4.4 for gallium). Add 0.5 ml of an ethanolic solution of the reagent (10^{-4} *M* for indium; 10^{-3} *M* for gallium), and dilute to the mark with buffer. Allow the solutions to stand for 30 min and then irradiate and measure the fluorescence at the appropriate wavelength (gallium $\lambda_{ex}=347$ nm, $\lambda_{em}=413$; indium $\lambda_{ex}=335$ nm, $\lambda_{em}=411$).

Precision and accuracy

Precision data were obtained by multiple (10) analyses of a series of solutions of each metal. The relative standard deviations found were as follows: for zinc at the 130 ng/ml^{-1} level, 1.1%; for indium at the 115 ng/ml^{-1} level, 2.3%; and for gallium at the 400 ng/ml^{-1} level, 4.8%.

A series of known mixtures was also prepared and the relevant metal was determined by the appropriate procedure outlined above; four analyses were done on each mixture, with the results shown in Table III.

The nature of the complexes

Plots were made of the mole ratios of reactants against the fluorescence of the complexes (compensated for the fluorescence due to the uncomplexed reagent). In all these cases, it was assumed that the stability of the complex was such that the amount of reagent in solution, caused by the dissociation of the complex, was practically negligible. Within the limits imposed by this assumption, the plots

TABLE III

ANALYSIS OF MIXTURES

Metal determined	*Mixture used*	*Metal found (nM)*	
		Maximum	*Minimum*
Zinc	50 nM Ga + 50 nM In + 10 nM Zn	10.6	9.45
Indium	100 nM Zn + 10 nM In	10.17	9.82
Gallium	100 nM Zn + 10 nM Ga	10.05	9.99

indicated that the metal complexes have a reagent: metal ratio of 2:1 for indium and 1:1 for both gallium and zinc (Fig. 3).

The complexes prepared for zinc, by reacting relatively concentrated solutions of zinc ions and the reagent, always had the composition $[Zn_1\ Reagent_2]^{2+}$. Attempts to elucidate the structure of the 1:1 complex have not been successful.

We wish to acknowledge the award of a Studentship to one of us (A.R.) by the Science Research Council.

SUMMARY

The spectrofluorimetric determination of nanogram amounts of gallium, indium and zinc with 2,2'-pyridylbenzimidazole is described. Zinc can be determined in the range 15–800 ng/ml, gallium 70–700 ng/ml and indium 110–1,000 ng/ml, with standard deviations of 1.1%, 4.8% and 2.3%, respectively. Interferences can be avoided by extraction, reduction or precipitation procedures. Methods are proposed for the determination of zinc in the presence of gallium and indium, and for gallium or indium in the presence of zinc.

RÉSUMÉ

On décrit une méthode d'analyse par spectrofluorimétrie pour le dosage du gallium, de l'indium et du zinc, à l'aide de 2,2-pyridylbenzimidazole. Les concentrations suivantes peuvent être mesurées: 15 à 800 ng/ml pour le zinc; 70 à 700 ng/ml pour le gallium et 110 à 1,000 ng/ml pour l'indium avec des déviations standards de 1.1%, 4.8% et 2.3% respectivement. Les interférences peuvent être évitées par des procédés d'extraction, de réduction ou de précipitation. On propose des méthodes pour le dosage du zinc en precence de gallium et d'indium, et pour le gallium ou l'indium en présence de zinc.

ZUSAMMENFASSUNG

Die spektralfluorimetrische Bestimmung von Nanogrammen Gallium, Indium und Zink mit 2,2'-Pyridylbenzimidazol wird beschrieben. Störungen können durch Extraktions-, Reduktions- oder Fällungsverfahren vermieden werden. Zink kann im Bereich von 15–800 ng/ml, Gallium von 70–700 ng/ml und Indium von 110–1000 ng/ml mit Standardabweichungen von 1.1%, 4.8% bzw. 2.3% bestimmt werden. Es werden

Methoden zur Bestimmung von Zink in Gegenwart von Gallium und Indium und für Gallium oder Indium in Gegenwart von Zink vorgeschlagen.

REFERENCES

1 C. E. WHITE, *Anal. Chem.*, 40 (1968) 116R.
2 J. L. WALTER AND H. FREISER, *Anal. Chem.*, 26 (1954) 217.
3 T. J. LANE, I. NAKAGAWA, J. L. WALTER AND A. J. KANDATHIL, *Inorg. Chem.*, 1 (1962) 267.
4 T. R. HARKINS, J. L. WALTER, O. E. HARRIS AND H. FREISER, *J. Am. Chem. Soc.*, 78 (1956) 260.
5 B. CHISWELL, F. LIONS AND B. MORRIS, *Inorg. Chem.*, 3 (1964) 110.
6 T. R. HARKINS AND H. FREISER, *J. Am. Chem. Soc.*, 78 (1956) 1143.
7 D. VON JERCHEL, M. KRACHT AND K. KRUCKER, *Ann. Chem.*, 590 (1954) 232.
8 P. JOB, *Ann. Chem.*, 9 (1928) 113.
9 E. B. SANDELL, *Colorimetric Metal Analysis*, 3rd Edn., Interscience, New York, 1959, p. 801.

Analytica Chimica Acta
Elsevier Publishing Company, Amsterdam
Printed in The Netherlands

THE SOLVENT EXTRACTION OF ALKALI METAL TETRAPHENYLBORATES

TATSUYA SEKINE* AND DAVID DYRSSEN
Department of Analytical Chemistry, University of Göteborg, 402 20 Göteborg 5 (Sweden)
(Received January 16th, 1969)

The use of tetraphenylborate (TPB) as an analytical reagent was, according to the review by FLASCHKA AND BARNARD[1], extended very widely during the decade 1950–1960. In most of the previous work, the reagent has been used to form insoluble precipitates mainly with ammonium, potassium, rubidium and cesium ions, and the alkali metal ions have then been separated by filtration or centrifugation of these precipitates. Attempts have, however, also been made to separate alkali metal ions by solvent extraction of their tetraphenylborates. FIX[2] studied the extraction of rubidium and cesium into nitrobenzene from aqueous 0.1 *M* sodium tetraphenylborate solution. HANDLEY AND BURROS[3] studied the extraction of cesium tetraphenylborate at tracer concentration into amyl acetate, and FINSTON[4], also studying this system, showed that cesium in the organic phase could be stripped by 3 *M* hydrochloric acid. In a similar manner, TESTEMALE AND GIRAULT[5] determined ^{137}Cs in radioactive wastes by extraction into 0.05 *M* NaTPB in isoamyl alcohol. The solvent extraction of cesium and francium tetraphenylborates has been studied by HARUYAMA *et al.*[6] and the extraction of ion-pairs into polar solvents has been described in the review by DIAMOND AND TUCK[7].

In the present work the extraction of potassium, rubidium and cesium tetraphenylborates has been studied at low concentrations. In addition we have tried to clarify the equilibria involved in these systems and to assess the possibility of separating the alkali metal ions by solvent extraction. Most of the previous work seems to have neglected the details of the equilibria involved in the systems.

EXPERIMENTAL

Reagents

Cesium-134 and rubidium-86 were obtained from the Radiochemical Center, Amersham, England. Each of the tracer solutions obtained was diluted with water and used as a stock solution. Potassium carbonate (100 mg) was irradiated with thermal neutrons in the R2 reactor at the Swedish Atomic Research Institute at Studsvik and was dissolved in dilute perchloric acid in order to provide a neutral potassium-42 stock solution.

All the reagents were of C.P. grade. Sodium perchlorate was recrystallized twice from water. Hexone (methyl isobutyl ketone) was obtained from Fisher

* Present address: Department of Chemistry, Science University of Tokyo, Kagurazaka, Shinjuku-ku, Tokyo, Japan.

Scientific Co., U.S.A., and TBP (tributyl phosphate) was obtained from Eastman Kodak Chemicals, U.S.A. The solvents were washed with 0.1 *M* perchloric acid, 0.1 *M* sodium hydroxide and finally several times with water. Nitrobenzene was obtained from Kistner Co., Sweden, nitromethane from Fisher Scientific Co. and nitroethane from Dr. Theodor Schuchardt Co., West Germany. These reagents were washed twice with water. Sodium tetraphenylborate (NaTPB, Kalignost reagent) was obtained from Merck AG, West Germany. Doubly distilled water was used in all cases.

Experimental procedure

All the determinations were carried out in a thermostatted room at 25°. Stoppered glass tubes (volume 50 ml) were used to equilibrate the organic and the aqueous phases. A given amount of one of the tracer solutions was placed in each tube followed by various amounts of the sodium tetraphenylborate solution. After addition of sodium perchlorate solution or water until the aqueous phase in each tube was 10.0 ml, 10.0 ml of one of the organic solvents was added. A small amount of cesium chloride was added as carrier in the experiments with cesium. The initial concentration of potassium, rubidium or cesium in the aqueous phase was always 10^{-4} *M*. The two phases were agitated vigorously for 3 min by a mechanical shaker and then separated by centrifugation. A 5-ml portion was pipetted from each phase and transferred to a small polyethylene test tube. The γ-radioactivity of the solution was measured with a well-type scintillation counter. Some measurements were carried out on the distribution of sodium ion with a Perkin-Elmer atomic absorption spectrometer, Model-303. A measured amount of sodium tetraphenylborate was dissolved in nitrobenzene and used as a standard and each organic phase was diluted with nitrobenzene until it contained 20–60 μM sodium ion before analysis. The sodium content in some organic layers was also checked gravimetrically, as follows. A 5-ml portion was pipetted from the organic phase which had been equilibrated with aqueous sodium tetraphenylborate solution and placed in a stoppered glass tube. The solvent was then shaken three times with 5 ml of 1 *M* hydrochloric acid to decompose tetraphenylborate ion and to back-extract the sodium into the aqueous phase, the aqueous phase being subsequently evaporated in a platinum dish. Hydrochloric acid was added to the residue in the platinum dish and the solution was re-evaporated. The residue was finally heated on a hot plate and the amount of sodium was determined as sodium chloride.

The net distribution ratio of the metal ions was calculated as follows:

$$D = \frac{[\mathrm{M}]_{\mathrm{org,\,total}}}{[\mathrm{M}]_{\mathrm{aq,\,total}}} = \frac{\gamma\text{-count-rate per ml org. phase}}{\gamma\text{-count-rate per ml aq. phase}}$$

The net distribution ratio of sodium ion was determined from the atomic absorption data or gravimetric data as follows:

$$D = [\mathrm{Na}]_{\mathrm{org}}/([\mathrm{Na}]_{\mathrm{initial}} - [\mathrm{Na}]_{\mathrm{org}})$$

RESULTS

Two-phase distribution of sodium tetraphenylborate

As tetraphenylboric acid is unstable in aqueous solution, this reagent is

generally supplied as the sodium salt. In the present study, this salt was always added initially to the aqueous phase containing the tracer of potassium, rubidium or cesium ion, and the tetraphenylborates of these heavy alkali metal ions were extracted into the organic phase. The distribution of sodium tetraphenylborate between water and nitrobenzene was, moreover, studied in the absence of sodium perchlorate in order to be able to determine the concentration of sodium tetraphenylborate in nitrobenzene in equilibrium with various initial concentrations of aqueous sodium tetraphenylborate. The results are given in Table I. It may be seen that about 90% is extracted into nitrobenzene.

TABLE I

DISTRIBUTION OF SODIUM TETRAPHENYLBORATE (NaTPB) BETWEEN NITROBENZENE AND WATER

$[NaTPB]_{initial,\,aq}$	$[Na]_{org}$	
(M)	*Atomic absorption*	*Gravimetry*
$1.0 \cdot 10^{-1}$	$7.8 \cdot 10^{-2}$	$9.0 \cdot 10^{-2}$
$5.0 \cdot 10^{-2}$	$4.5 \cdot 10^{-2}$	$4.4 \cdot 10^{-2}$
$3.0 \cdot 10^{-2}$	$2.7 \cdot 10^{-2}$	$2.6 \cdot 10^{-2}$
$1.0 \cdot 10^{-2}$	$9.1 \cdot 10^{-3}$	$9.4 \cdot 10^{-3}$
$3.0 \cdot 10^{-3}$	$2.7 \cdot 10^{-3}$	
$1.0 \cdot 10^{-3}$	$8.3 \cdot 10^{-4}$	
$3.0 \cdot 10^{-4}$	$2.7 \cdot 10^{-4}$	
$1.0 \cdot 10^{-4}$	$9.6 \cdot 10^{-5}$	

TABLE II

DISTRIBUTION OF ALKALI METAL IONS BETWEEN VARIOUS ORGANIC SOLVENTS AND SODIUM PERCHLORATE SOLUTIONS

Organic solvent	$[NaClO_4]$	*Distribution ratio* $\cdot 10^4$			
	(M)	Na^+	K^+	Rb^+	Cs^+
Nitrobenzene	0.1	1.2	63	400	1500
	1.0	0.94	44	220	980
	3.0	0.95	29	93	270
	5.0	1.4	14	32	95
Nitromethane	0.1	1500	5700		18000
	1.0	1200	3800		9600
	3.0	1000	2200		4600
	5.0	830	1300		2100
Nitroethane	0.1	380	1200		4000
	1.0	350	770		2100
	3.0	250	400		870
	5.0	100	170		230
Hexone	0.1	35	39		46
	1.0	67	82		67
	3.0	95	73		65
	5.0	120	68		49
TBP	0.1	610	510		530
	1.0	1600	1400		1500
	3.0	1200	980		890
	5.0	530	340		260

Extraction of alkali metal perchlorates

As sodium perchlorate solutions were used in most of the experiments, the extraction of the alkali metal perchlorates was studied in the absence of tetraphenylborate. Table II gives the net distribution ratios of the perchlorates as a function of the sodium perchlorate concentration in the aqueous phase. Table II shows that these metal ions are extracted into the organic phase to some extent even in the absence of tetraphenylborate ion; for example, more than 50% of cesium in 0.1 *M* sodium perchlorate solution is extracted into nitromethane by a single extraction. It was observed in the course of the experiments with nitromethane that at high sodium perchlorate concentrations the volume of the organic phase increased and that of the aqueous phase decreased after the two phases were equilibrated.

Extraction of heavy alkali metal ions in 0.1 M sodium perchlorate with 0.01 M (initial) sodium tetraphenylborate

Table III gives log *D* values and separation factors for the extraction of potassium, rubidium and cesium ions from 0.1 *M* sodium perchlorate solution,

TABLE III

DISTRIBUTION OF ALKALI METAL IONS BETWEEN VARIOUS ORGANIC SOLVENTS AND AN AQUEOUS SOLUTION CONTAINING 0.1 *M* SODIUM PERCHLORATE AND 0.01 *M* SODIUM TETRAPHENYLBORATE

(Initial concentrations in aqueous phase)

Solvent	*log D*			*Separation factor*	
	K^+	Rb^+	Cs^+	D_{Rb^+}/D_{K^+}	D_{Cs^+}/D_{Rb^+}
Nitrobenzene	0.888	1.603	2.476	5.2	7.5
Nitromethane	0.339	0.865	1.274	3.4	2.6
Nitroethane	0.516	1.164	1.696	4.4	3.4
Hexone	−0.629	−0.609	−0.377	1.0	1.7
TBP	−1.011	−1.028	−1.025	1.0	1.0

TABLE IV

SALTING-IN EFFECT OF ALKALI METAL TETRAPHENYLBORATES FOLLOWING THE ADDITION OF SODIUM PERCHLORATE TO THE AQUEOUS PHASE, INITIALLY CONTAINING 0.01 *M* NaTPB

Solvent	$[NaClO_4]$ *(M)*	*log D*		
		K^+	Rb^+	Cs^+
Nitrobenzene	0.1	0.863	1.603	2.490
	0.2	0.483	1.316	2.179
	0.5	0.086	0.841	1.658
	1.0	−0.401	0.324	1.130
	2.0	−0.810	−0.268	0.545
	3.0	−1.160	−0.614	0.124
	4.0	−1.436	−0.955	−0.237
Hexone	0.1	−0.679	−0.642	−0.377
	0.2	−0.955	−0.932	−0.717
	0.5	−1.388	−1.371	−1.188
	1.0	−1.680	−1.730	−1.638
	2.0	−1.889	−1.996	−1.963
	3.0	−1.935	−2.139	−2.132
	4.0	−1.917	−2.038	−2.174

initially containing 0.01 *M* sodium tetraphenylborate, into five organic solvents. It is clear that both the distribution ratios and the separation factors depend strongly on the organic solvent. Nitrobenzene gives the highest values for *D* and the separation factor.

Effect of sodium perchlorate on the tetraphenylborate extraction

Table IV and Fig. 1 illustrate the extraction of potassium, rubidium and cesium from aqueous solutions initially containing 0.01 *M* tetraphenylborate and various amounts of sodium perchlorate as a function of the initial concentration of

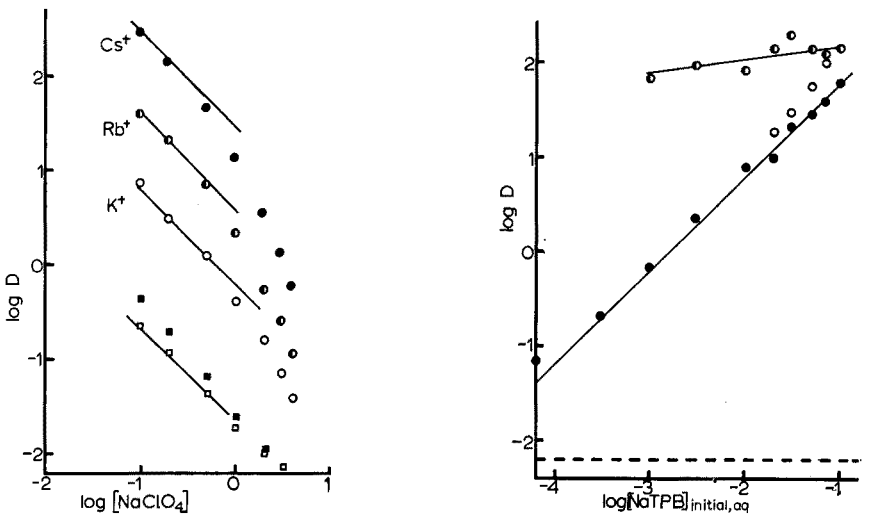

Fig. 1. The decrease in the distribution of alkali metal tetraphenylborate following the addition of sodium perchlorate to the aqueous solutions initially containing 0.01 *M* NaTPB. The open, semi-closed and closed circles represent data for the extraction of K^+, Rb^+ and Cs^+, respectively into nitrobenzene. The open and closed squares represent data for the extraction of Rb^+ and Cs^+, respectively, into hexone (the points representing the K^+ data are omitted since they coincide with the Rb^+ points). The lines are drawn with a slope of -1.

Fig. 2. The distribution of potassium tetraphenylborate between nitrobenzene and an aqueous phase of the following composition. (◐) NaTPB only (column A, Table V); (●) 0.1 *M* $NaClO_4$+ NaTPB (column C, Table V); (○) 0.1 *M* Na(TPB, ClO_4) (column B, Table V). For tetraphenylborate concentrations less than 10^{-2} *M* the results are represented by the closed circles. The straight line through the closed circles is drawn with the slope $+1$. The dashed line shows the distribution ratio for potassium when no sodium tetraphenylborate is added to the system (0.1 *M* $NaClO_4$ only).

sodium perchlorate in the aqueous phase. It can be seen that an addition of sodium perchlorate causes a remarkable decrease in the extraction of these ions as the tetraphenylborates (salting-in effect). For low concentrations of sodium perchlorate, the decrease in *D* is proportional to $[NaClO_4]$. Again, it should be noted that the separation factor is larger for nitrobenzene than for hexone.

The dependence of the extraction of potassium on the sodium tetraphenylborate concentration

Table V and Fig. 2 illustrate the extraction of potassium into nitrobenzene as

TABLE V

DEPENDENCE OF THE EXTRACTION OF POTASSIUM ON THE TETRAPHENYLBORATE CONCENTRATION

$[NaTPB]_{initial,aq}$	(A)	(B)	(C)
0.1	2.161	2.161	1.794
0.7	2.090	1.998	1.600
0.05	2.143	1.746	1.456
0.03	2.297	1.464	1.328
0.02	2.146	1.260	0.998
0.01	1.914	0.903	0.888
0.003	1.970	—	0.358
0.001	1.829	—	−0.178
0.003	—	—	−0.690
0.0001	—	—	−1.166
—	—	−2.200	−2.200

Column (A): log D for potassium when the aqueous phase initially contains NaTPB only.
Column (B): log D for potassium when the aqueous phase is a mixture of 0.1 M NaTPB and 0.1 M $NaClO_4$, *i.e.* 0.1 M Na(TPB,ClO_4).
Column (C): log D for potassium when the aqueous phase contains 0.1 M $NaClO_4$ in addition to NaTPB of various concentrations.

a function of the initial concentration of sodium tetraphenylborate in the aqueous phase. The semi-closed circles in Fig. 2 correspond to data obtained with an aqueous phase containing sodium tetraphenylborate and 10^{-4} M potassium ion only, while the open circles correspond to those obtained with an aqueous phase initially containing 0.1 M Na (TPB, ClO_4) and 10^{-4} M potassium ion (*i.e.* the aqueous phase was, in this case, prepared by mixing various amounts of 0.1 M sodium perchlorate solution and 0.1 M sodium tetraphenylborate solution). The closed circles represent the results obtained with an aqueous phase initially containing 0.1 M sodium perchlorate in addition to various amounts of sodium tetraphenylborate and 10^{-4} M potassium ion. The data corresponding to the open and the closed circles coincide for tetraphenylborate concentrations less than $3 \cdot 10^{-3}$ M, and the results in this region are therefore represented by closed circles only.

The results for rubidium and cesium showed a similar tendency to those for potassium, but it was not possible to determine the distribution ratios of these ions accurately under the same conditions as potassium, owing to their high distribution ratios, especially when the aqueous phase contained no sodium perchlorate. Figure 3 shows the distribution ratios of these ions between nitrobenzene and 0.1 M sodium perchlorate as a function of the initial sodium tetraphenylborate concentration in the aqueous phase. The straight lines in Fig. 3 show that D is proportional to $[NaTPB]_{initial,aq}$, although the distribution ratio for cesium deviates somewhat from linearity.

Effect of the addition of perchloric acid to the aqueous phase

The extraction of alkali metal ions with tetraphenylborate is decreased by the addition of perchloric acid to the aqueous phase. The decrease in the distribution ratio of rubidium with the hydrogen ion concentration of the aqueous phase, initially containing 0.05 M sodium tetraphenylborate and 0.05 M (Na, H)ClO_4 is exemplified in Table VI, and the graph log D *vs.* log $[NaTPB]_{initial,aq} - [HClO_4]_{initial,aq} + [H^+]$

obtained from the data in Table VI is shown in Fig. 4. It may be seen from Fig. 4 that the distribution ratio is proportional to the remaining concentration of tetraphenylborate ion if it is supposed that phenylboric acid, $C_6H_5B(OH)_2$ is the main product of the acid hydrolysis[1]. When an excess of perchloric acid is added the extraction becomes identical with that of rubidium perchlorate into nitrobenzene (*cf.* Table II).

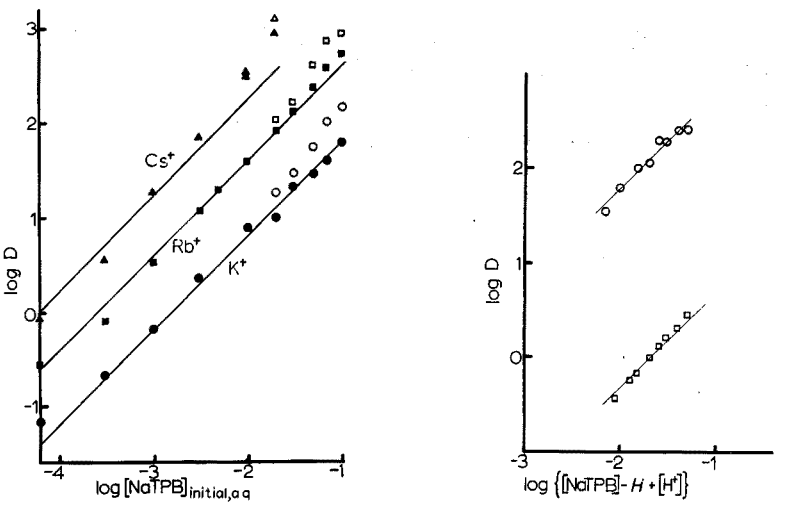

Fig. 3. The distribution of potassium (●, ○), rubidium (■, □) and cesium (▲, △) tetraphenylborate between aqueous solutions and nitrobenzene. The closed symbols indicate data obtained when the aqueous phase initially contained 0.1 *M* $NaClO_4$ and various amounts of NaTPB. The open symbols indicate data obtained when the aqueous phase was initially 0.1 *M* Na(TPB, ClO_4). The straight lines are drawn with slopes +1.

Fig. 4. Decrease in the extraction of rubidium into nitrobenzene (○) and into hexone (□) caused by the addition of perchloric acid. The aqueous phase initially contained 0.05 *M* (Na,H)ClO_4 and 0.05 *M* NaTPB in all cases. The term *H* represents the molarity of the perchloric acid added, and $[H^+]$ is the molar ion concentration at equilibrium. The straight lines are drawn with slopes +1.

TABLE VI

DECREASE IN THE EXTRACTION OF RUBIDIUM FROM AN AQUEOUS PHASE CONTAINING 0.05 *M* NaTPB ON THE ADDITION OF VARIOUS MIXTURES OF $NaClO_4$ AND $HClO_4$

Initial composition of the aqueous phase			*pH and* $[TPB^-]$ *at equilibrium*					
			Nitrobenzene			*Methyl isobutyl ketone*		
$[NaTPB]$ *(M)*	$[HClO_4]$ *(M)*	$[NaClO_4]$ *(M)*	*pH*	$[TPB^-]$[a]	*log D*	*pH*	$[TPB^-]$[a]	*log D*
0.05	0	0.05	8.90	0.05	2.41	6.64	0.05	0.45
0.05	0.01	0.04	6.39	0.04	2.40	3.76	0.04	0.30
0.05	0.02	0.03	6.13	0.03	2.28	3.25	0.031	0.21
0.05	0.025	0.025	5.95	0.025	2.30	3.09	0.026	0.11
0.05	0.03	0.02	4.26	0.02	2.06	2.94	0.021	0.00
0.05	0.035	0.015	4.20	0.015	2.00	2.90	0.016	−0.17
0.05	0.04	0.010	4.16	0.01	1.80	2.51	0.013	−0.24
0.05	0.045	0.005	2.67	0.007	1.55	2.41	0.0089	−0.44

[a] The concentration of TPB^- at equilibrium is calculated by eqn. (24).

It was observed in the other experiments that an addition of sodium hydroxide to aqueous phases which had been acidified with perchloric acid as described in Table VI and Fig. 4 increased the pH, but left the distribution ratio unchanged. These results indicate that the addition of strong acid to the system destroys tetraphenylborate by irreversible acid hydrolysis and that phenylborate cannot replace tetraphenylborate as an extracting agent for alkali metal ions.

Other observations

The extraction of rubidium ion from 0.1 *M* sodium tetraphenylborate was performed with various organic solvents and an initial rubidium concentration of 10^{-4} *M*. In these experiments it was observed that the recovery of rubidium from the two phases was not quantitative when the organic phase was isopropylether,

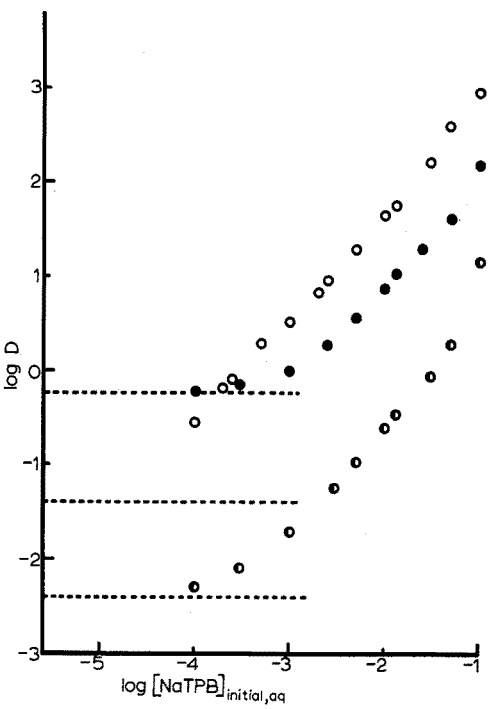

Fig. 5. The extraction of rubidium into nitrobenzene (○), into nitromethane (●) and into hexone (◐) from mixtures of 0.1 *M* Na(TPB, ClO_4) as a function of the initial concentration of tetraphenylborate. The dashed lines give the distribution ratio of rubidium perchlorate between these solvents and the aqueous phase in the absence of tetraphenylborate ion (−1.40 for nitrobenzene, −0.24 for nitromethane and −2.41 for hexone).

dichloroether, methyl isobutyl carbinol, benzene, chloroform, carbon tetrachloride or hexane, although rubidium tetraphenylborate was extracted to some extent into a number of these solvents. A quantitative recovery from the both phases was obtained only with the solvents listed in Table III. This is probably due to the low solubility of RbTPB.

Figure 5 illustrates the distribution of rubidium between 0.1 *M* Na(TBP, ClO_4)

and the organic solvents nitrobenzene, nitromethane and hexone as a function of the initial tetraphenylborate concentration.

It was, moreover, observed that the separation of the two phases was incomplete when solvents such as nitromethane, dichloroether or hexone were used; that is, even after a centrifugation at 2000 rev./min for 3 min, a turbidity was observed in the two phases or on the interface. The phase separation was very much improved when a small amount of sodium perchlorate was added to the aqueous phase.

DISCUSSION

The extraction of a monovalent ion, M^+, as an ion-pair with a monovalent anion, A^-, can be described by the following equilibrium

$$M^+ + A^- \rightleftharpoons MA(org) \quad (1)$$

The equilibrium constant is

$$K_{MA} = [MA]_{org}/[M^+][A^-] \quad (2)$$

The ion-pair in the organic phase may dissociate, especially in a solvent like nitrobenzene

$$MA(org) \rightleftharpoons M^+(org) + A^-(org) \quad (3)$$

$$K_{diss} = [M^+]_{org}[A^-]_{org}/[MA]_{org} \quad (4)$$

The constant $K_{MA}K_{diss} = K$ represents the equilibrium

$$M^+ + A^- \rightleftharpoons M^+(org) + A^-(org) \quad (5)$$

K being given by

$$K = [M^+]_{org}[A^-]_{org}/[M^+][A^-] \quad (6)$$

If it is assumed that M^+ and A^- do not associate in the aqueous phase and that no polymerization of any species occurs, then the net distribution ratio of the metal ion may be expressed as

$$D = [M]_{total,org}/[M]_{total,aq} = ([MA]_{org} + [M^+]_{org})/[M^+] \quad (7)$$

Distribution of sodium tetraphenylborate

Although the data in Table I are somewhat scattered, it can be concluded that about 90% of sodium tetraphenylborate in water is extracted into the same volume of nitrobenzene, and the distribution ratio of sodium tetraphenylborate ($D \approx 9$) is independent of its concentration in both phases. Thus, the following relations can be introduced:

$$[Na^+] = [TPB^-] \quad (8)$$

$$[Na^+]_{org} = [TPB^-]_{org} \quad (9)$$

From eqns. (2), (4), (7), (8) and (9), the distribution ratio for sodium can be obtained:

$$D = K_{MA}[Na^+] + \sqrt{K_{MA}K_{diss}} \quad (10)$$

According to the results in Table I, the distribution ratio of sodium is independent of the initial concentration of sodium tetraphenylborate in the aqueous phase. From eqn. (10) it can then be concluded that the extracted ion-pair in the organic phase is almost completely dissociated into sodium and tetraphenylborate ions *i.e.* K_{MA} is small, and the distribution ratio can be written as

$$D = \sqrt{K_{MA} K_{diss}} = \sqrt{K} \approx 9 \qquad (11)$$

As the ionic strength in the two phases is not constant when [NaTPB] is increased, the activity coefficients of the ionic species in each phase are altered, but since the total concentration of sodium tetraphenylborate is less than 0.1 *M*, eqn. (11) should be valid as a first approximation, and K for sodium tetraphenylborate is approximately 81.

Distribution of metal ions as perchlorates

In Table II, the distribution ratio of sodium ion between nitrobenzene and sodium perchlorate is almost independent of the sodium perchlorate concentration, while the ratios of the other metal ions decrease with increasing sodium perchlorate concentration above 0.1 *M*. The decrease is especially pronounced for cesium, not so pronounced for rubidium and still less for potassium. The same tendency is also observed with nitromethane and nitroethane, but not with hexone and TBP, which are usually regarded as solvating organic solvents.

Table II also shows that the distribution ratio for the nitro compounds increases in the order $Na^+ < K^+ < Rb^+ < Cs^+$, *i.e.* the order of decreasing hydration. This is not the case, however, for hexone and TBP. Further discussion should be postponed until the degree of dissociation of the ion-pairs $MClO_4$ in the organic phase has been ascertained.

Distribution of the heavy alkali metal tetraphenylborates

The distribution ratio of potassium tetraphenylborate in Table V and Fig. 2 may be summarized as follows: (i) if $[Na^+] > [K^+] = 10^{-4}$ *M*, the distribution ratio of potassium is almost independent of the sodium tetraphenylborate concentration when no sodium perchlorate is added to the aqueous phase, (ii) the distribution ratio is proportional to the initial tetraphenylborate concentration in the aqueous phase when the aqueous phase always contains 0.1 *M* sodium perchlorate and (iii) when the aqueous phase initially contains 0.1 *M* Na(TPB, ClO_4), the slope of the plot log D *vs.* $\log[TPB^-]_{initial, aq}$ is similar to that given in (ii) in the region of lower tetraphenylborate concentrations, but the slope increases somewhat in the region of higher tetraphenylborate concentrations.

It can be concluded from the results discussed above that in these distribution systems: (i) about 90% of the tetraphenylborate in the system is distributed into the organic phase together with an equivalent amount of sodium ion, (ii) the metal ion–tetraphenylborate ion ion-pairs in the organic phase are almost completely dissociated. This is in agreement with conductance measurements in anhydrous acetonitrile by KAY *et al.*[8]. The dipicrylaminates also seem to be dissociated in nitrobenzene[9,10].

Accordingly the following equations can be introduced.

The net distribution ratio of the metal ion is described by

$$D = [M^+]_{org}/[M^+] \quad (12)$$

and the extraction of the metal ions proceeds according to equilibrium (5). The balance of TPB is given by

$$[NaTPB]_{initial,\,aq} = [TPB^-] + [TPB^-]_{org} \quad (13)$$

Since the amount of potassium is small in comparison to NaTPB in most experiments, sodium will determine the $[TPB^-]_{org}/[TPB^-]$ ratio, according to

$$Na^+ + TPB^- \rightleftharpoons Na^+(org) + TPB^-(org) \quad (14)$$

Thus, if no sodium perchlorate is added, eqns. (8) and (9) are valid and $[TPB^-]_{org}/[TPB^-] = 9$. K, defined by eqn. (6), will then be for potassium

$$K = [K^+]_{org}9/[K^+] = 9 \cdot 10^{2.17} = 1330 \quad (15)$$

This equation, furthermore, says that the distribution ratio $D = [K^+]_{org}/[K^+]$ for amounts of potassium small in comparison with NaTPB will be constant.

If, however, $[Na^+]$ is kept practically constant at 0.1 M with sodium perchlorate, then eqn. (6) gives for sodium

$$K = [Na^+]_{org}[TPB^-]_{org}/0.1[TPB^-] = 81 \quad (16)$$

or from eqn. (9), as sodium perchlorate in the organic layer can be neglected (*cf.* Table II):

$$[TPB^-]^2_{org} = 8.1[TPB^-] \quad (17)$$

As $[TPB^-]_{org} \leq 0.1\ M$, it can be seen from this equation that $[TPB^-]_{org}/[TPB^-] \geq 81$ and eqn. (13) may be approximated to

$$[NaTPB]_{initial,\,aq} = [TPB^-]_{org} \quad (18)$$

The distribution ratio for potassium can then be derived from eqns. (6) and (12), *i.e.*

$$D = K[TPB^-]/[TPB]_{org} \quad (19)$$

or, if eqns. (17) and (18) are used,

$$D = K[NaTPB]_{initial,\,aq}/8.1 \quad (20)$$

The straight line in Fig. 2 is drawn with slope +1 and $K/8.1 = 10^{2.80}$ or $K = 5110$. Even if K has a different value when no sodium perchlorate is present, eqn. (20) explains the data in Table V (C) and Fig. 2 (filled circles). Deviation from linearity occurs at low $[NaTPB]_{initial,\,aq}$, where the amount of tetraphenylborate extracted with potassium cannot be neglected and the distribution of potassium perchlorate makes a contribution to D. The open circles connect the two cases discussed here, because in this case the sum of the initial concentrations of NaTPB and sodium perchlorate was kept constant at 0.1 M.

The filled circles in Fig. 3 may be explained by eqn. (20) in the same way as for potassium. The straight lines for rubidium and cesium in Fig. 3 are drawn with slopes +1 and K values of 32400 and 128000 for rubidium and cesium, respectively. The open symbols in Fig. 3 are also explained as above for potassium. The increase

of log D above the straight lines for rubidium and cesium at initial TPB concentrations larger than 0.01 M may be explained by ion-pair formation, which has been neglected in eqn. (12). One possible reason could be that these ions are less hydrated and thus smaller. This would favour the formation of ion-pairs.

Effect of the addition of sodium perchlorate

As can be seen in Fig. 1 and Table IV, the extraction of alkali metal ions in the presence of 0.01 M tetraphenylborate (initial concentration) is very much decreased by addition of sodium perchlorate to the aqueous phase. The slope of the log D *vs.* log[$NaClO_4$] plot is almost -1 in the lower sodium perchlorate concentration region, but the slope decreases as the perchlorate concentration increases.

This is explained by eqns. (6) and (9) which may be combined to give

$$K = [TPB^-]^2_{org}/[Na^+][TPB^-] = 81 \quad (21)$$

Equation (18) should be valid as $[Na^+] \geq 0.1\ M$ and the distribution constant K for the small amounts of potassium, rubidium and cesium should therefore follow

$$K = D[TPB^-]_{org}/[TPB^-] \quad (22)$$

Thus, from eqn. (21) we obtain

$$K = D81[Na^+]/0.01 \quad (23a)$$

and

$$D = K0.01/81[Na^+] \quad (23b)$$

The distribution ratio ought therefore to be inversely proportional to the sodium ion concentration. As, however, the ionic concentration in the aqueous phase alters considerably, changes in the activity coefficients of the chemical species may be large at high concentrations of sodium perchlorate. This may be one reason for the deviation of the plots from straight lines with slope -1. These lines have been drawn with the constants 5110, 36200 and 256000 for potassium, rubidium and cesium, respectively. Similarly, the data for hexone may be explained by eqn. (23b).

Effect of the addition of perchloric acid

If tetraphenylborate is hydrolyzed according to

$$Na(C_6H_5)_4B + HClO_4 + 2H_2O \rightarrow C_6H_5B(OH)_2 + 3C_6H_6 + NaClO_4$$

then the remaining unhydrolyzed NaTPB can be calculated from

$$[TPB^-]_{org} + [TPB^-] = [NaTPB]_{initial,\,aq} - [H^+]_{initial,\,aq} + [H^+] \quad (24)$$

where $[H^+]$ is the hydrogen ion concentration at equilibrium, determined by means of potentiometry. Thus, the distribution ratio should be proportional to the remaining TPB^- as above (Figs. 2 and 3). The data in Table VI and Fig. 4 confirm this. It should be observed that the equilibrium concentration of sodium perchlorate is practically constant and equal to 0.05 M.

Use of tetraphenylborate for the analysis of heavy alkali metal ions

From the results in Tables III–VI or those of Figs. 1–4, it may be concluded that (i) the extraction is greatest and the separation of the heavy alkali metal ions

most effective when nitrobenzene is used as the organic solvent, (ii) the extraction is greater when the concentration of the co-existing sodium ion in the aqueous phase is low, (iii) the extraction is greater when the concentration of tetraphenylborate is high if the system contains a certain amount of sodium salt, and (iv) the extraction is decreased by the addition of a strong acid.

This indicates how a satisfactory extraction or separation of the alkali metal ions may be achieved.

A good separation of potassium, rubidium and cesium is effected by the use of nitrobenzene and the separation will not be affected very much by increases in the tetraphenylborate concentration or in the co-existing sodium ion concentration. The distribution ratio of these ions with tetraphenylborate is too high for the ions to be separated effectively in the absence of co-existing sodium salt (*cf.* Fig. 2 or Table V) and the aqueous phase should therefore contain a certain amount of sodium salt to produce an effective separation of these metal ions. Too high a concentration of sodium salt (>1 *M*) may, however, decrease the separation factor (*cf.* Fig. 1). The concentrations of sodium salt and sodium tetraphenylborate should be chosen so that the distribution ratios for the ions to be separated are neither too high nor too low.

As the solubilities of potassium, rubidium or cesium tetraphenylborate in water are very low and not very different from each other[1,11,12], it is not possible to separate these ions by precipitation of the tetraphenylborates, but the use of an extraction cycle under controlled experimental conditions seems to be quite feasible, provided that the solubility products of the heavy alkali metal tetraphenylborates are not attained. However, as can be seen in Table I, an organic phase which has extracted these metal ions as tetraphenylborates always contains a large amount of sodium ions which will also be back-extracted (*e.g.* with acid) into the aqueous phase together with the heavy alkali metal ions. Thus, the separation of the latter from sodium must be achieved by precipitation with a carrier, preferably ammonium.

This work has been partly supported by the Swedish Natural Science Foundation. The English has been revised by Mrs. SUSAN JAGNER, M.A. and fil.lic.

SUMMARY

The extraction of sodium and small amounts of potassium, rubidium and cesium from aqueous solutions containing sodium tetraphenylborate (TPB), sodium perchlorate and perchloric acid has been studied for nitromethane, nitroethane, nitrobenzene, methyl isobutyl ketone and tributyl phosphate. Nitromethane gives the highest distribution ratio (org/aq) for the perchlorates, and nitrobenzene gives the highest distribution ratio and separation factor for the tetraphenylborates. Most distribution data could be explained by assuming that the tetraphenylborates were fully dissociated in both phases. The equilibrium constants and distribution ratios increase in the order sodium < potassium < rubidium < cesium. The distribution ratio of small amounts of the heavy alkali metal ions will thus not be appreciably influenced by the concentration of sodium tetraphenylborate, but will decrease on the addition of sodium chloride or perchlorate. The effect of perchloric acid can be explained by irreversible acid hydrolysis of the tetraphenylborate ion.

RÉSUMÉ

L'extraction du sodium et de faibles teneurs de potassium, de rubidium et de césium, en solutions aqueuses, renfermant du tétraphénylborate de sodium, a été étudiée pour les solvants suivants: nitrométhane, nitroéthane, nitrobenzène, méthylisobutylcétone et tributylphosphate. Le nitrométhane donne les coefficients de partage les plus élevés (org/aq) pour les perchlorates; le nitrobenzène donne les meilleurs coefficient de partage et facteurs de séparation pour les tétraphénylborates. Les valeurs obtenues peuvent s'expliquer en admettant que les tétraphénylborates sont totalement dissociés dans les deux phases. Les constantes d'équilibre et les coefficients de partage augmentent dans l'ordre sodium < potassium < rubidium < cesium. Les coefficients de partage des métaux alcalins lourds en faibles quantités ne sont pas influencés sensiblement par la concentration du tétraphénylborate de sodium, mais ils diminuent par addition de chlorure de sodium ou de perchlorate. L'influence de l'acide perchlorique peut s'expliquer par l'hydrolyse acide irréversible de l'ion tétraphénylborate.

ZUSAMMENFASSUNG

Die Extraktion von Natrium und kleiner Mengen Kalium, Rubidium und Cäsium aus wässrigen Lösungen, die Natriumtetraphenylborat (TPB), Natriumperchlorat und Perchlorsäure enthielten, wurde mit folgenden 5 Lösungsmitteln untersucht: Nitromethan, Nitroäthan, Nitrobenzol, Methylisobutylketon und Tributylphosphat. Nitromethan ergibt den grössten Verteilungskoeffizienten für Perchlorate, Nitrobenzol gibt die günstigsten Verteilungsverhältnisse und Trennfaktoren für die Tetraphenylborate. Die meisten Verteilungskoeffizienten konnten durch die Annahme erklärt werden, dass das Tetraphenylborat in beiden Phasen völlig dissoziiert ist. Die Gleichgewichtskonstanten und Verteilungskoeffizienten steigen vom Natrium zum Cäsium an. Die Verteilungskoeffizienten von kleinen Gehalten der schweren Alkalimetallionen werden deshalb kaum durch die Konzentration des Natriumtetraphenylborats beeinflusst; aber sie verringern sich bei Zugabe von Natriumchlorid oder Perchlorat. Der Einfluss der Perchlorsäure kann mit einer irreversiblen Säurehydrolyse des Tetraphenylborations erklärt werden.

REFERENCES

1 H. Flaschka and A. J. Barnard, Jr., *Advances in Analytical Chemistry and Instrumentation*, Vol. 1, Interscience, New York, 1960.
2 R. C. Fix, *Thesis*, Massachusetts Institute of Technology, 1956, cited in ref. 1.
3 T. H. Handley and C. L. Burros, *Anal. Chem.*, 31 (1959) 332.
4 H. L. Finston, private communication cited in ref. 1.
5 G. Testemale and J. Girault, *Comm. Energie At. (France)*, Rappt. CEA-R3391, 1967.
6 K. Haruyama, T. Ashizawa and T. Ashizawa, *Japan Analyst*, 14 (1965) 120; *Chem. Abstr.*, 63 (1965) 5213a.
7 R. M. Diamond and L. G. Tuck, *Progr. Inorg. Chem.*, 2 (1960) 109.
8 R. L. Kay, B. J. Hales and G. P. Cunningham, *J. Phys. Chem.*, 71 (1967) 3925.
9 M. Kyrš, *Collection Czech. Chem. Commun.*, 26 (1961) 155.
10 J. Rais and M. Kyrš, *Proc. Int. Conf. on Solvent Extraction Chemistry*, North-Holland Publishing Co., 1967, p. 595.
11 W. Geilmann and W. Gebauhr, *Z. Anal. Chem.*, 142 (1954) 241.
12 R. T. Pflaum and L. C. Howick, *Anal. Chem.*, 28 (1956) 1542.

Analytica Chimica Acta
Elsevier Publishing Company, Amsterdam
Printed in The Netherlands

STUDIES WITH DITHIZONE. PART XVII. THE EXTRACTION CONSTANTS OF ORGANOMERCURY(II) DITHIZONATES

H. M. N. H. IRVING AND A. M. KIWAN
Department of Inorganic and Structural Chemistry, University of Leeds, Leeds 2 (England)
(Received January 21st, 1969)

The reaction between an aqueous solution of an organomercury(II) cation, RHg^+, and a solution of dithizone (1,5-diphenyl-3-mercaptoformazan; H_2Dz) in an immiscible organic solvent leads to the formation of a yellow 1:1 complex, RHg(HDz), which is distributed between the two phases in accordance with eqn. (1):

$$RHg^+ + (H_2Dz)_{org} \rightleftharpoons RHg(HDz)_{org} + H^+ \quad (1)$$

where the subscript org distinguishes species in the organic phase from those in the aqueous phase. In previous papers[1] (and refs. therein), these examples of liquid–liquid extraction have been examined for a considerable variety of organomercurials; the influence of pH and the nature of the buffer substituents on the percentage extraction has been discussed and the spectral characteristics of the various dithizonates that can be exploited analytically have also been reported.

A knowledge of the relevant extraction constants (the equilibrium constants of eqn. (1)) defined by

$$K_{ex} = [RHg(HDz)]_{org}[H^+]/[RHg^+][H_2Dz]_{org} \quad (2)$$

would assist any reasoned attempts at separation based, *e.g.*, on adjustment of pH. However, in most cases the extraction is virtually quantitative even at pH 0–1, implying that the equilibrium in eqn. (1) lies far to the right. Increase in the concentration of acid to move the equilibrium to the left in order to obtain accessible values for the concentration terms $[RHg(HDz)]_{org}$ and $[H_2Dz]_{org}$, which can be determined absorptiometrically, introduces difficulties; first those inherent in the low buffer capacity of strong acids and secondly from the difficulty of maintaining a constant ionic strength.

An alternative approach is to reduce the value of the term $[RHg^+]$ by introducing an auxiliary complexing agent. Specifically, if an anion, X^-, is introduced that can form a complex (or series of complexes) with the organomercury(II) cation, the mass balance for an experimentally known total amount of mercurial can be written in the form

$$[Hg]_T = [RHg^+] + [RHgX] + [RHgX_2^-] + [RHgX_3^{2-}] + [RHgX]_{org} + [RHg(HDz)]_{org} + [RHg(HDz)] \quad (3)$$

for the possibility of the liquid–liquid extraction of the formally uncharged species RHgX must also be taken into consideration. In passing it should be noted that yellow complexes (HDz)HgX (X = Cl, Br, I) are extracted when solutions of mercury(II)

containing halide ions are treated with solutions of dithizone in organic solvents[2]. These observations explain some anomalous results reported in the literature.

If the partition coefficients of the species RHgX and RHg(HDz) are defined by

$$P_{RHgX} = [RHgX]_{org}/[RHgX] \tag{4a}$$

and

$$P_{RHg(HDz)} = [RHg(HDz)]_{org}/[RHg(HDz)] \tag{4b}$$

we can write

$$\begin{aligned} q &= [RHg(HDz)]_{org}/\{[Hg]_T - (1 + 1/P_{RHg(HDz)})[RHg(HDz)]_{org}\} \\ &= [RHg(HDz)]_{org}/\{[RHg^+] + [RHgX] + [RHgX_2^-] + \ldots + [RHgX]_{org}\} \\ &= K_{ex}[H_2Dz]_{org}/[H^+]\{1 + (1 + P_{RHgX})\beta_1[X^-] + \beta_2[X^-]^2 + \ldots\} \end{aligned} \tag{5}$$

where $\beta_1 = [RHgX]/[RHg^+][X^-]$, and $\beta_n = [RHgX_n^{(n-1)-}]/[RHg^+][X^-]^n$ are the first and n-th overall (cumulative) stability constants for the halide complexes.

Equation (5) can be rearranged in a form more suitable for graphical treatment:

$$\left\{\frac{[H_2Dz]_{org}}{[H^+]q}\right\} = \frac{1}{K_{ex}} + (1 + P_{RHgX})\frac{\beta_1}{K_{ex}} \cdot [X^-] + \frac{\beta_2}{K_{ex}} \cdot [X^-]^2 + \ldots. \tag{6}$$

Thus a plot of $[H_2Dz]_{org}/[H^+]q$ against $[X^-]$ should be a straight line if the term in $[X^-]^2$ is negligible (*i.e.* if β_2 is very small) and in any event would be a polynomial in $[X^-]$ that would extrapolate to $1/K_{ex}$ as $[X^-] \to 0$.

Unfortunately, values of q cannot be calculated directly unless the value of the partition coefficient $P_{RHg(HDz)}$ for the organomercury(II) dithizonate can be obtained by some independent method. If, however, we define a ratio

$$q^* = [RHg(HDz)]_{org}/\{[Hg]_T - [RHg(HDz)]_{org}\} \tag{7}$$

for which values can be calculated directly from experimental data, it is easy to show that

$$q^* = q/\{1 + (q/P_{RHg(HDz)})\} \tag{8}$$

so that, provided $q \ll P_{RHg(HDz)}$, we can replace q by q^* in eqn. (6). This appears to be a valid approximation (at least for systems involving iodide), for most values of q were less than 10 whilst that of $P_{RHg(HDz)}$ appears to be much greater than 10^3, as judged from preliminary measurements with ^{203}Hg as tracer.

The term $[X^-]$ in eqn. (6) refers to the free iodide concentration. If $[X]_T$ is the known total amount added, we have

$$[X]_T = [X^-] + [RHgX]_{org} + [RHgX] \tag{9}$$

Provided that the terms $[RHg^+]$, $[RHgX_n]$ $(n > 1)$ and $[RHg(HDz)]$ can be neglected in comparison with other terms in eqn. (3) (an assumption justified below), this leads to

$$[RHgX]_{org} + [RHgX] = [Hg]_T - [RHg(HDz)] = [Hg]_T/(1 + q^*) \tag{10}$$

so that

$$[X^-] = [X]_T - [Hg]_T/(1 + q^*) \tag{11}$$

When iodide was used as the auxiliary complexing agent in the system *p*-hydroxymethylphenylmercury(II)–dithizone, the plot of $[H_2Dz]_{org}/q^*[H^+]$ against $[I^-]$ was a straight line (Fig. 1, curve 1), showing that the data conform to eqn. (6) with no measurable contribution from a term in $[I^-]^2$ and demonstrating the absence of $[RHgI_2^-]$ and higher complexes. All the other systems studied in the present work (Table I) also gave linear plots although the scatter tended to be greater for measurements with bromide and chloride ions which had to be added in much greater concentration (Fig. 1, curves 2, 3). These results are in agreement with published data for aryl- and alkyl-mercury(II) cations which show that the co-ordination number does not normally exceed one. Whereas values of β_1 as high as 10^9 have been reported (*cf.* Table II), values of β_2 appear to be in the region of 1[3,4].

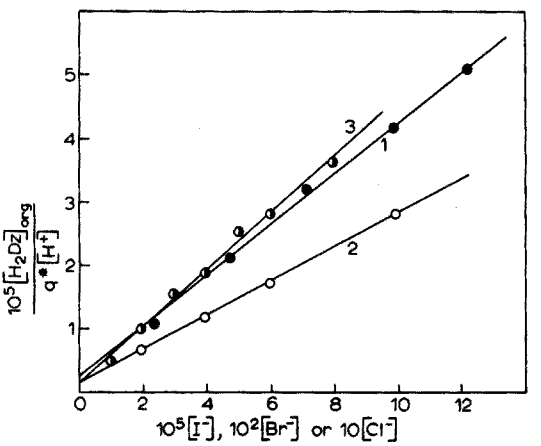

Fig. 1. The application of eqn. (6) to the distribution of *p*-hydroxymethylphenylmercury(II) dithizonate between carbon tetrachloride and perchloric acid containing halide ions and sodium perchlorate at $\mu = 1.0$ *M*. Curve 1, iodide; curve 2, bromide; curve 3, chloride ions.

It is not feasible to obtain accurate values of K_{ex} from the reciprocal of the intercept of plots of eqn. (6), at least by graphical extrapolation. The best straight line to fit the experimental data was computed by the least-squares method and the calculated values of log K_{ex} and log $(1+P_{RHgX})\beta_1$ are collected in Table I with their respective standard deviations.

Equation (6) predicts that linear plots of results for systems comprising the same organomercurial but different auxiliary complexing agents should extrapolate to a common intercept $(1/K_{ex})$ although the slopes will vary in accordance with the stability constant and partition coefficient of the complex RHgX. This is shown for the three complexing halides in Fig. 1 (curves 1, 2 and 3) in which the straight lines are computed from the data in Table I. The agreement is less satisfactory for *o*-carboxyphenylmercury dithizonate and poor for phenylmercuric dithizonate.

The extraction constant K_{ex} is compounded of four individual constants since

$$K_{ex} = \beta_{RHg(HDz)} P_{RHg(HDz)} / \beta_{H_2Dz} P_{H_2Dz} \qquad (12)$$

where $\beta_{M(HDz)}$ is the formation constant of the species M(HDz). Since both components of the numerator will change independently with changes in R and not necessarily

TABLE I

VALUES OF EXTRACTION CONSTANTS OF RHg(HDz) AND OTHER PARAMETERS FOR HALIDE COMPLEXES RHgX CALCULATED FROM PARTITION MEASUREMENTS

$R =$	*Anion*	$\log K_{ex}$	$\log (1 + P_{RHgX})\beta_1$
C_6F_5-	I^-	6.59 ± 0.02	5.09 ± 0.02
2,3-(HO)$(NO_2)C_6H_3-$	I^-	5.10 ± 0.22	4.37 ± 0.22
p-Cl·C_6H_4-	I^-	5.17 ± 0.27	4.72 ± 0.27
p-Br·C_6H_4-	I^-	5.00 ± 0.03	4.59 ± 0.03
C_6H_5-	I^-	4.62 ± 0.09	4.25 ± 0.09
	Br^-	5.53 ± 0.06	2.20 ± 0.06
o-$CH_3O\cdot C_6H_4-$	I^-	4.43 ± 0.03	4.15 ± 0.03
o-HO·C_6H_4-	I^-	5.63 ± 0.17	5.83 ± 0.17
p-HO·$CH_2\cdot C_6H_4-$	I^-	5.82 ± 0.11	5.43 ± 0.11
	Br^-	5.95 ± 0.09	2.38 ± 0.09
	Cl^-	6.11 ± 0.22	1.76 ± 0.22
o-HO·$CH_2\cdot C_6H_4-$	I^-	4.85 ± 0.08	5.34 ± 0.08
o-HOOC·C_6H_4-	I^-	4.52 ± 0.14	5.10 ± 0.14
	Br^-	4.47 ± 0.09	2.74 ± 0.09
	Cl^-	5.41 ± 0.05	1.39 ± 0.05
p-$CH_3\cdot CO\cdot NHC_6H_4-$	Cl^-	5.43 ± 0.13	2.06 ± 0.13
p-$Me_2N\cdot C_6H_4-$	Cl^-	5.98 ± 0.21	5.23 ± 0.21
C_2H_5-	I^-	4.46 ± 0.05	4.94 ± 0.05
CH_3-	I^-	5.12 ± 0.14	5.38 ± 0.14

in the same direction, no detailed analysis of the values of K_{ex} in Table I is justifiable although they will be useful for calculating the most favourable conditions for separations from each other or, more particularly, from other cations.

Values of $\log (1+P_{RHgX})\beta_1$ are not easy to interpret. It can confidently be expected that values of P_{RHgX} for any given mercurial will increase as the complex gets bulkier in the order X = Cl < Br < I and this is endorsed by the only published measurements for $MeHg^+$ (11, 45 and 400 ± 100 for toluene/water at $\mu = 0.1$). The present value for the partition of phenylmercury(II) chloride between carbon tetrachloride and an aqueous phase containing excess of chloride ions at $\mu = 1.0$ *M*

TABLE II

DECADIC LOGARITHMS OF STABILITY CONSTANTS AND PARTITION COEFFICIENTS OF ORGANOMERCURY COMPLEXES

Cation	*Ligand*								*Ref.*[c]
	OH⁻	*CN⁻*	*SCN⁻*	*F⁻*	*Cl⁻*	*Br⁻*	*I⁻*	*RS⁻*	
CH_3Hg^+	9.5, 9.89	14.2	6.1	—	5.45	6.7	8.7		A
					(~1.0)[a]	(1.65)[a]	(2.6)[a]		A
				1.5	5.25	6.62	8.60	16.1[b]	B
$C_2H_5Hg^+$	9.1								
$C_6H_5Hg^+$	10.0								A
					(1.11)[a]				C
CF_3Hg^+	10.76				5.78	7.24	9.63		A

[a] Values of $\log_{10} P_{RHgX}$ for toluene/water at 25° are given in parentheses.
[b] For R = HO·$CH_2\cdot CH_2S^-$: for cysteine $\log \beta_1 = 20.1$ (ref. 4).
[c] A: data from "Stability Constants of Metal-ion Complexes", *Chem. Soc. Special Publication No. 17*, London, 1964; B: G. SCHWARZENBACH AND M. SCHELLENBERG, ref. 4; C: present work: carbon tetrachloride/water.

($NaClO_4$) is $P_{C_6H_5HgCl}=12.85$. The fact that it remained constant over the range $[Cl]=0.075$–2.50 M confirmed the absence of higher complexes. Since RHg^+ will be a "type B" or "soft" cation, values of β_1 should also increase in the order $Cl < Br < I$. Both effects will lead to values of $\log (1+P_{RHgX})\beta_1$ increasing in the order $Cl < Br < I$ as found (Table I) for R = *p*-hydroxmethylphenyl-, *o*-carboxyphenyl- and phenyl-. What is most disconcerting, however, is that the orders of magnitude are quite wrong. For since P_{RHgX} is certainly greater than 10 in every case, the values of $\log \beta_1$ for iodide complexes never exceed 4.6 nor those for bromide and chloride 1.7 and 1.1 respectively, values quite inconsistent with the limited information in the literature (Table II). If we accept the reliability of $\log \beta_{CH_3HgI}=8.6$ and assume $\log P_{CH_3HgI}=2.6$ (Table II), we calculate $\log(1+P)\beta=11.2$ and the discrepancy with the value of 5.58 obtained by the present liquid–liquid extraction method deserves reinvestigation.

EXPERIMENTAL

Reagents

The preparation of the organomercurials used and the purification of dithizone and other reagents has been described in previous papers[1]. Solution sof AnalaR sodium chloride, bromide and iodide in deionised water were freed from heavy metals by extraction with successive portions of a solution of dithizone in carbon tetrachloride. Their concentrations were then determined titrimetrically against standard silver nitrate.

The extraction constant of p-*carboxyphenylmercury(II) dithizonate*

A series of mixtures was prepared containing the same initial amount of dithizone (10 ml of a $2.803 \cdot 10^{-5}$ M solution in carbon tetrachloride) and the same initial concentration of *p*-carboxyphenylmercury(II) chloride ($[Hg]_T=1.43 \cdot 10^{-5}$ M) with variable amounts of sodium iodide and sufficient perchloric acid and sodium perchlorate to achieve an acidity of 0.05 M and an ionic strength $\mu=1.0$ M in a total volume of 10 ml. Each mixture was equilibrated for 3–5 min after which the phases were separated and the optical density of the organic phase was measured (SP 500 spectrophotometer, matched 1 cm silica cells) at 480 and 620 nm the respective wavelength maxima for the dithizone complex and dithizone itself. The ratio $\varepsilon_{480}/\varepsilon_{640}$ was obtained from the spectrum of pure dithizone and was used to calculate the absorption due to dithizone alone at 480 nm: that due to the mercury complex alone was then determined by difference and is shown in the fourth row of the following Table of results

(*a*) Iodide as complexing agent. $[H^+]=0.05$ M; $\mu=1.0$ M.

$10^5[I^-]_T$	0.0	2.5	5.0	7.5
A_{480} obs.	0.668	0.651	0.638	0.625
A_{620} obs.	0.473	0.510	0.544	0.573
A_{480} calc.	0.452	0.418	0.389	0.363
q^*	(~65)	12.29	6.175	4.079
$10^5[H_2Dz]_{org}$	1.367	1.474	1.572	1.656
$10^5[H_2Dz]_{org}/q^*[H^+]$	(0.42)	2.399	5.096	8.120
$10^5[I^-]$	—	2.392	4.800	7.218

$10^5[I^-]_T$	10.0	12.5	15.0	17.5
A_{480} obs.	0.615	0.605	0.600	0.596
A_{620} obs.	0.590	0.608	0.620	0.640
A_{480} calc.	0.345	0.327	0.316	0.303
q^*	3.224	2.616	2.324	2.034
$10^5[H_2Dz]_{org}$	1.705	1.752	1.792	1.850
$10^5[H_2Dz]_{org}/q^*[H^+]$	10.58	13.43	15.42	17.99
$[I^-]$	9.661	12.104	14.570	17.029

(*b*) Bromide as complexing agent. $[H^+]=1.0\ M$; $\mu=1.0\ M$.
Initial concentration of dithizone $2.832\cdot10^{-5}\ M$.
$[Hg^+]_T=1.43\cdot10^{-5}\ M$.

$[Br^-]_T$	0.025	0.050	0.060	0.08	0.10
q^*	0.496	0.284	0.235	0.177	0.147
$10^5[H_2Dz]_{org}/q^*[H^+]$	5.10	8.98	11.1	14.7	18.0

(*c*) Chloride as complexing agent. $[H^+]=1.0\ M$; $\mu=1.0\ M$.
Initial concentration of dithizone $2.89\cdot10^{-5}\ M$.
$[Hg^+]_T=1.43\cdot10^{-5}\ M$

$[Cl^-]_T$	0.05	0.10	0.20	0.25	0.30	0.35	0.40	0.70
q^*	1.443	1.226	0.644	0.512	0.435	0.417	0.341	0.215
$10^5[H_2Dz]_{org}/q^*[H^+]$	1.37	1.65	3.52	4.58	5.53	5.82	7.34	12.2

Experimental results for other organomercurials are given below. Unless stated to the contrary $\mu=1.0\ M$.

Pentafluoromercury(II) dithizonate
Initial $[H_2Dz]_{org}=2.995\cdot10^{-5}$; $[Hg]_T=1.437\cdot10^{-5}$; $[H^+]=0.10\ M$.

$10^4[I^-]_T$	5.0	7.5	10.0	15.0	17.5
q^*	9.45	7.02	5.42	3.72	3.26
$10^5[H_2Dz]_{org}/q^*[H^+]$	1.62	2.40	3.26	4.85	5.60

2-Hydroxy-3-nitrophenylmercury(II) dithizonate
Initial $[H_2Dz]_{org}=2.867\cdot10^{-5}$; $[Hg]_T=1.421\cdot10^{-5}$; $[H^+]=0.10\ M$.

$10^4[I^-]_T$	2.5	5.0	7.5	10.0	12.5
q^*	3.22	2.07	1.30	1.11	0.92
$10^5[H_2Dz]_{org}/q^*[H^+]$	5.60	9.27	15.8	19.3	24.0

o-*Hydroxyphenylmercury(II) dithizonate*
Initial $[H_2Dz]_{org}=2.514\cdot10^{-5}$; $[Hg]_T=1.50\cdot10^{-5}$; $[H^+]=0.05\ M$.

$10^5[I^-]_T$	2.5	5.0	7.5	10.0	12.5	15.0	17.5
q^*	7.73	4.36	2.90	2.27	1.90	1.63	1.41
$10^5[H_2Dz]_{org}/q^*[H^+]$	3.98	7.45	12.0	15.8	19.5	23.3	27.3

p-*Chlorophenylmercury(II) dithizonate*
Initial $[H_2Dz]_{org}=2.968\cdot10^{-5}$; $[Hg]_T=1.436\cdot10^{-5}$; $[H^+]=0.10\ M$.

$10^4[I^-]_T$	2.5	5.0	7.5	10.0	15.0
q^*	1.955	1.245	0.800	0.653	0.437
$10^4[H_2Dz]_{org}/q^*[H^+]$	1.01	1.72	2.88	3.70	5.44

p-*Bromophenylmercury(II) dithizonate*

Initial $[H_2Dz]_{org} = 2.919 \cdot 10^{-5}$; $[Hg]_T = 1.43 \cdot 10^{-5}$; $[H^+] = 0.10\ M$.

$10^4[I^-]_T$	2.5	5.0	7.5	10.0	12.5	15.0	17.5
q^*	1.944	1.040	0.748	0.589	0.497	0.409	0.362
$10^4[H_2Dz]_{org}/q^*[H^+]$	1.01	2.08	3.05	4.01	4.88	6.06	6.88

p-*Hydroxymethylphenylmercury(II) dithizonate*

Initial $[H_2Dz]_{org} = 2.89 \cdot 10^{-5}$; $[Hg]_T = 1.66 \cdot 10^{-5}$; $[H^+] = 0.10\ M$.

$10^5[I^-]_T$	2.5	5.0	7.5	10.0	12.5
q^*	13.00	7.17	4.92	4.00	3.40
$10^5[H_2Dz]_{org}/q^*[H^+]$	1.06	2.10	3.19	4.12	5.00

Initial $[H_2Dz]_{org} = 2.572 \cdot 10^{-5}$; $[Hg]_T = 1.66 \cdot 10^{-5}$; $[H^+] = 1.0\ M$.

$10^2[Br^-]_T$	2.0	4.0	6.0	10.0
q^*	2.180	1.410	1.056	0.680
$10^5[H_2Dz]_{org}/q^*[H^+]$	0.682	1.17	1.66	2.81

Initial $[H_2Dz]_{org} = 2.933 \cdot 10^{-5}$; $[Hg]_T = 1.66 \cdot 10^{-5}$; $[H^+] = 1.0\ M$.

$[Cl^-]_T$	0.1	0.2	0.3	0.4	0.5	0.6	0.8
q^*	4.030	2.099	1.394	1.204	0.909	0.823	0.659
$10^5[H_2Dz]_{org}/q^*[H^+]$	0.448	0.964	1.52	1.82	2.50	2.79	3.60

o-*Hydroxymethylphenylmercury(II) dithizonate*

Initial $[H_2Dz]_{org} = 2.942 \cdot 10^{-5}$; $[Hg]_T = 1.43 \cdot 10^{-5}$; $[H^+] = 0.05\ M$.

$10^5[I^-]$	2.5	7.5	10.0	12.5	15.0
q^*	4.00	1.77	1.35	1.125	0.946
$10^5[H_2Dz]_{org}/q^*[H^+]$	8.65	22.3	30.7	37.6	45.9

o-*Methoxyphenylmercury(II) dithizonate*

Initial $[H_2Dz]_{org} = 2.890 \cdot 10^{-5}$; $[Hg]_T = 1.444 \cdot 10^{-5}$; $[H^+] = 0.10\ M$.

$10^4[I^-]_T$	2.5	5.0	7.5	10.0	15.0
q^*	1.20	0.767	0.537	0.439	0.311
$10^4[H_2Dz]_{org}/q^*[H^+]$	1.63	2.91	4.35	5.61	8.16

o-*Carboxyphenylmercury(II) dithizonate*

Initial $[H_2Dz]_{org} = 2.968 \cdot 10^{-5}$; $[Hg]_T = 1.499 \cdot 10^{-5}$; $[H^+] = 0.10\ M$.

$10^5[I^-]_T$	2.5	5.0	7.5	10.0	15.0	17.5	20.0
q^*	1.955	1.245	0.80	0.578	0.465	0.387	0.344
$10^4[H_2Dz]_{org}/q^*[H^+]$	1.01	1.72	2.88	4.18	5.35	6.52	7.44

Initial $[H_2Dz]_{org} = 2.851 \cdot 10^{-5}$; $[Hg]_T = 1.499 \cdot 10^{-5}$; $[H^+] = 0.10\ M$.

$10^2[Br^-]$	2.5	4.0	6.0	8.0
q^*	0.466	0.311	0.223	0.170
$10^4[H_2Dz]_{org}/q^*[H^+]$	4.95	8.00	11.5	15.4

Initial $[H_2Dz]_{org} = 3.04 \cdot 10^{-5}$; $[Hg]_T = 1.499 \cdot 10^{-5}$; $[H^+] = 1.0\ M$.

$[Cl^-]$	0.10	0.20	0.30	0.40	0.50	0.60	0.70	0.80
q^*	1.68	0.948	0.761	0.595	0.476	0.421	0.377	0.333
$10^5[H_2Dz]_{org}/q^*[H^+]$	1.24	2.42	3.15	4.18	5.37	6.18	6.96	8.00

Phenylmercury(II) dithizonate

Initial $[H_2Dz]_{org} = 2.979 \cdot 10^{-5}$; $[Hg]_T = 1.456 \cdot 10^{-5}$; $[H^+] = 0.10$ *M*.

$10^4[I^-]_T$	2.5	5.0	7.5	10.0	12.5
q^*	1.56	0.95	0.723	0.535	0.455
$10^4[H_2Dz]_{org}/q^*[H^+]$	1.30	2.34	3.23	4.52	5.47

Initial $[H_2Dz]_{org} = 2.952 \cdot 10^{-5}$; $[Hg]_T = 1.33 \cdot 10^{-5}$; $[H^+] = 1.25$; ionic strength 1.30 *M*.

$10^2[Br^-]_T$	1.00	2.00	3.00	4.00	6.00
q^*	2.35	1.30	1.06	0.859	0.634
$10^5[H_2Dz]_{org}/q^*[H^+]$	0.652	1.325	1.714	2.159	3.038

p-*Acetylaminophenylmercury(II) dithizonate*

Initial $[H_2Dz]_{org} = 3.02 \cdot 10^{-5}$; $[Hg]_T = 1.5 \cdot 10^{-5}$; $[H^+] = 0.10$; ionic strength 0.50 *M*.

$10^2[Cl^-]_T$	2.5	5.0	7.5	10.0	15.0	20.0	25.0	30.0
q^*	13.10	6.66	5.07	3.65	2.64	2.04	1.83	1.54
$10^5[H_2Dz]_{org}/q^*[H^+]$	1.24	2.53	3.45	4.94	7.12	9.53	10.80	13.32

p-*Dimethylaminomercury(II) dithizonate*

Initial $[H_2Dz]_{org} = 3.057 \cdot 10^{-5}$; $[Hg]_T = 1.539 \cdot 10^{-5}$; $[H^+] = 0.10$ *M*; ionic strength 0.50 *M*.

$10^5[I^-]_T$	2.5	5.0	7.5	10.0	12.5
q^*	3.24	1.904	1.34	1.208	0.918
$10^4[H_2Dz]_{org}/q^*[H^+]$	0.534	1.002	1.520	1.718	2.392

Ethylmercury(II) dithizonate

Initial $[H_2Dz]_{org} = 2.943 \cdot 10^{-5}$; $[Hg]_T = 1.581 \cdot 10^{-5}$; $[H^+] = 0.05$ *M*.

$10^5[I^-]_T$	5.0	10.0	15.0	20.0	25.0	35.0	40.0
q^*	2.68	1.33	0.89	0.68	0.61	0.463	0.409
$10^4[H_2Dz]_{org}/q^*[H^+]$	1.34	3.02	4.87	6.67	7.60	10.37	11.93

Methylmercury(II) dithizonate

Initial $[H_2Dz]_{org} = 2.993 \cdot 10^{-5}$; $[Hg]_T = 1.437 \cdot 10^{-5}$; $[H^+] = 0.05$ *M*.

$10^5[I^-]_T$	2.5	5.0	7.5	10.0	12.5	17.5	20.0
q^*	7.145	3.91	2.976	2.137	1.775	1.367	1.234
$10^5[H_2Dz]_{org}/q^*[H^+]$	4.84	9.20	12.86	18.79	23.22	32.21	35.36

Distribution of phenylmercury(II) chloride

A series of solutions containing $2.98 \cdot 10^{-5}$ *M* phenylmercury(II) chloride (10 ml) were shaken mechanically for 1 h with 10 ml of aqueous phases containing various amounts of sodium chloride and sodium perchlorate (pH 5.5; $\mu = 1.0$ *M*). After the phases had been separated, the concentration $[C_6H_5HgCl]_{org}$ was determined absorptiometrically.

$[Cl^-]$	0.075	0.100	0.150	0.175	0.200	0.300	0.400	0.500
q	13.11	12.82	12.84	12.85	12.90	13.10	12.60	12.71
$[Cl^-]$	0.600	0.700	0.800	0.900	1.000	1.500[a]	2.500[a]	
q	13.10	12.80	12.84	12.84	12.72	12.80	12.70	

[a] The last two measurements were carried out at $\mu = 3.0$ *M*. The average was $P_{C_6H_5HgCl} = 12.85 \pm 0.05$.

SUMMARY

Extraction constants are reported for the distribution of fourteen different organomercury(II) dithizonates, RHg(HDz), between carbon tetrachloride and aqueous phases of constant ionic strength containing complexing halide ions.

RÉSUMÉ

Des constantes d'extraction sont données pour le partage de quatorze dithizonates organomercuriques différents, RHg(HDz), entre tétrachlorure de carbone et phases aqueuses de force ionique constante, contenant des ions halogénures complexants.

ZUSAMMENFASSUNG

Extraktionskonstanten für die Verteilung von 14 verschiedenen Organoquecksilber(II)-dithozonaten, RHg(HDz), zwischen Tetrachlorkohlenstoff und wässrigen Phasen mit konstanter Ionenstärke und komplexbildenden Halogenidionen werden angegeben.

REFERENCES

1 H. M. N. H. IRVING AND A. M. KIWAN, *Anal. Chim. Acta*, 45 (1969) 00, 00, 00.
2 H. M. N. H. IRVING, Unpublished observations.
3 R. BARBIERI, M. GUISTINIANI AND E. CERVO, *J. Inorg. & Nuclear Chem.*, 27 (1966) 1325; G. C. STOCCO, E. RIVAROLA, R. ROMEO AND R. BARBIERI, *J. Inorg. & Nuclear Chem.*, 30 (1968) 2409.
4 G. SCHWARZENBACH AND M. SCHELLENBERG, *Helv. Chim. Acta*, 48 (1965) 28.

Analytica Chimica Acta
Elsevier Publishing Company, Amsterdam
Printed in The Netherlands

SUR UN DOSAGE INDIRECT PAR GRAVI-AMPEROMETRIE DU CALCIUM DANS DES ECHANTILLONS A FORT POURCENTAGE, AU MOYEN DE L'EDTA

W. HAERDI, D. MONNIER ET A. DAÏNA
Laboratoire de Chimie Analytique, Université de Genève, Genève (Suisse)
(Reçu le 18 novembre, 1968)

Le dosage de traces de calcium par ampérométrie proposé dans divers articles précédents[1-3] permet de titrer de 1 à 500 μg de cet élément au moyen d'EGTA ou d'EDTA avec une erreur souvent très inférieure à 3% et ceci en présence ou non de magnésium.

Pour des échantillons qui renferment un fort pourcentage de calcium, la méthode devient moins précise. En effet, les erreurs des titrages ampérométriques proviennent essentiellement des lectures de burette, du titre de la solution du réactif et de l'évaluation du point final. Nous avons cherché à améliorer au maximum la précision de ce dosage et pour cela, nous proposons une méthode mixte qui se fait en deux temps (méthode "gravi-ampérométrique"). Elle consiste à ajouter à la solution de l'échantillon une masse exactement pesée de réactif (éthylènediaminetétraacétate de sodium ou EDTA) et légèrement inférieure à celle nécessaire pour complexer la totalité du calcium. Le dosage est alors achevé par ampérométrie selon la méthode proposée.

On associe ainsi la précision de la pesée (gravimétrie) et la sensibilité de la méthode ampérométrique. Il est en effet généralement admis qu'une pesée est plus précise que les manipulations et les lectures inhérentes à la titrimétrie lorsque l'élément à doser est en pourcentage élevé dans l'échantillon.

DOSAGE D'UN CARBONATE DE CALCIUM PAR GRAVI-AMPÉROMÉTRIE À L'EDTA

Pour tester la valeur de cette méthode et en déterminer la précision, nous avons effectué une série d'analyses de carbonate de calcium pur.

Mode opératoire

L'échantillon de carbonate ($\sim$100 mg, puriss. p.a.) est dissous avec précaution dans une quantité minimum de l'acide chlorhydrique concentré. Il faut prendre soin de chasser complètement le CO_2, c'est pourquoi il est recommandé de chauffer la solution chlorhydrique à l'ébullition durant 1 min environ. Dans un second bécher, une masse appropriée, légèrement inférieure à celle stoechiométriquement nécessaire, d' EDTA (purum séché 2 h à 80°) est exactement pesée et dissoute dans l'éthanolamine *M* (0.2 ml pour 500 mg d'EDTA). Les deux solutions sont réunies, le pH est ajusté à 10.5 par une addition d'éthanolamine *M* (5 ml environ). On effectue le

dosage ampérométrique avec une solution d'EDTA (ou d'EGTA) 10^{-2} *M*. Résistance: R/Ca: 10^7 Ω (v. article précédent[3]).

Résultats

Les résultats de ces dosages sont donnés au Tableau I. Les erreurs extrêmes sont calculées par rapport à la moyenne.

TABLEAU I

DOSAGE GRAVI-AMPÉROMÉTRIQUE DU CALCIUM(II) DANS UN CARBONATE DE CALCIUM PUR PAR L'EDTA. CALCUL D'ERREUR

Ca introduit (mM)	*EDTA pesé (mM)*	*EDTA 10^{-2} M écoulé (mM) ou (ml)*	*Ca trouvé (mM)*	*Rapport Ca trouvé/ Ca introduit*
1.2512	1.2393	0.0113 (1.13)	1.2506	1.000
1.2440	1.2423	0.0060 (0.60)	1.2483	1.003
1.2673	1.2404	0.0210 (2.10)	1.2604	0.995
1.2510	1.2418	0.0040 (0.40)	1.2458	0.996
1.7120	1.6978	0.0156 (1.56)	1.7134	1.001
1.2296	1.2169	0.0047 (0.47)	1.2216	0.993
1.8450	1.8353	0.0039 (0.39)	1.8392	0.997
1.7350	1.7219	0.0105 (1.05)	1.7324	0.999
0.9144	0.9020	0.0118 (1.18)	0.9138	0.999
1.0703	1.0575	0.0120 (1.20)	1.0695	0.999
Erreur extrême		: ± 5 ‰		Moyenne
Déviation standard		: ± 2.5‰		0.998
Limite de confiance (95%)		: ± 5.6‰		

DOSAGE D'UN NITRATE DE CALCIUM PAR GRAVI-AMPÉROMÉTRIE À L'EDTA

Il était intéressant de voir si l'absence de l'ion chlore dans le milieu améliorait la précision du dosage.

Mode opératoire

Comme ci-dessus, avec une seule différence: l'échantillon et l'EDTA sont pesés dans le même bécher, on évite ainsi un transvasage de solutions. Nous avons effectué une série d'analyses de nitrate de calcium (pro anal.).

Résultats

Les résultats de ces dosages de nitrate de calcium sont donnés au Tableau II.

L'absence de l'ion chlore n'a pas amélioré la configuration des courbes ampérométriques de titration. Celles-ci présentent toujours un point d'inflexion. Les résultats du dosage du nitrate de calcium sont plus précis que ceux obtenus sur le carbonate. Il est vrai que dans le cas du nitrate nous avons évité le transvasage des solutions.

Si l'on complexe la grande partie du calcium par l'EDTA, le dosage ampérométrique peut se faire indifféremment avec une solution d'EDTA ou d'EGTA. Par contre, et sans qu'on puisse l'expliquer, si l'on ajoute de l'EGTA solide, la détermination de la fin du dosage par ampérométrie n'est plus possible ni avec une solution d'EDTA ni avec une solution d'EGTA ou du moins elle est très peu précise; une étude est en cours.

TABLEAU II

DOSAGE GRAVI-AMPÉROMÉTRIQUE DU Ca(II) DANS UN NITRATE DE CALCIUM PUR PAR L'EDTA (ET L'EGTA)

Calcium introduit (mM)	*EDTA pesé (mM)*	*EDTA 10^{-2} M écoulé (mM) ou (ml)*	*Calcium trouvé (mM)*	*Rapport Ca trouvé/ Ca introduit*
1.0747	1.0534	0.0195 (1.95)	1.0729	0.998
1.1735	1.1538	0.0199 (1.99)	1.1737	1.000
1.2769	1.2562	0.0194 (1.94)	1.2756	0.999
		EGTA 10^{-2} M écoulé (mM) ou (ml)		
1.0116	1.0055	0.0040 (0.40)	1.0093	0.999
0.8661	0.8596	0.0066 (0.66)	0.8659	1.000
1.1584	1.1488	0.0097 (0.97)	1.1581	1.000
0.6792	0.6718	0.0059 (0.59)	0.6774	0.997
Erreurs extrêmes		: ± 1.5‰		Moyenne
Déviation standard		: ± 1.2‰		0.999
Limite de confiance (95%)		: ± 2.7‰		

Dosage direct du carbonate de calcium

A titre comparatif, nous avons effectué une série de dosages du carbonate de calcium par la méthode directe (v. *Mode opératoire*[3]). Les résultats sont donnés dans le Tableau III.

TABLEAU III

DOSAGE AMPÉROMÉTRIQUE DIRECT DU CALCIUM(II) DANS UN CARBONATE DE CALCIUM PUR PAR L'EDTA

Calcium introduit (mM)	*EDTA 10^{-2} M écoulé = Ca^{2+} trouvé (mM) ou (ml)*	*Rapport Ca trouvé/ Ca introduit*	*Erreur relative*
0.948	0.947 (94.7)	0.999	
0.996	0.991 (99.1)	0.995	
0.961	0.963 (96.3)	1.002	Moyenne Ca trouvé/Ca introduit
0.997	0.991 (99.1)	0.994	0.999
0.998	0.995 (99.5)	0.997	
0.981	0.987 (98.7)	1.006	Erreurs extrêmes:
0.991	0.993 (99.3)	1.002	± 7‰
0.962	0.959 (95.9)	0.997	
0.996	0.998 (99.8)	0.992	
0.966	0.971 (97.1)	1.005	

APPLICATION

Titrage d'un échantillon renfermant du $CaCO_3$ de teneur inconnue par la méthode gravi-ampérométrique au moyen d'EDTA

Le premier dosage n'est qu'approximatif, il permet de situer la valeur recherchée. Le sel est séché, pesé puis dissous dans l'acide chlorhydrique concentré. On

chauffe à l'ébullition une minute et on alcalinise avec l'éthanolamine M jusqu'au pH de 10.5. Cet essai préliminaire utilise l'EDTA 10^{-1} M et est effectué selon le procédé classique[3]. Il conduit à des valeurs du calcium(II) comprises entre 25 et 26%.

Les résultats du dosage gravi-ampérométrique sont donnés dans le Tableau IV. Le poids d'EDTA ajouté est calculé pour une valeur du Ca égale à 25%.

TABLEAU IV

RÉSULTATS D'UN DOSAGE GRAVI-AMPÉROMÉTRIQUE DU CALCIUM(II) (env. 25.3 mg) DANS UN MÉLANGE INCONNU DE $CaCO_3$ + Na_2CO_3

Echantillon pesé (en mg)	*EDTA pesé (en mg)*	*EDTA 10^{-2} M écoulé (en ml)*	*Ca trouvé (en mg)*	*Ca trouvé (en %)*
111.12	257.58	1.14	28.14	25.31
113.74	243.81	6.30	28.72	25.25
128.01	297.58	0.76	32.28	25.27
		Moyenne:	en % Ca^{2+}	25.28
			en % $CaCO_3$:	63.19

La durée totale d'un tel dosage est de 30 à 40 min prédosages compris et d'environ 15 min si la teneur en calcium est approximativement connue.

Pour l'essai 2, nous avons pesé trop peu d'EDTA afin d'augmenter le volume de réactif nécessaire au dosage ampérométrique et de voir l'incidence sur la précision des résultats.

Remarques et conclusion

Pour le dosage ampérométrique[4] on a utilisé deux concentrations de complexon 10^{-1} et 10^{-2}. Comme on pouvait s'y attendre les sauts ampérométriques obtenus au point équivalent avec la concentration la plus élevée sont mieux marqués. Néanmoins, un rapide calcul nous a permis de constater que l'emploi de la concentration 10^{-2} M est recommandé car l'erreur faite sur le point final est inférieure au facteur 10 existant entre les deux concentrations.

Précisons pour conclure que la méthode décrite ci-dessus n'est valable que dans le cas où le calcium n'est pas accompagné du magnésium (une étude est en cours). Elle peut donc être utilisée actuellement dans des milieux où ce dernier est absent ou en faible quantité, notamment dans les ciments, etc. Pratiquement, nous constatons que pour les masses de calcium mises en oeuvre dans cette étude ($\sim$50 mg) la méthode indirecte (gravi-ampérométrique) se justifie, l'erreur extrême engendrée sur le résultat final étant de ± 1–$2^0/_{00}$ dans les meilleures conditions, tandis qu'elle se monte à $\pm 7^0/_{00}$ pour la méthode directe.

ÉTUDE THÉORIQUE DES ERREURS

Nous présentons maintenant une étude théorique de la précision de cette détermination et des causes d'erreur. Il est intéressant de rechercher quelles conditions pouvaient améliorer la précision du dosage.

Pour mettre en évidence les avantages d'une telle méthode, nous avons calculé les erreurs maximum du titrage ampérométrique (direct) et celles du dosage gravi-ampérométrique (indirect).

Symboles utilisés

Δp = précision de la balance analytique utilisée (mg)
P = masse de l'échantillon contenant le calcium à analyser (mg)
x = masse de calcium dans P mg d'échantillon (mg)
k_e = coefficient d'analyse Ca/EDTA ($=PA_{Ca}/PM_{EDTA}=0.1077$)
k_c = coefficient d'analyse Ca/$CaCO_3$ ($=PA_{Ca}/PM_{CaCO_3}=0.4004$)
V = volume du ballon jaugé renfermant la solution titrée d'EDTA (ml)
ΔV = précision de la graduation du ballon jaugé (ml)
b = masse d'EDTA pesée pour la préparation de la solution titrée (mg Ca)
t = titre réel (mg Ca.ml^{-1})
t' = titre théorique $b \cdot k_e/V$ (mg Ca.ml^{-1})
Δt = erreur de titre (mg Ca.ml^{-1})
a = masse d'EDTA ajoutée sous forme solide (méthode indirecte) (mg Ca)
N = volume (ml) de la solution titrée, nécessaire à la complexation du calcium (en admettant qu'il n'y a pas d'erreur de pesée)
Δn = précision des graduations de la burette utilisée pour le titrage (ml)
σ = facteur de proportionnalité reliant les précisions de deux burettes
f = excès de solution titrée nécessaire pour observer le point final (ml)

L'erreur maximum comprend: l'erreur de pesée de l'échantillon (δP), celle de la pesée de l'EDTA (δp) (par gravi-ampérométrie), l'erreur due au titre de la solution (δN), les erreurs de graduation et de lecture des burettes (δn) et l'erreur, toujours positive, de l'excès de réactif nécessaire à la détermination de la fin du titrage, décelable sur l'ampéromètre (δf). On a donc:

(*a*) erreur absolue de pesée de l'échantillon:

$$\delta P = \frac{\Delta p \cdot x}{P} \text{ (mg Ca)} \tag{1}$$

(*b*) erreur absolue de pesée de l'EDTA:

$$\delta p = \Delta p \cdot k_e \text{ (mg Ca)} \tag{2}$$

(*c*) erreur absolue due au titre:

$$\Delta t = t - t' = \frac{b \cdot k_e + \Delta p \cdot k_e}{V - \Delta V} - \frac{b \cdot k_e}{V}$$

$$\Delta t = \frac{V \cdot \Delta p \cdot k_e + \Delta V \cdot b \cdot k_e}{V(V - \Delta V)} \text{ (mg Ca.ml}^{-1}\text{)} \tag{3'}$$

masse de calcium à titrer: $x - a \cdot k_e = N \cdot t'$ (mg Ca) d'où:

$$\delta N = \frac{\Delta t}{t'}\left(x - a \cdot k_e + \frac{x \cdot \Delta p}{P} + \Delta p \cdot k_e\right) \text{ (mg Ca)} \tag{3}$$

(*d*) erreur absolue due à la lecture de la graduation de la burette:

$$\delta n = \Delta n(t' + \Delta t) \text{ (mg Ca)} \tag{4}$$

Cette erreur intervient deux fois.

(*e*) erreur absolue de fin de titrage:

$$\Delta f = (t' + \Delta t) \cdot f \text{ (mg Ca)} \tag{5}$$

Cette erreur est toujours positive et on peut en tenir compte en la déterminant au préalable, sur un essai à blanc.

En posant:

ε^{I} erreur absolue maximum (positive) de la méthode indirecte (en mg Ca),

ε^{D} erreur absolue maximum (positive) de la méthode directe (en mg Ca),

Δn^{I} précision des graduations de la burette utilisée en gravi-ampérométrie (ml),

Δn^{D} précision des graduations de la burette utilisée dans la méthode ampérométrique directe (ml),

on obtient finalement (en utilisant la même solution titrée pour les deux méthodes):

$$\varepsilon^{I} = \delta P + \delta p + \delta N^{I} + 2\delta n^{I} + \delta f \tag{6'}$$

$$\varepsilon^{D} = \delta P + \delta N^{D} + 2\delta n^{D} + \delta f \tag{7'}$$

$$\varepsilon^{I} = \frac{x \cdot \Delta p}{P} + \Delta p \cdot k_e + \frac{\Delta t}{t'}\left(x - a \cdot k_e + \frac{x \cdot \Delta p}{P} + \Delta p \cdot k_e\right) + 2\Delta n^{I}(t' + \Delta t) + f(t' + \Delta t) \tag{6}$$

$$\varepsilon^{D} = \frac{x \cdot \Delta p}{P} + \frac{\Delta t}{t'}\left(x + \frac{x \cdot \Delta p}{P}\right) + 2\Delta n^{D}(t' + \Delta t) + f(t' + \Delta t) \tag{7}$$

Conditions pour lesquelles la gravi-ampérométrie est plus précise que la titration directe ($\varepsilon^{I} < \varepsilon^{D}$)

En posant $\varepsilon^{I} \leqslant \varepsilon^{D}$, on tire des équations (6) et (7):

$$a \geqslant \Delta p\left(1 + \frac{t'}{\Delta t}\right) - \frac{t'}{k_e}\left(\frac{\Delta n^{D} t'}{t} + \Delta n^{D} - \frac{\Delta n^{I} t'}{t} - \Delta n^{I}\right) \tag{8}$$

Admettons que: $\Delta n^{D} = \sigma \Delta n^{I}$ ($\sigma \geqslant 1$)

Alors, en remplaçant dans (8):

$$a \geqslant 1 + \frac{t'}{\Delta t}\Delta p - \frac{2t'}{k_e} \cdot \Delta n^{I}(\sigma - 1) \tag{9}$$

Plus a sera petit, plus les limites d'applications de la méthode gravi-ampérométrique seront grandes; plus le terme compris dans le deuxième crochet sera petit, plus la méthode indirecte sera bonne. Pour réaliser ceci, il faut donc que Δp soit le plus petit possible et que, au contraire, $(2t'/k_e)\,\Delta n^{I}(\sigma - 1) = R(\sigma - 1)$ soit grand, c'est-à-dire σ grand.

La précision de la balance (Δp) ainsi que le rapport $\Delta n^{D}/\Delta n^{I} = \sigma$ des précisions des burettes utilisées jouent un grand rôle. Il y a donc compétition entre Δp et σ: plus $(\sigma - 1)$ est grand, plus Δp pourra être grand, c'est-à-dire la balance moins précise.

Comme il est impossible de déterminer Δn^{I} sans connaître a priori la valeur de $(x - a)$ (masse de calcium qui reste à titrer) et ainsi de pouvoir choisir la burette

adéquate, le terme $R(\sigma-1)$ n'a qu'une signification théorique, ne permettant de tirer de la relation (9) que des considérations générales.

Par contre, en posant $\sigma=1$ (soit $\Delta n^{I}=\Delta n^{D}$), ce terme tombe et

$$a \geqslant \Delta p \left(1+\frac{t'}{\Delta t}\right) \qquad (10)$$

ce qui nous permet de déterminer, en utilisant des burettes de même précision, la valeur limite de a à partir de laquelle la méthode indirecte est moins précise que la directe.

On remarque que cette limite va dépendre beaucoup de la précision (Δp) de la balance analytique utilisée pour la détermination de la masse d'EDTA solide (méthode indirecte). Dans ces conditions, la valeur limite de a calculée est utilisable pratiquement. Elle permet par exemple de déterminer à partir de quelle valeur de a un changement de burette s'impose pour garder: $\varepsilon^{I}<\varepsilon^{D}$. Si un tel changement n'est plus possible, aucune amélioration de Δn possible, la valeur de a déterminée nous donnera la limite absolue de la méthode indirecte pour laquelle il est inutile de la mettre en oeuvre. Ces considérations vont être illustrées par un exemple numérique.

Exemple numérique

La précision (tolérance) du matériel le plus couramment utilisé pratiquement (balance, ballon jaugé, burette graduée, etc.) est donnée par le fabricant. Dans cette étude, nous avons utilisé les normes indiquées par DOERFFEL[5].

TABLEAU V

VOLUME D'EDTA 10^{-2} M THÉORIQUEMENT NÉCESSAIRE POUR LE TITRAGE DE DIVERSES MASSES DE CALCIUM ET LES BURETTES CORRESPONDANTES AVEC LEUR PRÉCISION

Ca^{2+} à titrer (x) (mg)	*EDTA 10^{-2} M nécessaire (N) (ml)*	*Burette volume total (ml)*	*Précision (Δn) de la burette (ml)*
100	249.50	250	0.2
50	124.75	250	0.2
20	49.90	50	0.04
10	24.95	25	0.03
5	12.47	25	0.03
2	4.99	5	0.01
1	2.49	5	0.01
0.5	1.24	2	0.01

TABLEAU VI

VALEURS DE BASE POUR LA DÉTERMINATION DE ε^{I} ET ε^{D} AU MOYEN DES RELATIONS (6) ET (7)

	Précision de la balance (Δp)		
	0.1 mg	*0.01 mg*	*0.001 mg*
$t'=10^{-2}$ M (mg Ca.ml^{-1})	0.40080	0.40080	0.40080
Δt (relation (3')) (mg Ca.ml^{-1})	0.00016	0.00015	0.00015
$\Delta t/t$	0.00037	0.00037	0.00037
$t=t'+\Delta t$ (mg Ca.ml^{-1})	0.40096	0.40095	0.40095

Anal. Chim. Acta, 45 (1969) 457–466

TABLEAU VII

RÉSULTATS OBTENUS, POUR L'EXEMPLE DÉCRIT CI-DESSUS

(MD = méthode directe, MI = méthode indirecte (gravi-ampérométrique))

Masse à doser (x) (mg Ca)	*Masse EDTA (a) ajoutée (mg Ca)*	*A titrer (x − a) (mg Ca)*	*Précision balance Δp (mg Ca)*	*MD δP (mg Ca)*	*MI δP + δp (mg Ca)*	*MD et MI*		*MD et MI*		*MD et MI δf (mg Ca)*	ε^D *(mg Ca)*	ε^I *(mg Ca)*	ε^D *et* ε^I *(‰)*
						δN^D *(mg Ca)*	δN^I *(mg Ca)*	δn^D *(mg Ca)*	δn^I *(mg Ca)*				
	0	50		0.04000	—	0.01851	—	0.16038	—	0.02	0.23889	—	4.78
50	49.0	1	0.1	—	0.05077	—	0.00039	—	0.00802	0.02	—	0.07918	1.58
	49.5	0.5		—	0.05077	—	0.00020	—	0.00802	0.02	—	0.07899	1.58
	0	5		0.04000	—	0.00186	—	0.02406	—	0.02	0.08592	—	17.18
5	4.0	1	0.1	—	0.05077	—	0.00039	—	0.00802	0.02	—	0.07918	15.84
	4.9	0.1		—	0.05077	—	0.00006	—	0.00802	0.02	—	0.07885	15.77
	0	0.5		0.04000	—	0.00019	—	0.00802	—	0.02	0.06821	—	136.42
0.5	0.3	0.2	0.1	—	0.05077	—	0.00009	—	0.00802	0.02	—	0.07888	157.76
	0.4	0.1		—	0.05077	—	0.00006	—	0.00802	0.02	—	0.07885	157.70
	0	50		0.00400	—	0.01850	—	0.16037	—	0.02	0.20287	—	4.06
50	49.0	1	0.01	—	0.00508	—	0.00037	—	0.00801	0.02	—	0.03346	0.67
	49.5	0.5		—	0.00508	—	0.00018	—	0.00801	0.02	—	0.03327	0.67
	0	5		0.00400	—	0.00185	—	0.02405	—	0.02	0.04090	—	8.18
5	4.0	1	0.01	—	0.00508	—	0.00037	—	0.00801	0.02	—	0.03346	6.69
	4.9	0.1		—	0.00508	—	0.00004	—	0.00801	0.02	—	0.03313	6.63
	0	0.5		0.00400	—	0.00018	—	0.00801	—	0.02	0.03219	—	64.38
0.5	0.3	0.2	0.01	—	0.00508	—	0.00008	—	0.00801	0.02	—	0.03317	66.34
	0.4	0.1		—	0.00508	—	0.00004	—	0.00801	0.02	—	0.03313	66.26

Soit à doser le calcium (de 0.5 à 100 mg) dans des masses diverses de $CaCO_3$ pur. Le Tableau V donne les volumes d'EDTA 10^{-2} M nécessaires pour titrer les masses de Ca^{2+} considérées.

Le Tableau VI indique les valeurs de t', Δt, $\Delta t/t$ et $(t'+\Delta t)$ déterminées au moyen de la relation (3'), pour des précisions de pesées (balances) diverses. Ballon jaugé utilisé pour la préparation de la solution titrée: 1000 ml (précision: ± 0.38 ml).

Conclusions

Les valeurs théoriques trouvées (Tableau VII) confirment celles obtenues pratiquement. En effet, lors du titrage direct de 50 mg de calcium: erreur pratique: $\pm 7^0/_{00}$, erreur théorique: $\pm 4.78^0/_{00}$. Le dosage indirect de la même masse de calcium (à titrer environ 0.5 mg): erreur pratique: $\pm 1.5^0/_{00}$, erreur théorique: $\pm 1.58^0/_{00}$.

Cette étude théorique nous a donc permi de constater que la méthode gravi-ampérométrique proposée améliore sensiblement la précision du dosage titrimétrique du calcium (ampérométrie directe). Cependant cet avantage est limité par le matériel de titrage à disposition. En effet, à partir du moment où il n'est plus possible d'améliorer la précision des graduations des burettes par une diminution du volume de celles-ci, l'application de la méthode indirecte ne se justifie plus. La masse limite de calcium pour laquelle $\varepsilon^I \leqslant \varepsilon^D$, peut alors se calculer au moyen de la relation (10) en posant:

$$x = a = \Delta p\left(1 + \frac{t'}{\Delta t}\right) \tag{11}$$

En considérant l'exemple ci-dessus (v. Tableau VI) et une précision de la pesée de $\Delta p = 0.01$ (balance semi-micro): $x = 25$ mg.

Dans ces conditions, en dessous d'une masse absolue de calcium à doser de 25 mg, la méthode indirecte proposée est à rejeter si aucune amélioration de la précision des graduations de la burette ne peut être envisagée ($\sigma = 1$). Par contre, pour une masse de calcium supérieure à 25 mg et en choisissant judicieusement la valeur de a (au moyen de la relation (9)), l'application de la méthode indirecte se justifie. Enfin, un changement de burette entraînant une valeur de $\sigma > 1$ est toujours en faveur de la méthode gravi-ampérométrique.

RÉSUMÉ

Un dosage gravi-ampérométrique du calcium en fort pourcentage (de l'ordre de 50 mg) est proposé. La méthode consiste à ajouter une masse exactement pesée de réactif (EDTA) et légèrement inférieure à celle nécessaire pour complexer la totalité du calcium. Le dosage est alors achevé par ampérométrie selon une méthode ampérométrique. Une étude comparative prouve que la méthode proposée est plus précise que le dosage ampérométrique direct au moyen d'EDTA. Les erreurs relatives sont: méthode proposée ± 1–$2^0/_{00}$, méthode directe $\pm 7^0/_{00}$.

Une étude théorique des erreurs intervenant au cours des diverses manipulations, démontre que théoriquement la méthode gravi-ampérométrique de dosage est plus précise que le dosage ampérométrique direct. Les résultats théoriques confirment les résultats pratiques.

SUMMARY

A gravimetric–amperometric determination of high percentages of calcium is proposed. An exactly weighed amount of EDTA, slightly less than the theoretical amount, is added and the determination is then completed amperometrically. The proposed method is more precise than direct amperometric titration for large amounts of calcium; relative errors in determining 50 mg Ca are: ± 1–$2‰$ for the proposed method, $\pm 7‰$ for the direct method. A theoretical study of the errors involved confirms the greater precision of the proposed method at the 50-mg Ca level.

ZUSAMMENFASSUNG

Es wird eine gravimetrisch–amperometrische Bestimmung für hohe Prozentgehalte Calcium vorgeschlagen. Dazu wird eine genau gewogene Menge EDTA, welche etwas geringer ist als der theoretische Betrag, zur Calciumlösung gegeben und die Bestimmung dann amperometrisch durchgeführt. Die vorgeschlagene Methode ist genauer als die direkte amperometrische Titration für grosse Gehalte Calcium. Der relative Fehler beträgt bei der Verwendung von 50 mg Calcium $\pm$ 1–2%, bei der vorgeschlagenen Methode und $\pm$ 7% bei der direkten Methode. Theoretische Überlegungen bestätigen die grössere Genauigkeit der vorgeschlagenen Methode.

BIBLIOGRAPHIE

1 D. MONNIER ET A. ROUÈCHE, *Helv. Chim. Acta*, 47 (1964) 102.
2 A. ROUÈÇHE ET D. MONNIER, *Anal. Chim. Acta*, 31 (1964) 426.
3 D. MONNIER, G. DELPIN ET W. HAERDI, *Anal. Chim. Acta*, 35 (1966) 231.
4 Pour plus de détails, consulter: A. DAÏNA, *thèse n. 1453*, Université de Genève, 1967.
5 K. DOERFFEL, *Z. Anal. Chem.*, 185 (1962) 1.

Analytica Chimica Acta
Elsevier Publishing Company, Amsterdam
Printed in The Netherlands

THE USE OF THERMOGRAVIMETRIC ANALYSIS IN KINETIC STUDIES OF THE THERMAL DEGRADATION OF POLYMERS

FRANCISCO FARRÉ-RIUS*, JEAN HURET, MARC PUYO AND GEORGES GUIOCHON
Laboratoire du Professeur Jacque, Ecole polytechnique, Paris 5ème (France)
(Received January 17th, 1969)

The application of thermal methods of analysis to polymer studies is expanding rapidly but the collection of data has tended to outstrip the necessary theoretical background. There is some general agreement on a few rules based on general kinetics but no experimental study has been made to test their validity and to determine the fastest and most accurate method of deriving useful information from the experimental data[1]. The purpose of this paper is to show how useful kinetic data may be easily and accurately derived from simple thermogravimetric analysis.

Thermogravimetry is not a good method for determining the rate order of a reaction. Although the reaction rates do depend on the concentration of the reactants in a more or less complicated way (the rate equation leading sometimes to a reaction order), the rate is usually proportional to the mass of the reactants: if the initial sample mass is doubled, the reaction rate at any time will be twice as great. Moreover, during the decomposition of a given sample, the rate of decomposition will be proportional to the mass of the sample insofar as its concentration remains constant and equal to 1. Thermogravimetric experiments are very seldom carried out in solution because most solvents are too volatile. The thermogravimetric or apparent order of the decomposition is unity in most cases.

The only exceptions result either from diffusion being the rate-controlling step, because the reaction products diffuse slowly to the gas–liquid interface, or from some autocatalytic effect; *e.g.*, an involatile product or intermediate may act as a catalyst or an inhibitor of the pyrolysis. These conditions are, however, quite rare and the usual practice, which is to analyze only small samples in the form of very thin layers, drastically limits the possibility of diffusion-controlled reactions.

Practically the only reasons which may prevent the weight loss rate from being proportional to the mass of the undecomposed polymer are that the reaction mechanism may change during the course of the reaction[2] or that the degradation may be a zero-order reaction[3]. This is not the general case although changes in the reaction mechanism occur occasionally[2].

If the decomposition mechanism changes during the reaction, the rate will not decrease in proportion to the mass of the polymer. However, the decomposition rate at any time after the beginning of the reaction will be proportional to the initial mass of the sample. The variations of $(1/m) \cdot (dm/dt)$ are those of the total rate constant during the reaction and may give some indication of a possible change of mechanism[2].

The determination of the apparent "mass order" is therefore of no direct

* Present address: Perkin-Elmer Hispania, Madrid, Spain.

interest, but it is sound experimental practice to check if the compound under study undergoes a normal decomposition reaction. In some cases, samples thinner than usual should be used to speed up diffusion of some reaction products. In other cases, difficulties could be encountered because some intermediate compounds of high or medium molecular weight may either decompose further or volatilize and react in the gas phase. The reaction rate then does not correspond exactly to the rate of weight loss. These are some of the main difficulties found in accounting for thermogravimetric results[4,5]. It should always be borne in mind, however, that any difference between unity and the apparent order should originate from the experimental conditions of the decomposition, or from changes in the decomposition mechanism, or from an unusual mechanism.

THEORETICAL

In the subsequent discussion, it is assumed that the decomposition reaction is normal, *i.e.* it proceeds at a rate which is proportional to the mass of the undecomposed sample:

$$dm/dt = -km \tag{1}$$

The theoretical conclusions will be illustrated by the results obtained in the study of the decomposition of polyethyleneglycol adipate (PEGA) which satisfies these requirements[6].

In dealing with such a first-order reaction, the advantages of programmed-temperature gravimetric analysis, better known as thermogravimetric analysis, are well known[7], and can be summarized as follows. There is no warm-up and equilibration period during which a large part of the sample may decompose, leading to less accurate results; only a few samples are necessary for a series of experiments, the value of the activation energy and the values of the rate constant in a large temperature range being obtained for each sample, so that the reproducibility of these results and the homogeneity of the product can be studied simultaneously.

Practically all published papers in programmed-temperature thermogravimetric analysis make use of linear programs, hence these are discussed first. Subsequently, it is shown that other programs can be used with advantage.

Linear programming

The derivation of the first-order rate constant from thermogravimetric records has been the subject of many papers[6,8-12]. No rigorous solution is possible when a linear program is used but some convenient and reasonably accurate approximations have been worked out. The determination of the rate constant is made in two steps: the derivation of the activation energy, and then the derivation of the rate constant for a given value of the temperature.

Determination of the activation energy. If the reaction is assumed to be first order:

$$dm/dt = -Z \exp(-E/RT)m \tag{2}$$

where Z is a constant and E the activation energy, and if the temperature of the sample

varies linearly with time:

$$T = T_0 + qt \tag{3}$$

then eqn. (2) may be integrated to:

$$\ln \frac{m}{m_0} = -\frac{Z}{q}\int_{T_0}^{T} \exp(-E/RT)\mathrm{d}T \tag{4}$$

but the integral in eqn. (4) cannot be solved rigorously. Several authors[8-10] have given numerical solutions using various types of series and have published tables to help solve eqn. (4) in practical cases[9]. These solutions are, however, complicated and, as in many other cases in physical chemistry[13], the best answer does not appear to lie in forcing eqn. (4) to numerical solution.

A general solution may be obtained[11] which is valid with one simple condition: if a characteristic temperature is defined as the temperature at which a fraction 1/e of the initial sample weight remains undecomposed, it can be assumed that:

$$\Theta = T - T_S \tag{5}$$

is small compared to T_S in the temperature range where the reaction takes place. Practically, as is shown later, in the temperature range where more than 90% of the weight loss takes place, Θ/T_S is smaller than a few percent. HOROWITZ AND METZGER[11] have shown that with this assumption eqn. (4) can be solved. A more rigorous treatment has been published together with some experimental results[6]. This solution of eqn. (4) is:

$$\ln \ln(m_0/m) = (E/RT_S^2)\,\Theta \tag{6}$$

Thus a plot of $\ln \ln(m_0/m)$ *vs.* Θ should be linear and from the slope of this straight line it is possible to derive the activation energy.

The main drawback of this method is its relative inaccuracy. When Θ is large, eqn. (6) is not valid, so that the above plot deviates from linearity; when Θ is small, E is the ratio of two small quantities and the experimental error is very large, so that the points corresponding to large Θ values are given too much weight in the computation of E.

Determination of the rate constant. It has also been shown[6] that the calculation suggested by HOROWITZ AND METZGER[11] makes it possible to derive the rate constant at any temperature. This constant is given by:

$$k = Z \exp(-E/RT) = \frac{qE}{RT_S^2} \exp\left\{\frac{E}{R}\left(\frac{1}{T_S} - \frac{1}{T}\right)\right\} \tag{7}$$

thus the value of the rate constant at the characteristic temperature T_S is:

$$k\,(T_S) = qE/RT_S^2 \tag{8}$$

Of course, T_S and $k\,(T_S)$ are functions of q, and one of the main drawbacks of this method is that it is not possible to derive an explicit relationship between the characteristic temperature and the rate constant: T_S is an empirical parameter which must be calculated for each experiment, from the weight and temperature records. Equation (8) gives the value of the rate constant at the characteristic temperature. To calculate the value of the rate constant at any other temperature, the simplest

method is to draw, on a $\ln k$ *vs.* $1/T$ plot, a straight line of slope E/R through the point of coordinates $\ln k\ (T_S)$ and $1/T_S$.

Determination of the activation energy from the inflexion slope. It is possible to show that the characteristic point defined by HOROWITZ AND METZGER[11] on the thermogravimetric record is the inflexion point of this sigmoidal curve. Differentiation of eqn. (2) with respect to time, substitution of the value of dm/dt from eqn. (2), and replacement of dT/dt by q (eqn. 3), gives:

$$\frac{d^2m}{dt^2} = -Z \exp(-E/RT)m \left\{\frac{qE}{RT^2} - Z \exp(-E/RT)\right\} \quad (9)$$

The temperature T_I corresponding to the inflexion point of the thermogravimetric curve is thus given by the equation:

$$k\ (T_I) = qE/RT_I^2 \quad (10)$$

Equations (8) and (10) cannot be fulfilled simultaneously when $T_I \neq T_S$ because the function:

$$z = T^2 \exp(-E/RT) \quad (11)$$

is uniform and increases monotonically with increasing temperature, so that the equation:

$$z = qE/RZ \quad (12)$$

has only one root with a physical meaning thus:

$$T_I = T_S \quad (13)$$

and therefore:

$$m_I = m_0/e \quad (14)$$

Introducing eqns. (10) and (14) into eqn. (2) gives:

$$E = \frac{e\ RT_S^2}{qm_0}\left(\frac{dm}{dt}\right)_S \quad (15)$$

Equation (15) allows the activation energy to be calculated from the most important part of the thermogravimetric curve, the part around the inflexion point which corresponds to roughly one half of the weight loss.

Temperature range where the pyrolysis takes place. Equation (6) can be used to determine the temperature range where the pyrolysis takes place, *i.e.* the values of Θ between which a given percentage of the total weight loss takes place. A pyrolysis ratio m/m_0 equal to $e^{-\alpha}$ is reached for a temperature such that:

$$\Theta = (RT_S^2/E) \ln \alpha \approx 4.6(T_S^2/E) \log \alpha \quad (16)$$

As shown in Table I, a relatively large pyrolysis ratio is reached for moderate values of α. For example, $\alpha = 3$ gives a weight loss of 95%. Then:

$$\Theta_{95} = 2.17(T_S^2/E)$$

However, a small pyrolysis ratio is obtained only for very small values of α. For example, a weight loss of 5% corresponds to $\alpha^{-1} = 19.4$. Then:

$$\Theta_5 = -5.92(T_S^2/E)$$

As shown in Table II, for pyrolysis of PEGA, the practical range of values of the characteristic temperature is 580 to 660°K. With an activation energy of 44 kcal/mole this gives values of T_S^2/E between 7.6 and 9.9. Thus:

$$-59 < \Theta_5 < -45^\circ$$

$$16 < \Theta_{95} < 22^\circ$$

90% of the total weight loss takes place in the temperature range 60–80°C.

TABLE I

VALUES OF THE PYROLYSIS RATIO

α	m_0/m [a]	$\Delta m/m_0$ (%)
1/16	1.065	6
1/8	1.133	12
1/4	1.284	22
1	2.72	63
2	7.39	87
3	20.1	95
4	54.6	98.2

[a] $m/m_0 = e^{-\alpha}$.

Theory of nonlinear temperature programs

Although the theoretical treatment leads to calculations which are relatively easy to carry out and which, as shown below, give results in good agreement with experimental facts, it would be more satisfactory, and perhaps more precise to use a temperature program which would lead to a more rigorous mathematical treatment[14].

Assuming that the sample temperature is a function of time:

$$t = f(T) \tag{17}$$

and combining this with eqn. (2) gives:

$$(dm/m) = -Z \exp(-E/RT) f'(T) dT \tag{18}$$

where $f'(T)$ is the first derivative of $f(T)$. This equation obviously cannot be integrated for linear programs. However, there is an infinity of functions $f(T)$ such that eqn. (18) could be integrated. Any functions $f(T)$ such that $f'(T)dT = g(1/T)d(1/T)$ allow this integration. We shall discuss only two particular cases because of their practical interest.

Hyperbolic temperature program. The simplest function such that the right half of eqn. (18) could be integrated is given by:

$$f'(T)dT = -a\,d(1/T) = (a/T^2)dT \tag{19}$$

where a is a positive constant. (A program during which the temperature decreases with increasing time is obviously of no interest.) Equation (18) is then integrated to:

$$\ln(m/m_0) = (RZa/E)\{\exp(-E/RT_0) - \exp(-E/RT)\} \tag{20}$$

If it is assumed that the starting temperature T_0 is small enough for the re-

action rate at that temperature to be neglected, which is practically always the case, then:

$$\ln \ln(m_0/m) = \ln(RZa/E) - (E/RT) \tag{21}$$

E can be derived from the slope of a plot of $\ln \ln(m_0/m)$ *vs.* $1/T$ and Z from the ordinate of the plot.

It is interesting to note that, for the hyperbolic program also, the inflexion point corresponds to a relative mass of undecomposed sample equal to 1/e, as far as the simplified eqn. (21) is valid.

Differentiation of eqn. (2) with respect to time gives:

$$\frac{d^2m}{dt^2} = -Zm \exp(-E/RT)\left[Z \exp(-E/RT) - \frac{1}{f'(T)}\frac{E}{RT^2}\right] \tag{22}$$

Combining this equation with eqn. (19) and equating to zero gives the rate constant at the temperature T_i, corresponding to the inflexion point:

$$Z \exp(-E/RT_i) = E/aR \tag{23}$$

Combining eqns. (21) and (23) gives $m_0/m_i = e$.

It is thus easy to derive from the thermogravimetric record the activation energy, the temperature corresponding to the inflexion point and the rate constant at that temperature and then the rate constant at any other temperature.

Integration of eqn. (19) gives the program law:

$$t = a(1/T_0 - 1/T) \tag{24}$$

The hyperbolic temperature program can alternatively be written:

$$T = aT_0/(a - T_0t) \tag{25}$$

Exponential temperature program. Another possible solution is to use a program such that:

$$f'(T)dT = -b \exp(-c/RT)d(1/T) \tag{26}$$

where b and c are positive constants. Integration of this equation gives the program law:

$$t = f(T) = (b/c)[\exp(-c/RT) - \exp(-c/RT_0)] \tag{27}$$

Integration of eqn. (18) with such a program law gives:

$$\ln (m/m_0) = -\{bZR/(c+E)\}[\exp\{-(c+E)/RT\} - \exp\{-(c+E)/RT_0\}] \tag{28}$$

If the initial temperature is small enough for the decomposition rate at the starting temperature to be ignored, eqn. (28) may be simplified to:

$$\ln \ln (m_0/m) = \ln \{bZR/(c+E)\} - (c+E)/RT \tag{29}$$

In this case the relative sample mass at the inflexion point is not equal to 1/e. Combining eqns. (22), (26) and (28) shows that:

$$\ln (m_0/m_i) = E/(c+E) \neq 1$$

EXPERIMENTAL

A Thermobalance TH 59 Adamel (6, Passage Louis-Philippe, Paris, France) was used. This balance has a wire suspension and magnetic damping; it is very stable

and reliable. The deflexion of the beam is proportional to the weight variation of the sample. This deflexion is recorded by a spot-follower. The sensitivity can be changed easily if needed; for these experiments, it was about 0.15 mg/mm and was determined before and after each run by adding a calibrated weight. This can be done in a controlled atmosphere. Careful attention was given to avoiding any source of artefacts[4,5,7] known to play an important role in the measurements. For each run the sample weight and sample temperature were simultaneously recorded *vs.* time on the same sheet of paper.

The sample weight was 15–20 mg and the sensitivity of the weight measurements was about 0.2 mg. The crucible had an internal diameter of 16 mm and a height of 8 mm. The ratio of sample mass per unit surface of the sample holder was thus 0.1 mg/mm^2 in agreement with MADORSKY's specifications[2]. Loss of sample by spattering was prevented by the crucible height.

The pyrolyses were carried out in pure argon (Argon U, Air Liquide, Paris). The balance cell was evacuated to 0.1 torr and filled with argon several times; then a flow of 40 cm^3/min of argon was maintained. The temperature of the furnace was controlled within 0.5°. The temperature of the sample was measured by a thermocouple in contact with the bottom of the crucible, and recorded with the sample weight; the temperature could be measured with an accuracy of 1°.

The temperature of the furnace was programmed by a mechanical system with a rotating cylindrical cam; cams for linear programs are easy to build by fitting a straight, thick plastic ribbon on the rotating cylinder. The cam corresponding to the hyperbolic program was more tedious to build. However, the same fluctuations ($\pm 1°$) of the temperature around the ideal law of variations were obtained in all cases.

For all experiments, the samples were taken from the same batch of polyethyleneglycol adipate with an average molecular weight of 2400[6].

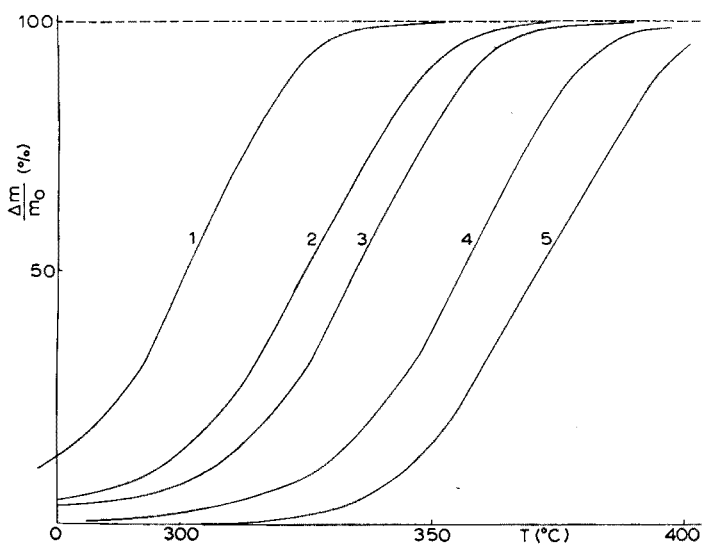

Fig. 1. Variation with the temperature of the weight of PEGA samples at various program rates. (1) 20°/h; (2) 45°/h; (3) 76°/h; (4) 180°/h; (5) 338°/h. The horizontal dotted line corresponds to a pyrolysis ratio 1.

RESULTS

Figure 1 shows the variations of the relative sample weight with temperature for samples of PEGA pyrolyzed with linear programs at various rates. The program rate, the characteristic temperature corresponding to each of these runs and to a few others are given in Table II, as well as the activation energy derived from the slope of a ln ln (m_0/m) *vs.* Θ plot. Figure 2 shows such a plot for one of the curves given in Fig. 1. For each of the experimental points on Fig. 2, the horizontal and vertical segments are equal to twice the absolute standard deviation of the measurement. The slight curvature which can be seen on Fig. 2 at large values of Θ, both positive

TABLE II

ACTIVATION ENERGY OF THE PYROLYSIS OF POLYETHYLENEGLYCOL ADIPATE

N[a]	*Program rate q (°/h)*	T_s (°)	*Activation energy (kcal/mole)*		
			H and M method	*Inflexion method*	*Other method*
	18.6	305	45.5	45.4	
	18.6	306	46.0	45.7	
1	20	308	45.5	45.5	
2	45	338	45.0	45.1	
3	76	342	45.0	45.2	
	170	367	44.5	44.7	
4	180	372	45.5	45.3	
	180	370	44.5	45.1	
	180	372	44.5	44.8	
5	338	383	44.5	45.0	
	Isothermal				45.7
	Hyperbolic				45.6

[a] Curve number on Fig. 1.

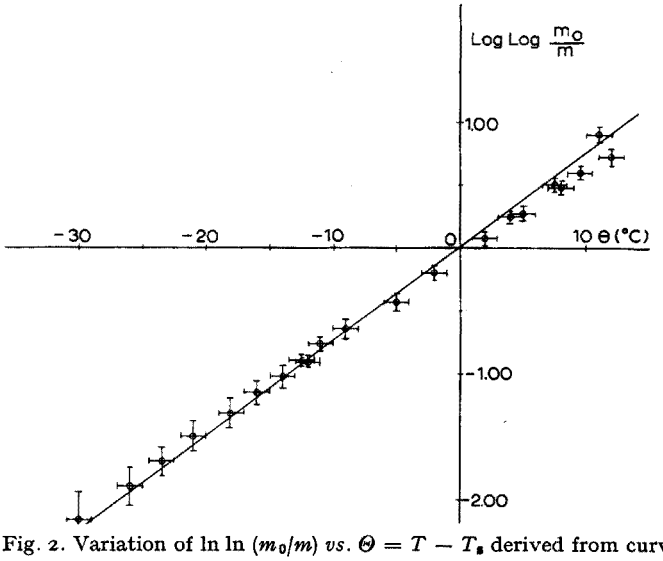

Fig. 2. Variation of ln ln (m_0/m) *vs.* $\Theta = T - T_s$ derived from curve 1, Fig. 1.

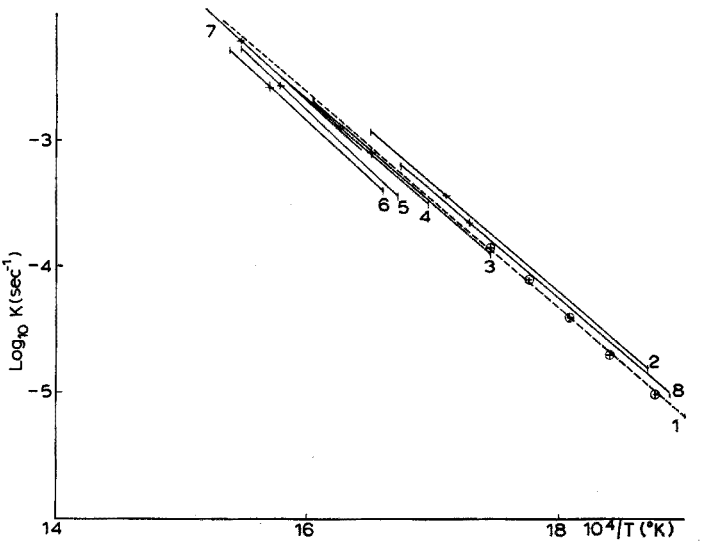

Fig. 3. Variation of the logarithm of the first-order rate constant of the pyrolyis of PEGA with the inverse of the absolute temperature. Dotted line (1), isothermal results. Solid lines, programmed temperature experiments, program rates: (2) 20°/h; (3) 45°/h; (4) 76°/h; (5) 170°/h; (6) 180°/h; (7) 338°/h; (8) 18.6°/h.

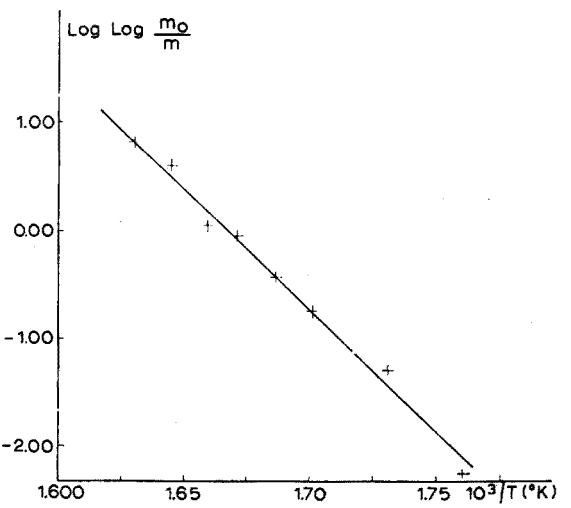

Fig. 4. Variation of ln ln (m_0/m) *vs.* $1/T$ for a PEGA sample analyzed with an hyperbolic program of temperature $1/T = -1.25 \cdot 10^{-6} t + 1.95 \cdot 10^{-3}$ ($°K^{-1}$, t in sec).

and negative, results from the fact that, when Θ is no longer small compared to T_S, the assumptions made in deriving eqn. (6) are not valid. The same linear plots were obtained for all the experiments.

Equation (8) allows a calculation of the value of the rate constant at the characteristic temperature from the program rate, the activation energy and the characteristic temperature. The results corresponding to the curves shown in Fig. 1

are given in Fig. 3 on a log k *vs.* $1/T$ plot. In each case a straight line with a slope equal to E/R is drawn through the point log k (T_S), $1/T_S$. This straight line starts and ends at the points corresponding to the values of the temperature at which the sample weight is 0.95 and 0.05 times the initial weight.

The thermogravimetric records obtained with hyperbolic programs were very similar to those obtained with linear programs. Figure 4 shows the plot of ln ln (m_0/m) *vs.* $1/T$ obtained from one of these records. The corresponding value of the activation energy is given in Table II.

DISCUSSION

All the experimental results obtained and described above are consistent and in agreement with the theoretical predictions. Before the extent of this agreement and some of its consequences are discussed, it is interesting to examine the validity of the first assumption, *i.e.* that the decomposition of PEGA is first-order.

Determination of the order of the reaction

A study of the kinetics of the decomposition of PEGA has been published previously[6]. It has been shown, by means of isothermal thermogravimetric analysis, that in the temperature range studied here this reaction is first-order. However, a later study of the mechanism of the thermal decomposition of PEGA[15] has shown that three completely different and competitive reactions occur. The activation energies of these reactions are very close (36–42 kcal/mole) so that their relative rates do not change practically between at least 280 and 330° [16]. Despite this rather complex mechanism a first-order weight loss is observed by thermogravimetry.

It is much more difficult, with programmed temperature thermogravimetry, to determine if the rate order is one, because in these conditions the reaction rate depends on two variables, sample mass and sample temperature, instead of only one, sample mass, in isothermal conditions. Thus the profile analysis of the thermogravimetric record must be very subtle, in order to recognize slight deviations from first-order law. This is probably the most important drawback of programmed temperature thermogravimetry. As is shown below, however, this method makes it possible to study the kinetics of the decomposition in a much broader temperature range than isothermal analysis.

The most important deviations observed when the reaction is not first order are that the inflexion point of the curve is no longer observed at a relative sample mass equal to 1/e, that the corresponding mass depends on the program rate, and that the ln ln (m_0/m) *vs.* Θ or $1/T$ (depending on the program law) plots are no longer linear.

Influence of the program rate

The thermogravimetric curve depends strongly on the program rate (*cf.* Fig. 1). The curves obtained are nearly identical, but they do not derive from each other by mere translation: the higher the program rate, the higher the temperature range in which the reaction appears to proceed, but also the less steep the curves.

On the kinetic data. This displacement of the thermogravimetric curve should not be considered as a kind of artefact, as some authors have done, since it results

directly from the dependence of the reaction rate constant on the temperature; with a fast program rate, the reaction has less time to proceed at low temperature, where its rate is relatively slow. The time scale is different for the various curves which on m *vs.* t plots are steeper and steeper with increasing program rate. As is shown by Fig. 1, the temperature at which a given pyrolysis ratio is reached seems to increase with the logarithm of the program rate.

It is shown below that this relationship, although it holds quite satisfactorily over a limited range, is only approximate. The kinetic results derived from these different curves are in very good agreement, despite the large variation in the temperature range where the decomposition occurs. The standard deviation of the values of the activation energy derived from experiments made with various linear program rates is 0.5 kcal/mole or 1.2% (Table II). These values are also in agreement with those derived from isothermal experiments. The values of the rate constant are also in good agreement, but there is a wider fluctuation in the values of the frequency factor Z than in those of the activation energy (Fig. 3). A slight decreasing trend is observed at higher temperatures.

On the decomposition ratio observed at a given temperature. Equation (4) may be written as follows

$$\log (m/m_0) = -(1/q) \int_{T_0}^{T} k\mathrm{d}T = -(A/q) \tag{30}$$

where A is a function of the temperature only. Accordingly, at high temperature where A/q is large, the relative amount of undecomposed sample, m/m_0, increases exponentially with increasing program rate and the relative weight loss decreases steadily (*cf.* Table III). Figure 5 shows the variation of log (m/m_0) with $1/q$ at different

TABLE III

VARIATION OF THE RELATIVE WEIGHT LOSS WITH THE PROGRAM RATE

q (°/min)	$1/q$	$\Delta m/m_0$ (%)[a]			
		$T = 300°$		$T = 350°$	
		Experiment	*Theory*	*Experiment*	*Theory*
45				95.0	98.0
76	$1.32 \cdot 10^{-2}$	12.0	14.0	90.5	91.0
101				85.5	83.5
138				72	73.5
170	$5.88 \cdot 10^{-3}$	5.0	6.5	64	64.5
180	$5.55 \cdot 10^{-3}$	4.0	5.0	60.0	62.5
180	$5.55 \cdot 10^{-3}$	6.0	5.0	64.5	62.5
338	$2.76 \cdot 10^{-3}$	3.0	3.1		

[a] In both cases A is obtained from Fig. 5b.

values of the temperature. At low or moderate temperatures only negligible weight losses are observed when the usual program rates (100 to 200°/h) are used. This is the reason why, in programmed temperature experiments, the reaction takes place in a temperature range much higher than that used in isothermal conditions. For PEGA it was not possible to measure the decomposition rate at temperatures higher than 300° by isothermal experiments whereas with programmed temperatures it

was difficult to make measurements under 300°: with the slowest program rate (18°/h), the characteristic temperature was 309°. In many cases the two methods would thus be complementary, especially if data over a large temperature range were needed.

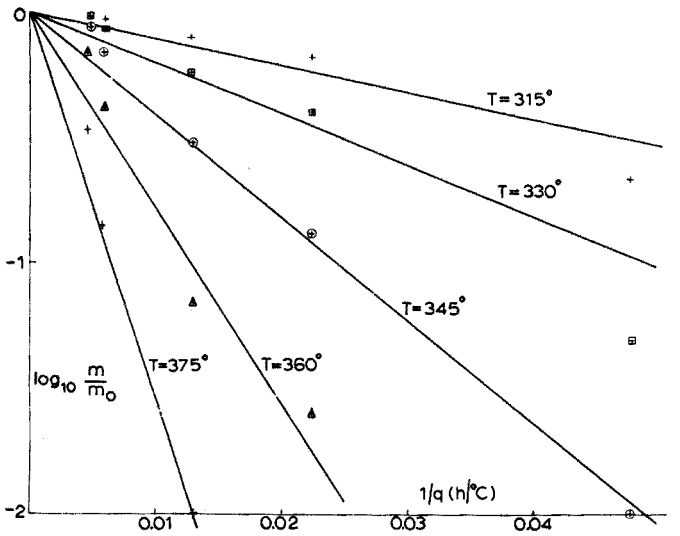

Fig. 5. Variation of the relative mass m/m_0 of the unreacted part of the sample observed when the sample temperature reaches certain values, with the inverse of the program rate, q.

This also explains the origin of a serious misconception, *i.e.* that there exists a definite temperature of initial decomposition or a critical limit of thermal stability, usually defined as the temperature at which a small proportion of the sample weight is lost. However, this temperature depends largely on the program rate (*cf.* eqn. (30)); with a rate of 170°/h, which is quite representative of the usual practice, 1% of the sample is decomposed at 290° (Fig. 1), but at that temperature, the isothermal decomposition is quite fast, since it needs only 2 min to reach a pyrolysis ratio of 1%[6]. The temperature of decomposition is thus a mere artefact[5].

At the beginning of the decomposition A/q is small and with a known approximation, the relative weight loss can be written as:

$$\Delta m/m_0 = 1 - \exp(-A/q) \sim A/q \qquad (31)$$

In that range the weight loss is proportional to $1/q$. This makes it possible to select the proper program rate to obtain any given pyrolysis ratio at any temperature, provided that A is known.

If $k(T)$ is known, and therefore A can be calculated for any temperature, it is possible to predict the relative weight loss at any temperature and for any value of the program rate. This was done at two different temperatures with values of $k(T)$ derived from previous isothermal experiments (Table III). The values of k are in agreement with those derived from programmed-temperature experiments (Fig. 3). It is thus not surprising that the agreement is good between these theoretical results and the experimental data.

On the temperature at which a given relative weight loss is observed. Equation (4) gives:

$$q \ln (m_0/m) = \int_{T_0}^{T} Z \exp(-E/RT)\mathrm{d}T = A \qquad (32)$$

Although the integral cannot be solved, its value may easily be calculated for any temperature when the rate constant is known. Figure 6 shows the variation with the temperature of the rate constant $k(T)$ (Fig. 6a) and the integral $\int_0^T k\mathrm{d}T$ (Fig. 6b),

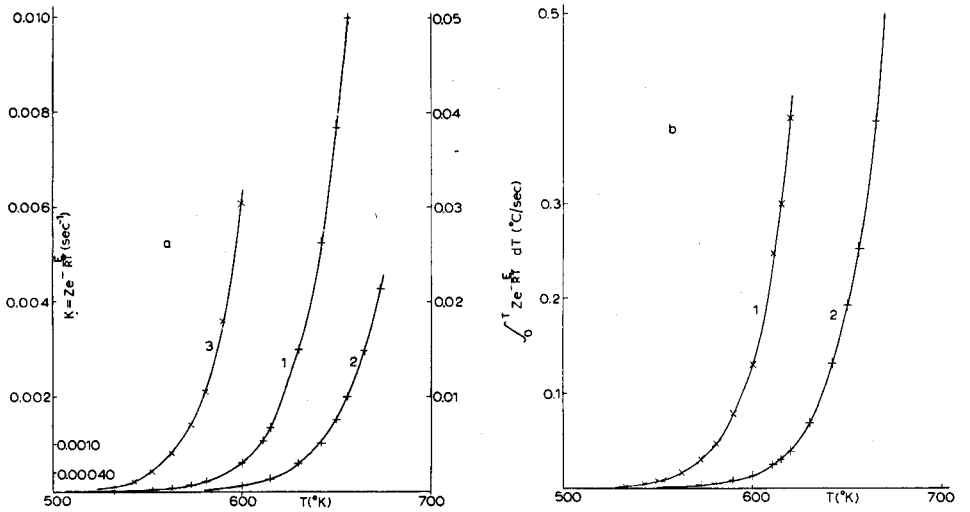

Fig. 6. Variation with the absolute temperature of: (a) the rate constant of the pyrolysis of PEGA. (1) rate constant scale on the right, (2) same scale contracted 5 times, (3) same scale expanded 10 times; (b) the integral $\int_0^T k\,\mathrm{d}T$. (1) scale on the left, (2) same scale expanded 10 times. These curves are derived from isothermal data (dotted line on Fig. 3).

which is practically identical to $\int_{T_0}^{T} k\mathrm{d}T$, where T_0 is the ambient temperature at which the decomposition is negligible. The values of the rate constant used are the same as for Table III. Equation (32) is then solved for any value of the relative mass of undecomposed product by taking the intersection of the curve $y=A$ with the horizontal straight line of ordinate $q \ln (m_0/m)$.

Another test of the agreement between isothermal and programmed-temperature data may be obtained by comparing the experimental results to those obtained by solving eqn. (32). Table IV gives the values of the integral obtained from the iso-

TABLE IV

COMPARISON OF THEORETICAL AND EXPERIMENTAL RESULTS[a]

T (°)	300	315	330	345
$\int_0^T k\mathrm{d}T$	0.0030	0.0073	0.0163	0.0356
$q \ln (m_0/m)$	0.0029	0.0070	0.0150	0.0300

[a] Pyrolysis of PEGA.

thermal data and the values of $q \ln (m_0/m)$ at the same temperature, derived from the thermogravimetric curve obtained with one of the slowest programs (20°/h), and for which decomposition takes place in a range very similar to that in which the isothermal measurements were made. The agreement between the two sets of results is very good, except at the highest temperature where the decomposition is near completion and where deviation of the kinetics from the first-order law may be expected.

On the value of the characteristic temperature. The variations of T_S with q are important, since T_S corresponds to a ratio $(m_0/m) = e$, so that, for practical purposes, the decomposition takes place between $T_S - 50°$ and $T_S + 20°$ (*cf.* Fig. 1), and since T_S is equal to the temperature at which the inflexion point of the thermogravimetric curve is reached. From eqn. (8) the characteristic temperature is given by the equation:

$$Z \exp(-E/RT_S) = qE/RT_S^2 \qquad (33)$$

The variations of:

$$z' = (RT^2/E)\, Z \exp(-E/RT)$$

are plotted *vs.* T on a logarithmic scale in Fig. 7. The values of T_S are obtained from the intersection of the curve $z'(T)$ with the horizontal line $z' = q$. The corresponding values of T_S are plotted *vs.* q in Fig. 8. The experimental values corresponding to the curves given in Fig. 1 are also plotted on Fig. 8. There is an excellent agreement between these results derived from either programmed-temperature experiments or isothermal ones. It may be seen from Fig. 8 that the practical range of variations of T_S is not very large and does not greatly exceed 100° for PEGA, between 300 and 400°.

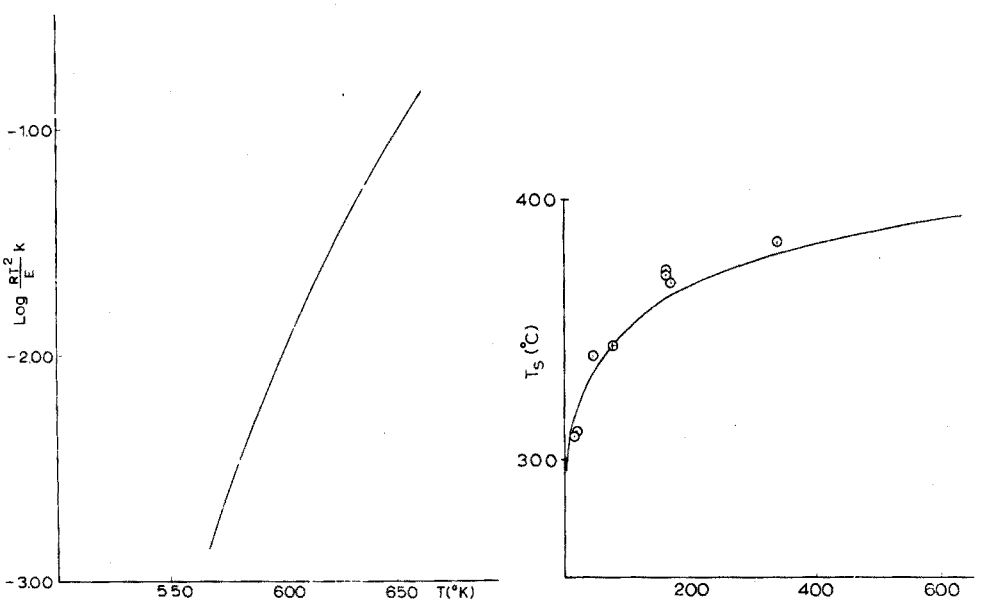

Fig. 7. Variation of the function $(RT^2/E)\, k$ with the absolute temperature, derived from Fig. 6a.

Fig. 8. Variation with the program rate, q, of the characteristic temperature, at which the mass of undecomposed product is equal to m_0/e. Theoretical curve derived from isothermal data and experimental points.

Precision of the determination of the activation energy

A very important drawback of the method suggested by HOROWITZ AND METZGER[11] for the derivation of the activation energy from thermogravimetric curves is its lack of precision. From eqn. (6) it can be seen that for $\Theta=0$ or $T=T_S$ the activation energy takes the indefinite form 0/0. Around $\Theta=0$, the error for E is very large (see Fig. 2) if E is derived from the slope of the straight line joining the origin to the experimental point. The absolute temperature and the sample mass are known with good precision, but the error in $\Theta=T-T_S$ may be very large; it is difficult to measure the sample temperature to better than 0.5° and the inaccuracy on Θ is at least 1°. The relative error on the coordinates of the experimental points around the origin is very large. It is therefore not possible to use values of Θ less than 5–7° in the determination of E. This is unfortunate because, in the derivation, excessive weight is given to the two portions of the curve where the assumption that Θ is small is less satisfactory, and where the reaction is slow. The kinetics is more prone to deviate from the first-order law at the end of the reaction, where side reactions may become important.

It would be more precise to use the portion of the curve near the inflexion point to determine the activation energy. This can be done more precisely as follows than by any previous method. The values m_0 and T_S can easily be established with an error of less than 0.5%; it is more difficult but not impossible to have a value of q which does not fluctuate by more than 1% for the linear program. The most difficult parameter to measure with great accuracy is the slope of the inflexion tangent to the thermogravimetric curve; this slope can be determined with an error of a few percent, which is thus the error in the activation energy.

Practically, the value of the characteristic temperature is derived from the experimental m *vs.* T record as the temperature at which the relative sample mass is 1/e. The activation energy is then calculated by means of eqn. (15) and the rate constant at the characteristic temperature is obtained from eqn. (10). Finally the method described above to obtain Fig. 3 is used to determine the value of the rate constant at any temperature.

The values of the activation energies calculated by this procedure from the experiments described above, to which the HOROWITZ AND METZGER's treatment was previously applied, are given in Table II. The standard deviations of both series of results are very similar but when the slope of the inflexion tangent is used, the calculation needs only two measurements, the inflexion temperature and the slope itself, instead of about twenty measurements for each run by HOROWITZ AND METZGER's method.

The drawback of the new method is of course that only one value of the activation energy is obtained for each thermogravimetric curve and thus the results cannot be tested for self-consistency. However, this is more than compensated by the excellent accuracy obtained; when necessary, consistency with the less precise value derived from 3–4 points by the HOROWITZ AND METZGER process can be looked for.

It should be noted that eqn. (6) is valid within the same limits as eqn. (2); eqn. (14) is also rigorous since it results from HOROWITZ AND METZGER's calculation on the assumption that $T-T_S$ is small and this difference is zero in that particular case.

When an hyperbolic temperature program can be used, the precision of the determination of the activation energy, and thus of the rate constant, is much better

than that achieved by the method of HOROWITZ AND METZGER and is even better than that obtained when the newly proposed method involving the coordinates of the inflexion point of the thermogravimetric curve is used. Only one hyperbolic program has been used, however. The mean value of the activation energy derived from several replicate experiments by that program is given in Table II. It is in excellent agreement with the values obtained by the other methods. The standard deviation for these results was 0.3 kcal/mole. The experimental difficulties are larger with an hyperbolic program than with a linear program. With the Adamel thermobalance, the temperature of which is programmed by a mechanical system, it is possible to achieve the same fluctuations of the temperature around the ideal law of variation ($\pm 1°$) but it is much longer and more difficult to prepare the cam corresponding to a given program. In spite of these difficulties the use of non-linear programs should receive more attention.

F.F.R. thanks Fondation Juan March, Madrid (Spain) for a research grant.

SUMMARY

Various thermogravimetric methods can be used to determine the activation energy and the rate constant of the pyrolysis of compounds, when only one mechanism is involved or when several mechanisms occur simultaneously with a relative extent which does not depend much on the temperature. Although the experimental results can be explained by simple kinetic theory, the mechanism of the pyrolysis is in most, if not all, cases much more complicated than is indicated by the thermogravimetric results. This is certainly true in the pyrolysis of polyethyleneglycol adipate. This does not reduce the interest of thermogravimetric analysis but illustrates the great difficulties which can be encountered in accounting for thermogravimetric measurements.

RÉSUMÉ

Diverses méthodes thermogravimétriques peuvent être utilisées pour déterminer l'énergie d'activation et la vitesse de pyrolyse de composés, lorsqu'un seul mécanisme entre en jeu ou lorsque plusieurs mécanismes se produisent simultanément, mais que leur importance relative ne dépend pas trop de la température. Bien que les résultats expérimentaux puissent être expliqués par simple théorie cinétique, le mécanisme de pyrolyse dans la plupart des cas, si ce n'est dans tous, est plus compliqué qu'il est indiqué par les résultats thermogravimétriques. Ceci est certainement vrai pour la pyrolyse d'adipate de polyéthylèneglycol, ce qui ne diminue pas l'intérêt de l'analyse thermogravimétrique, mais illustre les grandes difficultés rencontrées lors de l'interprétation de mesures thermogravimétriques.

ZUSAMMENFASSUNG

Verschiedene thermogravimetrische Methoden können zur Bestimmung der Aktivierungsenergie und der Geschwindigkeitskonstante bei der Pyrolyse von Verbindungen verwendet werden, wenn nur ein Mechanismus vorliegt oder wenn

verschiedene Mechanismen gleichzeitig auftreten und diese nicht stark von der Temperatur abhängen. Obgleich die experimentellen Ergebnisse mit Hilfe einfacher kinetischer Theorien erklärt werden, ist der Mechanismus der Pyrolyse in den meisten, wenn auch nicht in allen Fällen komplizierter als es durch die thermogravimetrischen Ergebnisse angezeigt wird. Das ist besonders der Fall bei der Pyrolyse von Polyäthylenglykol. Dadurch wird das Interesse an thermogravimetrischen Analysen nicht vermindert aber es zeigen sich die grossen Schwierigkeiten, welche bei thermogravimetrischen Messungen auftreten können und berücksichtigt werden müssen.

REFERENCES

1 G. GUIOCHON, *Communication to the International Symposium on Thermal Analysis, London, April 1965.*
2 S. L. MADORSKY, *Thermal Degradation of Polymers*, Wiley, New York, 1964.
3 R. SIMHA AND L. A. WALL, *J. Phys. Chem.*, 56 (1952) 707.
4 A. NEWKIRK, *Anal. Chem.*, 32 (1960) 1558.
5 G. GUIOCHON, *Anal. Chem.*, 33 (1961) 1124.
6 F. FARRÉ-RIUS AND G. GUIOCHON, *Bull. Soc. Chim. France*, (1965) 455.
7 A. W. COATS AND J. P. REDFERN, *Analyst*, 88 (1963) 906.
8 C. DUVAL, *Anal. Chim. Acta*, 31 (1964) 301.
9 P. VALLET, *Compt. Rend.*, 249 (1959) 823.
10 C. D. DOYLE, *J. Appl. Polymer Sci.*, 5 (1961) 285.
11 H. HOROWITZ AND G. METZGER, *Anal. Chem.*, 35 (1963) 1464.
12 R. M. FUOSS, I. O. SALYER AND H. S. WILSON, *J. Polymer Sci.*, A2 (1964) 3147.
13 J. C. GIDDINGS, *Méthodes Physiques d'Analyse*, 2 (1966) 13.
14 S. SZEPE, *J. Gas Chromatog.*, 5 (1967) 180.
15 F. FARRÉ-RIUS AND G. GUIOCHON, *J. Gas Chromatog.*, 5 (1967) 457.
16 F. FARRÉ-RIUS, *Thesis*, Paris, 1969.

Analytica Chimica Acta
Elsevier Publishing Company, Amsterdam
Printed in The Netherlands

THE SYNTHESIS OF SOME NITRATED POLYAMINE RESINS AND THEIR USE AS ION-EXCHANGERS FOR THE ALKALI AND ALKALINE EARTH METALS*

CASIMIR A. JANICKI** AND CARL E. MOORE
Department of Chemistry, Loyola University, Chicago, Ill. (U.S.A.)
(Received December 28th, 1968)

The useful ion-exchange resins have a selectivity which permits closely related ions to be separated by ion-exchange chromatography. However, the use of these resins is often time-consuming for separations of large amounts of similar ions, though separations may be improved by the use of complexing agents such as citric acid[1], ethylenediaminetetraacetic acid[2] and nitrilotriacetic acid[3].

Attempts have been made to obtain resins of higher selectivity by the preparation of materials which have a preference for certain counter ions and bind them to the fixed ionic groups or other components of the matrix. Thus, a cation which forms strong complexes with, or is precipitated by, a certain reagent should be preferred by a resin into which this reagent has been incorporated as a structural unit. SKOGSEID[4], who was the first to use this approach to ion-exchange resin preparation, incorporated dipicrylamine into a styrene-type resin. He found that the resin had considerably greater affinity for potassium than the existing cation-exchange resins. Dipicrylamine is a well known analytical reagent which precipitates potassium selectively from the lighter alkali metal cations as a red to yellow precipitate of low solubility.

The work of SKOGSEID suggested that other resins based on the dipicrylamine moiety and similar structures are possible and that more favorable structural cases may exist. Among these are the nitro-polyamines which are easily synthesized by the condensation of aromatic diamines and their hydrochlorides, and the subsequent nitration of the resulting polymer. It was felt that the resin based on *m*-phenylenediamine presented a particularly favorable case for checking this hypothesis and when compared to the resin prepared by SKOGSEID would have a greater similarity to dipicrylamine (Fig. 1). Because of this greater similarity it would possess a greater ability to selectively remove potassium and the heavier alkali metals from large amounts of sodium in systems such as sea water.

Five resins were prepared and studied. They are nitro-poly-*m*-phenylenediamine, nitro-poly-*p*-phenylenediamine, nitro-poly-3,3'-diaminodiphenyl, nitro-poly-4,4'-diaminodiphenyl, and nitro-poly-2,7-diaminonaphthalene.

* Presented at the 1966 Anachem Conference, Wayne State University, Detroit, Michigan.
** Present address: McNeil Laboratories, Fort Washington, Pa., 19034.

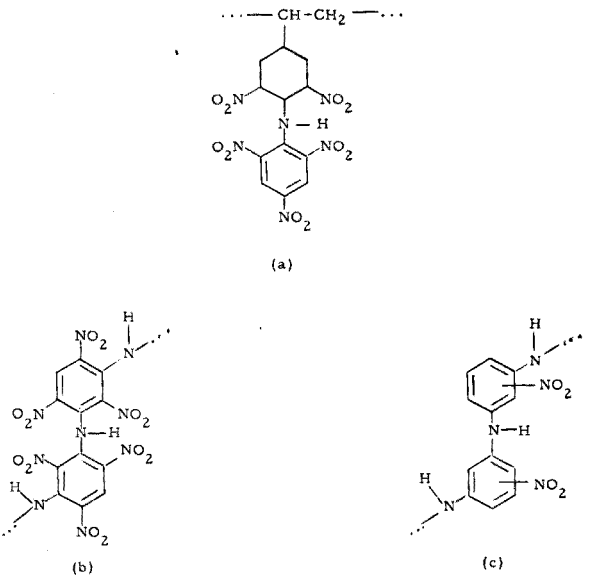

Fig. 1. (a) SKOGSEID's resin; (b) structure of proposed resin; (c) proposed structure of resin synthesized (nitro-poly-*m*-phenylenediamine).

EXPERIMENTAL

Apparatus

A 300-ml Magne-Dash Autoclave (Autoclave Engineer's, Inc., Erie, Pa.) was used in the synthesis of the polyamines. A Beckman battery-operated DU Spectrophotometer with the 4300 photomultiplier, Spectral Energy Recording and Flame Photometry Attachments, a Brown Recorder, and the oxygen–hydrogen flame were used for the assay of the metallic cations.

Materials

Practical grades of *m*-phenylenediamine and *p*-phenylenediamine were purified by distillation under reduced pressure and 4,4'-diaminodiphenyl was used as obtained. The 2,7-diaminonaphthalene was synthesized from 2,7-dihydroxynaphthalene by the BUCHERER reaction[5]. The 3,3'-diaminodiphenyl was synthesized from *m*-nitroaniline which was converted to *m*-iodonitrobenzene[6]. The 3,3'-dinitrodiphenyl was prepared from *m*-iodonitrobenzene by the ULLMANN reaction[7]. The diamine was obtained by reduction of 3,3'-dinitrodiphenyl[8].

The hydrochloride salts of the amines were prepared by passing dry hydrogen chloride gas through an ether or benzene solution of the amine.

The test solutions used to determine the effect of pH on the exchange were Clark and Lubs buffers, using only potassium salts. The modified sea water solution was composed of the acetate salts of sodium (10,600 p.p.m.), potassium (383 p.p.m.), magnesium (1,270 p.p.m.) and calcium (400 p.p.m.). The acetate salts were arbitrarily chosen to have a common anion in solution and as a means to control pH. The pH was controlled so that another variable could be kept constant.

Resin preparation

The condensation technique, heating an amine with an amine hydrochloride, was successfully used in synthesizing diphenylamine from aniline and aniline hydrochloride as well as tetramethyldiphenylamine from 3,5-dimethylaniline and its hydrochloride salt[9]. These reactions served as model reactions for the resin preparations.

Equimolar amounts of the aromatic amine and its corresponding hydrochloride salt were mixed, transferred to a glass tube, inserted into the autoclave, and heated under nitrogen. In some instances iron wire, iron(III) chloride or aluminum chloride were used to effect the condensation. The black product obtained was washed in turn with dilute hydrochloric acid, acetone, water, dilute ammonia, ethanol and finally acetone. The washing procedure removed starting materials and low-molecular-weight products.

Nitration of the polyamines

The polyamine was dissolved in oleum at room temperature and the solution cooled to 0°. Red fuming nitric acid was added dropwise with vigorous stirring, the temperature being kept below 10°. The solution was stirred for an additional 3 h. The solution was poured over ice and the precipitated product collected on a fritted glass funnel, washed with water, and dried at 60°.

Ion-exchange study of the resins

A batch method was used to determine the exchange capacities and effect of pH on the exchange. The nitrated polyamines were ground to 270 mesh, conditioned by several exchange cycles, and the acid form of the resin washed with water and dried at 60°. The resin (0.2–0.5 g) was transferred to a flask, shaken with 50 ml of the test solution and equilibrated for 48 h at 25 $\pm$1°. The mixture was filtered through a fine fritted glass funnel, washed free of test solution, air-dried, and washed with a known amount of 0.1 *M* hydrochloric acid. The acid solutions were diluted and assayed.

Cation determination

The acid solutions were assayed for the various cations by flame photometry. The standards used were nearly identical in composition to the samples. Preliminary assays of solutions of mixtures of cations were performed so that standards, containing approximately the same concentrations of the samples, could be prepared. Calcium was measured at 554 nm, magnesium at 383 nm, potassium at 767 nm and sodium at 589.6 nm.

RESULTS AND CONCLUSIONS

The five polyamines that were synthesized are listed in Table I with the synthesis conditions, yields, and nitrogen analyses. The ash found in the last three polymers was entirely due to the particular agent used to effect the condensation. The polyamines were usually very black and found to be insoluble in most common organic solvents. The polymer of *m*-phenylenediamine, one of the more soluble polymers, was soluble in N,N-dimethylformamide (DMF), dimethylsulfoxide, N-methylpyrrolidine, sulfuric acid, and formic acid. The molecular weights of the polymers

TABLE I

THE CONDITIONS, YIELDS AND NITROGEN ANALYSES FOR THE POLYAMINES

	No. of moles of amine	*Temp.* (°)	*Time (h)*	*Yield (g)*	*N analysis (%)*	*Ash*
m-Phenylenediamine	0.056	275 ± 10	24	9.68	Calcd: 15.38	
					Found: 14.82	
p-Phenylenediamine	0.073	265 ± 10	24	8.50	Calcd: 15.38	
					Found: 12.82	
3,3′-Diaminodiphenyl	0.010	280 ± 10	72[a]	2.50	Calcd: 8.38	
					Found: 6.44	5.95
4,4′-Diaminodiphenyl	0.029	265 ± 10	57[a]	5.58	Calcd: 8.38	
					Found: 7.77	3.66
2,7-Diaminonaphthalene	0.106	275 ± 10	24[a]	2.45	Calcd: 9.92	
					Found: 10.93	3.25

[a] Iron wire, iron(III) chloride or aluminum chloride used.

were very difficult to obtain because of the lack of solubility in a suitable solvent. A molecular weight of 4200 to 5200 was obtained for poly-*m*-phenylenediamine. This was determined on a vapor-pressure osmometer at a temperature of 37° with DMF as the solvent.

The nitrated polyamines were soluble in diluted alkali and acetone. Only one nitro group per monomer unit could be accounted for by analysis for nitrogen. More vigorous nitrating conditions did not improve the nitrogen values and in many cases destroyed the polymers. The same method was successfully used to nitrate diphenylamine to obtain dipicrylamine in very high yields, and hexanitrotetramethyldiphenylamine from tetramethyldiphenylamine[9].

Since the nitrated polymer of *m*-phenylenediamine was studied more extensively than the other polymers and it also resembles dipicrylamine more closely than the other polymers, most of the discussion will relate to it. Any major differences between nitro-poly-*m*-phenylenediamine and the other four nitrated polymers will be pointed out. The nitrated polymers were tested for their ion-exchange properties as well as the reversibility of the exchange. A small column of nitro-poly-*m*-phenylenediamine was prepared, washed with dilute hydrochloric acid, and washed with water.

TABLE II

THE RECOVERY AND REVERSIBILITY OF THE EXCHANGE FOR NITRO-POLY-*m*-PHENYLENEDIAMINE

Sample	*Mg exchanged/g resin*	*Mg recovered/g resin*
Potassium	31.7	31.9
	30.2	29.9
	28.2	28.7
Potassium	29.6	31.9
	30.5	32.6
	30.7	31.8
Calcium	23.6	23.1
Sodium	14.9	15.5

A 50-ml aliquot of a solution of 164 p.p.m. of potassium (as potassium chloride) was poured through the column, collected and assayed. The column was washed free of excess reagent and eluted with 25 ml of 1 *M* hydrochloric acid. The acid was collected and assayed. The cycle was repeated twice (Table II). A second sample from an entirely different batch of nitro-poly-*m*-phenylenediamine was used to obtain another set of results for the potassium exchange. An additional sample was used for the sodium and calcium exchange (Table II). The results indicate that the resins exhibit cation-exchange properties and that the exchange was fully reversible.

The effect of pH on the exchange was determined by the batch method using MacIlvaines buffers of pH 2, 4, 6, and 8. Sodium ion was the only metal ion present. The results obtained for nitro-poly-*m*-phenylenediamine and nitro-poly-*p*-phenylenediamine are given in Fig. 2. The polymers were found to dissolve slowly above pH 7, and rapidly above pH 10. From the data the polymers would have to be classified as weak ion exchangers. The capacities of the five polymers for potassium at pH 6 are given in Table III.

TABLE III

THE CAPACITIES TOWARD POTASSIUM AT pH 6 FOR THE FIVE NITRATED POLYAMINES

Nitrated polymer of	*Meq potassium/g*
m-Phenylenediamine	1.80
p-Phenylenediamine	1.35
3,3'-Diaminodiphenyl	1.30
4,4'-Diaminodiphenyl	1.08
2,7-Diaminonaphthalene	1.09

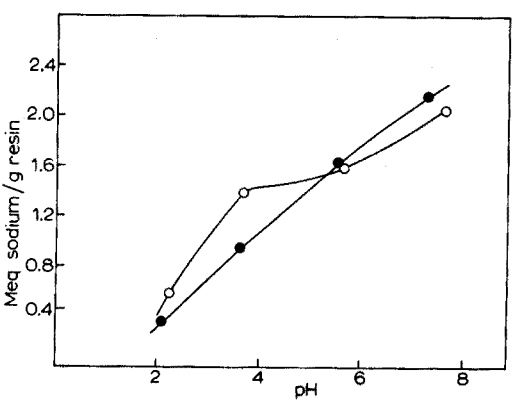

Fig. 2. Titration curve for the nitro-poly-*m*-phenylenediamine (●), and nitro-poly-*p*-phenylenediamine (○).

The selectivity of the resins is characterized by the ion-exchange isotherm. When the equivalent ionic fraction of the ion in the resin is plotted against the equivalent ionic fraction of the ion in solution, a curve is obtained. The theoretical curve, if the resin had no selectivity, is represented by a diagonal (Fig. 3). The deviation from the diagonal is an indication of the selectivity of the resin for a particular ion in an ion-pair. The data obtained for nitro-poly-*m*-phenylenediamine are given in Fig. 3.

The general nature of the selectivity of the polymer is of the same order as the commercial exchangers, calcium, magnesium, potassium and sodium being preferred the least.

In order to compare the nitro-polyamines with SKOGSEID's resin, the nitro-polyamines were tested against an artificial sea water solution. The solution (pH 6) was added to the nitro-polyamine and the batch technique was used. SKOGSEID calculated separation factors which were obtained by dividing the mole fraction of cation in the ion-exchanger by the mole fraction in solution. His separation factors are

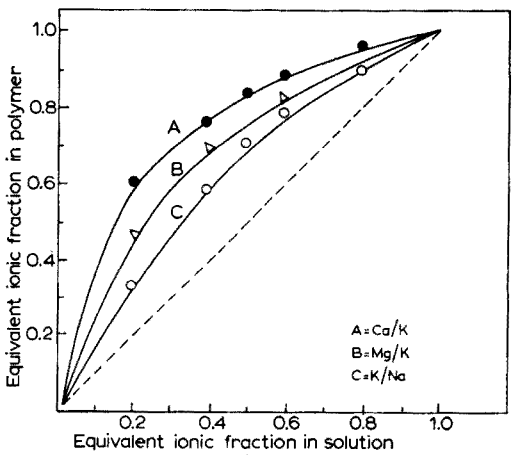

Fig. 3. Ion-exchange isotherm for the nitrated polymer of *m*-phenylenediamine.

TABLE IV

COMPARISON OF THE SEPARATION FACTORS[a] OF SKOGSEID'S RESIN WITH THE NITRATED POLYAMINE RESINS

Resin	*Sodium*	*Magnesium*	*Calcium*	*Potassium*
SKOGSEID'S	0.650	1.62	3.04	6.00
Nitrated poly-*m*-phenylenediamine	0.632	2.82	7.18	2.27
Nitrated poly-*p*-phenylenediamine	0.501	3.65	9.20	1.95
Nitrated poly-3,3'-diaminodiphenyl	0.544	3.43	8.51	1.73
Nitrated poly-4,4'-diaminodiphenyl	0.527	3.20	9.95	2.32
Nitrated poly-2,7-diaminonaphthalene	0.544	3.16	9.15	2.60

[a] Mole fraction in exchanger divided by mole fraction in solution.

presented in Table IV with those calculated for the five nitropolyamines. The separation factor for SKOGSEID's resin for potassium is very large, being 6. For nitro-poly-*m*-phenylenediamine, which has a separation factor for sodium of less than SKOGSEID's resin, the sodium occupies 39% of the exchange sites of the polymer. Because sea water contains comparatively little potassium, an exchanger would have to have a SKOGSEID separation factor much larger than 6 to be considered for separating potassium from systems such as sea water.

Although nitro-poly-*m*-phenylenediamine did not have such a good selectivity towards potassium as that of SKOGSEID's resin, it is felt that a fully nitrated polyamine

could be more selective. The sites are available for nitration, since bromination and chlorination of poly-*m*-phenylenediamine resulted in products having two halogens per monomer unit.

SUMMARY

Five polyamines were synthesized by the condensation of an amine with its corresponding amine hydrochloride salt, and the polyamines were nitrated, averaging 1 nitro group per monomer unit. The nitro-polyamines were found to be weak cation-exchangers. The resins did not have the same selectivity towards potassium as the exchanger synthesized by SKOGSEID, who incorporated dipicrylamine onto a polystyrene resin.

RÉSUMÉ

Cinq polyamines ont pu être synthétisées par condensation d'une amine avec son chlorhydrate d'amine correspondant. Ces polyamines sont ensuite nitrées, en moyenne un groupe nitro par unité monomère. Les polyamines nitrées constituent des échangeurs de cations faibles. Les résines n'ont pas la même sélectivité envers le potassium que les échangeurs synthétisés par SKOGSEID qui incorporent de la dipicrylamine sur une résine polystyrène.

ZUSAMMENFASSUNG

Es wurden fünf Polyamine synthetisiert durch Kondensation eines Amins mit seinem korrespondierenden Aminhydrochloridsalz. Diese Polyamine wurden im Durchschnitt mit einer Nitrogruppe pro monomerer Einheit nitriert. Die Nitropolyamine sind schwache Kationenaustauscher. Die Harze besitzen nicht die gleiche Selektivität gegenüber Kalium wie die Austauscher, welche durch Skogseid synthetisiert wurden und welche Dipicrylamin auf ein Polystyrolharz enthalten.

REFERENCES

1 F. H. SPEDDING, *Discussions Faraday Soc.*, 7 (1949) 214.
2 E. J. WHEELWRIGHT AND F. H. SPEDDING, *J. Am. Chem. Soc.*, 75 (1953) 2529.
3 J. LORIERS AND D. CARMINATI, *Compt. Rend.*, 237 (1953) 1328.
4 A. SKOGSEID, *Dissertation*, Oslo, 1948.
5 H. T. BUCHERER, *J. Prakt. Chem.*, 69 (1904) 49.
6 D. A. SHIRLEY, *Preparation of Organic Intermediates*, Wiley, New York, 1943, p. 184.
7 F. ULLMANN AND J. BIELECKI, *Ber.*, 34 (1901) 2174.
8 A. H. BLATT, *Organic Synthesis Coll.*, Vol. II, Wiley, New York, 1943, p. 160.
9 C. E. MOORE, T. S. MEYER AND J. W. HUDSON, *Talanta*, 13 (1966) 171.

Analytica Chimica Acta
Elsevier Publishing Company, Amsterdam
Printed in The Netherlands

POTENTIOMETRIC TITRATIONS WITH ION-EXCHANGING MEMBRANE ELECTRODES

PART V. TITRATION CURVES FOR PRECIPITATION TITRATIONS INVOLVING IONS OF HIGHER VALENCIES

F. P. IJSSELING AND E. VAN DALEN
Analytical Department, Chemical Laboratory, Free University, Amsterdam (The Netherlands)
(Received January 20th, 1969)

In previous papers of this series, the theoretical[1,2] and experimental[3,4] aspects of the use of ion-exchanging membrane electrodes for potentiometric indication of the equivalence point in precipitation titrations were discussed, but the discussion was restricted to the case that only univalent ions are present in the solution to be titrated, the reference solution and the reagent.

In the present paper the influence of the presence of ions of higher valencies is considered. In order to calculate titration curves for potentiometric titrations with ion-exchanging membrane electrodes, the membrane potential must be calculated as a function of the composition of the solutions surrounding the membrane during the titration. The membrane potential is composed of three separate potential differences: (1) the Donnan potential at the side of the reference solution (E_{D1}); (2) the Donnan potential at the side of the solution to be titrated (E_{D2}); (3) the diffusion potential inside the membrane (E_{im}). The methods for the calculation of the Donnan potentials and the intramembrane diffusion potential will be explained separately, with the same notation as in the previous papers.

CALCULATION OF THE DONNAN POTENTIALS AND DISCUSSION OF THE RESULTS

The Donnan potentials are dependent on the concentrations as well as on the valencies of the ions present in the solutions surrounding the membrane. However, specific ionic properties, such as the diffusion coefficients, do not enter into the calculations. For this reason all ionic species with the same valency are combined into one group with valency k. The concentration of the valency group is found by adding the concentrations of the separate ionic species of which the valency group is composed. It is supposed that the reference solution is not contaminated by constituents of the membrane or of the solution at the titration side. Thus the Donnan potential at the interface membrane/reference solution remains constant during the titration, and only the Donnan potential at the interface membrane/test solution has to be calculated.

For the calculation of the Donnan potentials, the following equation is used[5]:

$$\sum_k z_k c_k E_D^{-z_k} = -wX \qquad (1)$$

in which z_k is the valency of valency group k; c_k is the concentration of valency

group k (meq/cm^3); E_D is the Donnan potential, defined as $E_D = \exp(F\Delta\varphi/RT)$; F, R and T have the usual meaning and $\Delta\varphi$ is the physically measurable potential difference between the inner side of the membrane and the adjacent solution; w is $+1$ for anion-exchanging and -1 for cation-exchanging membranes; and X is the capacity of the membrane (meq/cm^3).

The change in the Donnan potential during the titration was calculated for the general case:

$$M^+X^- \,//\, \text{membrane} \,//\, N_n{}^pY_y{}^q + A_a{}^rB_b{}^s \rightarrow N_n{}^pB_b{}^s\downarrow + A_a{}^rY_y{}^q$$

The compounds $N_n{}^pY_y{}^q$, $A_a{}^rB_b{}^s$ and $A_a{}^rY_y{}^q$ are assumed to be completely dissociated in solution.

As is readily seen the calculation of Donnan potentials generally consists of the solution of a high-order equation. The method of calculation was programmed for use with a computer, which involved the following considerations.

1. The reagent solution is added to the solution to be titrated in equal increments. The number of steps in which the reagent solution is added before the reaction is completed, can be chosen. After the equivalence point, the membrane potential is calculated automatically for the same number of increments:

2. The reference solution is of the same composition as the solution to be titrated; when, in practice, a different reference solution is used, only a linear displacement of the titration curve along the potential axis is introduced, the shape of the titration curve being retained.

The following data were incorporated into the computer programme:

(*a*) the valencies of the ions N, Y, A and B;

(*b*) the composition of the molecules NY, AB, NB and AY;

(*c*) the initial concentration of NY in the solution to be titrated;

(*d*) the volume of the solution to be titrated;

(*e*) the concentration of the reagent AB;

(*f*) the capacity of the membrane;

(*g*) the number of additions of reagent solution necessary to complete the titration reaction.

The computations were carried out for the case of an anion-exchanging membrane ($w = +1$ in eqn. (1)), because the titration curves for cation-exchanging membranes could be derived directly from these.

For each addition of reagent solution the following computations were carried out successively:

(*a*) The concentrations of the ionic species N, Y, A and B at the side of the solution to be titrated were calculated.

(*b*) The Donnan potential E_{D2} at the test-solution side of the membrane was found by solving eqn. (1) numerically, by means of the physically sound assumption that only one positive root exists. This is caused by the normalization of the physically measurable Donnan potential as $E_D = \exp(F\Delta\varphi/RT)$. The Donnan potential equation was solved by locating an interval in which the Donnan function changes sign. This was done by starting with the interval (10^{-12}, 1) and assessing the signs of the Donnan function at the end-points of the interval. If necessary, the search was continued with the intervals (1,2), (2,4), (4,8), etc. When the desired interval was located, it was narrowed by a process of bisection and interpolation until the final value for E_{D2} did

not differ significantly from its predecessor. The tolerance was defined by $\varepsilon = E_{D2} \cdot e_r + e_a$, where e_r and e_a are the relative and absolute errors, respectively, in E_{D2}. In all these computations, both e_r and e_a had the value $2 \cdot 10^{-7}$.

(*c*) The Donnan potentials were converted to the physically measurable values by $\Delta\varphi_2 = (RT/F) \ln E_{D2}$.

(*d*) The algebraic difference of the Donnan potentials $\Delta\varphi_2$ and $\Delta\varphi_1$ was found by subtraction; as the reference solution and the solution to be titrated have the same composition, the value of $\Delta\varphi_2$ as found for zero reagent solution can be substituted for $\Delta\varphi_1$.

When the differences between the Donnan potentials computed in this way are plotted against the total volume of added reagent solution, titration curves are obtained for the case of zero intramembrane diffusion potential. Figure 1(a–h) shows the results obtained for the 32 possible combinations of univalent and divalent ions. For the case of a cation-exchanging membrane, similar titration curves were obtained, when the potential sign of the appropriate reaction was inverted; for example, the reaction $N^{2+}Y_2^- + A_2^+B_2^- \rightarrow NB_2\downarrow + 2\ A^+Y^-$ for an anion-exchanging membrane is equivalent to the titration reaction $N^{2-}Y_2^+ + A_2^-B_2^+ \rightarrow NB_2\downarrow + 2\ A^-Y^+$ for a cation-exchanging material.

Figure 1(i–p) shows the titration curves for the possible combinations of univalent and trivalent ions. In all cases, 20 ml of a 0.01 or 0.1 *M* solution of NY was titrated with a 0.1 or 1.0 *M* reagent solution, and the membrane used had a capacity of 1 meq/cm^3.

With regard to the titration curves in Fig. 1, the following conclusions can be drawn.

1. The presence of co-ions of higher valency has only a very limited influence on the shape of the titration curves (a, e, i, m).

2. In titrations where only counter-ions of higher valencies are present, the Donnan potentials are somewhat lower than in the corresponding case of only univalent ions present (compare d with a, h with e, l with i, p with m).

3. The most interesting cases occur when the counter-ions present in the solution to be titrated have a valency different from that of the counter-ions added with the reagent solution (b,c,f,g,j,k,n,o). As can be deduced from the calculations, the influence of the counter-ion with the higher valency predominates in defining the ultimate shape of the titration curves.

These conclusions are in accordance with the two basic rules concerning the values of the Donnan potentials[5]: (*a*) when the concentration of the solution outside the membrane increases, the Donnan potential decreases; and (*b*) an increase in the valency of the counter-ions results in a decrease of the Donnan potential.

CALCULATION OF THE INTRAMEMBRANE DIFFUSION POTENTIAL

For this calculation, a simplified method was used as proposed by SCHLÖGL[6]. In this method, the inner diffusion potential (E_{im}) is found from the equation:

$$E_{im} = \frac{RT}{F} \ln \frac{z_{jk} D_{jk} (C_{1.jk} - C_{2.jk})}{\frac{1}{2} z_{jk}^2 D_{jk} (C_{1.jk} + C_{2.jk})} \qquad (2)$$

where R = molar gas constant; T = temperature in the Kelvin scale; F = faraday;

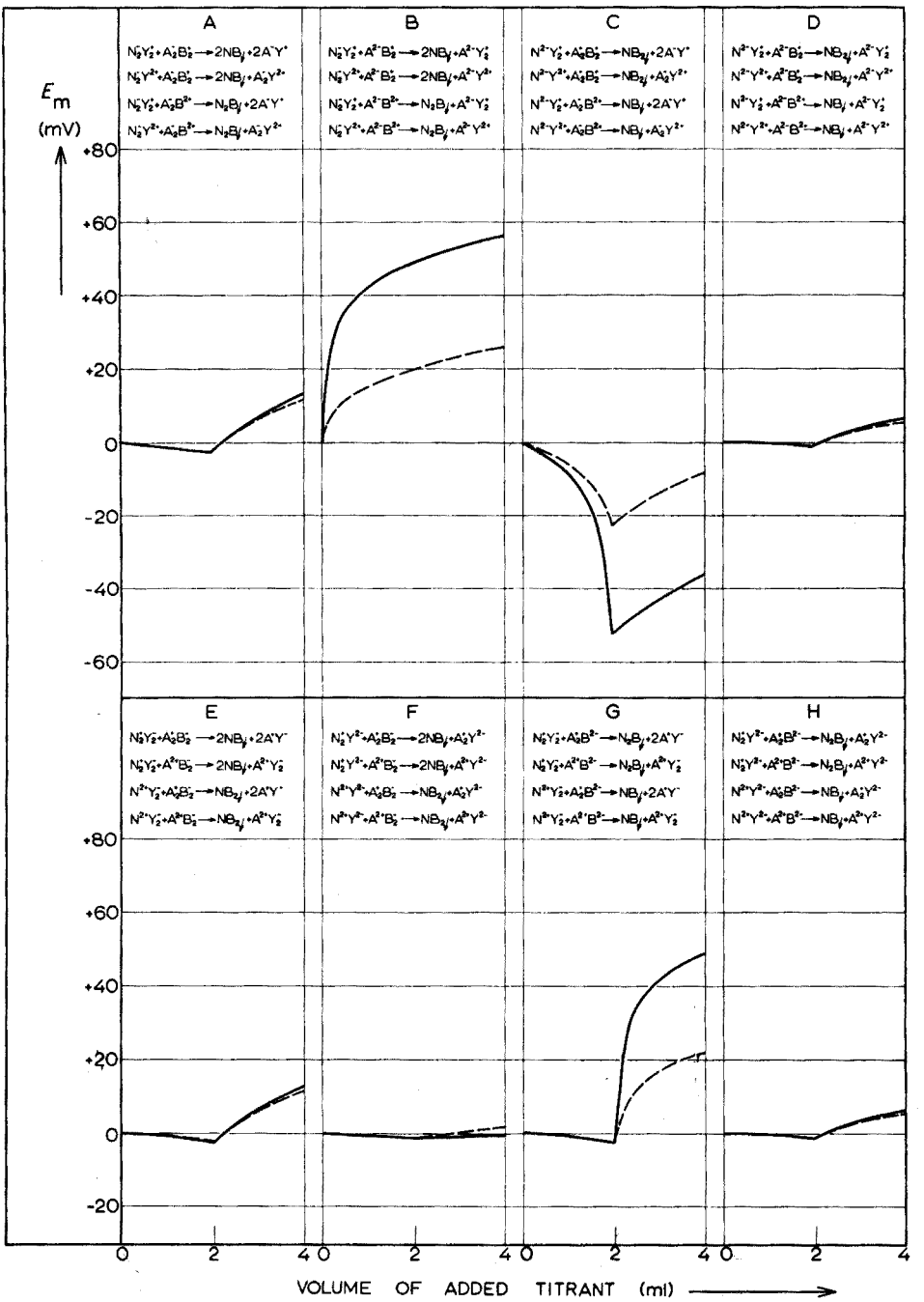

Fig. 1. Calculated values of the Donnan potentials for an anion-exchanging membrane during a precipitation titration:

$$N_n{}^pY_y{}^q \,//\, \text{membrane} \,//\, N_n{}^pY_y{}^q + A_a{}^rB_b{}^s \rightarrow N_n{}^pB_b{}^s\downarrow + A_a{}^rY_y{}^q$$

The calculations were performed for all possible combinations of univalent and bivalent ions

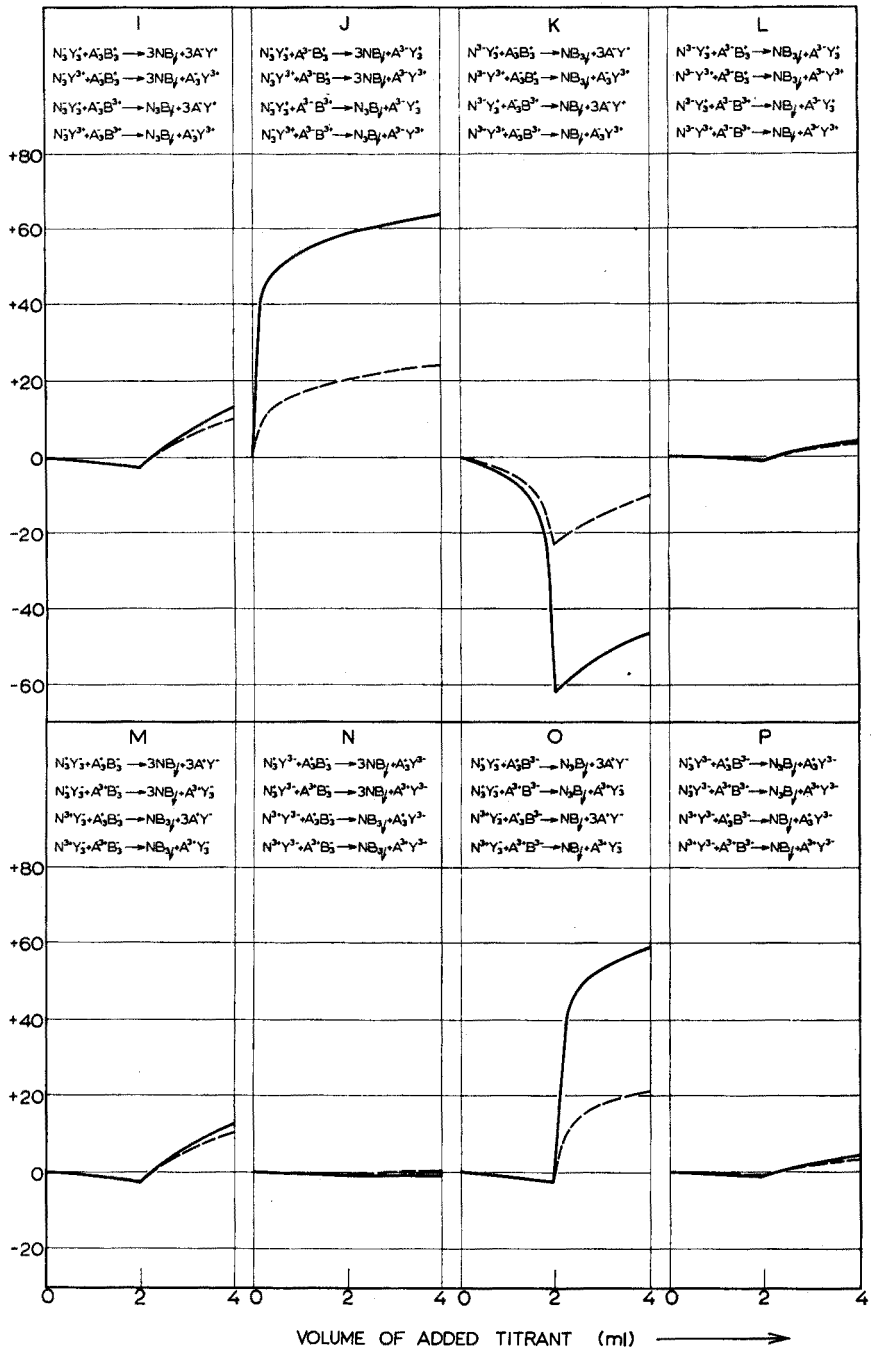

(a–h) as well as for univalent and tervalent ions (i–p). The titration conditions were as follows: (a) capacity of the membrane 1 meq/cm³; (b) 20 ml of a 0.1 *M* solution of $N_n^pY_y^q$ was titrated with a 1 *M* solution of the reagent $A_a^rB_b^s$ (broken lines), or 20 ml of a 0.01 *M* $N_n^pY_y^q$ solution was titrated with 0.1 *M* reagent solution (continuous lines).

z_{jk} = valency of ionic species jk; D_{jk} = diffusion coefficient of ionic species jk; $C_{1.jk}$ = concentration of ionic species jk at one side of the membrane; $C_{2.jk}$ = concentration at the other interface membrane/solution (both concentrations $C_{1.jk}$ and $C_{2.jk}$ are the concentrations at the inner surface of the membrane).

The surface concentrations are calculated by means of the equation:

$$C_{1.jk} = c_{1.jk} E_{D1}^{-z_k} \text{ (and a similar equation for } C_{2.jk}) \quad (3)$$

For the calculations the Donnan potentials required are found as described in the above paragraphs.

In the first series of calculations made in this work[1,2], a more elaborate method was used, which was also proposed by SCHLÖGL[7]. The relation used in the present paper is much easier to handle, but the application of the equation is restricted to the case that $z_{jk}D_{jk}(C_{1.jk}-C_{2.jk})/\frac{1}{2}z_{jk}^2D_{jk}(C_{1.jk}+C_{2.jk})$ is sufficiently small compared to unity. This restriction is necessary because the equation used holds only for systems without flow of electric current and when the intramembrane diffusion potential as well as the intramembrane osmotic pressure are not too large.

Moreover, for the simplified, as well as for the more elaborate method, it is assumed that: (*a*) there is no convection flow of the solution through the membrane phase; (*b*) the diffusion coefficients D_{jk} and the membrane capacity X are constant; (*c*) the overall process is controlled only by membrane diffusion; and (*d*) that a stationary state exists, *i.e.* the membrane does not act to accumulate matter.

In order to compare the two methods of calculation, the titration curves for several cases were calculated (Fig. 2). As can be seen, the differences between the

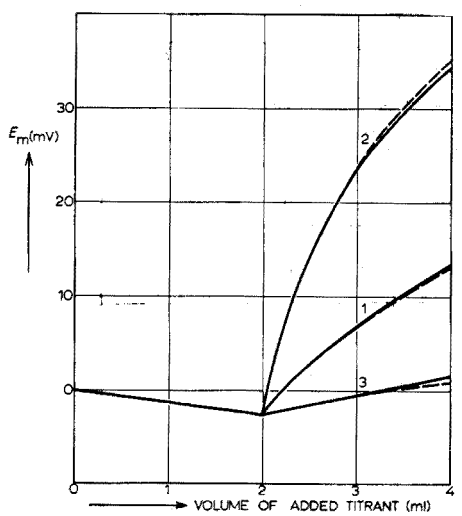

Fig. 2. Comparison of two methods of calculation of the membrane potentials. For the case of an anion-exchanging membrane with a capacity of 1 meq/cm³, 20 ml of a 0.1 *M* solution of N^+Y^- was titrated with a 1 *M* solution of A^+B^-. The continuous titration curves were calculated by the simplified method[6]; the broken curves were calculated by the more elaborate method[7]. Values of the diffusion coefficients used in the calculations:

	N^+	A^+	Y^-	B^-	
curves 1	4	4	6	6	$\cdot 10^{-6}$ cm²/sec
curves 2	4	4	1.5	6	
curves 3	4	4	6	1.5	

two calculated values of the membrane potentials during the titrations are quite acceptable, considering the fairly severe assumptions underlying the calculations. When the simplified method is used, the calculated membrane potentials should not differ by more than 5% from the values obtained by the more elaborate method. Even when the more elaborate method is used, the calculated values of the membrane potentials can deviate by 5–10% from the true values, hence the error in the calculation of the membrane potentials by the simplified method seems fully acceptable.

For a few cases, in which both univalent and bivalent ions are present in the solutions surrounding the membrane, the titration curves were calculated by the simplified method (Fig. 3). As can be seen from the figures, the influence of the diffusion potential on the shape of the titration curves is primarily dependent on the ratio of the diffusion coefficients of the counter-ions present in the solution to be titrated and in the reagent solution. Just as in the case that only univalent ions are present in the solutions, this rule holds only for a given capacity of the membrane and given concentrations of the solutions taking part in the titration reaction.

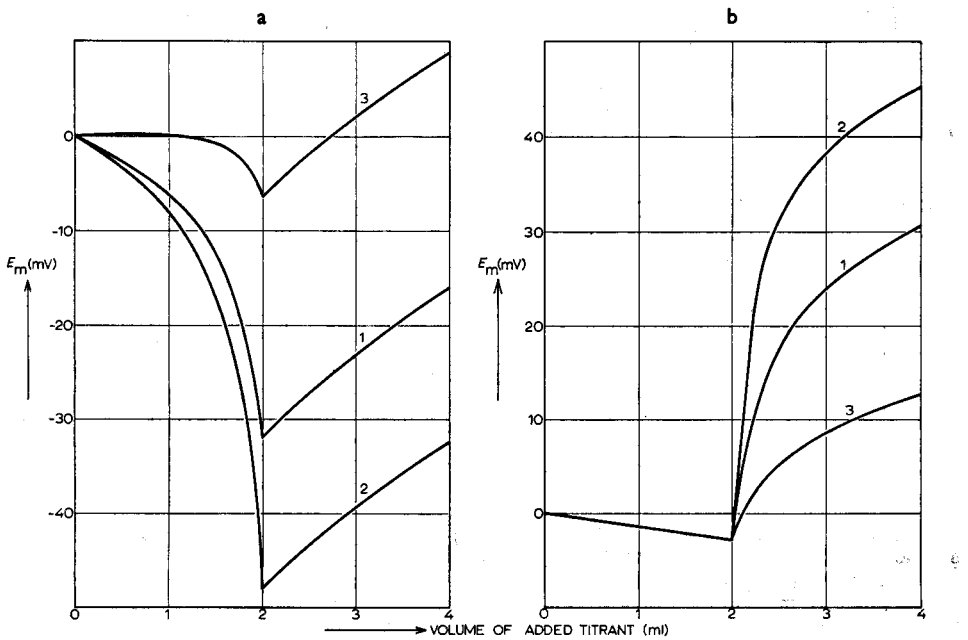

Fig. 3. Calculated curves for various titrations, with anion-exchanging membranes with a capacity of 1 meq/cm³.

(a) Reaction $N^{2-}Y_2^+ + A_2^-B^{2+} \rightarrow NB\downarrow + 2\,A^-Y^+$; 20 ml of 0.05 *M* $N^{2-}Y_2^+$ are titrated with 0.5 *M* $A_2^-B^{2+}$; the values of the diffusion coefficients are (in units of $1 \cdot 10^{-6}$ cm²/sec):

	N^{2-}	Y^+	A^-	B^{2+}
curve 1	6	4	6	4
curve 2	6	4	1.5	4
curve 3	1.5	4	6	4

(b) Reaction $N^{2+}Y_2^- + A_2^+B^{2-} \rightarrow NB\downarrow + 2\,A^+Y^-$; the concentrations used are the same as in case a; the values of the diffusion coefficients are (expressed in units of $1 \cdot 10^{-6}$ cm²/sec):

	N^{2+}	Y^-	A^+	B^{2-}
curve 1	4	6	4	6
curve 2	4	1.5	4	6
curve 3	4	6	4	1.5

Otherwise, the same rules apply to the more complicated case of ions of several valencies present in the solutions surrounding the membrane as to the case of univalent ions only.

EXPERIMENTAL

The titration apparatus and method described previously[3,4] were used for the following titrations:

(*a*) Solutions of barium chloride were titrated with potassium, sodium or lithium sulphate solution (Fig. 4a, to be compared with Fig. 1c). The reverse titrations were also performed (Fig. 4b, to be compared with Fig. 1g).

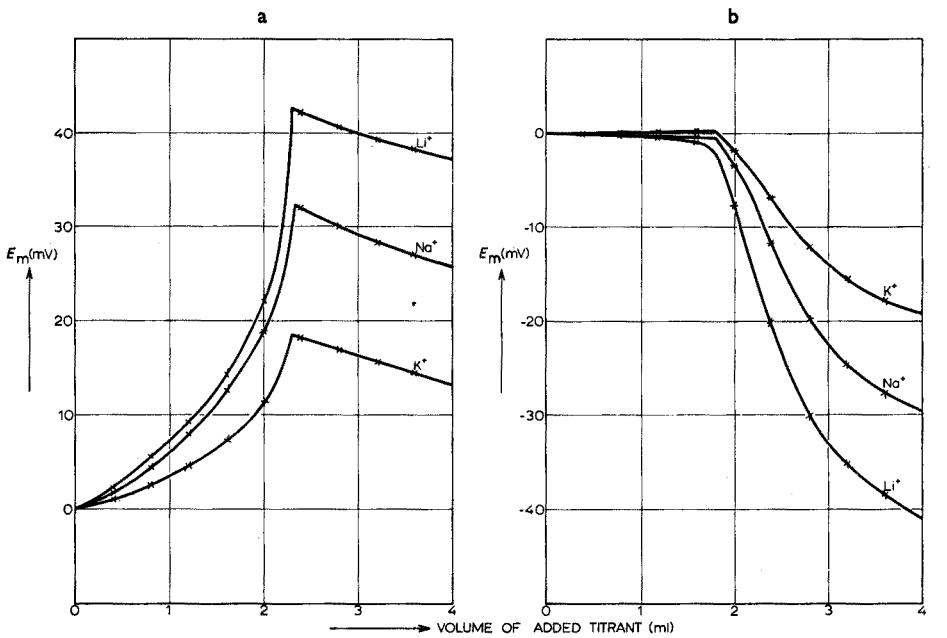

Fig. 4. Experimental curves for the titration of: (a) 20 ml of 0.029 *M* $BaCl_2$ solution with 0.26 *M* solutions of K_2SO_4, Na_2SO_4 or Li_2SO_4; (b) 20 ml of 0.026 *M* K_2SO_4, Na_2SO_4 or Li_2SO_4 with 0.29 *M* solution of $BaCl_2$. The membranes used were of the cation-exchanging type (Asahi CK 1). With Permaplex C 20 membranes the same results were obtained. The results are to be compared with the theoretically calculated titration curves of Figs. 1c and 1g (after reversing the sign of the calculated values, because in the experiments cation-exchanging membranes were used in place of anion-exchanging membranes). The membranes were used in the Na^+-form with 0.05 *M* KCl as reference solution.

(*b*) Solutions of barium nitrate and lead nitrate were titrated with sodium sulphate solution (Fig. 5a, to be compared with Fig. 1c); the reverse titrations were again carried out (Fig. 5b, to be compared with Fig. 1g). In all these cases, cation-exchanging Permaplex C 20 and Asahi CK 1 membranes were used, hence the titration curves indicated in Fig. 1 must be read with the opposite values of the membrane potentials.

(*c*) Anion-exchanging Asahi CA 2 membranes were used, and solutions of barium chloride, bromide, iodide, nitrate or acetate were titrated with sodium

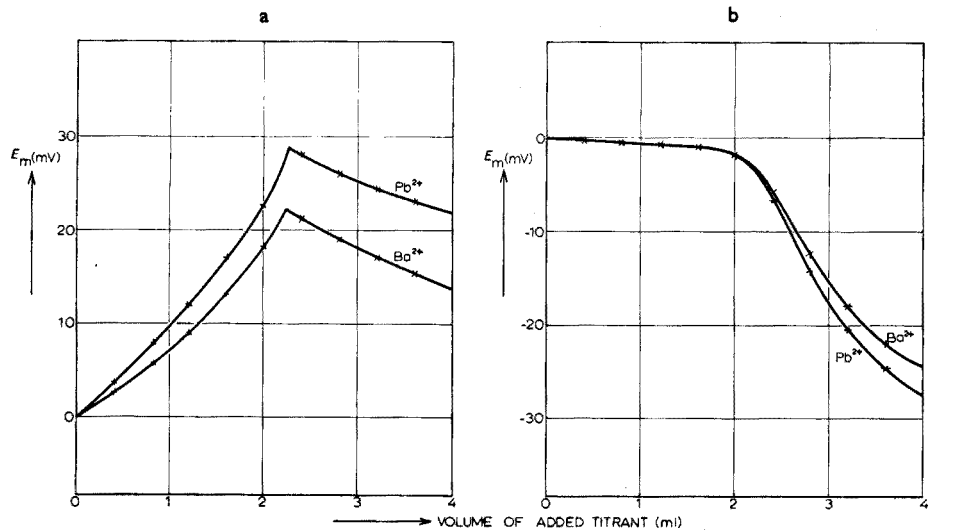

Fig. 5. Experimental curves for the titration of: (a) 20 ml of 0.029 *M* solutions of $Ba(NO_3)_2$ or $Pb(NO_3)_2$ with 0.26 *M* Na_2SO_4 solution; (b) 20 ml of 0.026 *M* Na_2SO_4 with 0.029 *M* $Ba(NO_3)_2$ or $Pb(NO_3)_2$. The cation-exchanging Permaplex C 20 membranes were used in the Na^+-form and 0.05 *M* KNO_3 was used as the reference solution.

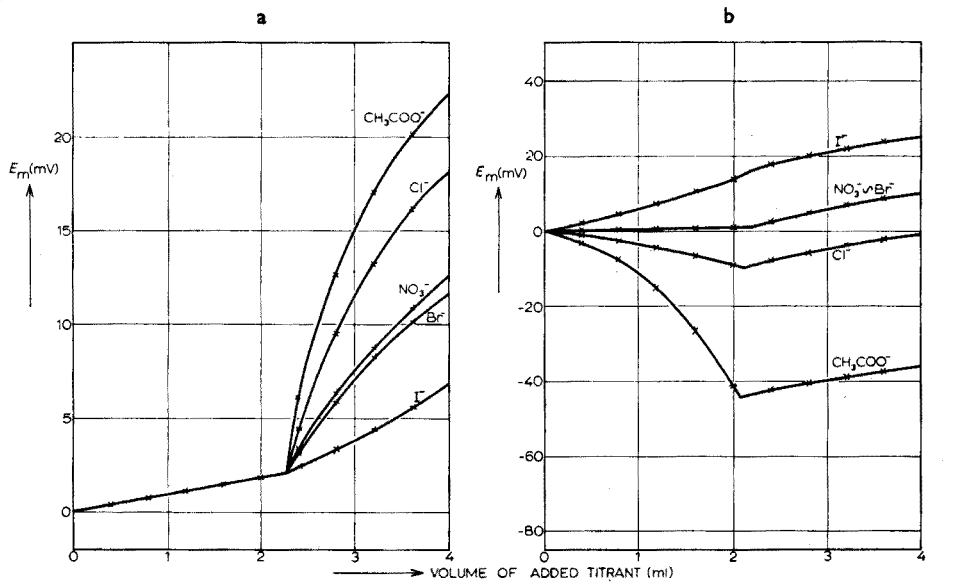

Fig. 6. Experimental curves for the titration of: (a) 20 ml of 0.029 *M* solutions of $Ba(CH_3COO)_2$, $BaCl_2$, $BaBr_2$, $Ba(NO_3)_2$ or BaI_2 with 0.26 *M* Na_2SO_4 solution; (b) 20 ml of 0.026 *M* Na_2SO_4 with 0.29 *M* solutions of $Ba(CH_3COO)_2$, $BaCl_2$, $BaBr_2$, $Ba(NO_3)_2$ or BaI_2. Anion-exchanging membranes (Permaplex A 20) were used in the Cl^-- form; the reference solution was 0.05 *M* KCl. The results should be compared with the theoretically calculated titration curves of Figs. 1g and 1c. As can be seen from Fig. 6b, the experimentally found equivalence point is somewhat too late (theoretically 1.8 ml). This is caused by the uptake of sulphate ions by the membrane during the first stage of the titration; when the concentration of the sulphate ions in the solution decreases during the titration, these ions return to the solution by reversal of the exchange reaction. With this kind of titration, the greatest errors were found from this phenomenon.

sulphate solution (Fig. 6a, to be compared with Figs. 1g and 3b); the reverse titrations were also performed (Fig. 6b, to be compared with Figs. 1c and 3a).

Titrations of potassium chloride with silver sulphate, barium chloride with silver sulphate, sodium hydroxide with sulphuric acid, and hydrochloric acid with barium hydroxide were performed, as well as the reverse titrations for all these cases. The titration curves obtained experimentally were also in accord with the calculated curves for these cases.

DISCUSSION OF THE RESULTS

In all cases the shape of the obtained titration curves is qualitatively in accordance with the calculated theoretical curves, although in a few cases the slope of the titration curves before the equivalence point deviates somewhat (Figs. 5b and 6a, and partly Fig. 4b). Typically, in these cases the co-ion present in the solution to be titrated is precipitated. Just as in the previously described cases of univalent ions, the ratio of the diffusion coefficients of the counter-ions present in the solution to be titrated and in the reagent solution is an important parameter in determining the shape of the titration curves.

The sequence of the values of the diffusion coefficients of the ions taking part in the titrations as mentioned above can be given as follows:

$$H^+ > K^+ > Na^+ > Li^+$$

$$Ba^{2+} > Pb^{2+}$$

$$I^- > Br^- > NO_3^- > Cl^- > CH_3COO^-$$

These results are in agreement with the sequence described earlier[3].

The authors gratefully acknowledge the valuable assistance of Dr. W. T. DE VRIES of this laboratory, who carried out the programming of the calculations.

SUMMARY

Theoretical titration curves were calculated for the cases when univalent and bivalent or univalent and trivalent ions are present in the titration system. As was found previously, the factor that primarily determines the shape of the titration curves for a given combination of ionic valencies is the ratio of the diffusion coefficients of the counter-ions present in the solution to be titrated and in the titrant. The experimental results obtained with solutions containing univalent and bivalent ions are in accordance with the theoretical expectations. The use of a simplified method for the calculation of the intramembrane diffusion potential is justified.

RÉSUMÉ

Des titrages potentiométriques sont effectués à l'aide d'une électrode à membrane échangeuse d'ions. On examine les cas de systèmes de titrage d'ions monovalents et polyvalents. Les courbes de titrage obtenues expérimentalement correspondent qualitativement à celles qui ont été calculées.

ZUSAMMENFASSUNG

Es wurden Titrationskurven für potentiometrische Titrationen berechnet für den Fall, dass einwertige und zweiwertige oder einwertige und dreiwertige Ionen im System anwesend sind. Es wurde früher bereits gefunden, dass der Faktor, der im wesentlichen die Gestalt der Titrationskurve bestimmt, durch die Kombination der Ionenwertigkeiten und dem Verhältnis der Diffusionskoeffizienten bestimmt wird. Die experimentellen Ergebnisse, welche mit Lösungen erhalten wurden, welche einwertige und zweiwertige Ionen enthalten, stimmen mit den theoretischen Überlegungen überein. Für die Berechnung der Membranpotentiale wurde ein vereinfachtes Verfahren gewählt, welches sich bewährt hat.

REFERENCES

1 F. P. IJSSELING AND E. VAN DALEN, *Anal. Chim. Acta*, 36 (1966) 166.
2 F. P. IJSSELING AND E. VAN DALEN, *Anal. Chim. Acta*, 40 (1968) 421.
3 F. P. IJSSELING AND E. VAN DALEN, *Anal. Chim. Acta*, 43 (1968) 77.
4 F. P. IJSSELING AND E. VAN DALEN, *Anal. Chim. Acta*, 45 (1969) 121.
5 F. HELFFERICH, *Ion Exchange*, McGraw-Hill, New York, 1962, chapter 5, pp. 134–146; R. SCHLÖGL, *Stofftransport durch Membrane*, Dr. Dietrich Steinkopf Verlag, Darmstadt, 1964, pp. 67–72.
6 R. SCHLÖGL, *Ber. Bunsenges. Physik. Chemie*, 70 (1966) 400.
7 R. SCHLÖGL, *Z. Physik. Chem. (Frankfurt)*, 1 (1954) 305.

Analytica Chimica Acta
Elsevier Publishing Company, Amsterdam
Printed in The Netherlands

ZUR ANALYTIK DES HYPOBROMITS UND BROMITS

H. FUCHS UND R. LANDSBERG*
Institut für physikalische Chemie, Technische Hochschule für Chemie "Carl Schorlemmer", Leuna-Merseburg, Merseburg (D.D.R.)
(Eingegangen den 20. Dezember, 1968)

Die geringen Unterschiede in den Eigenschaften und die mangelhafte Stabilität, die besonders das Hypobromit auszeichnet, sind die entscheidenden Gründe für die Schwierigkeiten bei der Simultanbestimmung der beiden Anionen. Nach bereits dargelegten Untersuchungen[1] ist Bromit ein sehr häufiger Begleiter des Hypobromits, was oftmals unberücksichtigt blieb. Eine Reihe von Verfahren zur Bestimmung des Hypobromits[2-5] ist daher nur für bromitfreie Lösungen anwendbar, da wir im Rahmen unserer polarographischen Untersuchungen feststellen konnten, dass unter den Bedingungen dieser Methoden auch Bromit mit den zugesetzten Reduktionsmitteln reagiert. Mehrere Arbeiten[6-9] haben sich mit der Lösung dieses Problems auf titrimetrischem Wege beschäftigt. Die bisher existierenden Verfahren zur Simultanbestimmung haben im wesentlichen zwei Nachteile:

(*a*) Mangelhafte Selektivität der zur Zerstörung des Hypobromits zugesetzten Stoffe, die vor allem infolge des Überschusses auch mit Bromit reagieren. Die besten Ergebnisse lieferte die von CHAPIN[7] vorgeschlagene Methode.

(*b*) Disproportionierung des Hypobromits in schwach alkalischen Lösungen durch Zugabe von Natriumhydrogencarbonat, eine Fehlerquelle, die sich um so stärker bemerkbar macht, je höher die Konzentration des Hypobromits und je niedriger die des Bromits ist, weil die Konzentrationsänderungen zu Beginn der Konzentrations–Zeit-Kurve der Disproportionierung des Hypobromits am grössten sind.

Besonders beim Hypobromit, als dem reaktionsfähigerem und instabilerem der beiden Anionen, ist ausserdem folgenden zu berücksichtigen:

(*a*) Von den durch POLAK *et al.*[10] untersuchten, die Stabilität beeinflussenden Faktoren ist vor allem die Zersetzung durch Verunreinigungen in der Lösung zu beachten.

(*b*) Oxydation des Quecksilbers bei der polarographischen Bestimmung, deren Geschwindigkeit jedoch mit steigendem pH-Wert sinkt.

Bei Berücksichtigung dieser Fehlerquellen ist auch eine polarographische Bestimmung des Hypobromits möglich[11].

EXPERIMENTELLES

Für die Untersuchungen an der Quecksilbertropfelektrode wurde ein Polarograph vom Typ OH-102 (Metrimpex, Budapest) und eine Apparatur zur punktweisen Aufnahme von Stromspannungskurven benutzt. Der Potential–Zeit-Verlauf bei den

* Sektion Chemie der Humboldt-Universität, 108 Berlin, Bunsenstr. 1, D.D.R.

chronopotentiometrischen Messungen wurde mit einem Oszillographen Uniskop EO 1/130 (VEB Technisch-Physikalische Werkstätten Thalheim/Erzgebirge) registriert. Als Stromquelle dienten Anodenbatterien. Die Goldelektrode wurde in Form einer Scheibenelektrode verwendet. Ein Goldzylinder war so in eine Teflonkappe gebracht worden, dass die Grundfläche als Elektrode wirksam wurde. Alle Potentiale werden gegen die gesättigte Kalomelelektrode (GKE) angegeben. Die Lösungen wurden mit sauerstofffreiem Stickstoff gespült und die Messungen bei $20 \pm 0.2°$ durchgeführt. Das Bodenquecksilber ersetzen wir durch ein Platinblech als Gegenelektrode.

Die Herstellung des Bromits und der Hypobromitlösungen wurde bereits beschrieben[1]. Der Berechnung des Äquivalentgewichts ist die Reduktion zum Bromid zugrunde gelegt. Bei Gegenwart von Hypobromit wurde als Grundelektrolyt ausschliesslich 0.5 *M* Natronlauge verwendet. Sie wurde aus Natriumhydroxid zur Analyse (Chemapol, Prag) mit bidestilliertem Wasser bereitet und einer Elektrolyse an Platinelektroden unterworfen. Alle übrigen für Grundelektrolyten verwendeten Chemikalien besassen den Reinheitsgrad "zur Analyse" und wurden unmittelbar eingesetzt.

Erfolgte die Simultanbestimmung auf chronopotentiometrischem Wege, so wurde die Goldelektrode vor den Messungen 5 min bei -500 mV im Grundelektrolyten vorpolarisiert. Das weitere Vorgehen entsprach der üblichen Arbeitsweise. Bei der Bestimmung mit der Quecksilbertropfelektrode wurde das Potential dieser Elektrode auf das der Grenzströme des Hypobromits und Bromits eingestellt. Wenn eine wässrige Harnstofflösung zur Zerstörung des Hypobromits benutzt wurde, erfolgte die Messung des Grenzstromes bei -750 mV. Diese Lösung wurde tropfenweise zugesetzt, wobei während jeder Zugabe gerührt wurde, um einen örtlichen Überschuss zu vermeiden. Nach jedem Zusatz wurde bis zur Einstellung eines konstanten Stroms gewartet. Bei der Schnellmethode wurde die Zugabe unterbrochen, wenn die Abnahme des Grenzstroms einen bestimmten Wert erreicht hatte. Eine genauere Bestimmung des Bromitgrenzstromes ist möglich, wenn der Grenzstrom gegen die zugesetzte Lösungsmenge aufgetragen wird (Abb. 1). Die Differenz der Grenzströme entspricht der Hypobromitkonzentration.

CHRONOPOTENTIOMETRISCHE BESTIMMUNG AN DER GOLDELEKTRODE

Bei dieser Methode entfällt das Problem der selektiven Zerstörung des Hypobromits, da jedes der beiden Anionen einen gut ausgebildeten Einschaltsprung bei der Reduktion ergibt (Abb. 2). Der erste Einschaltsprung mit der Transitionszeit τ_1 entspricht dem Hypobromit und der zweite mit der Transitionszeit τ_2 dem Bromit. Die Transitionszeiten sind diffusionsbedingt. Die Transitionszeit des Bromits in Gegenwart von Hypobromit wurde nach BERZINS UND DELAHAY[12] ausgewertet, da während der Reduktion des Bromits auch noch Hypobromit zur Elektrode diffundiert, wodurch diese Transitionszeit gegenüber der alleinigen Anwesenheit von Bromit verlängert wird. Diese Erscheinung ist die Ursache der hohen Empfindlichkeit für Bromit. Abb. 3 gibt die Abhängigkeit des Produktes aus der Stromdichte i und der Quadratwurzel aus der Transitionszeit τ in Abhängigkeit von der Konzentration wieder. Dieses Verfahren ist besonders zum Nachweis geringer Bromitmengen in einer Hypobromitlösung hoher Konzentration geeignet. Der Fehler wächst mit

steigender Konzentrationsdifferenz zwischen Hypobromit und Bromit und beträgt 5%, wenn sich die Transitionszeiten τ_1 und τ_2 nur wenig unterscheiden.

Bei hypobromitfreien Bromitlösungen wurden chronopotentiometrische Messungen auf den gesamten alkalischen pH-Bereich ausgedehnt. In keinem Falle konnte aber die Existenz der freien bromigen Säure nachgewiesen werden. Es wurde stets nur der Einschaltsprung des Anions erhalten.

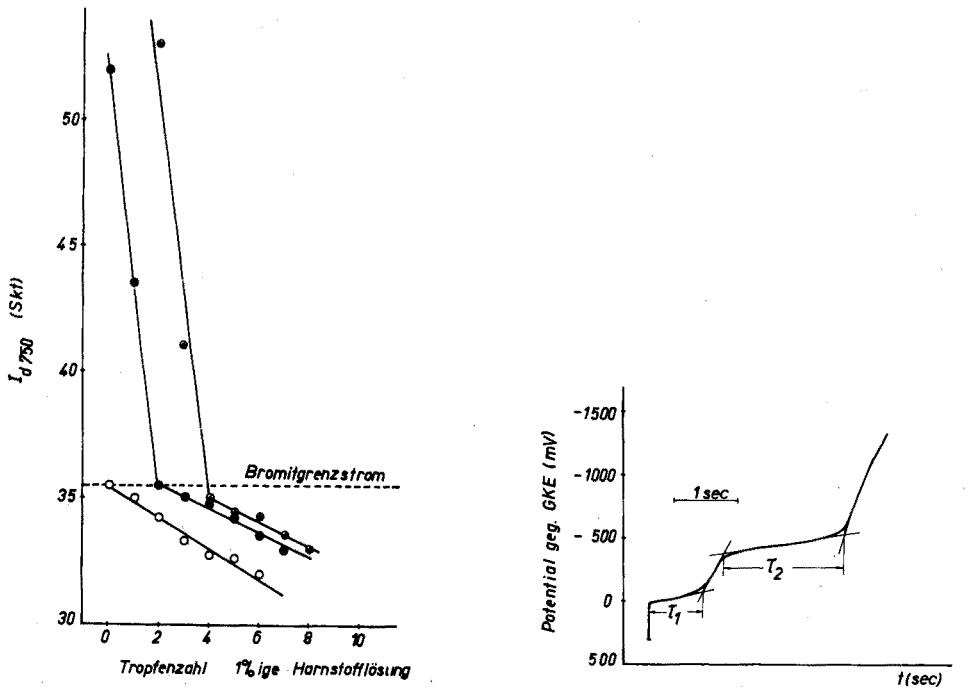

Abb. 1. Simultanbestimmung von BrO^- und BrO_2^- an der Quecksilbertropfelektrode in 0.5 *M* NaOH. (○) $1.5 \cdot 10^{-3}$ *M* BrO_2^- hypobromitfrei; (●) $1.5 \cdot 10^{-3}$ *M* BrO_2^-; $1.4 \cdot 10^{-3}$ *M* BrO^-; (⊕) $1.5 \cdot 10^{-3}$ *M* BrO_2^-; $2.9 \cdot 10^{-3}$ *M* BrO^-.

Abb. 2. Potential–Zeit-Verlauf von $1.3 \cdot 10^{-2}$ *M* BrO^- und $5.5 \cdot 10^{-3}$ *M* BrO_2^- in 0.5 *M* NaOH an der Goldelektrode.

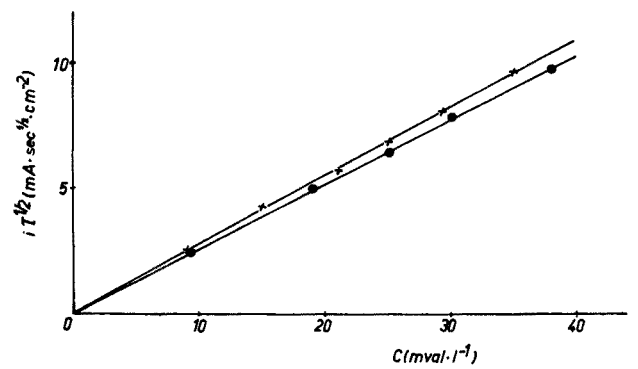

Abb. 3. Konzentrationsabhängigkeit von $i\tau^{\frac{1}{2}}$. (×) BrO^-; (●) BrO_2^-.

POLAROGRAPHISCHE BESTIMMUNG

Im Zusammenhang mit der Darstellung des Natriumbromits war es notwendig, ein Verfahren zu entwickeln, das bei geringem Aufwand in kurzer Zeit ein Ergebnis liefert. Die stationären Reduktionsstufen an der rotierenden Platinelektrode konnten für ein Analysenverfahren nicht benutzt werden, da katalytische Erscheinungen auftraten. Beim Hypobromit wurde eine vom Elektrodenzustand abhängige, kinetisch bedingte Vorstufe beobachtet. Die Hauptstufe des Hypobromits und die Stufe des Bromits überlagern sich und im Grenzstromgebiet dieser Stufen wird Bromat reduziert. Die Reduktion des Bromats wird ebenfalls in hohem Masse vom Elektroden zustand beeinflusst. Auch die stationären Stromspannungskurven an der rotierenden Goldelektrode waren wenig geeignet. Wir wandten uns deshalb der Quecksilbertropfelektrode zu[11]. Die Reduktionsstufen des Hypobromits und Bromits beginnen beim Potential der anodischen Quecksilberauflösung. Da die Potentiallage der Stufen übereinstimmt, überlagern sich die diffusionsbedingten Grenzströme der beiden Anionen, so dass Hypobromit als das reaktionsfähigere beseitigt werden muss: Ein das Hypobromit völlig selektiv zerstörender Stoff wurde nicht gefunden. Eine wässrige Harnstofflösung wurde den gestellten Anforderungen am besten gerecht. Harnstoff war erstmals von CLARENS[6] vorgeschlagen worden. Auch eine wässrige Phenollösung[7] wäre anwendbar. Sie führt jedoch zu einer Verschiebung der Bromitstufe zu negativeren Potentialen. Bei der zur Natriumbromitdarstellung[1] verwendeten Schnellmethode wurde nur die Bromitkonzentration verfolgt. Da das Probenvolumen in diesem Fall 50 ml betrug und die Summe der Konzentrationen des Bromits und Hypobromits zum Teil über 10^{-2} *N* lag, wurde eine 10%ige Harnstofflösung benutzt. Die Bromitkonzentration entspricht im Falle der 10%igen Harnstofflösung dem Grenzstrom dann, wenn dessen Abnahme nach Zugabe eines Tropfens gleich oder kleiner als 5% geworden ist. Günstiger für die Bestimmung beider Anionen sind kleinere Probenvolumina und niedrigere Konzentrationen. Abb. 1 zeigt Beispiele, bei denen das Volumen 25 ml war und eine 1%ige Harnstofflösung benutzt wurde. Die besten Ergebnisse wurden erhalten, wenn die Bromitkonzentration zwischen $2 \cdot 10^{-4}$ *M* und $2 \cdot 10^{-3}$ *M* lag und die Summe der Konzentrationen des Hypobromits und Bromits kleiner als 10^{-2} *N* war. Der Fehler beträgt bei Verwendung von 1%iger Harnstofflösung 2–3%. Bei grossen Konzentrationsunterschieden wächst

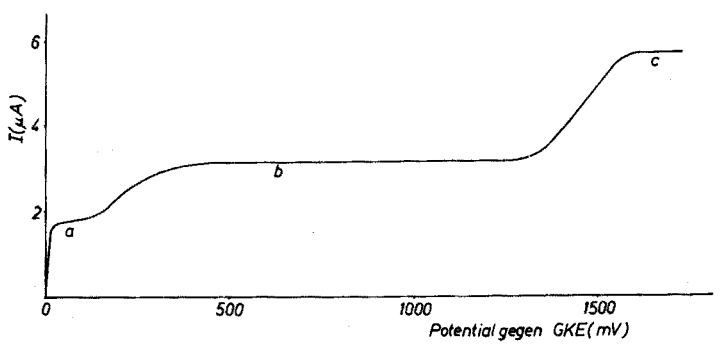

Abb. 4. Polarogramm von $1.75 \cdot 10^{-4}$ *M* BrO_2^- und $1.1 \cdot 10^{-4}$ *M* BrO_3^- in 0.3 *M* $CaCl_2$ (NaOH). (a) Vorstufe; (b) Grenzstrom des BrO_2^-; (c) Grenzstrom des BrO_3^-.

der Fehler bei demjenigen der beiden Anionen, das mit der niedrigeren Konzentration vorliegt. In Gegenwart von Calcium- oder Bariumionen versagte diese Methode.

In Abwesenheit von Hypobromit können mit der Quecksilbertropfelektrode in einem Calciumchloridgrundelektrolyten Bromit und Bromat bestimmt werden (Abb. 4). Zur Sicherung der Stabilität des Bromits wurde Natronlauge zugefügt, wobei der pH-Wert nur so weit erhöht wurde, dass es noch zu keiner Ausfällung von Calciumhydroxid kam. Die Vorstufe entsteht durch oberflächenaktive Anionen, in deren Gegenwart die Bromitreduktionsstufe ausserdem zu negativeren Potentialen verschoben wird. Der Grenzstrom der Vorstufe ist von der Behälterhöhe des Quecksilbers unabhängig. Mit wachsender Konzentration des oberflächenaktiven Anions wird die Verschiebung der Stufe grösser und der Grenzstrom der Vorstufe niedriger (Abb. 5). Die Wirksamkeit der oberflächenaktiven Anionen sinkt bei gleicher Konzentration in der Reihenfolge

$$I^- > SCN^- > Br^- > Cl^- > NO_3^-$$

Jodid und Rhodanid wurden nur in Natronlauge zugesetzt, da die Geschwindigkeit der Reaktion zwischen diesen Anionen und Bromit mit fallendem pH-Wert wächst.

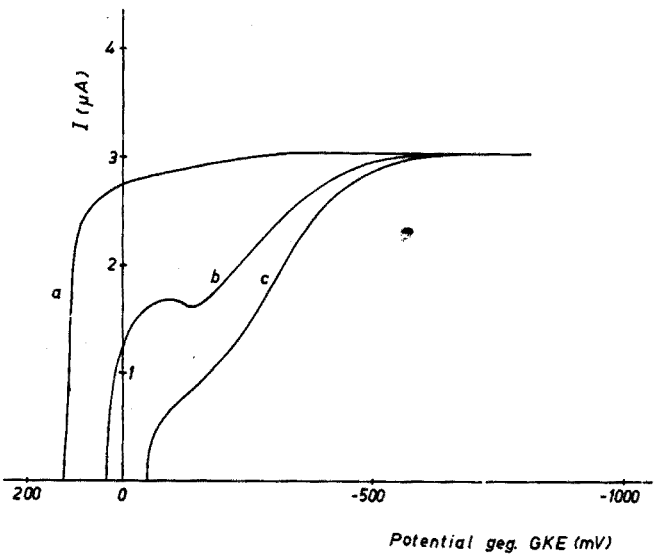

Abb. 5. Polarogramm von $1.75 \cdot 10^{-4}$ *M* BrO_2^-. Grundelektrolyt: Boratpuffer (pH = 9.1); 0.5 *M* Na_2SO_4. (a) nahezu bromidfrei; (b) $2.4 \cdot 10^{-2}$ *M* Br^-; (c) $1.0 \cdot 10^{-1}$ *M* Br^-.

Elektrokapillarkurven zeigen, dass die Erniedrigung der Reduktionsstufen durch oberflächenaktive Anionen in dem Potentialgebiet liegt, in dem diese Anionen an der Quecksilberoberfläche adsorbiert werden. Die Adsorption der Anionen führt zu einer Verdrängung des Bromits aus der Oberfläche, der Reduktionsvorgang wird dadurch gehemmt. Wird in Grundelektrolyten gearbeitet, deren Anionen nicht oberflächenaktiv sind (z.B. Sulfat, Fluorid oder Hydroxid), dann wird keine Vorstufe beobachtet. Hohe Grundelektrolytkonzentrationen wurden verwendet, um das Maximum in der Stufe bei hohen Bromitkonzentrationen zu unterdrücken, da im Falle eines Agar-Zusatzes relativ grosse Mengen notwendig sind.

ZUSAMMENFASSUNG

Nach Darlegung der Bedingungen für die Analytik des Hypobromits und Bromits werden Möglichkeiten zur Bestimmung mit der konventionellen Gleichspannungspolarographie und der Chronopotentiometrie an der Goldelektrode angegeben.

SUMMARY

Factors influencing the determination of hypobromite and bromite are discussed. A simultaneous determination of hypobromite and bromite is possible by chronopotentiometry with a gold electrode, or by conventional polarography.

RÉSUMÉ

On examine les divers facteurs influençant le dosage des hypobromites et des bromites. Un dosage simultané hypobromite–bromite est possible par chronopotentiométrie avec électrode d'or ou par polarographie conventionnelle.

LITERATUR

1 H. FUCHS UND R. LANDSBERG, *Z. Anorg. Allgem. Chem.*, im Druck.
2 R. SCHOLDER UND K. KRAUSS, *Z. Anorg. Allgem. Chem.*, 268 (1952) 279.
3 L. ERDEY UND J. INCZÉDY, *Z. Anal. Chem.*, 166 (1959) 410.
4 S. SUZUKI, K. HARIMAYA, M. UENO, N. TSUJI UND N. YAMAOKA, *Bull. Chem. Soc. Japan*, 30 (1957) 766.
5 J. P. TANDON UND K. L. CHAWLA *Bull. Chem. Soc. Japan*, 39 (1966) 2544.
6 J. CLARENS, *Compt. Rend.*, 156 (1913) 1998.
7 R. M. CHAPIN, *J. Am. Chem. Soc.*, 56 (1934) 2211.
8 M. H. HASHMI UND A. A. AYAZ *Anal. Chem.*, 35 (1963) 908; *Analyst*, 89 (1964) 147.
9 T. ANDERSEN UND H. E. LUNDAGER MADSEN, *Anal. Chem.*, 37 (1965) 49.
10 H. L. POLAK, G. FEENSTRA UND J. SLAGMAN, *Talanta*, 13 (1966) 715.
11 H. FUCHS UND R. LANDSBERG, *Z. Physik. Chem. (Leipzig)*, 232 (1966) 413.
12 T. BERZINS UND P. DELAHAY, *J. Am. Chem. Soc,*, 75 (1953) 4205.

Analytica Chimica Acta
Elsevier Publishing Company, Amsterdam
Printed in The Netherlands

EIN KATIONENTRENNUNGSGANG DURCH LÖSUNGSMITTELEXTRAKTION

HELMUT FÖRSTER
VEB Bergbau- und Hüttenkombinat "Albert Funk", Forschungsinstitut für Nichteisenmetalle, Freiberg
UND
KURT SCHWABE
Institut für Elektrochemie und physikalische Chemie, Technische Universität, Dresden (Deutschland)
(Eingegangen den 2. Februar, 1969)

Die Lösungsmittelextraktion nimmt heute einen hervorragenden Platz unter den Trennmethoden ein. Die grossen Fortschritte auf diesem Gebiet führten zur Aufstellung mehr oder weniger umfangreicher Trennschemata. Die Vollkommensten dienen dem qualitativen Nachweis, wie die Trennungsgänge von DOLL UND SPECKER[1], IWANTSCHEFF[2], WEST UND MUKHERJI[3], TÖLG[4] und CHALMERS UND DICK[5] beweisen. Quantitative Trennungen sind auf Gruppen oder einzelne Kationen beschränkt[5-12]. Die Durchführbarkeit vieler Trennungsgänge ist an niedrige Metallionenkonzentrationen und bestimmte Säureanionen geknüpft[13-18], so dass nur Spuren abtrennbar sind und bei der Aufarbeitung das wässrige Milieu wiederholt gewechselt werden muss. Wir bemühten uns um die Entwicklung eines Trennungsganges unter folgenden Gesichtpunkten:

1. In Analogie zum klassischen Trennungsgang sind die Kationen bei sinkender Azidität in wenigen Hauptgruppen zu extrahieren.
2. Auf die Anwesenheit von Hilfskomplexbildnern zur Unterdrückung der Hydrolyse wird verzichtet.
3. Als Gruppenreagentien sind nur Chelatkomplexbildner zu verwenden, um weitgehende Unabhängigkeit von der Art der Säureanionen zu erreichen.
4. Es sind nur leicht herstellbare Reagentien zu verwenden, die in organischen Lösungsmitteln gut lösliche Metallkomplexe bilden.
5. Aus dem organischen Lösungsmittel sind die Kationen mit selektiven Komplexbildnern zu reextrahieren.

Ein Trennungsgang unter diesem Blickwinkel lässt sich nur mit wenigen Reagentien verwirklichen. Als ungeeignet erwiesen sich alle Reagentien, die mit Metallionen Chelatkomplexe von geringer Stabilität und Löslichkeit in organischen Lösungsmitteln bilden, z. B. β-Diketone (Acetylaceton und Benzoylaceton), 8-Hydroxychinoline, Oxime, Nitrosophenole, Pyridylazonaphthole, Diphenylthiocarbazone, Dithiole, Merkaptochinoline, Flavon, Morin u.a. Ausgewählt wurde das N-Benzoyl-N-phenylhydroxylamin (BPHA) und das Diäthylammoniumdiäthyldithiocarbamidat (DÄDDTC). Diese durch Benzoylierung des Phenylhydroxylamins und durch Neutralisation des Diäthylamins mit Schwefelkohlenstoff leicht darstell-

baren Reagentien, bilden mit vielen Kationen in saurer Lösung Chelatkomplexe von grosser Beständigkeit und guter Löslichkeit. In zahlreichen Arbeiten wird darüber berichtet[4,19–33].

In vorliegender Arbeit wird ein Bericht über einen einfachen Kationentrennungsgang durch Lösungsmittelextraktion gegeben. In Analogie zum klassischen Schwefelwasserstoff–Ammoniak-Trennungsgang werden die Kationen bei sinkender Azidität in vier Hauptgruppen extrahiert; die Elemente der Sulfidgruppen mit DÄDDTC und die Ammoniakgruppe mit BPHA. Zur weiteren Aufspaltung dient die unterschiedliche Reextrahierbarkeit der im Chloroform gelösten Chelatkomplexe mit verschiedenen Reagenslösungen. In diesem Trennungsgang finden *ca.* 60 Kationen Berücksichtigung. Viele Kationen können im Mikro- und Milligrammbereich quantitativ abgetrennt werden. Die Durchführung des Trennungsganges ist unabhängig von der Art der Säureanionen und gelingt im Gegensatz zum klassischen Trennungsgang auch aus salpetersauren Lösungen. Alle Trennoperationen sind mit leicht herstellbaren Reagentien in einfachen Schüttelzylindern rasch ausführbar.

Die Entwicklung dieses Trennungsganges diente der Abtrennung von Radionukliden zur aktivierungsanalytischen Bestimmung von Verunreinigungen in hochreinen Werkstoffen. Dieses Ziel führte zur Vernachlässigung einiger Elemente, deren aktivierungsanalytische Bestimmung von geringem Interesse ist, z. B. des Eisens, Magnesiums und Titans. Bei der Aufstellung des Trennungsganges leisteten Radionuklide als Indikatoren wertvolle Hilfe. Der Trennungsgang wird im folgenden beschrieben, seine aktivierungsanalytische Anwendbarkeit wird in einer weiteren Publikation dargelegt werden.

Übersicht des Trennungsganges

Eine schematische Übersicht des gesamten Trennungsganges vermitteln die Abb. 1–7. Die erste Abbildung zeigt die Trennung der Kationen der mineralsauren Originallösung in fünf Hauptgruppen. Die Bedingungen der Trennung wurden in der

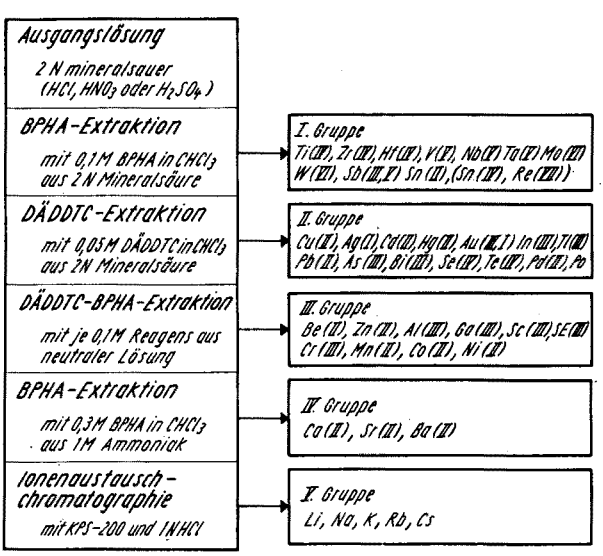

Abb. 1. Trennung der Originallösung in Hauptgruppen.

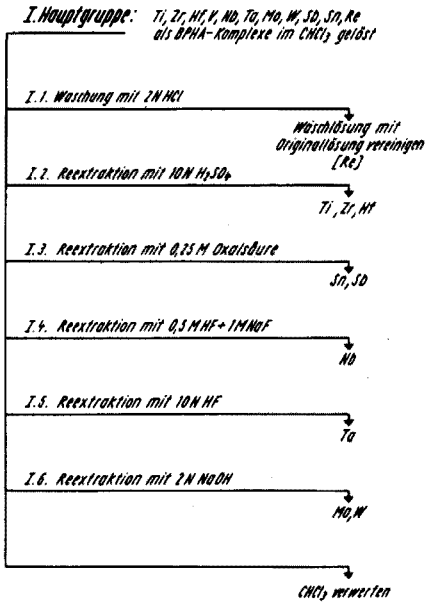

Abb. 2. Trennung der I. Hauptgruppe.

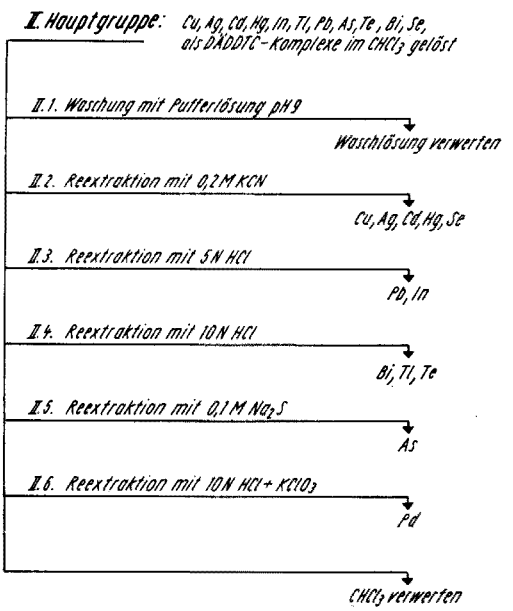

Abb. 3. Trennung der II. Hauptgruppe.

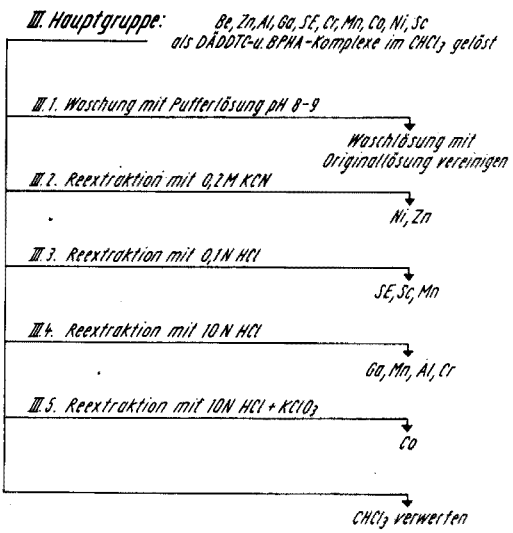

Abb. 4. Trennung der III. Hauptgruppe.

linken Spalte und rechts die in den betreffenden Gruppen abgetrennten Kationen vermerkt. Die weitere Aufspaltung der Hauptgruppen in Untergruppen durch selektive Reextraktion zeigen die Abb. 2–5. Diese Schemata enthalten die Klassifizierung der Untergruppen, die Art und die Konzentration der anzuwendenden Reextraktionsmittel, die Reihenfolge ihrer Anwendung und die in den Untergruppen abgetrennten

Kationen. In zahlreichen Untergruppen treten mehrere Kationen gleichzeitig auf, so dass weitere Trennoperationen notwendig sind. Einfache Trennstufen werden im Text erläutert, mehrstufige zusätzlich durch Schemata veranschaulicht.

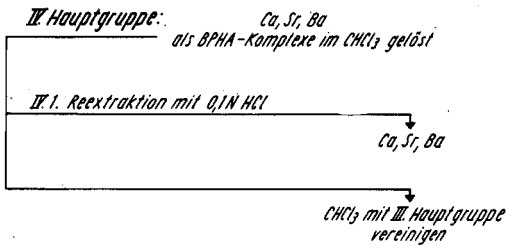

Abb. 5. Trennung der IV. Hauptgruppe.

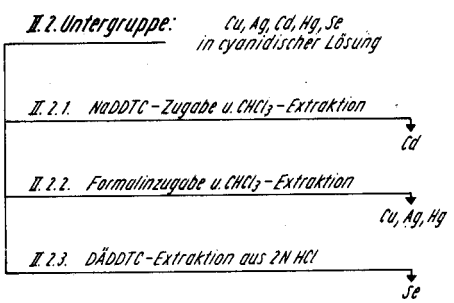

Abb. 6. Trennung der II.2. Untergruppe.

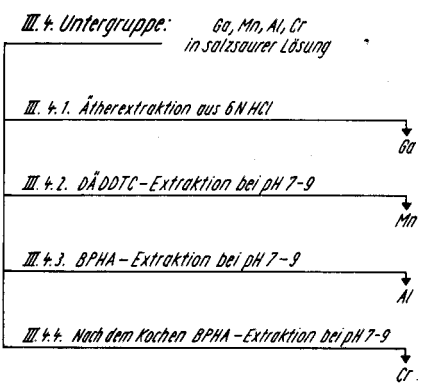

Abb. 7. Trennung der III.4. Untergruppe.

Erläuterungen zur Durchführung des Trennungsganges

Allgemeine Hinweise. Die Verteilung der Metallionen wurde in verschlossenen Glaszylindern vorgenommen. Geschüttelt wird bei der Extraktion, d. h. zur Überführung eines Kations aus der wässrigen in die organische Lösung, *ca.* 30 Sekunden und bei der Reextraktion, d. h. zur Zurückführung eines Kations in die wässrige Lösung, 1 Minute. Um dabei Vollständigkeit zu erzielen, wird jede Verteilung, falls nicht anders vermerkt, 1–2 mal mit frischem Reagens wiederholt. Die Volumina der Chloroformlösungen werden im allgemeinen doppelt so gross gewählt wie die wässriger Lösungen. Wir verwendeten insgesamt 50–60 ml Extraktions- und 15–25 ml Reextraktionslösungen. Bei der Abtrennung grösserer Mengen von Metallionen sind die Volumina der Extraktionslösung zu vergrössern, da die Trennbarkeit grösserer Mengen von Metallionen im allgemeinen durch die Löslichkeit der Chelatkomplexe im Chloroform begrenzt wird. Unvollständigkeit bei der Extraktion ist an der auftretenden Trübung beim Zutropfen alkoholischer Reagenslösung zur wässrigen Probelösung erkennbar.

Lösen der Proben. Die Durchführbarkeit des Trennungsganges ist an mineral-

saure Probelösungen gebunden. Das Lösen der Proben kann mit Salzsäure, Salpetersäure, Schwefelsäure oder deren Gemischen vorgenommen werden. Andere Mineralsäuren, wie z. B. Perchlorsäure, Bromwasserstoffsäure und Flusssäure, sind bisher noch nicht verwendet worden. Störungen im Trennungsgang sind nur in flusssauren Lösungen zu erwarten, z. B. sind Nb und Ta aus 2 *N* Flusssäure nicht mehr extrahierbar. Um beim Säureaufschluss Verluste an Ge, As, Sb, Cr, Re, Te, Se, Hg, Ru und Os zu vermeiden, ist es zweckmässig unter Rückfluss zu lösen. Dabei können die Oxidhydrate des Nb, Ta und W, die Sulfate der Erdalkalien, die Halogenide des Hg und Ag und die Oxide des Sn, Sb, Zr und Ti unlöslich zurückbleiben. Geringe Mengen dieser Metallionen vermögen in teilweise oder vollständig extrahierbaren Verbindungen in Lösung zu bleiben, z. B. sind 500 μg Ag aus 2 *N* salzsauren Lösungen vollständig abtrennbar, im Gegensatz zum Sb, Sn, Nb, Ta und Zr, die auch in 2 *N* salzsauren Lösungen rasch in unvollständig extrahierbare Oxidhydrate übergehen.

Die Trennung der Kationen der Originallösung in fünf Hauptgruppen (siehe Abb. 1)

In Analogie zum klassischen Schwefelwasserstoff–Ammoniak-Trennungsgang werden die Kationen bei sinkender Azidität durch BPHA- und DÄDDTC-Extraktion in fünf Hauptgruppen getrennt. In der I. Hauptgruppe werden aus 2 *N* mineralsaurer Lösung die Übergangselemente der 4.–7. Gruppe des Periodischen Systems als BPHA-Komplexe, in der II. Hauptgruppe bei gleicher Säurekonzentration Kationen der Schwefelwasserstoffgruppe als Diäthyldithiocarbamidate, in der III. Hauptgruppe Kationen der Ammoniak- und Ammon-Sulfidgruppe als BPHA- und DDTC-Komplexe und in der IV. Hauptgruppe aus 1 *M* ammoniakalischer Lösung die Erdalkalien als BPHA-Komplexe extrahiert. In der wässrigen Lösung bleiben die Alkalimetallionen zurück (V. Hauptgruppe).

Zu Beginn des Trennungsganges bringt man die Azidität der Probelösung auf eine Normalität von ~2. Die Extraktion der Ionen der I. Hauptgruppe erfolgt durch mehrmaliges Ausschütteln mit einer 0.1 *M* BPHA-Lösung in Chloroform. Bei Vollständigkeit der Abtrennung tritt beim Zutropfen einer alkoholischen BPHA-Lösung keine Trübung auf. Die Azidität der Probelösung darf zur Extraktion des Zr, Hf, Nb, Ta, Mo, W und Sb in salzsaurer Lösung bis 10 *N*, in schwefelsaurer und salpetersaurer Lösung bis 5 *N* und beim Zinn in salzsaurer Lösung bis 3 *N* und in schwefelsaurer Lösung bis 5 *N* ansteigen. Re(VII) und Sb(V) sind nur aus salzsauren Lösungen hoher Normalität extrahierbar. Zur Abtrennung dieser Ionen wird ein Aufschluss mit konzentrierter Salzsäure durchgeführt und, ohne zu verdünnen, mit 0.1 *M* BPHA vorextrahiert; z. B. sind 80% Re aus 10 *N* HCl, 1% aus 5 *N* HCl und nur 22% des Re aus 10 *N* H_2SO_4 extrahierbar.

Die Abtrennung der Kationen der I. Hauptgruppe gelingt nur dann vollständig, wenn keine Hydrolyse eingetreten ist. Da alle diese Ionen, ganz besonders W, Nb und Ta dazu neigen, ist es notwendig, die I. Hauptgruppe sofort nach der Säureeinstellung auszuschütteln. Selbst 1 mg Sn(II)-ionen unterliegen in 2 *N* Salzsäure der Hydrolyse, so dass dessen Extrahierbarkeit von Stunde zu Stunde absinkt. Die vereinigten Chloroformextrakte werden, wie im folgenden Kapitel beschrieben, in sechs Untergruppen aufgearbeitet.

Die Abtrennung der Kationen der II. Hauptgruppe findet bei gleicher Säurekonzentration durch mehrmaliges Ausschütteln mit 0.05 *M* DÄDDTC in Chloroform

statt. Bei Vollständigkeit der Trennung darf beim Zutropfen einer alkoholischen DÄDDTC-Lösung keine Trübung auftreten. Liegt die Azidität über 2 *N*, sind Cd aus schwefelsaurer Lösung und Cd, In, Pb und Tl aus salzsaurer nur unvollständig extrahierbar. Die Extraktion des Cu, Ag, Hg, As, Bi, Se, Te und Pd gelingt auch aus 5 *N* Mineralsäure vollständig. Sinkt die Azidität der Probelösung unter 1 *N*, dann können Zn und Co in die II. Hauptgruppe gelangen. Dabei ist zu berücksichtigen, dass die Azidität der wässrigen Lösung beim Schütteln mit DÄDDTC–Chloroform durch Reaktion mit Diäthylammoniumionen laufend vermindert wird. Deshalb muss bei der Abtrennung von Metallionen einer Gesamtkonzentration $\geqslant 0.1$ *N* die durch Neutralisation verbrauchte Säure ergänzt werden. Übersteigt das Volumen der Extraktionslösung das fünffache des Volumens der 2 *N* mineralsauren wässrigen Lösung, dann sind pro 100 ml 0.05 *M* DÄDDTC-Lösung ~1 ml 10 *N* Mineralsäure zuzufügen. Alle Chloroformauszüge der Diäthyldithiocarbamidate der II. Hauptgruppe sind zu sammeln, und wie im folgenden Kapitel beschrieben, in Untergruppen aufzuarbeiten.

Die Abtrennung der III. Hauptgruppe findet aus nahezu neutraler Lösung bei pH-Werten von 5–8 statt. Um Hydrolyse zu vermeiden, werden vor der Neutralisation BPHA und DÄDDTC in 0.5 *M* azetonischer Lösung im Überschuss zugesetzt. Die ausgefällten Chelatkomplexe der Kationen der III. Hauptgruppe werden mit reinem Chloroform ausgezogen. Bei Vollständigkeit der Trennung bleibt auch nach erneuter Reagenszugabe eine ungetrübte wässrige Lösung zurück. Die Abtrennung des Cr(III) gelingt nur dann vollständig, wenn die Fällung längere Zeit stand oder in der Wärme vorgenommen wurde. Die Abtrennung aller anderen Kationen bereitet auch in grösseren Mengen keine Schwierigkeiten. Die vereinigten Chloroformauszüge werden, wie im nächsten Kapitel beschrieben, weiter verarbeitet.

Die wässrige Probelösung wird 1 *M* ammoniakalisch gemacht und die IV. Hauptgruppe durch mehrmaliges Ausschütteln mit 0.3 *M* BPHA–Chloroform abgetrennt. Um Karbonatfällung der Erdalkalien zu vermeiden, ist es notwendig, karbonatfreien Ammoniak zu verwenden und nach dessen Zugabe sofort auszuschütteln. Die weitere Trennung der Erdalkalien siehe im nächsten Kapitel.

In der wässrigen Originallösung bleiben allein die Alkalimetallionen zurück. Da zu ihrer Trennung keine geeigneten Chelatsysteme verfügbar sind, wurden chromatographische Methoden herangezogen.

Die Trennung der Hauptgruppen in Untergruppen

Zur I. Hauptgruppe: Die Trennung der als BPHA-Komplexe im Chloroform gelösten Metallionen der I. Hauptgruppe beruht auf der unterschiedlichen Stabilität ihrer BPHA-, Sulfato-, Oxalato- und Fluorokomplexe. Wie Abb. 2 zeigt, werden zuerst die in geringen Mengen mitextrahierten Kationen der III. Hauptgruppe mit 2 *N* Salzsäure aus der Chloroformlösung ausgewaschen und wieder mit der Originallösung vereinigt. Re tritt an dieser Stelle nur nach BPHA-Extraktion aus konzentrierter salzsaurer Lösung auf, wobei Kationen der III. Hauptgrupppe nicht mitextrahiert werden. Durch erneutes mehrmaliges Ausschütteln der Chloroformlösung mit 5–10 *N* Schwefelsäure werden in der 2. Untergruppe Ti, Zr und Hf als Sulfatokomplexe reextrahiert; bei einmaligem Auswaschen mit 10 *N* Schwefelsäure bereits zu >90%. Alle übrigen in dieser Hauptgruppe vorhandenen BPHA-Komplexe zeigen hohe Beständigkeit gegen Schwefelsäure, ausser dem Sn-Komplex, welcher

zu einem geringen Anteil zerlegt wird. Sn und Sb sind als Oxalatokomplexe bei einmaligem Schütteln mit 0.25 *M* Oxalsäure zu >90% auswaschbar, wobei die Komplexe des Nb, Ta, Mo und W nicht angegriffen werden. Keine Vollständigkeit erzielt man bei der Nb–Ta-Trennung durch einmalige Verteilung. Zur Reextraktion des Mo und W ist dreimaliges Ausschütteln mit 2 *N* NaOH notwendig, da beim erstenmal nur das überschüssige Reagens entfernt wird.

Zur II. Hauptgruppe: Die Aufarbeitung der II. Hauptgruppe zeigt Abb. 3. Die in Chloroform gelösten Diäthyldithiocarbamidate werden nach Entfernung des Reagensüberschusses über die Cyano-, Chloro- und Thiokomplexe getrennt. Zur Entfernung des überschüssigen Reagenses ist kurzzeitiges Waschen mit Pufferlösung von pH 9 notwendig. In der II.2. Untergruppe sind Cu, Ag, Cd, Hg als Cyanokomplexe und Se vermutlich als Selenocyanat mit KCN vollständig reextrahierbar; selbst Cd und Se mit 0.2 *M* KCN bei einmaligem Waschen zu >95%. Der Behandlung mit KCN-Lösung folgt die Reextraktion des Pb, In, Bi, Tl und Te mit Salzsäure und des As mit Na_2S-Lösung. Pb- und In-Komplexe werden durch 3–5 *N* Salzsäure vollständig zerlegt, nur von geringen Mengen Bi und Tl begleitet. Zur Reextraktion der 4. Untergruppe mit 10 *N* Salzsäure ist mehrmaliges Ausschütteln notwendig. Im Chloroform verbleibt allein das Diäthyldithiocarbamidat des Pd zurück, da dieser Komplex sich durch grosse Beständigkeit gegen Laugen, Säuren, Cyanid- und Sulfidlösungen auszeichnet. Reextraktion gelingt nur durch Zerstörung des Komplexes beim Schütteln mit natriumchlorathaltiger 6 *N* Salzsäure.

Zur III. Hauptgruppe: Die Trennung der in Chloroform als BPHA- und DDTC-Komplexe gelösten Kationen der III. Hauptgruppe findet durch Reextraktion mit KCN- und HCl-Lösung statt. Zu Beginn der Trennung in Untergruppen wird wieder das überschüssige DÄDDTC durch Waschen mit Pufferlösung pH 9 entfernt. Der BPHA-Überschuss verbleibt im Chloroform, da zu dessen Entfernung nur Ausschütteln mit 2 *N* NaOH oder 25 *N* Schwefelsäure führt. In der III.2. Untergruppe sind $Ni(DDTC)_2$ und $Zn(DDTC)_2$ als Cyanokomplexe mit 0.2 *M* KCN leicht auswaschbar, ohne die anderen Komplexe anzugreifen. Die geringe Beständigkeit der BPHA-Komplexe des Sc und der Seltenen Erden gegen 0.1 *N* Salzsäure ermöglicht deren quantitative Abtrennung von Kationen der 4. und 5. Untergruppe. Zur vollständigen Reextraktion der BPHA-Komplexe des Cr, Al und Ga führt erst wiederholtes Ausschütteln mit 10 *N* Salzsäure. Im Chloroform verbleibt allein das Kobalt als grünes Diäthyldithiocarbamidat gelöst zurück. Die Reextraktion dieses Komplexes gelingt nur mit chlorathaltiger Salzsäure. Die Trennung der Kationen der III. Hauptgruppe verläuft vollständig bis auf Mn, welches sich auf die 3. und 4. Untergruppe verteilt.

Zur IV. Hauptgruppe: In der IV. Hauptgruppe sind die Erdalkalien als BPHA-Komplexe im Chloroform gelöst enthalten. Ihre leichte Zersetzlichkeit macht deren selektive Reextraktion unmöglich. Deshalb wurden die Erdalkaliionen gemeinsam durch zweimaliges Schütteln mit 0.1 *N* Salzsäure aus dem Chloroform ausgewaschen und chromatographisch am KPS getrennt[34,35].

Zur V. Hauptgruppe: In der V. Hauptgruppe liegen die Alkalimetallionen in wässriger ammoniakalischer Lösung vor. Ihre Trennung erfolgte nach Entfernung der Ammoniumsalze am Kationenaustauscherharz KPS. Zur Beseitigung der Ammoniumsalze ist einstündiges Erhitzen in der Muffel bei 350° notwendig. Den Glührückstand löst man in siedendem Wasser und gibt diese Lösung über das Harzbett.

Die getrennte Elution des Na vom K fand mit 1 *N* Salzsäure statt[34,35]. Das erforderliche Elutionsvolumen ergibt sich durch Multiplikation der Austauscherkapazität mit der Austauschkonstante[35].

Erläuterung der Untergruppen

Zu I.1.: Nach dem vorliegenden Trennschema wurden 500 μg Re mit >97%-iger Ausbeute von vielen Kationen in hoher Reinheit abgetrennt. Bei dreimaligem Ausschütteln des Re mit 0.1 *M* BPHA aus konzentrierter salzsaurer Lösung verblieben nur <1% in der wässrigen Lösung. Aus dem Chloroform lässt es sich mit alkalischen, neutralen und sauren Lösungen leicht reextrahieren, z. B. bereits zu 98% mit 2 *N* Salzsäure.

Zu I.2.: Zr und Hf sind gemeinsam mit hoher Ausbeute abgetrennt worden. Weniger als 0.5% verblieben bei zweimaligem Ausschütteln in der wässrigen Lösung und <2% im Chloroform. Die Trennung der Metallionen dieser Untergruppe ist nicht untersucht worden, da hierfür chromatographische Verfahren geeigneter erschienen[34,36]. Auf Ti wurde nur qualitativ geprüft.

Zu I.3.: Im Verhalten bei der BPHA-Extraktion ähnelt Zinn dem Antimon. Eine Trennung beider Metallionen ist nach Oxydation aus 2 *N* HCl durch längeres Schütteln möglich, da hierbei nur das Sn extrahiert wird[9]. Der Trennungsgang wurde mit 10 mg beider Metallionen durchgeführt und 9.5 mg wiedergefunden. *Ca.* 5% des Sn aber weniger als 0.5% des Sb begleiteten bei der schwefelsauren Waschung Zr und Hf in die I.2. Untergruppe.

Zu I.4.: Die Bestimmung des Nb ist nur qualitativ geführt worden. Vollständigkeit der Trennung wurde nur aus stärker als 2 *N* sauren Lösungen erzielt, z. B. sind aus 2 und 10 *N* Salzsäure Verteilungsverhältnisse um 1 und 100 gemessen worden. Der gebildete Nb–BPHA-Komplex zeigte Beständigkeit gegen 5 *N* Schwefelsäure und 0.1 *M* Oxalsäure, wurde aber durch 10 *N* Schwefelsäure und 0.2 *M* Oxalsäure teilweise aufgespaltet.

Zu I.5.: Der Trennungsgang wurde mit 500 μg Ta durchlaufen. Als grösste Verlustquellen erwiesen sich einerseits die Reextraktion des Nb mit verdünnter Flusssäure, wobei *ca.* 10% des Ta das Nb begleiteten, andererseits die Reextraktion mit 10 *N* Flusssäure, wobei keine Vollständigkeit erzielt werden konnte. Die Verluste in den übrigen Trennstufen sind vernachlässigbar, da sich der Ta–BPHA-Komplex durch grosse Beständigkeit gegen 25 *N* Schwefelsäure und 0.5 *M* Oxalsäure auszeichnet. Die Extraktion des Ta erfolgte auch aus verdünnten flusssauren Lösungen, z. B. sind aus 2 *N* mineralsauren und 0.1 *M* flusssauren Lösungen >98% des Ta bei einmaliger Verteilung abtrennbar.

Zu I.6.: Mo und W wurden gemeinsam abgetrennt. Die höchsten Verluste, bis 5% des Mo, traten bei der Ta-Reextraktion mit 10 *N* Flussäure auf, nur 1.4% gelangten in den Oxalatauszug und <1% gingen in anderen Trennstufen verloren. Den Mo- bzw. W-Nachweis führt man durch Extraktion der Rhodanide mit Methylisobutylketon, nach Reduktion des Mo mit Thioglykolsäure und des W mit $SnCl_2$. Beide Elemente sind an der Gelbfärbung der organischen Phase erkennbar[4].

Zu II.2.: Die Trennung des Cu, Ag, Cd, Hg und Se veranschaulicht Abb. 6. Nach Zugabe eines Überschusses an NaDDTC ist Cd und nach Demaskierung der Cyanokomplexe mit Formalin sind Cu, Ag und Hg erneut als Karbamidate extrahierbar[12].

Zu II.2.1.: Aus 0.2 *M* cyanidischer Lösung ist Cd nach Zugabe von 1 ml 20%igem NaDDTC pro 10 ml Lösung auch in Gegenwart von Zn selektiv extrahierbar. Aus der Chloroformlösung lässt es sich mit $\geqslant 2$ *N* Salzsäure ohne Schwierigkeiten in die wässrige Lösung zurückführen. Die quantitative Bestimmung kann mit Komplexon bei pH 10 oder in 1 *N* NaOH in Gegenwart von Cyanid mit Dithizon selektiv durchgeführt werden. 1–10 mg Cd wurden von vielen anderen Ionen abgetrennt. Nur 2% des Cd blieben in der cyanidischen Lösung zurück; die Summe der Verluste aller anderen Trennungen betrug $< 1\%$.

Zu II.2.2.: In Gegenwart von NaDDTC wurden die Cyanokomplexe des Cu, Ag und Hg mit ~10 ml Formalin abgebaut und diese Metallionen als Diäthyldithiocarbamidat gefällt und mit Chloroform ausgeschüttelt. Ihre Trennung beruht auf dem unterschiedlichen Verhalten der im Chloroform gelösten Diäthyldithiocarbamidate gegen KI-Lösung. Beim Schütteln des Chloroformextraktes mit angesäuerter 1 *M* KI-Lösung wird das Quecksilber als HgI_4^{2-}-Komplex ausgewaschen und der AgDDTC-Komplex unter AgI-Fällung vollständig zerlegt. Im Chloroform verbleibt allein der braun gefärbte, zur photometrischen Bestimmung geeignete $Cu(DDTC)_2$-Komplex. Der AgI-Niederschlag wird durch Filtration abgetrennt. Aus der KI-Lösung ist das Quecksilber bei pH $\geqslant 4$ wieder als Diäthyldithiocarbamidat extrahierbar. Je 1 mg Cu und Ag wurden nach diesem Schema von vielen anderen Ionen vollständig abgetrennt.

Zu II.2.3.: Aus der wässrigen Lösung ist das Selen nach dem Ansäuern auf 2 *N* und Oxydation mit Chlorat als Diäthyldithiocarbamidat extrahierbar. Bei der Abtrennung des Selens nach dieser Vorschrift gingen von 1000 μg nur 70 μg verloren.

Zu II.3.: Pb und In sind durch Bromokomplexextraktion mit Äther leicht voneinander trennbar[12]. Bei der Abtrennung von 0.5–10 mg In gingen $< 1.5\%$ des In bei der DÄDDTC-Extraktion und $< 1.5\%$ bei der Chlorokomplexreextraktion verloren.

Zu II.4.: Zur Abtrennung des Tl wird der salzsaure Reextrakt mit Wasser auf 6 *N* verdünnt und mit Isopropyläther ausgeschüttelt. Die Tl-Bestimmung führe man mit Dithizon[24] oder Komplexon in wässrigem Reextrakt durch. Je 1 mg Bi und Tl sind nach diesem Schema vollständig abgetrennt worden. Te wurde bisher nur qualitativ bestimmt.

Zu II.5.: Auf As wurde nur qualitativ geprüft.

Zu II.6.: Pd wurde zu $>90\%$ in der II.6. Untergruppe wiedergefunden.

Zu III.2.: Ni und Zn sind gleich der II.2. Untergruppe nach Demaskierung ihrer Cyanokomplexe mit Formalin erneut als Diäthyldithiocarbamidate extrahierbar. Zu ihrer Trennung kann die unterschiedliche Beständigkeit der DDTC-Komplexe gegen Salzsäure benutzt werden. Aus der Chloroformlösung ist Zn durch zweimaliges Schütteln mit 2 *N* HCl rasch und vollständig auswaschbar, im Gegensatz zum $Ni(DDTC)_2$-Komplex, der noch gegen konzentrierte Salzsäure Beständigkeit zeigt. Je 1000 μg beider Metallionen wurden diesem Trennungsgang unterworfen und in beiden Fällen >950 μg wiedergefunden. Vollständigkeit ist bei der Zn-Trennung nur dann zu erreichen, wenn aus der II.2.2. Untergruppe mitextrahierte Zn-Anteile durch 3 *N* Salzsäure zurückgewaschen werden. Die Verluste an Zn in der anderen Trennstufe sind gering.

Zu III.3.: Aus dieser Untergruppe wurde nur das Mn als Diäthyldithiocarbamidat abgetrennt; die Seltenen Erden und Scandium sind gemeinsam auf-

gearbeitet worden. Im Trennungsgang bildet das Mangan(II)-ion sowohl BPHA- als auch DDTC-Komplexe. Ihre unterschiedliche Beständigkeit gegen Salzsäure führt zur Verschleppung des Mn über die 3. und 4. Untergruppe. In Anwesenheit eines Reduktionsmittels, z. B. Ascorbinsäure oder Hydroxylamin wird die Bildung des säurebeständigen $Mn(DDTC)_3$ erschwert und die des säurezersetzlichen BPHA-Komplexes begünstigt; so dass Mn gemeinsam mit den Seltenen Erden reextrahiert werden kann. Vollständigkeit der Trennung ist jedoch nur dann erreichbar, wenn auch die 4. Untergruppe aufgearbeitet wird. Zur Durchführung der Mn-Trennung werden die salzsauren Auszüge der III. Hauptgruppe 0.01 *M* an Weinsäure gemacht und mit Ammoniak neutralisiert. Durch mehrmaliges Ausschütteln mit 0.05 *M* DÄDDTC wird Mn(II) von SE, Sc, Al und Cr getrennt; Vollständigkeit ist an der Farblosigkeit des Extraktes erkennbar.

Die Abtrennung aller Metallionen dieser Untergruppe gelang quantitativ. Die aufgetretenen Verluste in den einzelnen Trennstufen überschritten 0.5% nicht.

Zu III.4.: Die Trennung des Ga, Mn, Al und Cr wird in Abb. 7 veranschaulicht. Sie beruht auf der Extrahierbarkeit der Chlorokomplexe des Galliums mit Äther aus 6 *N* Salzsäure, des Mn-Diäthyldithiocarbamidates mit Chloroform aus neutraler Lösung und bei Al und Cr auf der unterschiedlichen Geschwindigkeit der BPHA-Chelatkomplexbildung.

Zu III.4.1.: Zur Ga-Abtrennung wird der 10 *N* salzsaure Reextrakt mit Wasser auf 5–6 *N* verdünnt und mit Äther mehrmals ausgeschüttelt. Aus dem Äther lässt sich das Gallium mit Wasser leicht zurückwaschen und quantitativ mit Komplexon gegen Xylenolorange titrieren. Die Ga-Bestimmung kann auch mit Rhodamin B photometrisch durchgeführt werden. Dazu macht man den 5–6 *N* salzsauren Reextrakt ~3%ig an Rhodamin B, schüttelt den violettfarbenen Ga-Komplex mit Benzol aus und misst die Extinktion bei 565 nm. Nach diesem Trennungsgang gelang es von 690 μg Ga > 620 μg von vielen anderen Kationen abzutrennen.

Zu III.4.2.: Zur Mn-Trennung wird die salzsaure Probelösung 0.01 *M* an Weinsäure gemacht, mit Ammoniak neutralisiert und mit 0.05 *M* DÄDDTC ausgeschüttelt, wie unter III.3. beschrieben.

Zu III.4.3.: Nach Abtrennung des Mn wird die wässrige Phase zweimal je 10 Minuten mit 0.1 *M* BPHA ausgeschüttelt. Aus den vereinigten Chloroformauszügen lässt sich das Al mit 10 *N* Salzsäure zurückwaschen.

Nach dieser Vorschrift konnten 10 mg Al nur begleitet von 3–4% Cr von allen anderen Ionen getrennt werden.

Zu III.4.4.: Aus der wässrigen Lösung ist Cr(III) gleich dem Al nach erneuter Reagenszugabe und 10 minutenlangem Kochen als BPHA-Komplex extrahierbar. Der gebildete Cr-Komplex zeigt Beständigkeit gegen schwach alkalische und saure Lösungen; mit 10 *N* Salzsäure wird er zerlegt.

Zu III.5.: Kobalt(II) wird in der III. Gruppe als DDTC-Komplex ausgeschüttelt. Aus der Chloroformlösung lässt sich das Kobalt nur nach Zerstörung des $Co(DDTC)_3$-Komplexes mit chlorathaltiger Salzsäure reextrahieren.

Verwendete Reagentien

Diäthylammoniumdiäthyldithiocarbamidat (DÄDDTC). Täglich frisch bereitete 0.05 *M* Lösung in Chloroform und 0.5 *M* in Alkohol bzw. in Azeton. Hergestellt wurde das Reagens aus 25 g Schwefelkohlenstoff und 50 g Diäthylamin in je 100 ml

Äther gelöst und unter Kühlen allmählich vereinigt. Das ausgefallene Reagens wird aus Essigester umkristallisiert und mit Äther gewaschen. Im Dunklen aufbewahrt ist es über Monate haltbar.

N-Benzoyl-N-phenylhydroxylamin (BPHA). 0.1 *M* und 0.3 *M* Lösung in Chloroform und 0.5 *M* Lösung in Alkohol bzw. Aceton. Hergestellt wurde das Reagens durch Benzoylierung von Phenylhydroxylamin. 300 g Phenylhydroxylamin wurden in 7 l heissem Wasser gelöst und bei 0° unter kräftigem Rühren in kleinen Anteilen mit 450 g Benzoylchlorid und 300 g $NaHCO_3$ versetzt. Zur Trennung von gleichzeitig gebildeten Dibenzoylderivat wird das Rohprodukt mit konzentriertem Ammoniak gelaugt und die erhaltene Lösung in −10° kalte 3 *N* Schwefelsäure getropft. Das wieder ausgefällte BPHA wird aus Essig, Toluol oder Dioxan umkristallisiert, *F* 122°.

Natriumdiäthyldithiocarbamidat. 10%ige wässrige Lösung.

Chloroform, p.A. Bei der Regeneration des Chloroforms ist der Gehalt an sulfidischem Schwefel durch Schütteln mit alkalischer H_2O_2-Lösung und Einwirkung von Brom zu beseitigen.

Äthyläther. Formalin, *ca.* 35%ig. *Weinsäure.* 10%ige wässrige Lösung. *Kationenaustauscherharz.* KPS. *Äthylendiamintetraessigsäure.* 0.1 *M*. *Kaliumcyanid.* 0.2 *M* wässrige Lösung. *Mineralsäuren* und *Laugen* verschiedener Normalität. *Pufferlösung.* pH 9, 0.1 *M* an NH_4Cl und 0.1 *M* an NH_4OH. *Natriumsulfid.* 0.1 *M*. *Kaliumchlorat.* p.A. *Fluoridlösung.* 0.5 *M* an H_2F_2 und 1 *M* an NaF. *Jodidlösung.* 1 *M* KI und 2.5 *N* an H_2SO_4. *Oxalsäurelösung.* 0.25 *M*.

ZUSAMMENFASSUNG

Es wird ein Bericht über einen einfachen, rasch durchführbaren Kationentrennungsgang gegeben. In diesem Trennungsgang finden *ca.* 60 Kationen Berücksichtigung. Viele Kationen sind im Mikro- und Milligrammbereich quantitativ trennbar. In Analogie zum klassischen Schwefelwasserstoff–Ammoniak-Trennungsgang werden die Kationen bei sinkender Azidität durch BPHA- und DÄDDTC-Extraktion in fünf Hauptgruppen getrennt. In der I. Hauptgruppe werden aus 2 *N* mineralsaurer Lösung die Übergangselemente der 4.–7. Gruppe des Periodischen Systems als BPHA-Komplexe, in der II. bei gleicher Säurekonzentration Kationen der Schwefelwasserstoffgruppe als Diäthyldithiocarbamidate, in der III. aus neutraler Lösung Kationen der Ammoniak- und Ammoniumsulfidgruppe mit BPHA und DÄDDTC und in der IV. aus 1 *M* ammoniakalischer Lösung die Erdalkalien als BPHA-Komplexe extrahiert. Zur weiteren Trennung dient die unterschiedliche Reextrahierbarkeit dieser im Chloroform gelösten Chelatkomplexe mit verschiedenen Reagenslösungen.

SUMMARY

A simple and rapid cation separation scheme has been developed, covering about 60 cations, many of them being quantitatively separable in the micro- and milligram ranges. By analogy with the classical hydrogen sulphide–ammonia separation process, the cations are divided with decreasing acidity by BPHA and DDDC extraction into five main groups. In group I the transition elements of groups 4 to 7 of the periodic system are extracted from 2 *N* mineral acidic solution, as BPHA

complexes; in group II, from the same acid concentration, cations of the hydrogen-sulphide group are extracted by DDDC; in group III, from neutral solution, cations of the ammonia and ammonium sulphide group are extracted by BPHA and DDDC; and in group IV, from 1 *N* ammoniacal solution are extracted the alkaline earths as BPHA complexes. For further separation, the differing reextractability of these chelate complexes dissolved in chloroform with solutions of reagents is utilised.

RÉSUMÉ

Un schéma de séparation simple et rapide est proposé, comprenant environ 60 métaux. Un grand nombre d'entre eux peuvent être séparés quantitativement (à l'échelle du micro- et du milligramme). Par analogie avec le procédé classique de séparation à l'hydrogène sulfuré–ammoniaque, les cations sont divisés en cinq groupes principaux par extraction à l'aide de BPHA et de DDDC, avec acidité décroissante. Groupe I: les éléments de transition des groupes 4 à 7 du système périodique sont extraits, en milieu acide minéral 2 *N*, comme complexes BPHA; Groupe II: les cations du groupe hydrogène sulfuré, extraits dans le même milieu comme diéthyldithiocarbamates; Groupe III: les cations du groupe ammoniaque–sulfure d'ammonium extraits en milieu neutre par BPHA et DDDC; Groupe IV: les alcalino-terreux en milieu ammoniacal 1 *N*, extraits comme complexes BPHA. Pour des séparations ultérieures, on utilise les réextractabilités différentes de ces chélates dissous dans le chloroforme, avec divers réactifs.

LITERATUR

1 W. DOLL UND H. SPECKER, *Z. Anal. Chem.*, 161 (1958) 354.
2 G. IWANTSCHEFF, *Das Dithizon und seine Anwendung in der Mikro- und Spurenanalyse*, Weinheim, 1958.
3 P. W. WEST UND A. K. MUKHERJI, *Anal. Chem.*, 31 (1959) 947.
4 G. TÖLG, *Z. Anal. Chem.*, 190 (1962) 161.
5 R. A. CHALMERS UND D. M. DICK, *Anal. Chim. Acta*, 31 (1964) 520; 32 (1965) 117.
6 P. C. VAN ERKELENS, *Anal. Chim. Acta*, 24 (1961) 526; 25 (1961) 129.
7 G. H. FAYE UND W. R. INMAN, *Anal. Chem.*, 35 (1963) 985.
8 N. M. KUZMAN, V. P. BELYAEV UND V. P. KALINACHENKO, *Zavodsk. Lab.*, 29 (1963) 691.
9 S. J. LYLE UND A. D. SHENDRIKAR, *Anal. Chim. Acta*, 32 (1965) 575; 36 (1966) 286.
10 G. B. MARSHALL UND T. S. WEST, *Talanta*, 14 (1967) 823.
11 S. MEYER UND O. G. KOCH, *Mikrochim. Acta*, (1958) 744; (1959) 720.
12 H. FÖRSTER, *Dissertation*, TU Dresden, Fakultät für Mathematik und Naturwissenschaften, 1964 und *Proc. Conf. Appl. Phys.-Chem. Methods Chem. Anal., Budapest, 1966*, 2.416–25.
13 K. KASIURA, *Chem. Anal. (Warsaw)*, 11 (1966) 141.
14 O. G. KOCH, *Mikrochim. Acta*, (1958) 92, 151, 347, 402.
15 C. L. LUKE, *Anal. Chim. Acta*, 39 (1967) 447.
16 Z. MARCZENKO UND K. KASIURA, *Chem. Anal. (Warsaw)*, 10 (1965) 449.
17 J. MINCZEWSKI, J. CHWASTOWSKA UND Z. MARCZENKO, *Chem. Anal. (Warsaw)*, 6 (1961) 501 und 509.
18 G. H. MORRISON UND J. F. COSGROVE, *Symposium on Radiochemical Analysis, 136th Meeting ACS, September 1959*.
19 I. P. ALIMARIN, F. P. SUDAKOV UND B. G. GOLOVKIN, *Usp. khim.*, 31 (1962) 8, 989.
20 H. BODE UND F. NEUMANN, *Z. Anal. Chem.*, 169 (1959) 410; 172 (1960) 1.
21 H. BODE UND K. TUSCHE, *Z. Anal. Chem.*, (1957) 414.
22 H. BODE, *Z. Anal. Chem.*, 142 (1954) 414; 143 (1954) 182; 144 (1955), 165, 90.
23 J. CHWASTOWSKA UND J. MINCZEWSKI, *Chem. Anal. (Warsaw)*, 9 (1964) 791.
24 H. FREISER, *Anal. Chem.*, 38 (1966) 131 R; 40 (1968) 522 R.
25 O. G. KOCH UND G. A. KOCH-DEDIC, *Handbuch der Spurenanalyse*, Springer-Verlag, 1964.
26 A. E. MARTELL UND M. CALVIN, *Die Chemie der Metallchelatverbindungen*, Weinheim, 1958.

27 G. H. MORRISON UND H. FREISER, *Anal. Chem.*, 30 (1958), 632; 32 (1960) 37 R; 34 (1962) 64 R; 36 (1964) 93 R.
28 R. G. MONK, *Anal. Chim. Acta*, 28 (1963) 217.
29 G. H. MORRISON UND H. FREISER, *Solvent Extraction in Analytical Chemistry*, Wiley, New York, 1957.
30 V. SEDIVEC UND J. FLECK, *Chem. Listy*, 52 (1958) 545.
31 J. STARÝ UND K. KRATZER, *Anal. Chim. Acta*, 40 (1968) 93.
32 J. STARÝ, *The Solvent Extraction of Metal Chelates*, Pergamon Press, 1964.
33 J. STARÝ, *Anal. Chim. Acta*, 28 (1963) 132, 149.
34 K. DORFNER, *Ionenaustauschchromatographie*, Akademieverlag, Berlin, 1963.
35 G. GEBHARDT, *Z. Phys. Chem.*, 229 (1965) 225.
36 J. INCZÉDY, *Analytische Anwendung von Ionenaustauschern*, Akadémiai Kiadó, Budapest, 1964.

Analytica Chimica Acta
Elsevier Publishing Company, Amsterdam
Printed in The Netherlands

SHORT COMMUNICATIONS

Colorimetric determination of organic peroxides

The use of benzoyl leuco methylene blue as a reagent for peroxides provides a convenient method of analysis. Benzoyl leuco methylene blue in a benzene/trichloroacetic acid solution reacts with peroxides and hydroperoxides with the aid of zirconium naphthenate to form the characteristic methylene blue color. EISS AND GIESECKE[1] found the benzoyl leuco dye peroxide reaction to be fairly slow. They attempted several heating variations to accelerate the color development but the results were not quantitative. They report that all work should be done at $24 \pm 1°$, since at 30° the results become very erratic. When the method was studied in this laboratory, even slower reaction rates were observed. In the work reported here, the reaction is carried out smoothly at an elevated temperature to yield a rapid and quantitative analysis. The reaction time for benzoyl peroxide has been reduced from 30 h to 35 min.

Reagents

Zirconium naphthenate, 0.24%. Dilute 1 ml of commercial (6%) zirconium naphthenate (Advance Division, Carlisle Chemical Works, New Brunswick, New Jersey) to 25 ml with benzene.

Benzoyl leuco methylene blue (National Cash Register Co., Dayton, Ohio). Dissolve 0.05 g in 100 ml of benzene. Store in a dark bottle.

Procedure

To obtain a calibration curve, or for sample analysis, pipet a suitable aliquot of the test solution into a 25-ml volumetric flask which contains 10 ml of 1.0% trichloroacetic acid in benzene. Add 0.5 ml of 0.24% zirconium naphthenate and 1 ml of leuco dye. Set the flask on a steam bath and allow 35 min for color development. The flask should be protected from direct light. Remove the flask, cool and dilute to volume with benzene. Measure the absorbance at 662 nm. On occasion, a slight cloudiness develops in the reaction flask. This is dissolved through the addition of a small amount of ethanol (less than 1% by volume).

Results and discussion

Observations in this laboratory were not consistent with those found by EISS AND GIESECKE. Apparently, subsequent lots of zirconium naphthenate are different from the initial lot, and give a much slower reaction time; it has been suggested that an impurity may have been the active principle in the original lot[2]. Since even under optimum catalytic conditions, benzoyl peroxide requires a 30-h reaction period, a slower time would detract from the convenience and practicality of the analysis. Heating allows the reaction time for *tert.*-butyl hydroperoxide, cumene hydroperoxide, lauroyl peroxide and benzoyl peroxide to be reduced to 35 min. For benzoyl peroxide, the same absorbance value was found after 35 min with heat as was reported by EISS AND GIESECKE for a 30-h reaction without heat.

Various catalysts were evaluated in the original paper[1]. Although a few catalysts did increase the rate of peroxide decomposition, several caused an excessive reagent blank. In the method reported here, although the reaction rate is markedly increased, the blank is not; in fact the blank averages about one-half that originally found[1]. Although the zirconium naphthenate does not function as a suitable catalyst at 24°, it does serve some purpose at the elevated temperature. With zirconium naphthenate, the absorption maximum occurs at 662 nm while without it, the maximum lies at 650 nm.

The suggested heating step does not seem to be critical in terms of specific temperatures and time limits (minimum reaction time is 35 min). At reaction times of less than 25 min, the color development is incomplete. Complete color development after 35 min was observed for the peroxides analyzed. A solution of lauroyl peroxide possessed the same absorbance after heating on the steam bath for 1.5 h and 35 min.

3M Company Central Research,
Box 3221,
St. Paul,
Minn. 55101 (U.S.A.)

JON BELISLE

1 M. I. EISS AND P. GIESECKE, *Anal. Chem.*, 31 (1959) 1558.
2 P. GIESECKE, American Cyanamid Co., Stamford, Conn., personal communication, 1968.

(Received January 22nd, 1969)

Anal. Chim. Acta, 45 (1969) 525–526

A rapid method for calibration of micropipets

LOWRY *et al.*[1] have described a method for the calibration of micropipets. Aliquots of a highly colored solution are drawn by micropipets and the optical absorbance is determined after appropriate dilution. Standards for comparison are prepared similarly employing gravimetrically calibrated pipets. The method, although precise, is time-consuming when many pipets are to be calibrated and does not lend itself to automation. By using radioactive solutions it is possible to eliminate the need for tedious sample dilutions, save time, and take advantage of automated radioactivity counting equipment, without loss of precision.

To compare the two methods, a series of Lang-Levy constriction pipets, constructed as described by BESSEY *et al.*[2], was calibrated colorimetrically. A pipetful of 0.5% (w/v) *p*-nitrophenol in 0.1 *N* sodium hydroxide was delivered to an exactly measured volume of 0.1 *N* sodium hydroxide of about 1,000 times the volume of the pipet. The optical absorbance of this solution at 400 nm was compared to that of standard solutions prepared in a similar manner with larger pipets that had been calibrated gravimetrically. The same pipets were recalibrated by delivering a pipetful of $5.5 \cdot 10^6$ counts/min/ml $Na_2H^{32}PO_4$ (New England Nuclear Corp., Boston, Mass.) to 10 ml of scintillation fluid[3] contained in standard vials. Radioactivity was estimated with a Model 3375 Tri-Carb liquid scintillation spectrometer (Packard Instrument

Co., Downers Grove, Ill.). No quenching was detectable. All vials were counted for 1 min and counts were compared to standards prepared with pipets calibrated gravimetrically. All calibrations, both colorimetric and radioisotopic, were done in triplicate.

TABLE I

COMPARISON OF PIPET VOLUMES AS DETERMINED BY CALIBRATION WITH ^{32}P AND *p*-NITROPHENOL

Volume (µl)		*Ratio* ^{32}P*:*
^{32}P	p-*Nitrophenol*	p-*nitrophenol*
10.86 ± 0.054[a]	10.90 ± 0.045	0.996
8.45 ± 0.041	8.34 ± 0.052	1.013
6.30 ± 0.029	6.54 ± 0.029	0.963
4.94 ± 0.020	4.79 ± 0.024	1.031
2.65 ± 0.013	2.68 ± 0.027	0.989
2.25 ± 0.010	2.39 ± 0.003	0.941
2.09 ± 0.009	2.05 ± 0.049	1.020
1.88 ± 0.013	1.87 ± 0.018	1.005
1.33 ± 0.007	1.37 ± 0.010	0.971
0.575 ± 0.007	0.595 ± 0.002	0.966
	Average	0.990

[a] Standard error of the mean.

Table I compares the results of calibrations of 10 pipets by both methods. When subjected to the "t" test there is no significant difference between the two methods.

Since the volume of scintillation fluid is not critical, within practical limits, for calibration with the radioisotopic method, automatic dispensing devices can be used for this step of the procedure. This, in conjunction with automatic counting, results in a great saving of time. The calibration of large numbers of pipets by the radioisotopic method requires about one-tenth the amount of operator time as does the colorimetric method.

Other radioisotopes should be as suitable as ^{32}P. When larger pipets are being calibrated, however, the use of an emitter of energetic β-particles such as ^{32}P obviates the need for quench correction of the observed counts.

National Institute of Dental Research,
National Institutes of Health,
Bethesda, Md. 20014 (U.S.A.)

J. F. GOGGINS
J. M. TANZER

1 O. H. LOWRY, N. R. ROBERTS, K. Y. LEINER, M. WU AND A. L. FARR, *J. Biol. Chem.*, 207 (1954) 1.
2 O. A. BESSEY, O. H. LOWRY AND M. J. BROCK, *J. Biol. Chem.*, 164 (1946) 321.
3 G. A. BRAY, *Anal. Biochem.*, 1 (1960) 279.

(Received December 28th, 1968)

Determination of plutonium by controlled-current coulometry*

One of the most precise methods for determining plutonium—that of SEILS *et al.*[1]—involves oxidation of plutonium to the hexavalent state with silver(II) oxide, destruction of excess oxidant by heating, and direct titration of the plutonium(VI) with standard iron(II) solution to an amperometric end-point. This method has been evaluated[2] and compared with other precise titrimetric methods for assaying plutonium[3] and in general found to be extremely precise ($\sigma \cong 0.06\%$) and satisfactory. Other workers have attempted to simplify the procedure. For example, an indirect titration has been studied[4] in which an excess of iron(II) was added and then back-titrated with cerium(IV) in an automatic titrator; this indirect approach avoids the nuisances caused by sluggishness of the Pu(VI)–Fe(II) reaction. Other workers[5,6] have modified the indirect procedure by using different electrode systems and by adding sulfamic acid to the oxidized sample to eliminate the heating step; this not only destroys excess silver(II) without reducing plutonium(VI), but also makes possible titrations of samples that contain moderate amounts of nitric acid. However, the convenience of sulfamic acid was apparently gained at the expense of some loss in precision, because relative standard deviations of 0.2–0.5% were reported. In the present work, similar results were obtained when the indirect titration procedures with cerium(IV)[5] or dichromate[6] as the titrant were evaluated. The major inconvenience in these procedures is that it is necessary to prepare and store the iron(II) solution with care and to standardize it frequently. It seemed that this inconvenience could be easily avoided by generating the reagents coulometrically from the dual-intermediates, Fe(III) and Ce(III). The results are reported in the present communication.

Experimental

Apparatus. An ORNL Model Q-2564 Controlled-Potential Coulometric Titrator[7], operated in the controlled-current mode, was used. This instrument provides a direct measurement (by analogic integration) of the total charge required during an electrolysis, and hence does not require a well regulated, constant, accurately known electrolysis current or an electrolysis timer. Indeed, the use of analog integration for controlled-current coulometric titrimetry allows one to adjust the electrolysis current during the titration according to the demands of the chemical system. In the present procedure, for example, the electrolysis current is reduced to a small value near the end-point to insure that the chemical and indicator electrode systems are near equilibrium. It is also convenient to display the integrator readout voltage along the X-axis of Moseley Model 2D-2A X-Y recorder, and to display the potential of the indicator electrode system along the Y-axis, so as to record the titration curve. It must be emphasized, however, that the procedure reported here could easily be performed with other types of controlled-potential or controlled-current coulometric instruments.

A titration vessel similar to that described previously[7] was used. The working electrode was a 45-mesh platinum gauze (2 × 6 cm); the auxiliary electrode was a small platinum wire isolated from the solution by a porous Vycor tube containing

* Research sponsored by the U.S. Atomic Energy Commission under contract with Union Carbide Corporation.

1 *N* sulfuric acid. Indicator electrodes were 16-gauge gold wires sealed in glass tubing with epoxy cement. The electrodes were polarized with a current of 1.3 μA by a 1.35-V mercury battery connected in series with a 1 megohm resistor. The potential of the polarized electrodes was measured with a Beckman Research Model pH meter whose output was connected to the Y-axis of the recorder.

Reagents. All reagents used in this work were analytical reagent grade or equivalent. Standard plutonium solutions were prepared from the pure (< 100 p.p.m. total impurities) metal in calibrated glassware.

Procedure. Place a sample aliquot containing 1–10 mg of Pu in the titration vessel, and adjust the solution to 0.5 *N* in sulfuric acid with a volume of about 5 ml. Add a few milligrams of solid silver(II) oxide and stir until the brown color of the dispersed oxide persists. Continue stirring for 5 min to ensure that the oxidation to Pu(VI) is complete. Add three drops of 1 *M* sulfamic acid to destroy excess of silver(II). At this time, rinse the inside walls of the vessel with a little water to wash any adhering silver(II) oxide into the solution. Add 5 ml of a solution that is 0.3 *M* in iron(III) ammonium sulfate, 0.05 *M* in cerium(III) nitrate, and 3 *M* in sulfuric acid. The solution is now ready for titration.

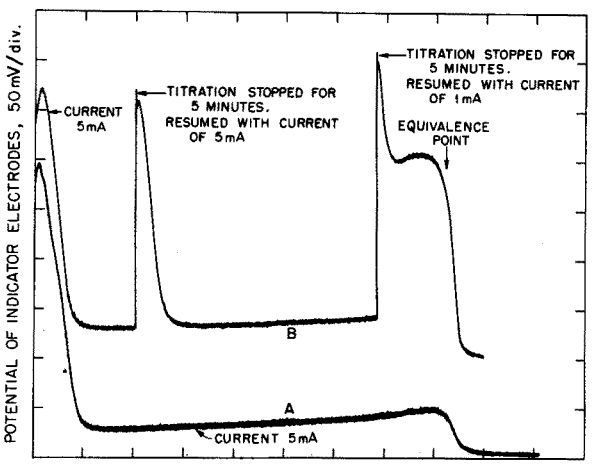

Fig. 1. Coulometric titration curves for titration of Pu(VI) with Fe(II).

Mount the vessel to the electrode assemblage and sparge with pure argon for 5 min to remove oxygen. Start the stirrer, zero the integrator, and begin coulometric reduction with a current of *ca.* 5 mA. Immediately after starting the electrolysis, the potential of the indicator electrodes decreases to 10–100 mV and then slowly increases as Pu(VI) is reduced (Curve A, Fig. 1). The presence of excess iron(II) is signalled by a second moderately abrupt decrease in potential. End the reduction electrolysis when the potential of the indicator electrodes decreases to 20 mV, and obtain the voltage of the integrator to four significant figures with a Rubicon potentiometer. This voltage corresponds to the amount of iron(II) generated. Then re-zero the integrator and titrate excess iron(II) with cerium(IV) generated electrolytically with an oxidizing current of about 100 μA. The potential of the indicator electrode system is observed as a function of the integrated current, which is displayed on a sensitive range of the

recorder, during this electrolysis. In the end-point region, the potential increases 300–400 mV and then decreases abruptly upon generation of excess cerium(IV) (Curve C, Fig. 2). Take the end-point as the maximum in the back-titration curve. Compute the results by subtracting the readout voltage corresponding to back-titration from the potentiometer readout corresponding to reduction, and converting the difference voltage to a weight basis by means of the electrical calibration factor of the instrument and Faraday's Law, assuming a two-electron reaction.

Results and discussion

The procedure for chemical oxidation of plutonium to Pu(VI) is essentially the same as that described by DRUMMOND AND GRANT[6], except that dilute sulfuric acid was preferred to nitric acid as the medium. No detrimental effect was observed with this alteration.

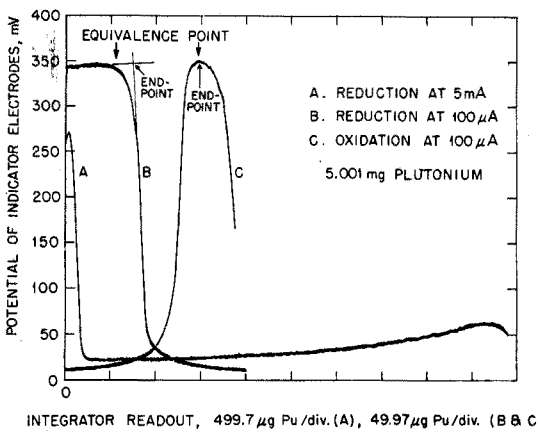

Fig. 2. Coulometric titration curves for titration of A and B: Pu(VI) with Fe(II); and C: Fe(II) with Ce(IV).

The change in indicator electrode potential during electrolysis warrants some discussion. Curve A in Fig. 1 presents a titration curve for complete reduction of Pu(VI) with Fe(II) generated electrolytically with a 5 mA current. If the electrolysis is terminated before complete reduction of Pu(VI) has been accomplished, the potential of the indicator electrode system increases several hundred millivolts in a few minutes (Curve B, Fig. 1). Moreover, a larger indicator electrode potential is observed with 1-mA electrolysis current than with 5-mA electrolysis current (*cf.* the later portion of Curve B, Fig. 1). These observations may be explained if one assumes that Pu(VI) is rapidly reduced to Pu(V) by either direct reduction at the electrode surface or by chemical reaction with electrogenerated Fe(II) and that the Pu(V) undergoes a slower disproportionation to yield Pu(VI) and Pu(IV). This is reasonable in view of the known reversibility of the Pu(VI)–Pu(V) couple and the irreversibility of the Pu(V)–Pu(IV) couple[8]. At the beginning of the titration, the potential of the indicator electrode system is determined by the reduction of Pu(VI) to Pu(V) at the cathode and the oxidation of Ce(III) to Ce(IV) at the anode. As Pu(VI) is reduced to Pu(V), the potential of the indicator electrode system decreases due to the accumula-

tion of Pu(V) in the solution; Pu(V) becomes the potential-controlling species at the anodic indicator electrode because it is oxidized at a lower potential than is Ce(III). Now, if the electrolysis is stopped for a few minutes, the Pu(V) disproportionates to yield a solution of Pu(VI) and Pu(IV), and again the Ce(III)–Ce(IV) couple determines the potential of the anodic indicator electrode. The electrode potential ultimately attains its initial value or slightly more. Upon resumption of the electrolysis with a smaller current (later portion of Curve B, Fig. 1), larger indicator electrode potentials are observed because less Pu(V) accumulates in the solution at the lower current level. The behavior of dual polarized electrodes during titrations of reversible and irreversible couples, and the factors governing that behavior have been discussed in detail[9].

Reduction curves are not exactly reproducible from one titration to another; variations in acid concentration, temperature, and plutonium concentration all affect the disproportionation rate of Pu(V)[10] and hence cause minor changes in the shape of the titration curve. Nevertheless, the approximate end-point for complete reduction is signaled by a decrease in the potential of the indicator electrodes, and the electrolysis may be terminated in the vicinity of the end-point. Attempts were made to decrease the reduction current immediately before the equivalence point, and to finish the titration with a slow rate of generation of ferrous to allow the chemical system to approach equilibrium. Curve B in Fig. 2 indicates the type of potential change that occurs in the end-point region at a current level of 100 μA. Even though the potential change is very sharp and the system appears to be at equilibrium near the end-point, the extrapolated end-point (shown on the figure) does not correspond to the equivalence point. This direct titration was found to give precise ($\sigma = 0.14\%$ at the 5 mg level, $n = 6$) but inaccurate (bias $= +0.7\%$) results when performed as described above and when the end-point indicated on Curve B of Fig. 2 was used. Accordingly, the indirect titration procedure given in the preceding section is preferable.

TABLE I

TYPICAL RESULTS FOR ANALYSIS OF STANDARD PLUTONIUM SOLUTIONS BY INDIRECT TITRATION PROCEDURE

Number of determinations	*Pu added (mg)*	*Pu found (mg)*	*Error (%)*	*Relative standard deviation*
7	5.001	5.010	+ 0.2	0.1
6	1.000	0.999	− 0.1	0.5

The accuracy and precision of the indirect titration procedure were estimated by replicate analysis of standard plutonium solutions. Typical results are shown in Table I; these results are similar to those reported in references 5 and 6, but are less precise than those reported in references 1–4. The results are based upon volumetric aliquots; weighed aliquots and larger quantities of plutonium would improve the precision and accuracy. However, this procedure was developed to supplement the controlled-potential coulometric procedures for determining plutonium[11], which are used routinely with 3–5 mg quantities of plutonium, and the present procedure is ideally suited for this purpose. When compared with the controlled-potential coulo-

metric method, the present method gives similar results at the 3–5 mg level, uses much of the same instrumentation, can be faster for large numbers of samples, is insensitive to relatively large amounts of iron or sulfate in the sample, and, finally, can be used for samples that are contaminated by traces of organic materials. The last two points can be particularly troublesome in the controlled-potential coulometric method.

Analytical Methodology Group,
Analytical Chemistry Division,
Oak Ridge National Laboratory,
Oak Ridge, Tenn. 37830
(U.S.A.)

J. R. STOKELY, JR.
W. D. SHULTS

1 C. A. SEILS, JR., R. J. MEYER AND R. P. LARSEN, *Anal. Chem.*, 35 (1963) 1673.
2 K. S. BERGSTRESSER AND G. R. WATERBURY, *USAEC Rept. LA-3091*, 1964.
3 G. R. WATERBURY AND C. F. METZ, *USAEC Rept. LA-3141*, Jan. 1965.
4 G. W. C. MILNER, A. J. WOOD AND G. E. CASSIE, *UKAEA Rept. AERE-R 4975*, Aug. 1965.
5 J. CORPEL AND F. REGNAUD, *Anal. Chim. Acta*, 35 (1966) 508.
6 J. L. DRUMMOND AND R. A. GRANT, *Talanta*, 13 (1966) 477.
7 H. C. JONES, W. D. SHULTS AND J. M. DALE, *Anal. Chem.*, 37 (1965) 680.
8 J. J. KATZ AND G. T. SEABORG, *The Chemistry of the Actinide Elements*, Methuen, London, 1957, p. 326.
9 C. N. REILLEY, W. D. COOKE AND N. H. FURMON, *Anal. Chem.*, 23 (1951) 1223.
10 J. J. KATZ AND G. T. SEABORG, *The Chemistry of the Actinide Elements*, Methuen, London, 1957, p. 321–325.
11 W. D. SHULTS, *Talanta*, 10 (1963) 833.

(Received December 9th, 1968)

Anal. Chim. Acta, 45 (1969) 528–532

Separation of the acidic sulfides of arsenic, antimony and tin from mixtures with basic sulfides by means of alkaline monochloroacetate

In order to separate the sulfides precipitated from acidic solution (H_2S group) into the sub-groups of basic and acidic sulfides, the mixture of sulfides is treated with ammonium polysulfide or with caustic alkali. In the first case, as shown by arsenic trisulfide, oxygen-free sulfo-salts are formed exclusively:

$$\underline{As_2S_3} + 2S_2^{2-} + S^{2-} \rightleftharpoons 2AsS_4^{3-}$$

Similar reactions occur with the sulfides of antimony and tin.

If the mixture of basic and acidic sulfides is treated with caustic alkali, a mixture of water-soluble oxygen-containing sulfo-salts results, according to the global reaction:

$$\underline{As_2S_3} + 6OH^- \rightleftharpoons AsOS_2^{3-} + AsO_2S^{3-}$$

In both cases, by controlled acidification of the solution, the sulfides of arsenic, antimony and tin are reprecipitated, and after filtration, the precipitate is analyzed by the usual processes.

An attempt was made to develop a new separation of basic and acidic sulfides by a process that maintains unaltered the basic sulfides and converts the acidic

sulfides to the respective soluble oxygen compounds, through digestion of the mixture of sulfides with alkali zincate or plumbite, whereby the following representative reaction could be expected:

$$\underline{As_2S_3} + 3Zn^{2+} + 12OH^- \rightleftharpoons 2AsO_3^{3-} + 3\underline{ZnS} + 6H_2O$$

The results were not satisfactory, because the low concentration of zinc(II) ions present in the zincate solution does not permit a complete transformation. If a plumbite solution is employed, the reaction is complete, but the residual lead in the digested sulfides and in the filtrate is inconvenient.

A sure separation was attained through the finding that the sulfides of arsenic, antimony and tin are quantitatively converted to the respective oxygen compounds through warming with an alkaline solution of alkali metal monochloroacetate. This desulfonation effect, which has recently been applied[1] for the total elimination of sulfide ions, is due to the formation of thiodiglycollate[2], according to:

$$S^{2-} + 2CH_2ClCO_2^- \rightarrow S(CH_2CO_2^-)_2 + 2Cl^-$$

If As_2S_3 reacts with alkaline monochloroacetate, the global reaction is:

$$\underline{As_2S_3} + 12OH^- + 6CH_2ClCO_2^- \rightarrow 2AsO_3^{3-} + 3S(CH_2CO_2^-)_2 + 6Cl^- + 6H_2O$$

Similar reactions occur with antimony and tin sulfides. In contrast, the basic sulfides remain unaltered if treated with caustic alkaline monochloroacetate. This different behaviour permits a sure separation of acidic and basic sulfides.

In this connection, it may be noted that MoS_3 and WS_3, which belong to the sub-group of acidic sulfides, are likewise dissolved by alkaline monochloroacetate solution whereby MoO_4^{2-} and WO_4^{2-} are produced.

If the alkaline solution of alkali metal monochloroacetate is employed as solubilizing and desulfurizing agent, the behaviour of mercury(II) sulfide deserves attention. This sulfide, although insoluble in caustic alkali, becomes soluble to a greater or smaller extent, if the acidic arsenic, antimony and tin sulfides are dissolved in caustic alkali[3]. This induced solubility of mercury(II) sulfide is due to the formation of HgS_2^{2-}. In the presence of monochloroacetate, HgS_2^{2-} is destroyed and HgS is regenerated:

$$HgS_2^{2-} + 2CH_2ClCO_2^- \rightarrow \underline{HgS} + S(CH_2CO_2^-)_2 + 2Cl^-$$

Accordingly, the presence of mercury(II) sulfide does not interfere in the complete separation of basic and acidic sulfides by means of caustic alkaline monochloroacetate.

When a mixture of sulfides is warmed with caustic alkaline monochloroacetate and then filtered, a solution is obtained which remains unaltered by acidification (no sulfide or sulfur is precipitated, nor hydrogen sulfide released) and therefore may be used for the direct identification of arsenic, antimony and tin by appropriate tests.

In order to identify arsenic and antimony, reduction with metallic aluminum to arsine and elemental antimony is recommended. Both reductions occur in the alkaline solution. Tin can be detected after reduction to tin(II), by means of metallic aluminum in acidified solution, followed by the familiar redox reaction with mercury-(II) chloride whereby calomel is formed.

Reagent

(*a*) 6 *M* potassium hydroxide solution,

(*b*) 2 *M* monochloroacetic acid solution.

Mix equal volumes of each reagent for use. (The solution is 3 *M* in KOH and 1 *M* in $CH_2ClCOOK$.)

Procedure

Transfer the hydrogen sulfide group precipitate obtained in the usual way, to a casserole, add 10–20 ml of the alkaline solution of potassium monochloroacetate and heat to 60–80° for 3–5 min, constantly stirring and breaking up any residue. Filter the mixture and wash the residue with 3 ml of the reagent diluted with 7 ml of water.

For the identification of arsenic, antimony and tin, an easy and rapid process is to add to the filtrate, contained in a small test tube, a piece of aluminum sheet. Place over the mouth of the tube a piece of filter paper moistened with 1–2 drops of 0.1 *M* silver nitrate solution. Warm the test tube gently to boiling. A grey to black precipitate of elemental silver on the filter paper confirms the presence of arsenic. A black deposit or precipitate of metallic antimony confirms the presence of antimony. In order to detect tin, acidify the filtrate with excess of 6 *M* hydrochloric acid, followed by addition of another piece of aluminum sheet. Warm the mixture gently until the aluminum has dissolved completely. Filter immediately into a test tube containing 1 ml of 3% mercury(II) chloride solution. A white or grey precipitate indicates tin.

The author is indebted to Professor FRITZ FEIGL for his many helpful suggestions.

Escola de Química,
Universidade Federal,
Rio de Janeiro (Brasil)

A. CALDAS

1 F. FEIGL, A. CALDAS AND E. LIBERGOTT, paper presented to *J. Indian Chem. Soc.*, for publication.
2 P. KLASON AND T. CARLSON, *Ber.*, 39 (1906) 733.
3 J. WALKER, *J. Chem. Soc. (London)*, 83 (1903) 184.

(Received January 12th, 1969)

Anal. Chim. Acta, 45 (1969) 532–534

Effect of substituents on dissociation constants of picramine reagents containing the *o,o'*-dihydroxyazo group

Derivatives of 2,7-bis-(azobenzene)-chromotropic acid, with picraminic acid as one azo-coupling component, have been suggested as colorimetric reagents for niobium, molybdenum, vanadium and some other elements[1–3]. The reaction with niobium and conditions for its spectrophotometric determination have been investigated in detail[3]. Reagents of this group are generally called "picramines" and are characterized by the *o,o'*-dihydroxyazo functional group.

The dissociation constants of the reagent and their ionic forms in media of different hydrogen ion concentrations have not previously been studied in detail. In earlier work[4], the protonation of these reagents together with some other mono- and

bis-azo derivatives of chromotropic acid, was investigated. The effects of substituents on protonation constants and molar absorptivities of the protonated form of the reagent were discussed.

It has already been noticed that dissociation of the last hydroxy group of the naphthalene nucleus of these reagents induces a hypsochromic effect in the absorption spectrum[5]. Such a spectrum is similar to the spectra of complexes of these reagents with metals, if the metal is bound over the peri-dihydroxy group of the naphthalene nucleus. It was therefore considered of interest to determine the dissociation constants of the second hydroxy group of the naphthalene ring, the effect of substituents on its value, and the dependence of the molar absorptivity of a completely ionized reagent on the corresponding dissociation constant.

Derivatives of 2,7-bis-(azobenzene)-chromotropic acid, in which one azo component is picraminic acid and the other is azobenzene with substituents in the benzene ring (I),

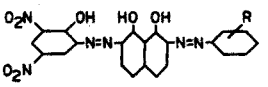

(I)

were investigated. The reagents, with the appropriate substituents, are listed in Table I.

Absorption spectra of reagents at different hydrogen ion concentrations

The absorption spectra of the investigated reagents are similar. In acidic medium they show a broad absorption band with a peak at about 500 nm. Decrease in the acidity of the medium above pH 1 leads to gradual dissociation of the reagent and the spectrum shifts towards longer wavelengths. Two peaks appear between 620 and 725 nm (Table I). This form of spectrum is found up to about pH 8 and then with increasing pH values, the absorption band shifts toward shorter wavelengths and has only one characteristic peak at about 620 nm. Figure 1 shows the absorption

TABLE I

CHARACTERISTICS OF ABSORPTION SPECTRA OF PICRAMINIC REAGENTS

Reagent	*R*[a]	*Medium*							
		pH > 8		*pH* 1–8		*pH* < 1		$H_0 < -1$	
		λ_{max}	$\varepsilon \cdot 10^{-4}$	λ_{max}	$\varepsilon \cdot 10^{-4}$	λ_{max}	$\varepsilon \cdot 10^{-4}$	λ_{max}	$\varepsilon \cdot 10^{-4}$
Picramine arsenazo	*o*-AsO_3H_2			595 620		540		680	
Picramine S	*o*-OH, *m,m'*-di-NO_2	620	3.6	665 725	4.2 4.3	550	3.8	670	5.4
Picramine M	*m*-SO_3H	590	4.4	620 680	5.9 3.9	550	5.6	650	8.4
Picramine K	*o*-COOH	620	3.9	635 685	4.3 3.0	550	3.9	655	6.6

[a] Substituent in I.

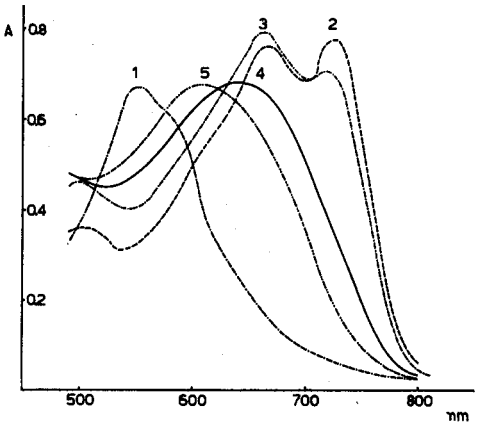

Fig. 1. Absorption spectra of picramine S at various hydrogen ion concentrations. (1) pH 1.22; (2) pH 3.98; (3) pH 9.02; (4) pH 10.75; (5) pH 12.48.

spectra for picramine S at various pH values, while Table I shows the molar absorptivities of particular ion species of the reagents. Data for the protonated form of the reagents[4] are also given in Table I.

Picramine arsenazo was not investigated in detail. The purity of the reagent could not be determined with sufficient accuracy by standard methods[1], and in alkaline solutions the reagent decomposed very quickly, its blue colour turning to pale rose.

Determination of dissociation constants

The ratio of the two forms of the reagents at different pH values was determined spectrophotometrically. The dissociation constant was determined from the expression:

$$pK = \log \frac{A - A_m}{A_s - A} + a\ pH$$

where A is the absorbancy of the solution at given pH; A_m the absorbancy of the solution when the total amount of reagent is in the ionized form RH_{m-n}; A_s the absorbancy of the solution when the total amount of reagent is in the form RH_n; and a is the number of protons released by the reagent on conversion from RH_n to RH_{m-n}.

Changes in the absorption spectra at various pH values were followed. The absorbancy at one or more characteristic wavelengths was measured as a function of the pH value. The pH values were adjusted with known buffer systems, and checked with a pH meter. Acetate, phosphate and glycine buffers were used for the pH ranges 1–5.2, 5.3–8.0, and 8.5–12.7, respectively.

The dissociation constant determined on transition from the acidic to the weakly acidic region is denoted as K_{n-1}, while on transition to the alkaline region, with a hypsochromic shift of the spectrum, it is denoted as K_n. Experimental results are given in Table II, which also contains values for the protonation constant (log K) from previous work[4].

TABLE II

DISSOCIATION AND PROTONATION CONSTANTS OF PICRAMINIC REAGENTS[a]

Reagent	pK_{n-1}[b]	pK_n[c]	*log K*
Picramine arsenazo	2.02	12	−4.51
Picramine S	2.55	10.2	−2.67
Picramine M	2.19	8.9	−1.62
Picramine K	2.79	8.8	−1.36

[a] $a = 1.0 \pm 0.2$.
[b] $K_{n-1} = [R^{1-m}][H^+]/[RH^{2-m}]$.
[c] $K_n = [R^{m-}][H^+]/[RH^{1-m}]$.

The value of pK_n has been assigned to the dissociation of the last hydroxy group of the naphthalene nucleus as a result of the hypsochromic effect accompanying this dissociation[5]. The value of K_{n-1} can be ascribed to the dissociation of the first hydroxy group of the naphthalene ring which induces a bathochromic effect in the spectrum of the reagent. According to this assumption the first hydroxy group of the benzene ring dissociates at pH below 2, together with other acid groups. This is also confirmed by the fact that in the case of picramine S, the constant $pK_{n-1}=2.55$ corresponds to the dissociation of only one hydroxy group ($a=1$). Titrimetric investigations[6] have also shown that, because of the presence of the nitro groups, the hydroxy groups of the benzene rings dissociate in a more acidic medium together with sulphonic groups.

Discussion

The results show that there is an analogy between the molar absorptivities of the completely dissociated reagents and the molar absorptivities of protonized forms of the reagents. Picramine M has the highest molar absorptivity. It has been observed that other reagents in the group of 2,7-bis-(azobenzene)-chromotropic acid derivatives, in which one of the components is metanilic acid (arsenazo M or anthranilic M), also have exceptionally high molar absorptivities[6].

The effect of substituents on the dissociation constants and on the protonation constants is similar. Picramine K was chosen as a "zero" reagent, since the effect of the *o*-carboxy group was found to be equal to zero[4]. The effect of the substituents can be expressed by $\log K_n/K_{n_0}$ as follows:

Substituent	$\log K_n/K_{n_0}$	$\log K/K_0$[4]
m-SO_3H	−0.10	−0.5
o-OH, *m,m'*-di-NO_2	−1.4	−1.5

The values are quite close, although they are slightly lower for the dissociation of the last hydroxy group of the naphthalene ring. Hence it may be concluded that dissociation proceeds less readily than protonation of the reagent.

A comparison of these results indicates that a substituent which reduces the basicity of the reagent and shifts its protonation to a more acidic region, also tends to shift the dissociation of the second hydroxy group of the naphthalene nucleus to a more alkaline region. Figure 2 shows the linear dependence between the logarithms

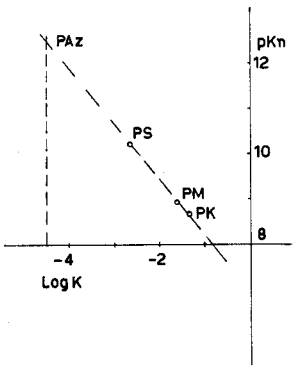

Fig. 2. Logarithm of the protonation constant *versus* pK_n.

of the protonation constants and the pK_n values for dissociation of the last hydroxy group of the reagent, indicating the similar effect of substituents on the protonation constant and on this dissociation constant. The results indicate that picramine arsenazo should dissociate above pH 12, but it was found to decompose in this pH region.

The constants denoted as K_{n-1} do not show any dependence on the substituents R in the benzene ring, which may indicate that K_{n-1} pertains to the hydroxy group farther from the substituents investigated.

We wish to express our thanks to Dr. L. A. OKHANOVA, V.I. Vernadsky Institute of Geochemistry and Analytical Chemistry, Moscow, for supplying the reagents.

Boris Kidrich Institute of Nuclear Sciences, A. A. MUK
Beograd (Yugoslavia) M. B. PRAVICA

1 S. B. SAVVIN, *Arsenazo III*, Atomizdat, Moscow, 1966.
2 S. B. SAVVIN AND YU. M. DEDKOV, *Zh. Analit. Khim.*, 17 (1962) 43.
3 I. P. ALIMARIN, S. B. SAVVIN AND L. A. OKHANOVA, *Talanta*, 15 (1968) 601.
4 A. MUK AND S. B. SAVVIN, *Anal. Chim. Acta*, 44 (1969) 59.
5 S. B. SAVVIN, R. F. PROPISTSOVA, YU. G. ROZOVSKII AND E. L. KUZIN, *Dokl. Akad. Nauk SSSR*, 181 (1968) 613.
6 A. MUK, S. B. SAVVIN AND R. F. PROPISTSOVA, *Zh. Analit. Khim.*, 23 (1968) 1277.

(Received December 11th, 1968)

Anal. Chim. Acta, 45 (1969) 534–538

Beam centering in a neutron generator

Recently, a technique for beam centering in a neutron generator, based on brief activation of a copper foil against which a KK X-ray film was later exposed for autoradiography, was described by SPELL AND IDDINGS[1]. Exposure times of 15–30 min were necessary, and the whole procedure required *ca.* 45 min. This method is successful for locating the beam and for determining the depleted areas in the target, but it requires a relatively long exposure time and a dark room for reprocessing films.

In a study[2] of the non-destructive determination of proteins from their nitrogen content, seeds of corn were irradiated in sets of four in a rotating holder. The low cross-section for the $^{14}N(n,2n)^{13}N$ reaction (6 mb) necessitated high beam currents, which resulted in rapid depletion of the tritium target. This called for the highest possible neutron economy by rotating the samples in the area of highest neutron density; because of the small sample size, flux configuration was also important. For rapid establishment of the most favourable position for irradiation, the indirect technique mentioned above proved tedious.

It has been shown that excellent radiographs can be made directly by fastening a photographic paper of low sensitivity on the target of the generator or in the position to be used for the irradiation. The paper can be processed on the spot provided that the irradiation area is adequately illuminated. This reduces the time for the whole operation to 10 min. Figure 1 shows a photocopy of a piece of commercial photographic paper which was irradiated on the target of the TMC Activatron III for 5 min at a beam current of 1.6 mA; the distortion of the beam and the depleted area can be seen clearly.

A systematic investigation of the effect was carried out with the neutron generator at the Nuclear Institute "Jožef Stefan". A holder of the form shown schematically in Fig. 2 was used for the tritium target, soldered to its backing by Wood's metal. The diameter of the deuteron beam on the target surface was about 2 mm. Pieces of photographic film (4 cm × 4 cm) were wrapped in aluminium foil (0.05 mm thick) and fastened to the backing of the holder with thin copper wire. The distance between the tritium target surface and the photographic emulsion was about 4 mm. The results reported here refer to the Agfa Gevaert 23D56 film, but other low-speed films and paper can also be used. The neutron flux during the irradiation of films was 10^9 n/sec into the 4π solid angle. Irradiated films were developed in the O81p developer. The blackening of films was similar to that shown on the left-hand side of Fig. 1.

In order to evaluate the films quantitatively, they were scanned with a photodensitometer. Details were clearest in films with a peak density about 1, but those with densities between 0.7 and 1.6 could still be used for centering purposes.

The relation between the peak density of exposed films and the corresponding maximum density of the integral neutron flux for the film Agfa Gevaert Scientia 23D56 is shown in Fig. 3. It is interesting to note that the density on the films, at the same density of neutron flux, is different if the emulsion or its backing is oriented towards the neutron source. The fact that the opacity of the photographic emulsion exposed to the neutron flux is more intense if the neutrons have to pass through its backing before reaching it, can be explained by the effect of the recoil protons. This explanation is supported by the results of irradiation experiments in which different foils (polyethylene, perspex, graphite, aluminium, iron, copper, cadmium, lead) up

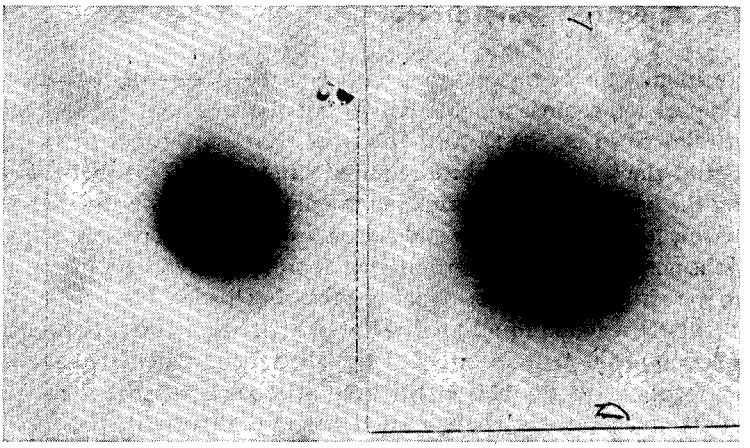

Fig. 1. Photocopy of a photographic paper irradiated in a 14-MeV neutron flux.

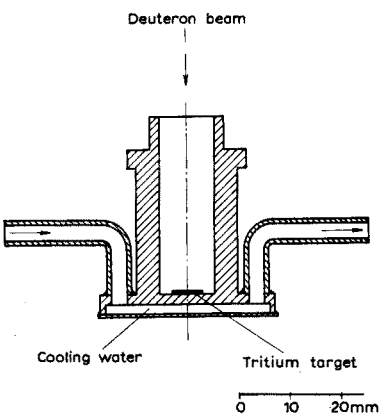

Fig. 2. Tritium target holder used for detailed study of the effect of neutron irradiation on photographic films.

to a thickness of 2 mm were inserted between the neutron source and photographic emulsion; only the hydrogen-containing polyethylene and perspex increased the density of films exposed to the neutrons. The inspection of films under the microscope confirmed this conclusion. The difference in opacity found when the emulsion was placed towards the source or away from it, indicated that the contribution of recoil protons from the backing is of the order of 25%. On the other hand, from the dependence of the film opacity on the thickness of the polyethylene in the above experiment, recoil protons from the emulsion itself contribute about 10% of the film density. In addition to recoil protons, other reactions contribute to the opacity of the exposed films; when the respective cross-sections are considered, it seems that inelastic scattering plays the most important role.

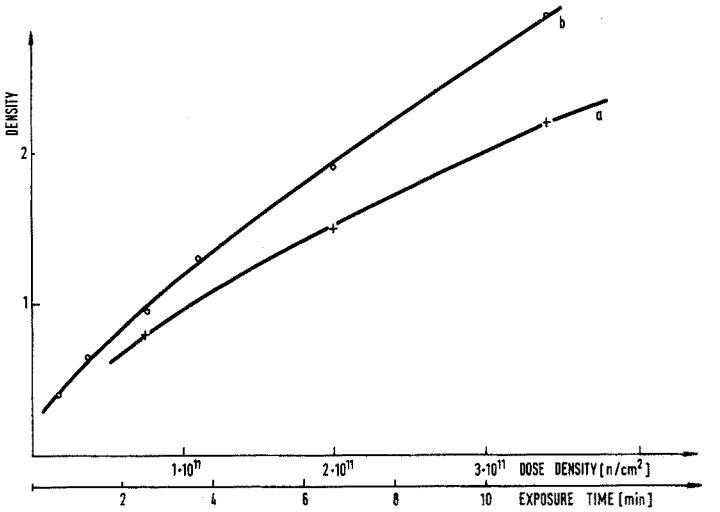

Fig. 3. Dependence of the maximum film density on the corresponding density of the integral neutron flux if emulsion is oriented towards (a) and away (b) from the neutron source. The time scale of the abscissa axis corresponds to the exposure time at the neutron flux of 10^9 n/sec/4π if the film is placed 4 mm away from the source.

The advantage of the suggested technique from the analytical point of view is that it quickly gives a picture of the configuration of the flux and its density at any cross-section in the irradiation field, which is very important in work with samples varying in size and geometry.

Nuclear Institute "Jožef Stefan" L. KOSTA
and the University of Ljubljana F. CVELBAR
(Yugoslavia) V. RAMŠAK

1 W. H. SPELL AND F. A. IDDINGS, *Anal. Chim. Acta*, 40 (1968) 515.
2 L. KOSTA, V. RAVNIK AND J. DUMANOVIĆ, Paper presented at the FAO/IAEA Panel on *New Approaches to Breeding for Plant Protein Improvement*, 17–21 June 1968, Swalöf, Sweden.

(Received November 28th, 1968)

Anal. Chim. Acta, 45 (1969) 539–541

Some observations on the determination of iodide by its catalytic effect on the decomposition of the monothiocyanate complex of iron(III)

The effect of iodide on the decomposition of the monothiocyanate complex of iron(III), in the presence of sodium nitrite and nitric acid, was first proposed as a method for the microdetermination of iodide by UTSUMI *et al.*[1]; analytical applications and the effect of many interfering ions have been described[2–5], and various improvements have been suggested[6–8]. This reaction would appear to be of considerable value in the determination of small amounts of iodide, iodine, iodate and periodate[4,5], particularly in the presence of high chloride concentrations[6].

However, there is one important factor which appears to have escaped notice previously, and which could cause difficulty in the determination of unknown concentrations of iodide; namely, two widely different iodide concentrations can lead to the same value of the measured parameter.

This communication reports the presence of this defect in the method of UTSUMI *et al.*[1] and suggests a possible means of detecting and overcoming its effect.

Experimental

The reaction solutions outlined previously[1] were used throughout, except that the overall volume was increased to 65 ml. AnalaR-grade reagents were used throughout. The reaction was followed by monitoring the absorbance of the iron(III) monothiocyanate at its wavelength of maximum absorbance, 460 nm. A Hitachi-Perkin Elmer 137 spectrophotometer coupled to a Honeywell Electronik Chart Recorder was used to give a continuous record of the variation in absorbance of the solution with time. All solutions and the 10-mm spectrophotometer cell were thermostatted at $25.0 \pm 0.1°$ for 30 min before use. The reaction solutions, except the acidified iron(III) solution, were mixed and kept in a stoppered flask. The reaction was started by addition of 10 ml of the iron(III) solution. The cell was then washed three times with the reaction solution and filled with it and finally transferred to the thermostatted cell compartment of the spectrophotometer.

Discussion

The effect of 0.4–154 p.p.m. of iodide on the rate of disappearance of the iron(III)–monothiocyanate complex is illustrated in Fig. 1. The curves obtained at the lower iodide concentrations are in general agreement with those reported previously[4,6,7]. Some interesting features are apparent on inspection of these curves.

1. At iodide concentrations up to 10 p.p.m. the reaction exhibits an induction period and the reaction rate increases with increasing iodide concentration. These are the properties used in the published methods[1,6,7].

2. At iodide concentrations above 10 p.p.m., three new features are observed. (*a*) The induction period is replaced by an initial increase in absorbance of the solution, the extent of the increase depending on the concentration of iodide present. (*b*) The reaction rate observed at half reaction decreases with increase in iodide concentration. (*c*) A residual absorbance becomes apparent above 20 p.p.m. of iodide, the value again depending on the initial iodide concentration.

The significance of (2) above on the analysis of unknown iodide concentrations is shown in the calibration curves obtained by this technique for the determination of iodide. In previous studies, two types of calibration curves have been used. The fixed-time method (Fig. 2) was favoured by UTSUMI *et al.*[1]. YATSIMIRSKII *et al.*[6] and PROSKURYAKOVA[7] plotted the logarithm of the absorbance during the reaction against time, and then plotted the slope of the linear portion found against the iodide concentration (Fig. 3). A third possible method would be to plot the time taken to reach a fixed absorbance (*e.g.* 0.500) against the iodide concentration. The second type of calibration curve is reported to give higher accuracy[6], whereas the first and third methods are simpler and faster.

However, all three calibration curves showed the same feature of two values of iodide concentration corresponding to each value of the parameter measured. The

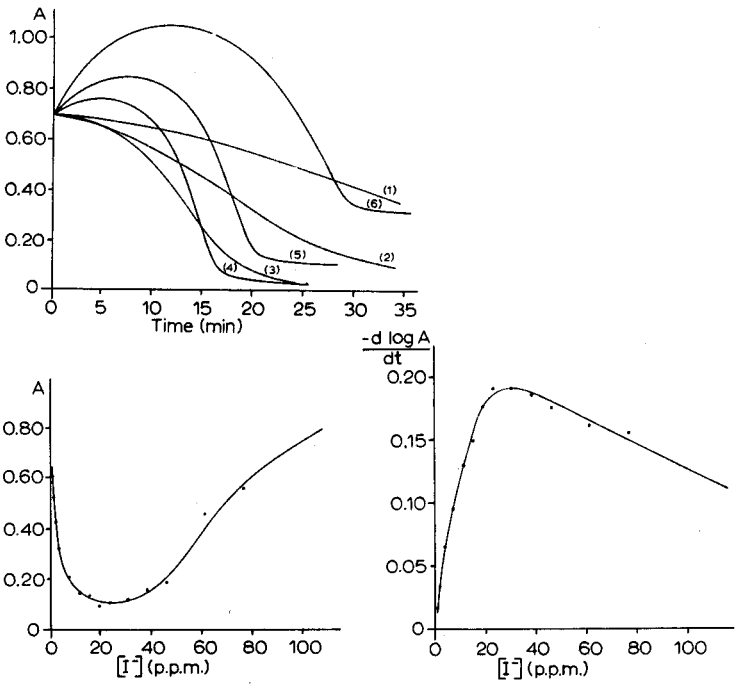

Fig. 1. Change in absorbance at 460 nm with time of a solution containing $1.91 \cdot 10^{-2}M$ iron(III), $2.31 \cdot 10^{-4}M$ potassium thiocyanate, $2.31 \cdot 10^{-5}M$ sodium nitrite, 0.88 M nitric acid and potassium iodide (p.p.m.): (1) 0.4, (2) 1.9, (3) 7.7, (4) 38.5, (5) 76.9, (6) 153.8.

Fig. 2. Calibration curve obtained by the fixed time method. Absorbance measured after 16 min. The concentration refers to the reaction mixture.

Fig. 3. Calibration curve obtained by the tangent method of YATSIMIRSKII *et al.*[6]. The concentration refers to the reaction mixture.

only differences were in the exact shapes of the calibration curves and the maximum iodide concentrations which could be determined before this feature became apparent. The failure in the system, which is apparent from Figs. 1–3, arises when the absorbance of the solution starts to increase at the beginning of the reaction, thus apparently delaying the decomposition of the iron(III)–monothiocyanate complex.

The residual absorbance, after complete reaction, was removed by shaking the solution with chloroform, when the aqueous layer became colourless and the chloroform layer attained the distinctive pink colour of iodine. The iron(III)–thiocyanate complex was not extracted and had apparently completely decomposed, since the aqueous layer was colourless. When the reaction was conducted in the presence of chloroform, with continual shaking, the reaction rate was reduced to that for the uncatalysed reaction and the chloroform layer again attained the characteristic iodine colour. Thus the initial increase in absorbance and the final residual absorbance, observed at the higher iodide concentrations must be due to iodine (λ max 470 nm[9]) which is produced during the reaction and remains throughout. Although no satisfactory kinetic information is available on the reaction, the rate of the catalysed reaction clearly depends on the formation of iodine during the reaction; the observed

effect of nitrite[1,6] on the induction period of the reaction is connected with the oxidation of iodide by nitrite.

Similar conclusions to those outlined above can be applied to the various other combinations of reaction solutions and temperatures proposed[6,7].

The concentration limits for iodide which have previously been determined by this method have been 0.001–10 p.p.m. If the concentration of iodide in a sample is known to fall within the appropriate range, then the available methods[1,6,7] can be applied without modification. If this information cannot be guaranteed, an alternative kinetic method[10,11] would normally be preferable. However, the present method can be used if required, provided that the production of iodine is checked by shaking the final reaction solution with 10 ml of chloroform and measuring the absorbance of the extract at 510 nm[9]. In checks of this technique, zero absorbance was found up to 15.4 p.p.m. of iodide in the reaction solution, and the absorbance increased from 0.217 to 1.180 as the iodide concentration increased from 38.5 to 77.0 p.p.m. Absorbance values greater than zero signify an excessively high concentration of iodide and the invalidity of the analysis. For the routine application of the method, visual observation on the chloroform extract would probably prove sufficient. In the event of a "significant amount" of iodine being detected, a further sample of the unknown iodide sample should be diluted by the required amount and the analysis repeated, although at such concentration levels, a more conventional method could readily be applied.

Department of Pure and Applied Chemistry,
University of Strathclyde,
Cathedral Street,
Glasgow C.1 (Scotland)

J. M. OTTAWAY
C. W. FULLER
W. B. ROWSTON

1 I. IWASAKI, S. UTSUMI AND T. OZAWA, *Bull. Chem. Soc. Japan*, 26 (1953) 108.
2 S. UTSUMI, *J. Chem. Soc. Japan, Pure Chem. Sect.*, 74 (1953) 298.
3 I. IWASAKI, S. UTSUMI, T. OZAWA AND R. HASEGAWA, *J. Chem. Soc. Japan, Pure Chem. Sect.*, 78 (1957) 474.
4 S. UTSUMI, M. SHIOTA, N. YONEHARA AND I. IWASAKI, *J. Chem. Soc. Japan, Pure Chem. Sect.*, 85 (1964) 32.
5 I. IWASAKI, S. UTSUMI AND N. YONEHARA, *J. Chem. Soc. Japan, Pure Chem. Sect.*, 85 (1964) 36.
6 K. B. YATSIMIRSKII, L. I. BUDARIN, N. A. BLAGOVESHCHENSKAYA, R. V. SMIRNOVA, A. P. FEDOROVA AND V. K. YATSIMIRSKII, *Zh. Analit. Khim.*, 18 (1963) 103.
7 G. F. PROSKURYAKOVA, *Zh. Analit. Khim.*, 22 (1967) 802.
8 M. P. BABKIN, *Lab. Delo*, 7 (1967) 429.
9 J. KLEINBERG AND A. W. DAVIDSON, *Chem. Rev.*, 42 (1948) 604.
10 E. B. SANDELL AND I. M. KOLTHOFF, *J. Am. Chem. Soc.*, 56 (1934) 1426.
11 H. P. LUNDGREN, *J. Am. Chem. Soc.*, 59 (1937) 413.

(Received December 8th, 1968)

Anal. Chim. Acta, 45 (1969) 541–544

An improved titrimetric method for the determination of uranium: oxygen ratios

A knowledge of oxygen: uranium ratios is essential in many applications of uranium oxides[1], but the analytical methods available are either not precise[2] or require elaborate apparatus[3–6]. NEUMANN'S[7] modification of determining uranium(IV) was an improvement but the reproducibility was found to be unsatisfactory; besides the inherent uncertainty arising from the volatility of iodine, the procedure involved many steps each contributing to the final uncertainty. A modification in which cerium(IV) sulphate was used as oxidant allowed a better precision to be achieved, as described below.

Reagents and samples

Cerium(IV) sulphate, iron(II) ammonium sulphate, sulphuric acid and 0.025 *M* ferroin indicator solution were all E. Merck G. R. grade chemicals.

Nuclear-grade uranium dioxide powder was obtained from the Atomic Fuels Division, B.A.R.C. (total metallic impurities less than 200 p.p.m.). The finely divided powder was first heated in hydrogen for 2 h at 1100°, ground in agate mortar and sieved. The sieved powder of particle size +300 to −100 was used in subsequent experiments. A small quantity of this sample was kept over anhydrous magnesium perchlorate in a desiccator before use. After the first portion was exhausted, a second portion (50 g) was taken from the stock bottle and dried over magnesium perchlorate (sample II). The U_3O_8 sample was prepared by oxidising a portion of the urania sample in air at 435° in a platinum boat and was kept over magnesium perchlorate.

Procedure

The uranium oxide samples (50–175 mg samples for nearly stoichiometric uranium dioxide and 100–250 mg samples for U_3O_8) were weighed and transferred to a known excess of 0.1 *M* cerium(IV) sulphate solution in 3 *N* sulphuric acid. The dissolution was completed by heating the mixture at 70° for the necessary length of time (30–40 min for UO_2 samples, or 10–15 min for U_3O_8 samples). Sufficient 5 *N* sulphuric acid was added to make the solution 3 *N* in sulphuric acid at the equivalence point, and the excess of cerium(IV) present was then titrated with a freshly prepared standard iron(II) ammonium sulphate solution using ferroin as indicator. The cerium(IV) solution was standardized just before each series of analyses; it was prepared by dissolving pure cerium(IV) sulphate in 5 *N* sulphuric acid, and diluting to give a 3 *N* acid solution.

The results are presented in Table I, which also shows the results obtained by NEUMANN'S method applied simultaneously.

Discussion

The oxygen: uranium ratio obtained for urania sample II was significantly higher than for sample I though both were drawn from the same stock. The sample II material was drawn from the stock bottle nearly 3 months after sample I. During this period, the nearly stoichiometric uranium dioxide was exposed to air inside the stock bottle and might have been oxidised further. It can also be observed that the precision for sample I is slightly poorer than that for sample II; this is probably due to the better

TABLE I

RESULTS OF O/U ANALYSES

Proposed method			*Neumann's method*		
No. of detns.	*Sample weight (mg)*	*O/U found (mean result)*	*No. of detns.*	*Sample weight (mg)*	*O/U found (mean result)*
UO_{2+x} sample I					
13	60.4–174.3	2.022 ± 0.0045[a]			
UO_{2+x} sample II					
15	54.95–118.45	2.0363 ± 0.0032[a]	11	58.94–150.79	2.0336 ± 0.0053[a]
U_3O_8					
20	100.8–288.90	2.671 ± 0.0038[a]	16	89.67–174.74	2.676 ± 0.013[a]

[a] Standard deviation.

accuracy of the burettes (graduated to 0.05 ml) and balance used for sample II and in all subsequent runs.

NEUMANN claimed a standard deviation of ±0.0016 for the O/U ratio of nearly stoichiometric urania samples. However, in the present work, a standard deviation of only ±0.005 was obtained for 11 O/U determinations by his method, compared with a standard deviation of ±0.0032 for 15 determinations by the proposed method. For U_3O_8 samples, the corresponding deviations were ±0.013 and ±0.0038, respectively. The simplicity of the proposed method makes it generally suitable for O/U analyses unless a deviation less than ±0.002 in O/U is required.

We are grateful for the valuable assistance and the encouragement given to us by Dr. J. SHANKAR and Dr. M. D. KARKHANAVALA of Chemistry Division, Bhabha Atomic Research Centre during this work.

Chemistry Division,
Bhabha Atomic Research Centre,
Trombay,
Bombay-74 (India)

S. R. DHARWADKAR
M. S. CHANDRASEKHARAIAH

1 *Thermodynamics and Transport Properties of Uranium Dioxide and Related Phases*, Technical Report No. 39, I.A.E.A., Vienna, 1965.
2 C. J. RODDEN, *Analytical Chemistry of Manhattan Project*, McGraw-Hill, New York, 1950, p.67.
3 R. W. STROMATT AND R. E. CONNALLY, *Anal. Chem.*, 33 (1961) 345.
4 C. M. BOYD AND O. MENIS, *Anal. Chem.*, 33 (1961) 1016.
5 H. KUBOTA, *Anal. Chem.*, 32 (1960) 610.
6 L. E. J. ROBERTS AND E. A. HARPER, *A.E.R.E. CIR-885/1952*.
7 L. NEUMANN, *Collection Czech. Chem. Commun.*, 25 (1960) 2235.

(Received January 1st, 1969)

Anal. Chim. Acta, 45 (1969) 545–546

The determination of sulphide in waters by an automatic method

The method[1] currently used in these laboratories for the determination of low levels of sulphide ions (1–10 p.p.m.) in waters, *e.g.* in trade effluents, is based on the liberation of hydrogen sulphide from an acidified sample and subsequent iodimetric titration; such procedures are not easily automated. In view of the large number of samples that are handled daily, the manual procedure is extremely time-consuming and tedious.

Colorimetric methods, in general, are more suitable for automation. An established procedure based on the synthesis of methylene blue[2,3] was considered but rejected in favour of a much simpler colorimetric procedure involving the formation of the transient violet colour produced from the reaction between nitroprusside and sulphide in alkaline solution[4]. The transient nature of the violet colour would be disadvantageous if it were measured conventionally. However, the Technicon Auto-analyzer has the advantage that samples can be treated in a reproducible manner, and the colour measured after a definite time from the addition of reagents. The variations caused by colour fading are thus minimized and a reproducible calibration is obtained.

A further novel feature of the proposed method is the inclusion of a distillation step to add selectivity to the procedure; this also eliminates the necessity of filtering any samples.

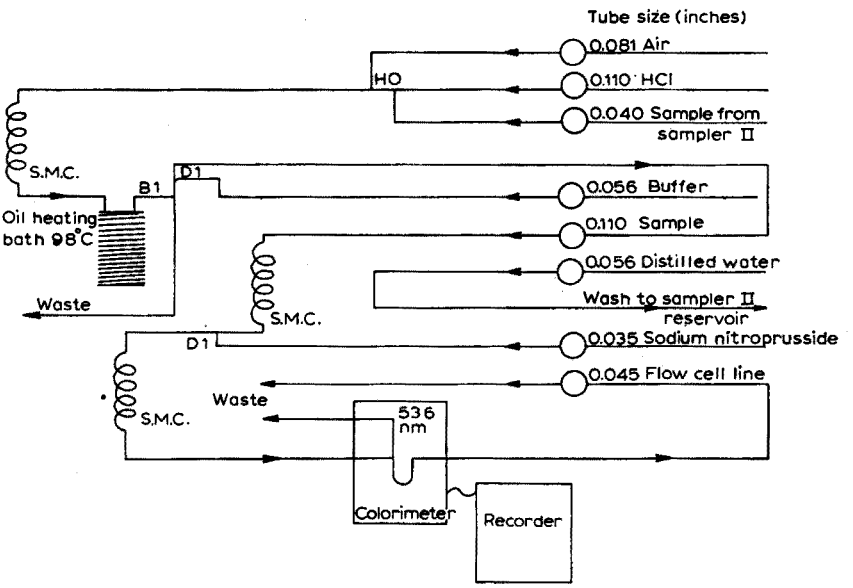

Fig. 1.

Apparatus

The apparatus, based on the "Technicon" Auto-analyzer modules, is shown schematically in Fig. 1. The sampling rate was chosen to be 40 samples per hour with a sample : wash ratio of 1:2; the wash used was distilled water.

There are several points of interest about the manifold:

1. The distillation temperature was 98°. Higher temperatures lead to splashing and carry-over at the B1 trap, whilst lower temperatures lead to somewhat reduced sensitivity.

2. The B1 trap which separates the air containing the gaseous hydrogen sulphide from the acidified sample should be as close as possible to the heating coil, otherwise sensitivity will be reduced.

3. The coil in which the solutions of buffered hydrogen sulphide and sodium nitroprusside are mixed should be as short as possible. This is a compromise between efficient mixing of the solutions and the extent to which colour fading occurs. Further, the connection between this mixing coil and the flow cell should be as short as possible or again sensitivity will be lost.

4. No wetting agent should be used during a run or excessive frothing will occur in the B1 trap, and unreliable results will be obtained.

Reagents

The solutions used were *ca.* 0.5 *N* hydrochloric acid, and aqueous 0.1% (w/v) sodium nitroprusside. Buffer solution (pH 12) was prepared by dissolving 58.2 g of disodium hydrogen phosphate dodecahydrate and 7 g of sodium hydroxide in water and diluting to 1 l.

Stock sulphide solution. Since there is no suitable primary standard for sulphide, a stock solution was prepared from sodium sulphide to contain *ca.* 100 p.p.m. of sulphide. This solution was made 0.1 *M* with respect to sodium hydroxide, and 20 p.p.m. of hydrazine sulphate was added; these served to minimize losses of sulphide by volatilisation and atmospheric oxidation. This solution was found to remain stable for a period of 2 weeks.

Calibration curve

The concentration range of interest was 1–10 p.p.m. of sulphide; accordingly, three dilutions of the stock solution were made to give *ca.* 2.5-, 5.0- and 10-p.p.m. sulphide solutions, which were stable for a period of one day only. These solutions were standardised by the manual procedure[1].

The calibration curve was prepared by submitting these standard sulphide solutions to the Auto-analyzer procedure outlined above; under these conditions a

TABLE I

STANDARD DEVIATIONS FOR THE MANUAL AND AUTO-ANALYZER PROCEDURES

Analytical procedure	*Mean sulphide content (p.p.m.)*	*No. of determinations*	*Standard deviation*
Manual	2.8	5	0.46
Auto-analyzer	2.8	16	0.12
Manual	6.2	11	0.83
Auto-analyzer	6.2	16	0.33
Manual	11.3	6	0.40
Auto-analyzer	11.3	16	0.48

return to baseline between samples was achieved. The plot was found to be linear and passed through the origin; the absorbance for *ca.* 10 p.p.m. of sulphide was *ca.* 0.250. It is perhaps pertinent to note that Beer's law was obeyed up to 40 p.p.m. of sulphide.

Precision of the method

A direct comparison between the precisions of the standard manual procedure[1] and the automated procedure was carried out. Three standard solutions were assessed for their sulphide contents over an 8-hour period; no trend in the results was observed. The results are summarized in Table I.

Analysis of water samples

About 1000 water samples (mostly trade effluents) were analysed over several months, in order to compare the results obtained for sulphide by the manual procedure and by the Auto-analyzer procedure.

More than 900 samples were found to contain less than 1 p.p.m. of sulphide by both procedures; since this level is the lower limit of detection of both procedures, they were not investigated further. However, twenty-six samples had a sulphide content of 1 p.p.m. or greater. The results (Table II) were analysed statistically by the Student "t"-test. The results of the Auto-analyzer procedure were not significantly different from those of the manual procedure.

TABLE II

DETERMINATION OF SULPHIDE IN WATERS BY THE MANUAL AND AUTO-ANALYZER PROCEDURES

Sulphide content (p.p.m.)		*Sulphide content (p.p.m.)*		*Sulphide content (p.p.m.)*		*Sulphide content (p.p.m.)*	
Manual	*Auto-analyzer*	*Manual*	*Auto-analyzer*	*Manual*	*Auto-analyzer*	*Manual*	*Auto-analyzer*
0.8	1.0	5.0	5.9	3.7	2.4	6.7	3.4
1.4	1.5	3.0	1.2	3.8	2.4	7.5	5.0
3.5	1.0	1.8	2.5	2.4	4.0	3.9	2.7
7.2	10.0	2.6	2.5	4.5	1.3	2.5	2.3
2.1	2.5	0.9	1.1	2.7	1.2	1.7	1.3
0.9	1.1	1.1	1.7	6.7	6.3	4.1	2.5
1.1	1.0	4.0	3.8				

Interferences

The inclusion of a distillation stage in the procedure, and the use of a selective reagent minimizes interferences. The concentrations of sulphite and thiosulphate ions which can be tolerated are 500 p.p.m. and 2000 p.p.m., respectively. These may be compared with a tolerable upper limit of 40 p.p.m. for those anions in the methylene blue method[2]. On the other hand, the manual procedure which involves a specific precipitation of zinc sulphide from the liberated hydrogen sulphide does not give interference.

The tolerable limit for both phenol and formaldehyde is 100 p.p.m.

Discussion

The nitroprusside method in conjunction with the Auto-analyzer for the determination of low level quantities of sulphide has been shown to be reliable. The precision is satisfactory in the concentration range 1–10 p.p.m. of sulphide, and in fact, is slightly better than that obtained for the manual procedure. The coefficients of variation at the 10-p.p.m. level for the Auto-analyzer procedure and the manual procedure are 4.2% and 3.6%, respectively. At lower levels, the coefficients of variation for the Auto-analyzer method are considerably less than those for the manual procedure.

If high selectivity is not required, the distillation may be omitted, so that the sensitivity of the method is increased by a factor of about 10. On the other hand, if less sensitivity is required (*i.e.*, concentrations greater than 40 p.p.m. of sulphide), this can be easily achieved by using different filters in the colorimeter or by including a dilution step in the manifold; no loss of selectivity occurs with either change, *i.e.*, a return to baseline between samples is obtained.

The Auto-analyzer procedure has been assessed under routine working conditions, the results of which have shown no significant differences from the manual procedure. The automated method allows a large increase in the number of samples that can be handled; the sampling rate of 40/h can readily be used to assess about 250 samples daily.

The authors are indebted to the Scientific Adviser (Dr. B. R. BROWN) for his permission to publish this work.

Scientific Branch,
Greater London Council,
The County Hall,
London S.E.1 (England)

P. CASAPIERI
R. SCOTT
E. A. SIMPSON

1 *Recommended Methods for the Analysis of Trade Effluents*, Society for Analytical Chemistry, London, 1967, p. 119.
2 *Standard Methods for the Examination of Water and Wastewater*, American Public Health Association Inc., New York, 1960, p. 332.
3 I. NUSSBAUM, *Water Sewage Works*, 112 (4) (1965) 113, 150.
4 V. N. BERNSTEIN AND V. G. BILIKER, *Russ. Chem. Rev.*, 30 (4) (1961) 227.

(Received December 15th, 1968)

Anal. Chim. Acta, 45 (1969) 547–550

ANALYTICA CHIMICA ACTA, VOL. 45 (1969)

AUTHOR INDEX

ANALYTICA CHIMICA ACTA, VOL. 45 (1969)

SUBJECT INDEX

Inorganic Macromolecules Reviews

Elsevier

Inorganic Macromolecules Reviews

The Chemistry, Physics and Technology of Macromolecular Inorganic Compounds and Materials

DECLARATION OF EDITORIAL INTENT

The editors and publisher of INORGANIC MACROMOLECULES REVIEWS intend to foster the increasing interest in the study and exploitation of inorganic macromolecules by providing a review periodical in which all aspects of their science and technology will be covered.

At present studies of inorganic macromolecular systems are reported in a variety of journals. INORGANIC MACROMOLECULES REVIEWS will provide a medium in which important aspects and developments of these studies are presented as a whole.

The Reviews should be of interest to chemists, physicists, polymer scientists, materials scientists and materials engineers working in the field, for the interpretation of inorganic macromolecules will be a broad one embracing both natural and synthetic systems and should help bridge the gap existing between organic polymer science, glasses and ceramics.

The editors' principal aim, however, is that the Reviews should make a significant contribution towards the development of the science and technology of inorganic macromolecules. For this reason only reviews of the highest quality will be published and the editors and referees will ensure that this standard is upheld.

FREQUENCY AND SUBSCRIPTION INFORMATION

Approximately one volume of four issues will be published per year. The size of the journal is 6½ x 9½". Subscription price is Dfl. 90.00 plus Dfl. 3.00 postage or equivalent (as at Jan. 1, 1969 US$25.00 plus US$0.85 or £10.9.6 plus 7s.). Subscriptions may be placed with your usual supplier or direct with Elsevier Publishing Company, P.O. Box 211, Amsterdam, The Netherlands. Specimen copies and advertising rates will be sent on request.

MANUSCRIPTS

Although the Editors will at times solicit review article manuscripts from established authorities in the field covered, unsolicited reviews will also be welcomed. It is, however, requested that subjects for such unsolicited reviews be cleared with the Editors before a manuscript is submitted so that duplication of effort may be avoided.

The Editors are:

F.G.R. Gimblett
Chemistry Department

and

K.A. Hodd
Department of Polymer Science and Technology

Brunel University
Acton, London W. 3, Great Britain

A brochure containing hints to authors is available free of charge from the publishers.

LANGUAGES

Reviews will be published in English, French and German, but manuscripts should preferably be submitted in English.

FORTHCOMING PAPERS:

The first issue will contain the proceedings of the International Symposium on Inorganic Polymers, held on April 9, 10 and 11, 1969 at the Northern Polytechnic, London.

CONTENTS

(continued on page 4 of cover)

(contents, continued from page 3 of cover)